HYDRODYNAMICS ~~MODELLING~~ OF A CIRCULATING FLUIDISED BED ~~REACTORS~~

by

CONSTANTINIA PANTOPIKOU

(BSc, MSc)

A thesis submitted for the degree of

DOCTOR OF PHILOSOPHY

at the

University of London

Department of Chemical and
Biochemical Engineering,
University College London.

JUNE 1991

ABSTRACT

The principle of circulation of solids in a gas-solid system had led to the development of a number of processes. These processes in the form of circulating fluidised beds (CFB) are usually large-scale operations, with the fluid catalytic cracking process (FCC) and combustion as the major examples.

In this work pressure drop and solid circulation rate measurements have been conducted during the operation of a circulating fluidised bed (CFB) consisting of a riser, a solid collecting system (cyclones), a slow bed, a ball valve and a riser distributor. Most of the experiments have been conducted with FCC powder of average particle diameter of 64μm and particle density of 884 kg/m^3. Some further experiments were conducted with either pure Poralox powder of particle diameter of 127μm and density of 1850 kg/m^3 or a 50/50 v/v mixture of Poralox and FCC. The gas velocities were varied between 1.5 and 4 m/s. The three riser distributor plates had the same free percentage of open area, divided into 1 nozzle, 7 and 13 holes.

The pressure profiles around the circulating fluidised system should be such that the higher pressure drop values should be located above and below the ball valve for safe operation of the riser type reactors.

Increasing the slow bed inventory from 21 to 60 cm resulted in an increase in the riser pressure drop and hence in the axial solids fraction present in the riser.

The design of the distributor plate affects the performance of the CFB. For the same operating conditions using the 7 and 13 hole distributors much higher solid circulation rates were observed compared with the 1 nozzle distributor.

Increasing the density and the size of particles from FCC to Poralox leads to higher solid circulation rates but also higher pressure drops.

Operating the CFB at high opening areas of the ball valve will normally leads to a downflow of solids in an annulus adjacent to the riser wall.

If the ball valve is fully open then the CFB cannot be operated without instabilities.

The Dense Annulus Lean Core model (DALC) is proposed which relates the pressure drop along the axis of the riser to particle and fluid properties. The DALC model is shown to give good predictions, both qualitatively and quantitatively when the CFB is operated so as to achieve high solid circulation rates.

The DALC model is then applied to the case in which a first order catalytic reaction takes place in the riser. By increasing the reaction rate constant to 15s^{-1} the model indicates a conversion of 55 % in the downflow region within a distance of less than 3m above the distributor. By increasing the gas velocity in the riser the model predicts that the conversion of a first order reaction decreases.

ACKNOWLEDGEMENTS

I wish to express my thanks and gratitude to:

My supervisor Prof. J. G. Yates, firstly for arranging a departmental studentship and secondly for his expert guidance and whose advice was easy to find during this work.

The Departmental Workshop and in particular Len Coates for constructing the experimental apparatus.

Costas and Christos for all the encouragement during the write up period of this work.

Dr. L. Al-Dhahir for his helpful discussion concerning this work.

BP Research International for financing the project.

CONTENTS

CHAPTER 1

INTRODUCTION

1.1 DEFINITION OF STATES OF FLUIDISATION

Fluidisation is the operation by which fine solids are transformed into a fluidlike state through contact with a gas or liquid. Suppose a quantity of finely divided solid particles is placed into a bed (ie a cylindrical container) supported with a porous plate and air is passed through the base in the upward direction. At relatively low air velocities, fluid merely percolates through the void spaces between stationary particles, and this is the state of the fixed bed. With an increase in fluid flow rate, particles move apart and a few are seen to vibrate and move about in restricted regions. This is the expanded bed. With further increase in the upward fluid velocity, the expansion of the bed continues until a point is reached when the particles are all just suspended in the upward flowing gas. At this point the drag (frictional) force between particles and fluid counterbalances the weight of the particles, the bed takes on the appearance of a liquid having a flat surface and the particles are then said to be 'fluidised'. The superficial gas velocity at which this occurs is called the 'minimum fluidisation velocity' U_{mf} and the bed is said to be in the state of incipient fluidisation. With an increase in gas velocity beyond minimum fluidisation, it is observed experimentally that instabilities and cavities are

developed in the form of gas bubbles. These bubbles form within the bed, rise to the surface where they burst in the same way as gas bubbles in a boiling liquid. At this gas velocity, the bed is divided essentially into two phases - the dense or emulsion phase where gas percolates through and the lean or bubble phase where much of the gas is out of contact with solids. Such a bed state is called an aggregative fluidised bed or a bubbling fluidised bed. A further increase in gas velocity leads to more vigorous bubbling with bigger gas bubbles appearing at the surface until at some velocity, the diameter of the surface bubble becomes equal to the diameter of the bed. This is the state of 'slugging' fluidisation and it is characterised by strong pressure flucuations, with many particles being thrown up into the space above the bed known as the 'freeboard'. At these high velocities much of the solid is lost from the bed by entrainment and elutriation, so that cyclones are needed to return particles to the bed. At relatively high gas velocities the particles will be transported out of the bed and only a low concentration of rapidly moving particles remain in contact with the gas. This state is known as vertical dilute phase flow and is sometimes found in pneumatic conveying systems. However, between the regions of slugging and dilute phase flow, there is evidence for the existence of another regime of flow, the so-called "fast" fluidisation regime, characterised by the highly turbulent motion of individual particles and aggregates or clusters of particles, high

solid concentrations compared with the condition obtained in dilute phase flow and extensive backmixing of solids. It may be possible to maintain a fast fluidised bed at atmospheric pressure and with velocities of 2-4.5 m/s with fine powders. The various states of gas-solid contacting as they have been described above are shown in Figure 1.1.

1.2 CHARACTERISTICS OF CIRCULATING FLUIDISED BEDS

The discovery of how to maintain a stable and continuous circulation of solids in a gas-solid system has led to the development of a number of processes using the principle of circulation. These processes are usually large-scale operations, especially in the petroleum industry with the fluid catalytic cracking process(FCC) as the major example.

Different forms of gas-solid contacting and flow occur in the various sections of any circulating system in order to achieve stable circulation. These forms may include pneumatic conveying (low solids concentration), moving beds ($U_{gas-solid} < U_{mf}$), fast fluidised solids transport (high solids concentration, $U_{gas-solid} > U_{mf}$) and nearly always one or more fluidised beds.

The basic problem then is to decide what type of flow and what pressures are to be maintained in the different sections of a circulating system, the size of pipes and vessels, the gas flowrate so as to design an assembly which is stable and has a circulation rate meeting the demands of the particular process.

Solid circulation systems have been used with liquid-solids (ion exchange, adsorption-desorption systems); however the most important applications are with gas-solids systems.

The most important and extensive use of circulation systems has been in the field of solid catalysed gas phase reactions, where they are used in one of the following two situations. The first is where the catalyst deactivates rapidly and requires frequent regeneration. In this situation, a steady-state solid circulation condition is achieved with the catalyst being continuously regenerated and returned to the reactor. A second use is where much heat must be brought into or removed from the reactor. Gases have a very small specific heat capacity relative to heats of reaction, whereas solids have a relatively large heat capacity. Hence a continous circulation of solids between two vessels (ie reactor and heat exchanger) can effectively transport heat from one vessel to the other and also control the temperatures in the units.

The circulation system can be treated as a whole, if the circulation rate for solids and the frictional losses for both the dense and lean mixtures are known. The principles involved in the circulation can be illustrated using as an example the water-steam system (Kunni and Levenspiel,1973).

Consider the circulation loop ABCDEA of Figure 1.2. Section AB is 1m high and filled with water. Section BC is horizontal and contains a heater that vaporises all the

water moving to the left from B to C. Section CD is filled with steam and section DA has a heat remover such that all steam moving to the right from D to A is condensed. The static head around the loop starting with point A can be estimated as follows:

$$P_B = P_A + 100 \text{ cmH}_2O$$

$$P_C = P_B = P_A + 100 \text{ cmH}_2O$$

If the density of steam is negligible with respect to the density of water then,

$$P_D = P_C = P_A + 100 \text{ cmH}_2O$$

and hence,

$$P_E = P_D = P_A + 100 \text{ cmH}_2O$$

Thus there is a pressure head of 100 cmH_2O between E and A tending to cause convection (because of the density difference of the fluid in the two sides of the loop) in the clockwise direction around the loop. If the valve is then opened, the fluid will circulate at a rate such that the pressure drop around the loop just matches the static head of 100 cm.

These principles of circulation apply to gas-solid systems, and from the above example one can see that such circulation systems must have regions of high bulk density and others of low bulk density.

A typical flow diagram of a circulating fluidised bed (CFB) with gas-solid contact is shown in Figure 1.3. It consists of a vertical tube, the riser, a separation system, the cyclones, and a bubbling fluidised bed. The latter is connected through an inclined pipe with

the high gas velocity riser .

A valve is used to regulate the solid rate within the riser. To illustrate the principle of the circulating fluidised bed loop of Figure 1.3, a typical pressure balance around the system, is presented in Figure 1.3. For all restrictions to the solid flow due to the valve, the maximum pressure drop is located above the valve at the bottom part of the bubbling bed. This prevents leakage of the high velocity gas from the riser side into the bubbling bed. To ensure proper operation of the riser type of reactor, the gas leakage should be avoided at all costs.

According to Geldart's classification, Group A powders are characterised by a relatively small particle size (d_p = 30-150 μm) and a low particle density (< 1500 kg/m^3). Frequently these powders show an increase in the void fraction of the emulsion phase as the fluidising gas velocity increases. Futhermore the minimum bubbling velocity U_{mb} is always greater than U_{mf}. They easily form bubbles which rise at velocities much in excess of that of the emulsion phase gas. Fluid cracking catalyst is a typical example of a Group A powder.

Squires et al. (1985) constructed a regime flow diagram for a Group A powder which is illustrated in Figure 1.4. This particular diagram is a plot of the solid volume fraction versus the superficial gas velocity, and introduces the different flow regimes of fluidisation. In each flow regime a schematic diagram of an industrial application is presented.

Diagram (I) shows the upflow design of the original fluid catalytic cracker (FCC model)

Diagram (II) indicates the downflow design with a meniscus. The first downflow FCC's (in the 1940's) operated at about 0.4m/s,with a dust loading of about 1.7kg per cubic meter of gas entering a single stage cyclone. Before 1955, FCC regenerators similar to (II) in mechanical arrangement, operated at about 0.75 m/s with about 70 kg/m^3 dust loading into a three stage cyclone.

Diagram (III) shows a CFB for Fischer-Tropsch synthesis at Sasol; steam tubes within the bed remove the heat of reaction.

Diagram (IV) shows a staged turbulent bed for the production of acrylonitrile.

Diagram (V) indicates a modern fluid cracker (Mobil-UOP) with a riser cracking zone and a CFB catalyst regenerator.

Diagram (VI) shows a CFB boiler.

The major advantages of gas-solid processing in CFB reactors in comparison to that of bubbling fluidised beds are the following:

1) A highly expanded bed of circulating fine-grain solids provides excellent gas-solid contact.

2) The high mean relative velocity between gas and solid results in high rates of heat and mass transfer.

3) The fluidised gas in the riser section of a CFB shows a plug flow behaviour.

4) The staged addition of one or more gaseous reagents at different levels in the riser is possible .

Although many of the above advantages describe the CFB reactor as an excellent gas-solid type of reactor, the high gas velocities and the recirculation of solids, may make the CFB system more expensive in terms of power requirement and investment in comparison with conventional fluidised bed reactors.

One of the main areas where CFBs have found commercial application is in combustion. Although initially most research and commercial development was centred on the bubbling form of fluidised bed, in more recent years much interest has focussed on circulating systems in particular for the finer and less dense forms of solid fuel such as some types of biomass. The Ahlstrom 'Pyroflow' system, which is based on the circulating fluidised bed principle, was initially developed in Finland for burning biomass fuels such as peat, wood wastes and paper mill sludges as well as coals. It is shown schematically in Figure 1.5.

This circulating bed is characterised by high fluidising velocities of the order of 5 m/s with entrainment of the majority of the bed particles which are collected by cyclone and returned to the combustor. The primary combustion air is fed through the main fluidised air distributor at the bottom while secondary air is introduced further up the reactor. Fine grains of sand are used as the bed material.

Fuels, such as peat, bark, sawdust and pulverised domestic waste are screw fed into the combustor which operates between 700^{o} C and 1000^{o} C depending on the fuel

being burnt. Because the circulating material is in a highly turbulent state and mixes rapidly, bed temperatures remain very uniform. Boiler tubes are situated in the upper part of the combustor and downstream after the cyclone.

In particular, it has proved to be a good system for burning biomass fuels of low density and small size which can be difficult in the more conventional 'bubbling' type of fluidised bed combustor as well as low reactivity coals.

Circulating fluidised bed systems for burning coal are also available from Lurgi (West Germany), Battelle (Columbus, USA) and Studsvik (Sweden). Lurgi have developed their system based on fast fluidised bed technology for the calcination of aluminium hydroxide to alumina. The coal is crushed to about 300 μm size. A novel feature of the Studsvic development is the use of a 'Labyrinth' particle separator instead of a cyclone for the recirculation of the bed material.

The Battelle process is called Multisolid Fluidised Bed Combustion. Essentially it superimposes the circulating bed of fine particles on a fluidised bed of large particles as is shown in Figure 1.6. This enables coal to be fed with a top size of up to 35 mm. By decoupling the combustion and heat transfer operations, this system allows greater fuel flexibility and better load following characteristics than a bubbling fluidised bed combustor.

Further technical advantages of this type of combustion system concern environmental matters. In particular, because of the low combustion temperatures employed,

emissions of sulphur dioxide to the atmosphere may be controlled by retaining much of the sulphur in the fuel using a fluidised bed containing crushed limestone or dolomite. Also, because of the low combustion temperatures, the formation of nitrogen oxides from atmospheric nitrogen is virtually eliminated and the conversion of fuel nitrogen to nitrogen oxides can be minimised by using appropriate operating conditions. There is also evidence that emissions of many of the trace elements associated with fuels are less than those obtained using alternative combustion techniques.

For over 10 years there has been considerable commercial interest worldwide in developing fluidised bed combustion, particularly for burning coal for power generation, industrial steam raising and furnaces producing hot gases. Much attention is also being directed to the use of biomass and lower grade fuels because of the increasing costs of premium fuels. At the same time, there are increasing numbers of combustible waste materials which require utilisation or disposal for environmental reasons. Frequently, these wastes contain sufficient combustibles to make incineration an attractive proposition, particularly if useful energy can be recovered.

Both bubbling and circulating types of fluidised bed combustion display certain characteristics, each having particular merit for different fuel types and applications. For example, very finely divided solid fuels of low density will be more suitable for circulating fluidised bed

combustion whereas a bubbling fluidised bed would be preferred for coarser, denser fuels.

The selection of the most suitable combustion equipment for each fuel will depend on its properties, such as chemical analysis, volatile content, calorific value, particle size and ash characteristics, as well as the specific application.

The choice between the circulating fluidised bed combustor and the "bubbling" bed combustor ultimately rests on their relative capital and operating costs. Where emission standards are not too onerous, the simplicity of the 'Shallow Bubbling Bed' technology is favoured; for example, at the smaller industrial scale, up to about 50 MW. The more complex and expensive circulating fluidised bed systems are more appropriate for the largest industrial and small power generation boilers where tight emissions standards need to be met.

1.3 OBJECTIVES OF THIS STUDY

The objective of this work is to study a circulating fluidised bed with regard to its hydrodynamics.
This means performing experiments to measure axial pressure differences and solid circulation rates.
Both monocomponent and binary component systems are to be investigated.

An important part of the work is taken up with theoretical aspects of predicting the axial pressure profiles and the axial distribution of solids.

Other researchers have attempted to predict pressure profiles and voidages along the axis of the riser. This has normally been by a combination of theory and empiricism. The resulting relationships can rarely be applied for general design purposes with satisfactory results. In some cases, the modelling has resulted in implications which are contradicted by visual observations.

It is hoped that this work will give rise to a more general means of accurately predicting the performance of a circulating fluidised bed (CFB).

Having developed a hydrodynamic model of a CFB, it is the intention to use this model for predicting the conversion of a chemical reaction taking place in the riser.

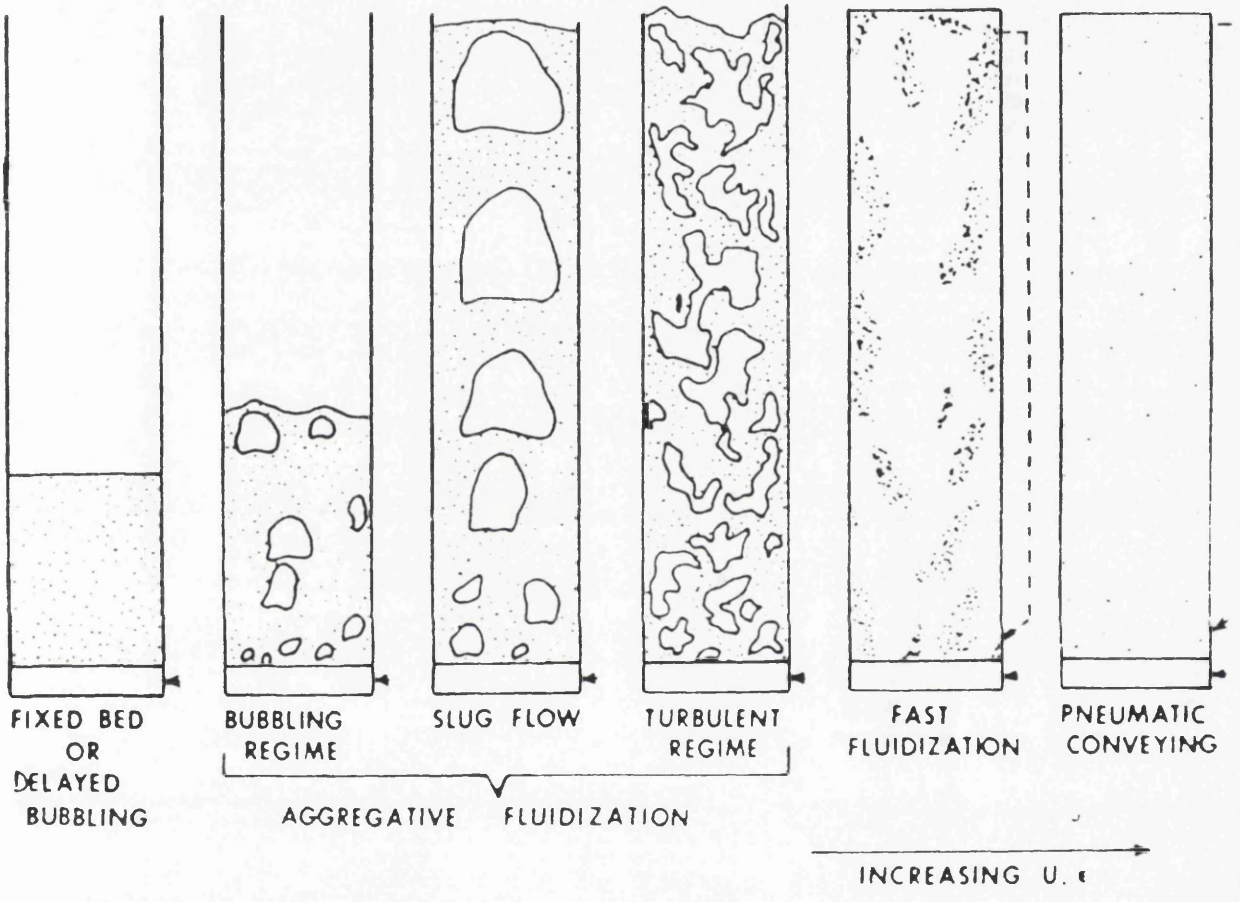

Figure 1.1 Principal flow regimes for upward flow of gas through solid particulate materials (Grace, 1986).

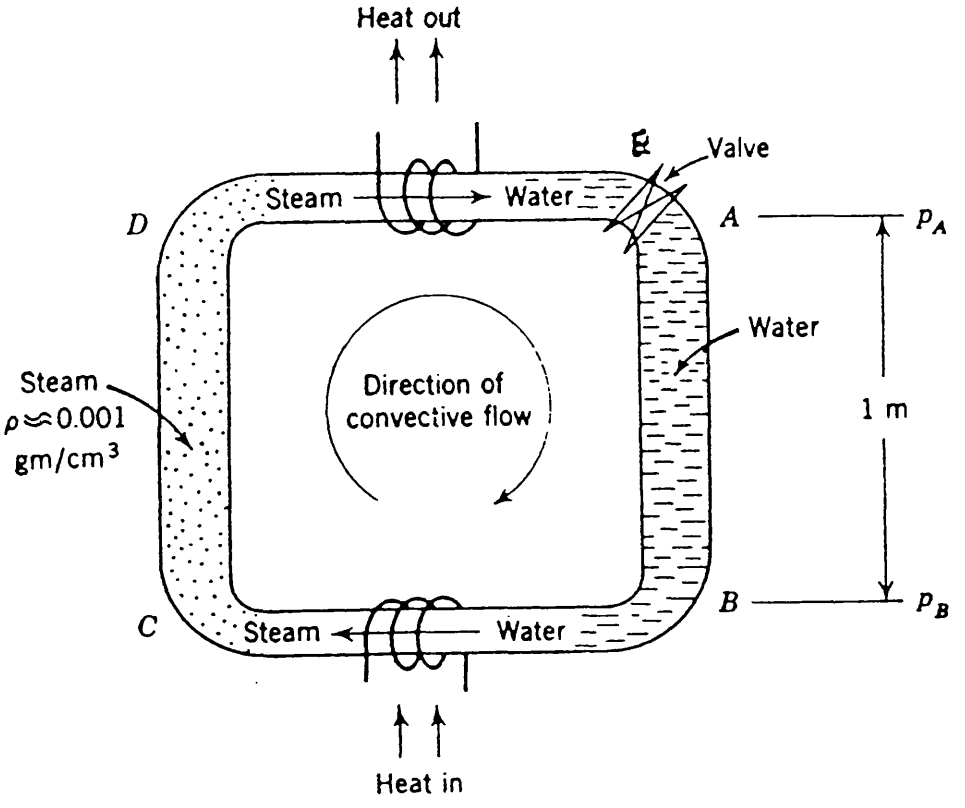

Figure 1.2 Sketch illustrating the principal of a circulating loop (Kunii & Levenspiel,1969).

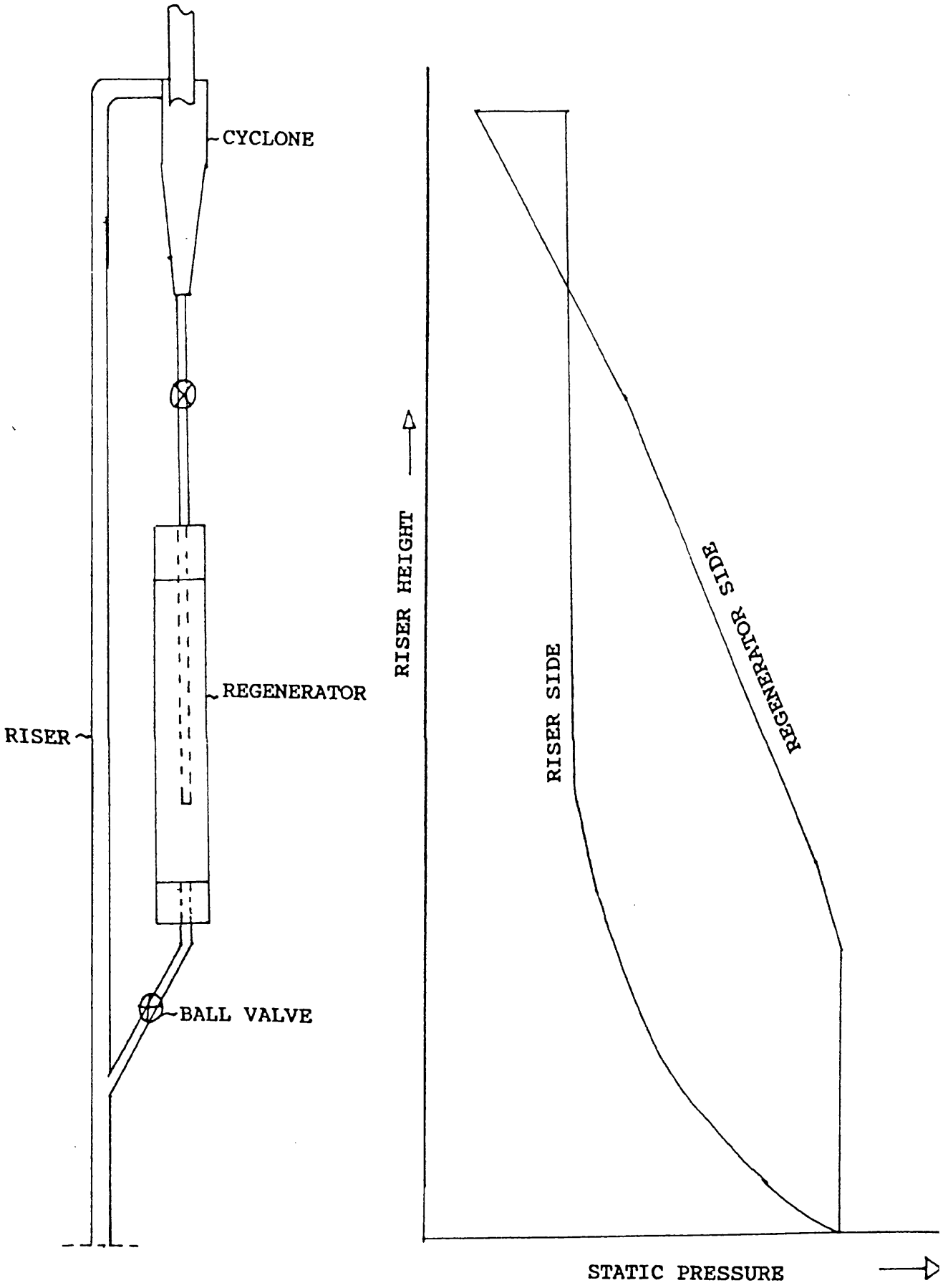

Figure 1.3 Pressure profile around a CFB.

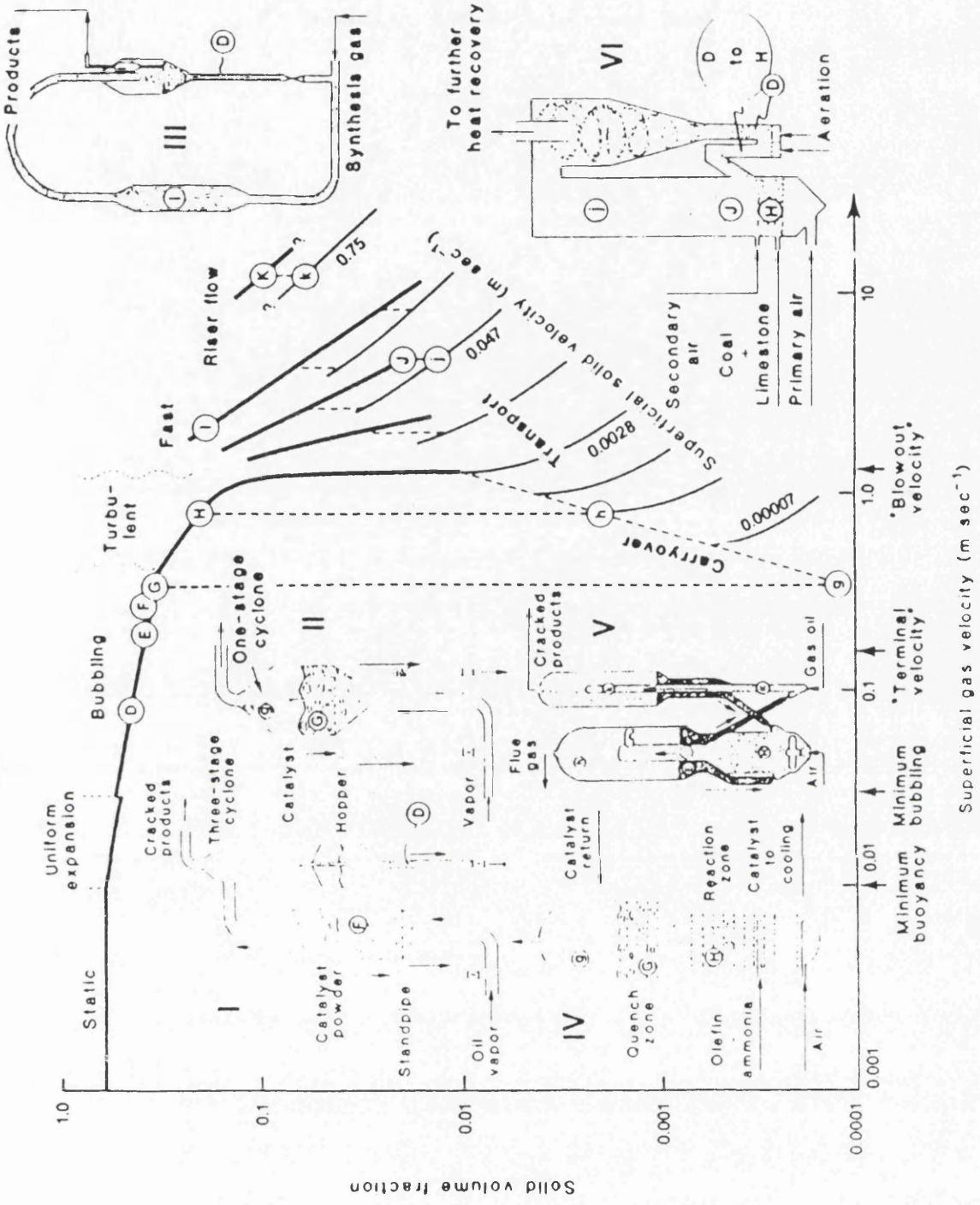

Figure 1.4 Regime diagram for fine powder (Squires et al., 1985).

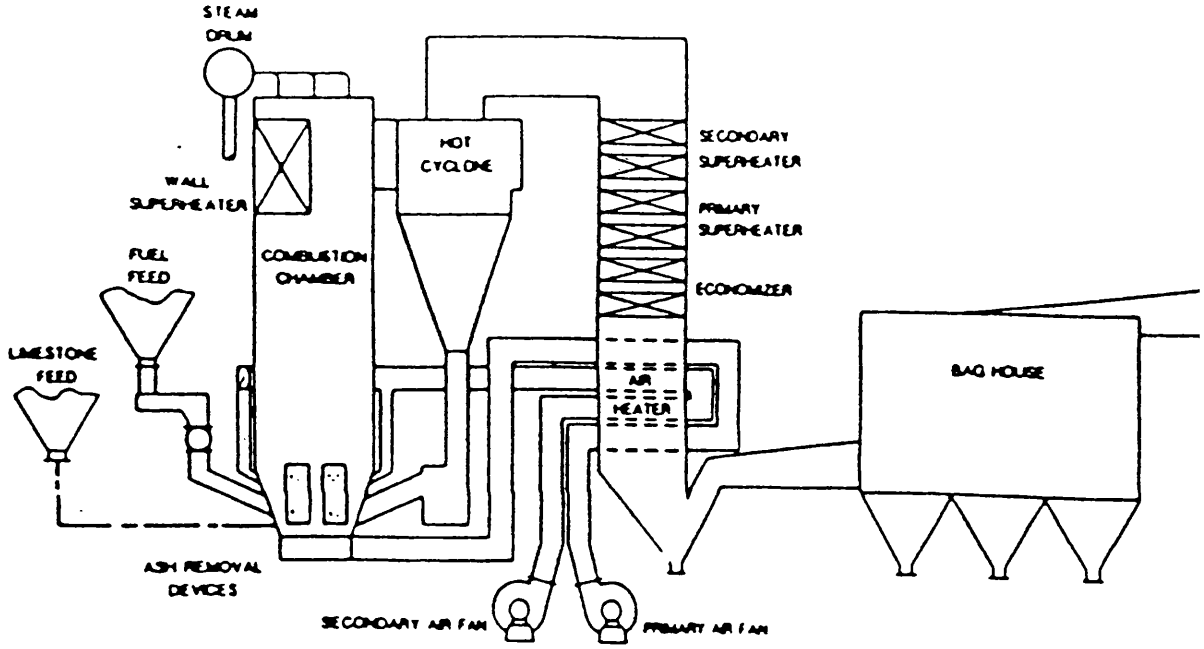

Figure 1.5 Circulating bed boiler system (Cooke, 1989).

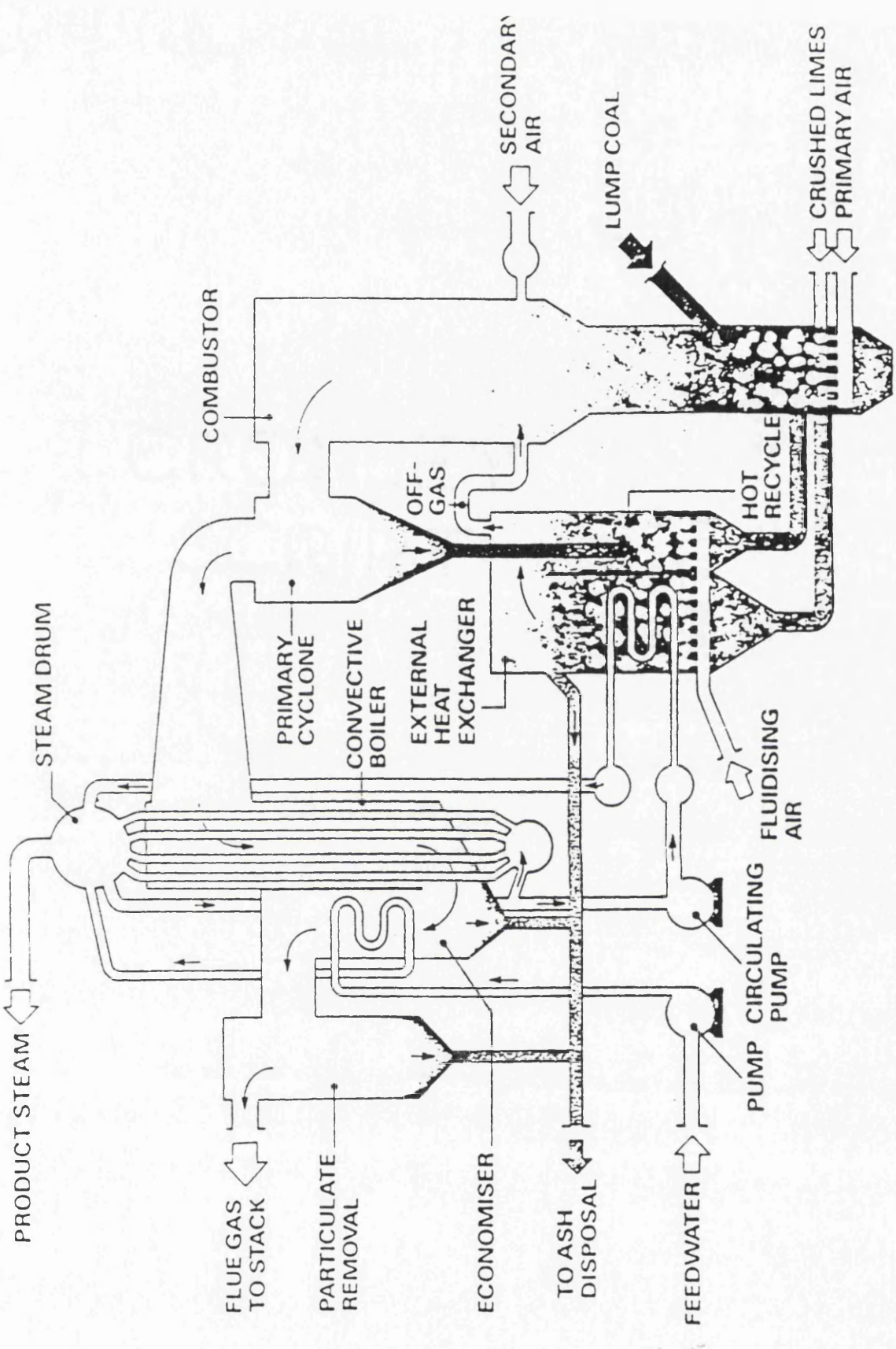

Figure 1.6 Battelle multisolid fluidised bed boiler (Cooke, 1989).

CHAPTER 2

LITERATURE SURVEY

The circulating fluidised bed (CFB) has been an important part of many idustrial processes for the last decade. The first known review of the CFB dates back to the Second World War. Squires (1985) devoted a paper in the First International Conference on CFBs which told the history of the development of the fluid catalytic cracking (FCC) process. According to this a consortium led by the Standard Oil Company of New Jersey and M.W.Kellogg Company used data obtained at the Massachusetts Institute of Technology (MIT) to design a fluid bed substitute for a 100 barrel per day pilot cracking reactor for the catalytic cracking of oil feed to gasoline.

However the first real attempt to study systematically the subject of circulating fluidised beds was carried out by Yerushalmi et al. (1976). This work, in common with much subsequent research, dealt only with the pressure gradient measurements over a range of solid circulation rates and gas velocities. A wide range of experimental conditions was examined by Yerushalmi et al. and the conclusions drawn from their studies are applicable for design purposes.

The first succesful attempt to produce general rules for predicting the voidage and hence the pressure gradient in the riser of a CFB came with the work of Li and Kwauk (1980) who conducted over a 1000 experiments using solids of different sizes and densities.

Although a great deal of empirical work has been

published, work of a theoretical nature has been limited, and in the last 10 years Yerushalmi's and Kwauk's work has remained as a basis with which subsequent research has been frequently compared.

For the purpose of this study, the literature survey is limited to work published on low concentration two-phase flows.

2.1 DEFINITIONS OF THE STATE OF TWO-PHASE FLOW IN CFBs

The riser of a circulating fluidised bed operates in gas velocity and bed density region between the extremes of bubbling fluidisation and vertical pneumatic transport. This regime has been subdivided into "turbulent fluidisation", "fast fluidisation" and "riser transport" Yerushalmi et al. (1976), but the criteria proposed to mark the boundaries of these regions are not yet fully developed. This can result in confusion and in order to avoid this these terms will not used in the discussion section. However the description of this subdivided regime as it is described in literature is considered below.

2.1.1 Definitions of the State of the Turbulent Regime

There are three main definitions of the turbulent regime which have been described in the literature.

(i) Increase in the gas velocity in the riser above that causing slugging, causes the fluidised bed to pass into a state in which continuous coalescence of slugs occurs leading to a channelling state with tongues of fluid darting in a zigzag fashion through the bed. This is the

state of turbulent fluidisation, as defined by Kehoe and Davidson (1971).

(ii) According to Yerushalmi et al. (1978) the turbulent regime is that which exists between two characteristic velocities Uc and Uk. These velocities are determined from variations in the amplitude of pressure fluctuations across a section of the fluidised bed. During observations the amplitude of pressure fluctuations first peaked and then fell to a relatively low level as the gas velocity was increased. The superficial velocity at the peak was called Uc and the velocity at which the amplitude levelled out was called Uk.

(iii) Rhodes (1986) defined the turbulent regime as that in which solids are transfered from the fluidised bed to freeboard by two competing processes: increase in bed height with increasing gas velocity due to bed expansion and decrease in bed height with increasing gas velocity as more solids are held in the freeboard.

2.1.2 Definitions of the Fast Bed Regime

There are three main definitions in the literature.

(i) Yerushalmi et al. (1976) defined as fast fluidisation a technique for bringing gas at high velocity into intimate contact with a finely divided solid in an entrained dense suspension characterised by extreme turbulence and extensive refluxing of dense packets and strands of particles. This technique was primarily orientated towards gas-solid reactor applications where it offered several important advantages over the conventional low-velocity

bubbling fluidised bed.

(ii) Fast fluidisation was defined by Rhodes (1986) as the transition at higher velocities where conditions in the riser of a CFB are relatively insensitive to changes in gas velocity or imposed solids flux. This results in a stable condition in which the proportions of dilute-phase and dense phase transport in the vertical column varied only gradually with changes in gas velocity or imposed solids flux.

(iii) According to Schnitzlein and Weinstein (1988), fast fluidisation is a two-phase flow with two distinct main regions, a dense region of solid at the bottom of the fluidisation column with similarities to bubbling and turbulent fluidised beds and a dilute region at the top. The solids are present in the dense region of the high velocity fluidised bed in at least three different forms; a) stagnant or down-flowing very near the wall at a void fraction close to minimum fluidisation conditions, b) travelling upwards in the form of dense packed solid aggregates with constant average velocity adjacent to the above region and c) dispersed dilutely in the upward flowing gas.

2.1.3 Definitions of the Dilute Phase Regime

Two definitions have been given in the literature.

(i) A dilute phase is said to be reached when all the particles are in motion and no particles remains at the bottom of the riser for more than a short time, while the gas is in the continuous phase.

(ii) The term circulating fluidisation is used in a general way to describe the gas-solid up-flow systems that exhibited carry-over of solid with an external recirculation leg.

2.2 UNIVERSITY WORK ON HYDRODYNAMICS OF CIRCULATING FLUIDISED BEDS

Although CFBs have been exploited commercially by a number of companies since the 1940's, university research was only started in the late 1970's. Yerushalmi and co-workers at City College New York, investigated the behaviour of a fine powder, (Group A according to Geldart's Classification), in fluidised beds operated at high gas velocity. They published a number of papers in which it was claimed that high velocity beds are favourable as gas-solid reactors compared to conventional fluidised beds. They referred to such a system as a "fast fluidised bed". Since then, a large number of researchers have investigated the phenomenon of fast fluidisation.

The studies of Yerushalmi et al. (1976-1979) focused on the definitions of different regimes of fluidisation as the gas velocity and solid circulation rate is increased.

Lanneau (1960) was the first to recognise the transition from bubbling to turbulent fluidisation by studying the fluidisation characteristics of a fine solid as the fluidising air velocity was increased to 1.7m/s. He used small capacitance probes and reported that the

heterogeneous character of the fluidised bed was changed to a condition of increasing homogeneity as the gas velocity increased beyond 1m/s.

Kehoe and Davidson (1971) also described the breakdown of the slugging regime at similar velocities into a state described as turbulent. Since then, the transition from bubbling to turbulent fluidisation has been the subject of investigation by Yerushalmi et al. (1976).

The first papers published by Yerushalmi et al. (1976,1977) focused on the three different regimes of fluoridation, bubbling, turbulent and fast.

As already mentioned the transition from the bubbling to the turbulent state, was characterized by two gas velocities, Uc the velocity at which the pressure fluctuations in the bed peak and Uk the gas velocity which marked the decay in the magnitude of pressure fluctuations in the bed. Visual observations have shown that the transition was also accompanied by the breakdown of large bubbles and slugs which continually coalesce and split. The solid in the bed was rearranged into clusters and streamers of particles whose motion was mostly downwards with smaller clusters and individual particles that were entrained upwards.

Yerushalmi et al. strongly supported the idea of the existence of clusters when a fine solid was used in a bed in the turbulent state. They claimed that the terminal

velocities of the clusters were greater than the gas velocity in the bed and individual particles are present due to the erosion of clusters.

It was stated, however, that no particle carry-over will be experienced provided that the freeboard is sufficiently high and hence there is no need for recirculation of the solid.

The studies of Yerushalmi et al. were carried out using high speed photography in three experimental set-ups: a rectangular two dimensional bed, a 75 mm diameter bed and a 152 mm diameter bed.

They presented their results in terms of pressure gradient across a range of sections of the riser, as a function of superficial gas velocity and solid circulation rate. They claimed that for a given gas velocity, the solid concentration in the riser increased with increasing solid circulation rate and they considered the possibility of achieving solid concentrations comparable to those in a bubbling bed. They also found that the pressure gradients were normally higher in the bottom section of the riser and lower towards the top.

They claimed high slip velocities in the fast bed and they proposed as in the above mentioned case of turbulent flow that the presence in the bed of dense packets of particles which had an effective free-fall velocity considerably in excess of that of a single particle. Because of its size the packet of particles would not be sustained by the upward flowing gas but would fall back into the bed and

disintegrate.

According to Yerushalmi et al. (1976), the fast bed condition was marked by high solid concentrations, clustering of individual particles which break apart and reform, extensive backmixing of solid and slip velocities much higher than the terminal velocity of an individual particle.

The slip velocity was defined as: $U_{sl} = U_g/\varepsilon - U_p$

The fast bed condition was stabilized only if the solid emerging from the top part of the reactor was recirculated by means of cyclones and a standpipe.

At velocities in excess of the transport velocity, Utr, the solid was fully entrained and its concentration within the column depended not only on the gas velocity but also on the solid circulation rate (Figure 2.1). When the solid circulating rate was low the dilute phase flow regime existed in which particles moved upwards in relatively straight paths and the slip velocities were of the same order as the terminal velocities of the individual particles. If the solid rate was increased further, the suspension became denser and at sufficiently high rates the fast bed state was established.

The structure of the fast bed was also explained in terms of clusters of particles (Yerushalmi et al.,1978) with high slip velocities. The equivalent diameter of a spherical cluster was calculated by neglecting the

acceleration and friction effects and assuming that:

a) all the particles were in densely packed clusters,

b) clusters were discreetly distributed in the bed and

c) clusters had a voidage equal to that at minimum fluidisation.

Based on these assumptions, the pressure drop per unit length was described by the following equations:

Pressure drop due to gravity in the vertical pipe:

$$dP/dL = (1-\varepsilon)\ (1-\varepsilon_{mf})\ \rho_s\ g \qquad (2.1)$$

where: ε is the effective voidage

ρ_s is the solid density

Pressure drop due to the drag exerted by the gas on the cluster:

$$dP/dL = 1/8\ N/A\ \rho_g\ (U_g/\varepsilon - U_p)^2\ c_{dp}\ f(\varepsilon)\ D_c^2 \qquad (2.2)$$

where: N is the number of clusters in the length dL

A is the cross-sectional area of riser

ρ_g is the gas density

U_p is the mean velocity of clusters

c_{dp} is a drag coefficient related to that of a single particle, c_{ds} by the expression:

$$c_{dp} = c_{ds}\ (\rho_g\ D_c\ (U_g/\varepsilon - U_p)\ /\ \mu) \qquad (2.3)$$

where: μ is the gas viscosity

The function $f(\varepsilon)$ accounted for the hindered settling

caused by the closeness of the aggregates. This function was related to the Richardson-Zaki (1954) index n by:

$$f(\varepsilon) = \varepsilon^{-2n} \qquad (2.4)$$

The value of n ranges from 4.65 to 2.4 for terminal Reynolds number, Re_t, $0.2<Re_t<500$.

Hence, $$D_c = 3/4\ \rho_s (Ug/\varepsilon - Up)^2\ c_{dp} \varepsilon^{-2n} / \rho_s\ g\ (1-\varepsilon_{mf}) \qquad (2.5)$$

The pressure drops obtained from these equations agreed well with the experimental data. The cluster voidage was an adjustable parameter which was used to allow the model to fit the data. The cluster diameter D_c was calculated and plotted as a function of the solids concentration, $(1-\varepsilon)$, for the 0.15m diameter pipe. Cluster diameters in the range 2 to 35 mm were calculated with this equation for the solids FCC and Dicalite 4200, though no visual observation suggesting the existence of such large cluster diameters was reported. The disadvantage of this model is that it required the use of many unmeasured parameters such as N, ε, D_c and U_{sl}.

Li and Kwauk (1980), emphasized the significance of the solid distribution in the axial direction of the riser and they presented experimental data obtained using a CFB, in the form of axial average voidage distribution.The values of average voidage were obtained by a detailed analysis of

the pressure gradient, entrance and acceleration effects being neglected. The experimental vertical average voidage profiles were of S-shaped form (Figure 2.2).

The characteristic voidage profile of the fast bed consisted of a dense phase at the bottom of the bed, a dilute phase at the top and an inflection point in the middle, that was the transition from a low voidage at the bottom to a high voidage at the top of the bed. Based on the experimental evidence of the voidage profile, Li propose a hydrodynamic model, based on the concept of clusters for powders belonging to Group A of Geldart's classification (Geldart 1973).

According to the model, the clusters at any height of the bed moved upwards through a diffusive mechanism from a relatively dense region in the lower section, and then, when they arrived at a higher region along the bed where the average density was lower, they tended to fall back to the lower region because of buoyancy. Under steady-state conditions dynamic equilibrium existed and the fluxes due to diffusion and buoyancy were equal. Figure 2.3 shows the physical picture of the model. The equation was of the form:

$$\ln(\varepsilon-\varepsilon_a/\varepsilon^*-\varepsilon_a) = -1/z_o\ (z-z_i) \qquad (2.6)$$

where: ε^* is the voidage for the dilute phase section

ε_a is the voidage for the dense phase section

z_i is the position of the inflection point in the

voidage curve

z_o is the characteristic length defining the ease of mixing and segregation for the clusters

The solution of the above equation required the determination of the four unknown parameters.

Li et al. (1982) correlated the above four parameters from experimental data. The following correlations were found to fit the data well:

$$\varepsilon_a = 0.756\ (18Re_s + 2.7Re_s^{1.687} / Ar)^{0.0741} \qquad (2.7)$$

$$\varepsilon^* = 0.924\ (18Re_s + 27\ Re_s^{1.687} / Ar)^{0.0286} \qquad (2.8)$$

where:
$$Re_s = \rho_g\ d_p\ (U - V\ \varepsilon/\ (1-\varepsilon))/m \qquad (2.9)$$

$$V = G_s/\rho_s \qquad (2.10)$$

$$Ar = d_p^3\ \rho_g\ g\ (\rho_s-\rho_g)\ /\ \mu^2 \qquad (2.11)$$

The position of the inflection point, z_i, was found to depend on the average particle residence time in the dense region, which was correlated from the experimental data by the expression:

$$t_o = 175.4\ ((\rho_g/\rho_s-\rho_g)\ (U-V_p)^2/d_p\ g)^{-1.922} \qquad (2.12)$$

and since $z_i = L - t_o\ V_p$

then, the inflection position

$$z_i = L-175.4\ ((\rho_g/(\rho_s-\rho_g)d_p\ g)^{1.922}\ V_p\ (U-V_p)^{-9.844} \quad (2.13)$$

where: L is the total length of the riser

The characteristic length, z_o, was given by the empirical correlation:

$$z_o = 500\ \exp\ (-69(\varepsilon^*-\varepsilon_a)) \quad (2.14)$$

Kwauk et al. (1985) presented modified correlations for the four unknown parameters and a full picture of the modeling of the fast fluidisation circuit.

The pressure drop in the downcomer, dP_d, was balanced by the pressure drops through the solid valve, dP_v, the fast bed, dP_f, and the overhead cyclone, dP_c.

Hence, $$dP_d = dP_v + dP_f + dP_c \quad (2.15)$$

This equation is written in terms of voidage and riser height and it was claimed that the major portion of the solids existed in the fast bed and downcomer. Hence, they presented an equation for determine the average bed voidage in the fast bed, for fixed rates of solid circulation.

$$\varepsilon = 1 - ((I/A) - (a/A)C) / (1+a/A)Z \quad (2.16)$$

where: I is the total inventory of solids

A is the c/s area of the fast bed

a is the c/s area of the downcomer

$C = (dP_v + dP_c)/\rho_s$

Z is the height of the fast bed

This mathematical model represented the best quantitative description of the fast fluidised bed, if the system was defined as consisting of two main regions, a dense region at the bottom of the bed and a dilute region on the top.

Cankurt and Yerushalmi (1978) investigated gas mixing in a CFB, using a tracer technique. They claimed that the radial concentration profile was uniform if a group A powder was used. For a riser diameter less than 0.1m however wall effects enhanced the gas velocity profile causing radial segregation. From those observations they concluded that the gas flow in the fast regime was of plug flow type.

Avidan (1980) using the same equipment, and a radioactive tracer technique, investigated solid mixing in the CFB. He found that the axial dispersion coefficients were higher near the top of a turbulent bed compared with a fast bed at the same gas velocity. He also claimed that the axial dispersion coefficient showed a minimum at a specific gas velocity of 3.5m/s and this value was constant in the CFB. Avidan also reported that the Peclet number increases

considerably when the gas velocity rises above 4m/s but below this value it remains constant. Since the Peclet number ($Pe_s = G_s L / \rho_s D_s$) gives the relative importance of solids movement by the mechanisms of convection and dispersion, Avidan proposed that below this critical gas velocity, the two mechanisms were of equal magnitude and due to this fact, the claims of good gas-solid contact and high heat transfer coefficients for the fast bed were basically true. However, he did not report anything on the radial distribution of solids.

Weinstein et al. (1983) found that the position of the inflection point was also dependent on the 'imposed' pressure drop set by the recirculation leg of the circulation system. In their experiments, an unrestricted standpipe was used for solid recirculation and it was stated that the solid inventory above the standpipe leg affected the position of the inflection point. Moreover the pressure profile in the bottom and the top of the riser seemed to be unchanged.

The radial voidage distribution in CFBs was first investigated by Weinstein et al. (1984). They made measurements with an X-ray source and a plate film with time exposures of about 5 s. To obtain density variations from the plate film an absorption technique was used. They plotted the experimental data as local value of voidage versus the radial position. For a set of flow parameters,

they claimed that the radial profiles showed a dilute core of high voidage in the range 0.9-0.99 surrounded by a dense annular region of voidage 0.6 to 0.85, along the axis of the riser. Under identical flow conditions, they also measured the variation of voidage along the riser height. From these observations they claimed that a dense phase occupied half the riser height and a transition to a dilute phase occurred near the top of the bed. Although the above mentioned radial profiles have been measured in positions, of what they claimed to be the dense lower part of the bed and within the transition region from dense to dilute phase, the radial profiles exhibited the same shape and variation ie high voidage of around 0.9 in the center of the riser and low voidage of around 0.7 in the annulus (Figure 2.4).

In a different paper, Weinstein et al. (1985), claimed the importance of the inflection point in the axial voidage profile and the behavior of this inflection point under different flow conditions. Hence, their approach towards describing the CFB system, was that according to their design of equipment, the riser two-phase flow consisted of: a) a dense region in the bottom part of the bed which occupied half of the riser height, with a radial profile of very high voidage in the center of the riser and a low voidage in the annulus, b) a dilute phase in the top part of the riser, where the radial voidage was not examined and c) an inflection point which showed the transition from the

dense phase towards the dilute phase and the position of which was examined under different conditions of solid flowrate, gas velocity and inventory. The radial voidage profile within the region of the inflection point for one set of flow conditions showed a high voidage in the center of the bed and a low voidage in the annulus of the bed. Hence the conclusion from the two papers was that there was strong radial variation and strong axial variation along the so called 'fast bed'.

In another paper, Weinstein et al. (1984) investigated the effect of particle density on the axial hold-up of solids in the fast bed. They used two powders with the same value of mean particle diameter, but whose densities differed by 35%. From their experimental data, they found two main differences: a) that the maximum solid rate was higher for the denser powder and b) that the variation of the solid fraction along the bed was smaller for the lighter solid. They offered an explanation based on the interchange of kinetic and potential energies between the gas and solid and the dissipation of the rest of the energy in the form of frictional losses. They concluded that the average solid loading in the fast bed was almost independent of solid particle density under identical operation conditions, however, they emphasized the magnitude of the variation which they said was greater for the denser solid.

It should be noted that Weinstein et al. (1984) used a

riser as part of the CFB system with no gas distributor at the lowest part of the bed, although, the U-tube connected to the riser from one side and to the slow bed from the other side, was aerated by means of nozzles.

Later Hartge et al. (1985) investigated the local hydrodynamics of two fast fluidised beds. They used a γ-ray absorption technique to measure the average solids hold-up and the data compared well with the measurements derived from pressure drop data for both fluidised beds. They then measured horizontal voidage profiles with a fibre optic probe. Since they accepted that the fast bed consisted of two distinct regions, a lower dense region and an upper dilute region, measurements of radial voidage profiles in both regions showed that in the dilute region, the profile was relatively flat with a wall zone of increased solids concentration and hence lower voidage. In the dense region of the bed, the voidage in the wall zone was as low as 0.7, while in the middle of the column the voidage was significantly higher. They therefore inferred that the segregation of gas-solid flow was present. This means that a dilute core region where the solids were transported upwards was surrounded by a denser annular region with downflow of the solids. These radial voidage profiles are comparable to the ones presented by Weinstein (1984).

Monceaux et al. (1985) reported axial pressure profiles in a CFB using Group A powders. According to these

authors, the axial pressure profile was divided into three sections , the acceleration section at the bottom of the riser, a section of constant pressure gradient ie the fully-developed flow, and a disengagement section, which only appeared at high loading ratios. In the fully-developed flow region, the pressure loss was due mainly to the solid hold-up. In this region, the radial solid flux profiles showed a downflow of solids near the wall in balance with the solid flux in the center of the riser.

All the above work supports the much earlier observations of Gajdos and Bierl (1978).

Rhodes and Geldart (1985) studied experimentally the hydrodynamics of a CFB. They presented plots of pressure gradient at different solid rates and over a range of gas velocities between 2.5 to 5m/s for a Group A powder. In order to explain the shape of the plots, they used the variation of entrainment flux E with distance h above the dense phase of the riser. The empirical equation for the rate of entrainment due to Wen an Chen (1982) was chosen to describe the flow of particles:

$$E = E^{*} + (Eo - E^{*})\, e^{-ah} \qquad (2.17)$$

The value of E^{*}, the entrainment rate above TDH was calculated from Geldart's (1979) correlation:

$$E^{*} / \rho_g U = 23.7 \exp(-5.4\, V_t/U) \qquad (2.18)$$

Values of E_o, the entrainment rate at the bed surface, were calculated from the correlation of Wen and Chen (1983)

$$E_o / Adb = 3.04E\text{-}9\ \rho_g^{3.5}\ g^{0.5} / \mu^{2.5}\ (U-U_{mf})^{2.5} \qquad (2.19)$$

The value of the coefficient in the exponent of equation (2.17) was taken to be 4 as recommended by Wen and Chen (1982). Hence they obtained the variation of entrainment flux with distance above the bed surface at high and low gas velocities. From their plots of axial solids concentration profiles they suggested that these profiles were the result of the changes in the bed level with solid circulation rate and gas velocity. The profiles of pressure gradient represented the rise in the level height with increase in solid circulation rate. Hence the variation of entrainment rate with distance was used to explain the characteristics of fast fluidisation.

Horio et al. (1985) investigated the hydrodynamics in a CFB. Optical fibre techniques were used for the measurement of particle velocity distributions, particle concentration and cluster structures. The cross correlation method was applied to determine the particle velocity in the riser. Their results showed that in the dilute phase flow, the average particle velocity was of the order of 2.8m/s when the gas velocity was 4m/s. They suggested that

clusters were surrounded by the dilute phase where fine particles were moving faster than the particles in the clusters. However, they were not capable of distinguishing dense phase particles from dilute phase particles, so they did not present any variation of particle velocity and hence any quantitative description of the fast fluidisation condition.

Later Rhodes et al. (1987) proposed an empirical model to predict the axial distribution of solids along the riser height. They applied the Wen and Chen (1982) correlation of the form:

$$G=E^{*}+(E_{o}-E^{*})\exp(-ah^{*}) \qquad (2.20)$$

This describes the variation of the entrainment flux with the distance above the surface of a bubbling fluidised bed which occupies a considerable distance within the riser of the CFB system. The above correlation was combined with a system pressure balance to predict the variation of voidage within the riser. Although the model was based on empirical correlations and it enables the axial solid distribution to be predicted, it might not be completely applicable to the riser conditions because it compares the fast fluidised bed with the freeboard of a bubbling bed and it underestimates the voidage in the dilute phase.

More recently, Schnitzlein et al. (1988), studied flow characteristics of fast fluidusation, by a method of instantaneous pressure signals in a fast bed.

They claimed that the mean voidage within both regions was constant and independent of height. The voidage in the dilute region was found to be independent of gas velocity and solid rate and they reported the presence of a wave within the dense region of constant speed of 1.6m/s. Because of this wave, they considered that the solid within the dense region was present in the form of a stagnant region near to the wall (down-flowing), as an upward movement of aggregates and as a dispersed solid of an upward flowing gas.

Bolton and Davidson (1988), studied the flowrates of particles down the wall of a high velocity fluidised bed using a sampling technique. By taking as a basis the model proposed by Rhodes et al. (1987) and from experimental evidence, they claimed that the flowrate of particles in the wall region decreased exponentially with increasing height above the gas distributor. They proposed a correlation similar to that of Wen and Chen (1982) of the form:

$$W = W_o + dW\ e^{-kz} \qquad (2.21)$$

where W_o and dW were constants. The exponential decay coefficient k accounted for the turbulent diffusion of particles in the freeboard since they reported that the solid layer in the wall region was due to deposition of particles from the dilute core to the wall because of the concentration difference between the two regions. Hence the diffusion mechanism was controlling the process of

backmixing of particles in a region where there was concentration equilibrium. According to this approach, they suggested a value of k in the range $3.5m^{-1}$ to $6.4m^{-1}$ which is contrary to the low value of $0.5m^{-1}$ presented by Rhodes (1986).

They explained the flow of the solids down the wall as being due to the geometry of the gas-solid separation system due to the increased particle concentration in the core with the increase of solid rate.

They proposed the use of an impingement device at the riser outlet in order to increase the mean solid concentration in the riser. Fortunately enough, they increased the solid concentration by increasing the depth of the bubbling bed and the backmixing of solids in the wall region was also further increased. However, they suggested that the most efficient operation of the riser of a CFB could be achieved if the depth of the bubbling bed at the bottom of the riser was reduced to zero.

Finally, they defined a fast fluidised riser as one consisting of two parts a) the lower part of the riser occupied by a violently bubbling or a slugging fluidised bed and 2) the upper part containing a core moving upwards in which the particles are entrained by the gas and a region adjacent to the wall in which a thin dense film of particles falls under gravity.

Horio et al. (1988) studied pressure distribution and solid circulation rates in a CFB with no riser distributor.

The pressure was measured by using semi-conductor sensors. They also measured cluster velocities by using a fibre optic probe technique. The conditions under investigation were: Ug in the range of 1.17 to 1.29m/s and Gs in the range of 11.7 to 11.25 kg/m^2s. Under such low superficial gas velocities in the riser section, they presented plots of the variation of the riser mean axial voidage with height and radial profiles of the variation of solid velocity. At the center of the riser the solid velocity for the above experimental conditions reached a maximum value in the range of 2.2 to 2.8m/s, while near the wall region the solid velocity was below 2m/s. From their measurements of radial velocity distributions, they claimed the formation of annular flow in the riser, where the thickness of annulus was not changed along the riser height and also that rates of internal and external circulation of solids were equal. They reported that for the values of Ug between 1.17 to 1.29m/s, the cluster diameter in the dilute core was small (5mm) and constant under the operating conditions, whereas in the annulus the size of clusters was greater than 10mm and it became larger as the solid moved downwards in the annulus. They concluded that a) the downflow circulation rate was higher than the external rate b) by using the cluster model (Yerushalmi et al., 1978) and by changing the value of cluster voidage they claimed that the cluster size was constant in the core irrespective of height, while it was large (10mm) in the downward flow, when a cluster voidage of 0.2 to 0.3 was used.

Brereton and Stromberg (1985) studied two aspects of the fluid mechanics in CFB, macroscopic density profiles in small and large units, and micro-structure of the flow. With regard to the first aspect, the CFB was described empirically by the following equations:

$$P = a\ h^{b} \qquad (2.22)$$

where: P is the static pressure

h is the riser height

a,b are constants depending on the gas velocity, solid circulation rate and solid and riser properties. When this equation was differentiated, it yielded the bulk density distribution:

$$g\ \rho_{b} = dP/dh = -\ (ab)\ h^{b-1} \qquad (2.23)$$

The plots of equations (2.22) and (2.23) on log/log paper gave straight lines for constant gas velocity and variable solid circulation rate. They stated clearly from equation 2.2.7 that the product 'ab' was independent of gas velocity and was a strong function of solid rate, while the slope 'b-1' was constant for the specific geometry of CFB. Although the above equations were applicable to CFB with no dense phase above the distributor, they suggested that if a dense saturated zone was formed in the CFB with secondary air then the Li and Kwauk (1982) equation could be used with good agreement between the experimental data and the

predicted line. As a result of this they showed that the secondary air did not influence the basic properties of the system. What is of interest to mention is the influence of geometry with respect to the separator and the recycle leg. The above researchers claimed without showing any graphs that by using six different separator designs they obtained different pressure drops for a given circulation rate. From their visual observations they reported that the different pressure drops were due to the clusters of particles reflecting off the top of the riser, colliding with other clusters and initiating a chain of downflow.

With respect to the second aspect of their studies, the microscopic structure of a CFB was examined by studying the solids distribution at Ug of 2.5m/s. They reported that at low circulation rates, there was no evidence for the two phase structure of the flow and that the solid was in the pneumatic transport regime; they calculated that the slip velocity (Ug/ε - Up) was twice the terminal velocity of a single particle. As the circulation rate was increased the high resolution trace of the capacitance signal showed a well defined two phase structure to be formed, where a refluxing of solids existed along the riser wall and small clusters of particles were present in the center of the column. Further studies of the radial distribution of solids in the riser using the same technique, proved that the cluster or dense phase concentration had its highest downflow value in the wall region. The explanation of the experimental evidence was due to transportation of clusters

and individual particles from the dilute core of the riser to the wall by the mechanism of turbulent diffusion, and at a critical point, the gas velocity was equal to the effective terminal velocity of the average cluster. At this point either the clusters were suspended and re-entrained into the core flow or fell along the wall as wave like sheets.

By offering this interpretation of the experimental evidence, they did not argue about the stability of the average cluster diameter because of a time averaged motion, but they suggested that the dense phase rose in an inner core and descended in an outer boundary layer.

This picture from the capacitance probe evidence, was also observed by Weinstein et al. (1984) and Bierl et al. (1980).

During the second conference on circulating fluidised bed technology (1988), the approach of most researchers was primarily to use more accurate techniques for the hydrodynamic measurements of a CFB and hence to obtain a clearer picture of the local structure of the riser. Secondly they used basic equations or well established models to explain theoretically or describe empirically the structure of two-phase flow in the riser.

Arena et al. (1988) studied and compared the hydrodynamic behavior of CFBs. Experimental techniques such as measurement of pressure gradients and slide valves

along the riser were used to determine voidage. They took as a basis, the elutriation theory as introduced by Horio et al. (1980) and Pemberton et al. (1983) and assumed that the solid was entrained upwards due to the high gas velocity and that part of it was transferred to the wall region by turbulent diffusion. Furthermore by neglecting the descending solid with respect to that in the ascending zone, they reported that the voidage above the inflection point is determined by the equation:

$$(d\varepsilon/dz)_i = C\rho_s g(1-\varepsilon)_i^2/G_s D(g/D)^{0.5} - C\rho_s(1-\varepsilon)_i^2(g/D)^{0.5}/G_s \qquad (2.24)$$

where: C is a constant

G_s is the solid mass flux

D is the riser diameter

ε is the voidage in the dilute phase

Of course, this was an empirical equation because it contains the term $(1-\varepsilon)_i$ which has to be evaluated from the model of Li and Kwauk (1980) and even so the equation was applicable only to the dilute part of the riser. The fact is that it takes into account the particle density and the riser diameter.

Rhodes et al. (1988) reported measurements of radial and axial solid fluxes in a riser using a sampling probe technique. Their results showed that there was an upward and a downward local solid flux, which decreased with

increasing height in the riser. This type of solid movement was explained as being due to the transfer of solids from the dilute core of the riser to the region of low gas velocity near the wall. When the particles reached the wall region they fall down the column height producing the downward flux. They also stated that this downward flux of solid would strongly influence the gas velocity profile causing a higher gas velocity in the core. Then they argued that although there was a continuous transfer of solid from the core to the wall, at the interface between these regions there would be an exchange of particles in both directions and that since the flux decreases with height, one might expect the upward flux in the core to be exponential in form. Their results did not indicate this trend. This might be an approach to the problem. However it should be noted that neither the velocities of solid and gas nor the voidage were measured. The local structure and in particular the motion of particles is unknown. The existence of the downward flux is however not accounted for. The transfer mechanism of solid from the core to the wall has been held responsible for the downward flux and the shape of the radial gas velocity profile which has been modified from the flat turbulent gas profile to that parabolic profile of laminar flow because of the great effect of solids in the wall region. If this is true it should be expected that the downward solid flux is equal to or greater than the upward flux. However, experimental measurements have shown that at three different axial riser

positions, the upward flux was at least twice the magnitude of the downward flux (Rhodes et al. 1988).

Kefa et al. (1988), proposed a two-dimensional gas-particle flow model to explain the performance of the CFB. The model takes into account the fluctuation of particle movement which is treated as a random Fourier series based on a gas-flow fluctuation spectrum. It ignores the influence of solid flow on the gas motion and is based on the turbulent diffusion of particles due to the fluid motion. The model predicts velocity particle trajectory for a range of particle sizes and particle concentration distribution in the axial direction. However, the researchers reported only one set of experimental conditions, that is at U_g=9m/s, to prove the agreement between theory and experimental data. The question arises whether this gas velocity is representative of the so called "fast" bed or dilute phase transport. The circulation rate is also unknown. Hence, the approach of mathematical modeling may be good but the physical picture of the CFB is not well described experimentally and in this case the CFB was operated in the vertical pneumatic type of mode.

Son et al. (1988), studied the hydrodynamics of a CFB. It is interesting to note that these researchers measured the solid circulation rate in the CFB, then used the model of Do et al. (1972) which was applicable to the bubbling fluidised bed and its freeboard, in order to determine the

variation of particle carry-over flux with gas velocity. They claimed that good agreement existed between their experimental data and the model prediction and they recommended the use of the model for determining the solid circulation rate.

Adams (1988) studied gas mixing in a CFB. A tracer gas technique was employed for determining gas phase diffusion coefficients, based on the mechanism of eddy diffusion. From the experimental evidence, it was reported that the presence of particles greatly reduced the gas diffusion coefficient, hence he confirmed the poor gas mixing in the riser reported by Cankurt and Yerushalmi (1978) and Yang et al. (1983). Then Adams investigated the effect of the riser gas velocity and solid circulation rate on gas diffusivity. Based on the above, it was reported that the diffusion coefficient was proportional to the gas velocity as in the case of single-phase flow but that it was inversely proportional to the solid circulation rate and bed density. This was explained as being due to the fact that the presence of particles suppressed the turbulent intensity of two-phase flow according to the size and density of the particles. As a result of the above findings, one would expect in a two-phase system to record either an increase or a decrease in diffusion coefficient with solids concentration depending on the particle properties.

During the Second International Conference on CFBs (1988), Burkell et al. (1988) presented a critique of five

different techniques for determining solid circulation rates in a CFB. The five methods were:
(i) closing a permeable valve in the return leg,
(ii) timing the descent of particles in the vertical standpipe of the return system stem,
(iii) recording the force imparted by returning solids as they cascade downward from the primary cyclone ,
(iv) measuring the pressure drop across a constriction in the return loop and
(v) estimating the solids flow from a heat balance on a calorimetric section in the vertical standpipe.

They investigated the above five methods by using a CFB.

Method (i) was the favored method, used previously by Yerushalmi et al. (1976), Hartge et al. (1986) and Arena et al.(1986). Burkell et al. stated that this method was acceptable for the cold model unit as long as the duration of a measurement was less than 30s. During this time interval, there was no discernible influence on the pressures in the riser.
The method (ii) involved measuring the time for identifiable particles to descend through a known distance in a section of a standpipe. This method was suggested to work well in both cold and hot circulating bed units.
The method (iii) included an impact flow-meter which was designed to measure the force of recirculating solids falling into a 'pan'. The impact flow-meter was located far enough below the primary cyclone so that falling particles

approached their terminal velocities before striking the pan. Forces transmitted through the lever and pivot were measured by a sensitive load beam. The signals obtained were seen to exhibit pulses. This was a sensitive method over a limited range of circulation rates.

The method (iv) involved the measurement of pressure drop across a constriction type flow-meter and was successfully demonstrated by Carlson et al. (1948) and Farbar (1953). Reh (1984) suggested that this technique could be adapted to measuring solid circulation rates in CFB units. The modified orifice meter did not appear to be successful under circulating bed conditions employing counter-current gas-solid motion in the return leg.

Finally method (v) used a jacketed heat transfer section in the vertical return standpipe of the high temperature CFB unit. In practice, this method was subject to uncertainty because of radial temperature gradients in the descending solids.

Takeuchi et al. (1986) examined the fluidisation state in a CFB based on data of the static pressure distribution. They presented their results in terms of pressure drop distributions along the riser height for different solid circulation rates. They concluded that when the solid circulation rate was controlled independently of the gas velocity, the state of fast fluidisation was characterized by two critical gas velocities U_{ff} and U_{dt}. U_{ff} was the minimum gas velocity to keep the solid circulation rate at

a steady level and U_{dt} was the velocity below which a gap appeared in the pressure drop distribution along the height when the velocity was reduced from that for dilute transport.

Yang (1988) developed a mathematical model which described the dynamics around the CFB loop. The dilute phase region of the fast bed, including the acceleration zone, was correlated with pneumatic transport equations developed previously (Yang, 1977). A dense phase pneumatic transport model with annular region was employed to characterize the dense phase region of the fast bed. The height of the dense phase was then obtained by pressure balance around the complete circulating fluidised bed loop. It was claimed that the model provided a good description of literature data reported by Kwauk et al. (1985), Weinstein et al. (1983) and Hartge et al. (1985).

Breault and Mathur (1989) investigated a CFB loop from the pressure data measurements for the development of a mathematical model to predict the pressure profile in CFBs. The CFB loop consisted of several gas-solid flow regimes such as aerated gas-solids downflow, aerated solids downflow and gas up-flow, horizontal pneumatic transport, vertical pneumatic transport and standpipe flow. Research workers have modeled the pressure drop in each of these regimes as the sum of individual contributions due to acceleration, kinetic energy, potential energy and

frictional effects. The model required solid flowrate, gas flowrate, equipment geometry and solids fraction as input to predict the pressure at any point in the system. They claimed that the predicted pressure profiles compared well with the experimental data.

In a recent paper Kato et al. (1989) studied particle holdup and axial pressure drop in fast fluidised beds. A perforated plate was used as the gas distributor. They claimed that the fast bed consisted of a dense region of particles in the lower part of the bed and a dilute region of particles in the upper part. The height of the inflection point between the dense region of particles and the dilute region was determined by the axial pressure drop profile. The location of the inflection point was affected by the superficial gas velocity, the circulation rate of particles and the particle Reynolds number. The following empirical equation was obtained:

$$Z_i = 360\ (M_s/\rho_p U_t)^{1.2}\ (U_a - U_t/U_t)^{-1.45}\ (Re_p)^{-0.29} \qquad (2.25)$$

The application range of Eqn. 2.3.1 was the following:

$$12 \leq M_s \leq 200\ ,\quad 1.6 \leq U_a \leq 6.0$$

$$0.45 \leq Re_p \leq 10\ ,\ 2.5 \leq U_a/\ U_t \leq 50$$

A particle sampling technique was used to determine the particle holdup. From their experimental data, they found that the particle holdup was affected by the superficial gas velocity, circulation rate of particles, particle

Reynolds number, tube diameter and axial distance above the distributor. The following empirical equation was obtained for the particle holdup:

$$\varepsilon/(1-\varepsilon) = 0.048 \exp(Z-Z_i)/(\exp(Z-Z_i)+1) \; (U_a-U_t/U_t)^{1.35} \times (M_s/\rho_p U_t)^{-1.28} \; (Re_p)^{0.23} \; (D_t)^{-1.28} \qquad (2.26)$$

The equation (2.26) was applicable under the conditions:

$1.4 \leqq U_a \leqq 6.0$ $\quad 0.1 \leqq U_t \leqq 0.9$ $\quad 30 \leqq M_s \leqq 130$

$0.45 \leqq Re_p \leqq 10$ $\quad 0.04 \leqq D_t \leqq 0.1$

More recently Louge and Chang (1990) developed a model to explain the discrepancy observed by Arena et al. (1985) between the voidage profiles inferred from pressure gradients and those measured by the quick-closing valve technique. The proposed model does not take into account radial profiles of voidage because it was claimed they did not contribute significantly to the transfer of momentum in the vertical direction. By neglecting the shear in the gas and solid phases the flow was considered one-dimensional. They claimed excellent agreement between the predicted voidage and Arena's voidage measurements using quick-closing valves although for their predictions the pressure gradient at a given section of the riser was required.

Ishii et al. (1989) presented the clustering annular

flow model to describe the annular flow structure in the riser of a CFB. This model was analyzed on the basis of an appropriate expression for the drag force acting on clusters and the minimum pressure gradient used previously by Nakamura and Capes (1973). In order to estimate the flow parameters including the dimensionless radius of the core, the values of both the diameter and the voidage of the cluster phase should be given. This model was based on assumptions such as :

(a) the solid suspension in the CFB consisted of clusters and a leaner continuous network

(b) the drag coefficient of the cluster was estimated from the spherical cluster approximation

(c) the particles in the dilute core were neglected in the material balance

(d) in the cluster the gas moved with the cluster and particles were uniformly suspended

(e) solids were ascending in the core and descending in the annulus

(f) clusters were homogeneously suspended both in the core and in the annulus

(g) the Richarson-Zaki equation was applicable to a cluster.

The most significant difference of the present model from that of Yerushalmi et al. (1978) was that annular flow was an essential assumption. Furthermore in this model, the voidages in the cluster were treated as variables for clusters in the core and annulus. The experimental

technique used involved optical probes for measuring cluster velocity and particle concentration in the cluster phase. From the experimental results an average cluster diameter of 10mm and a voidage of 0.8 were obtained, at operating conditions of gas velocity of 1.29 m/s and solid rate of 10.7 kg/m^2s. The origin and the mechanism of formation of clusters in the annulus and the core were not clearly explained. However they stated that most of the clusters in the riser were not transported but were only fluidised. The inflection point reported by Li and Kwauk (1980) in the voidage distribution was present at the surface of fluidised clusters. Above that surface clusters of small size were transported to the column exit. They concluded that the particle friction factor gave a good prediction for the core diameter and they claimed that the core-annulus shear stress cannot be neglected from calculations of the dimensionless core diameter.

As a continuation to the theoretical work Rhodes (1990) studied radial solids flux profiles in a CFB under a wide range of operating conditions. He developed a sampling probe to measure radial and axial solids flux variations within the riser. From the experimental results he presented radial solid flux profiles at three different axial positions of the riser. These profiles have a parabolic form and exhibited strong downwards solids flow near to the riser wall. The solid flux profiles were representative of what the author terms 'the refluxing dilute-phase transport

regime'. In order to explain this regime, the author proposed a model based on the following assumptions:

a) the flow structure consisted of a core region of solids rising in the dilute phase which was surrounded by the annulus of solids falling in the dense phase suspensions

b) all the gas passes through the core, giving no net flow of gas in the annulus

c) at any axial position there was a net transfer of solids from the core to the annulus. This rate of transfer was directly proportional to the product of the concentration of solids in the core and the interfacial area between the core and the annulus regions.

The last assumption was supported by the mechanism for particles transfer from a fast moving core to the slow moving annulus. Thus the rate of transfer increased with increasing solid concentration in the core and increasing interfacial area. The interface concentration between the core and annulus was neglected.

d) It was further assumed that the solids in the core behaved as individual particles such that the slip velocity between gas and particles was equal to the single particle terminal velocity

e) the superficial gas velocity was greater than the single particle terminal velocity

f) the voidage in the core did not vary with radial positions within the core

g) the downflow velocity of solids in the annular region was determined by a balance between gravitational forces

and wall friction forces and was constant for given powder properties

h) the voidage of the downward flowing suspension in the annulus was independent of axial position in the riser

i) the gas passing through the core exhibited a laminar velocity profile

j) the downward solids flow in the annulus was evenly distributed over the annulus area.

On the basis of these assumptions the core-annulus model successfully predicted radial solids flux profiles. However it is important to mention that the model could not predict the recirculation ratio and radial flux profiles from a knowledge of gas velocity, solid circulation rate, gas and particle properties and system geometry.

A summary of the experimental conditions used by the above mentioned authors is given in the following table.

TABLE 2.1 SUMMARY OF TEST CONDITIONS

REFERENCE	RISER DIAMETER mm	RISER HEIGHT m	d_p μm	ρ_p kg/m^3
Lanneau (1960)	76.2	4.6	70	---
Yerushalmi (1976),(1978)	75	7.2	33	1000
	152	8.4	268	1000
Li & Kwauk (1980)	90	---	Group A	Group A
Cankurt et al. (1978)	152	8.5	49	---
			33	---
Avidan (1980)	152	8.5	33	1670
			49	1070
			49	1450
Weinstein et al. (1984)	150	8	49	1450
Hartge et al. (1985)	50	3.3	56	---
	400	7.8	56	---
Monceaux et al. (1985)	144	8	59	900
Rhodes et al. (1985)	152	4	64	1800
			42	1020
			38	1310
Horio et al. (1985)	50	2.35	275	---
Schnitzlein et al. (1988)	152	8.4	59	1450
Bolton et al. (1988)	150	5.5	200	384
			60	1000
Brereton et al. (1985)	40x30	4	170	---
Arena et al. (1988)	41	6.4	70	1700
	120	5.75	90	2543
Son et al. (1988)	380	9.1	430	2630

TABLE 2.2 SUMMARY OF TEST CONDITIONS

REFERENCE	RISER DIAMETER mm	RISER HEIGHT m	d_p μm	ρ_p kg/m^3
Burkell et al. (1988)	152	9.3	64 148 220	2400 2650 2600
Takeuchi et al. (1986)	100	5.5	57	1080
Kato et al. (1989)	40 66	3 3	51 158 61	1650 1490 1700
Ishii et al. (1989)	50	2.79	60	1000
Horio et al. (1988)	50	2.79	60	1000
Rhodes et al. (1988)	152	4	64	1800
Kefa et al. (1988)	200	4	260 300 675	1023 2630 1700
Weinstein et al (1984)	152	8	49 49	1450 1070
Adams (1988)	300x400	4	250 200	3300 1020

2.3 CONCLUSIONS ON HYDRODYNAMICS OF CFBs

With the help of the above review of fast fluidisation, some conclusions can be drawn that will provide a clear definition of fast fluidisation itself. Fast fluidisation is the flow pattern which seems to be evident under the following conditions:

1) Solid circulation is necessary to maintain a steady state flow in the fluidisation column where the solid circulation rate strongly affects the solid hold-up.

2) The pressure gradient changes along the riser height in a dense lower section and in a dilute upper section of the bed.

3) The axial variation of voidage along the riser height shows that the dense phase occupies the lower region of the riser height and the transition to the dilute phase occurs near the top of the riser.

4) The radial voidage profile in the dense phase has a very high voidage in the centre of the riser and a low voidage in the annulus.

5) In the dilute phase, the radial voidage profile is relatively flat with a wall zone of increased solids concentration and hence a lower voidage.

Hence, the description of the riser of a CFB leads to the fact that a segregation of gas-solid flow is present so that the riser consists of a dilute core region where the particles are transported upwards and is surrounded by a denser annular region with downflow of solids.

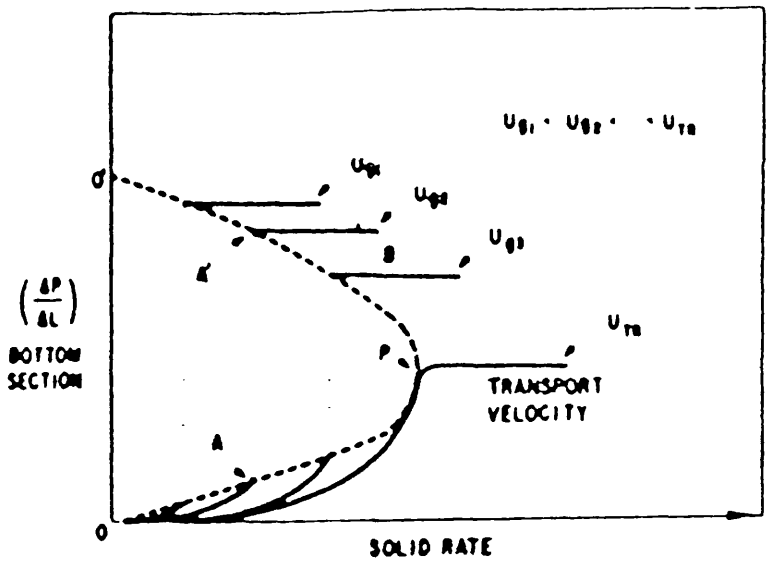

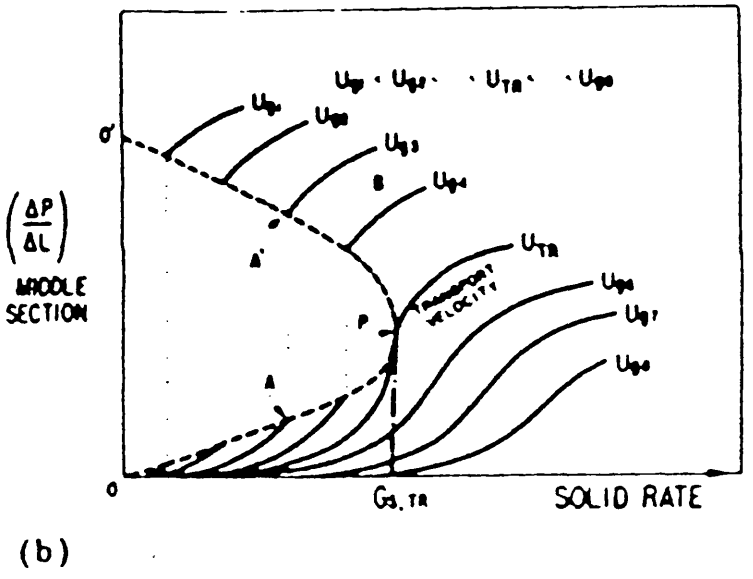

Figure 2.1 Qualitative representation of the pressure gradients measured in the modified 15.2cm system (a) across the bottom section, (b) between pressure taps no.1 and 2 (Yesushalmi et al., 1976).

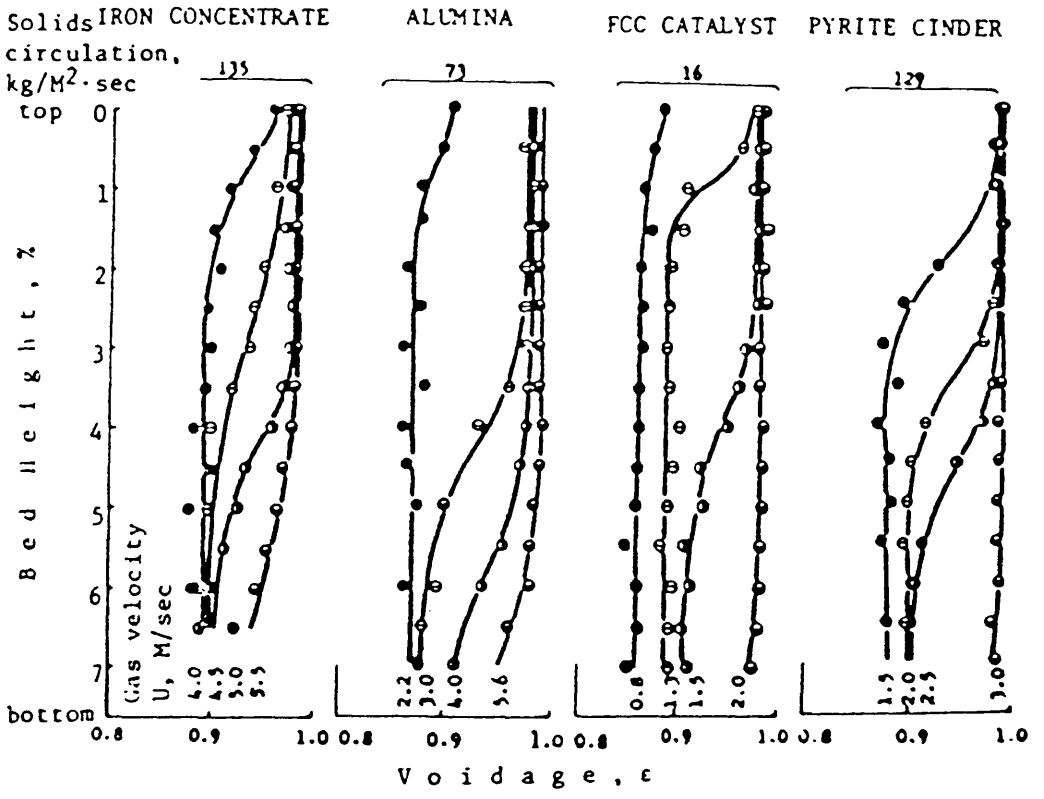

Figure 2.2 Vertical voidage distribution in fast fluidisation (Kwauk et al., 1985).

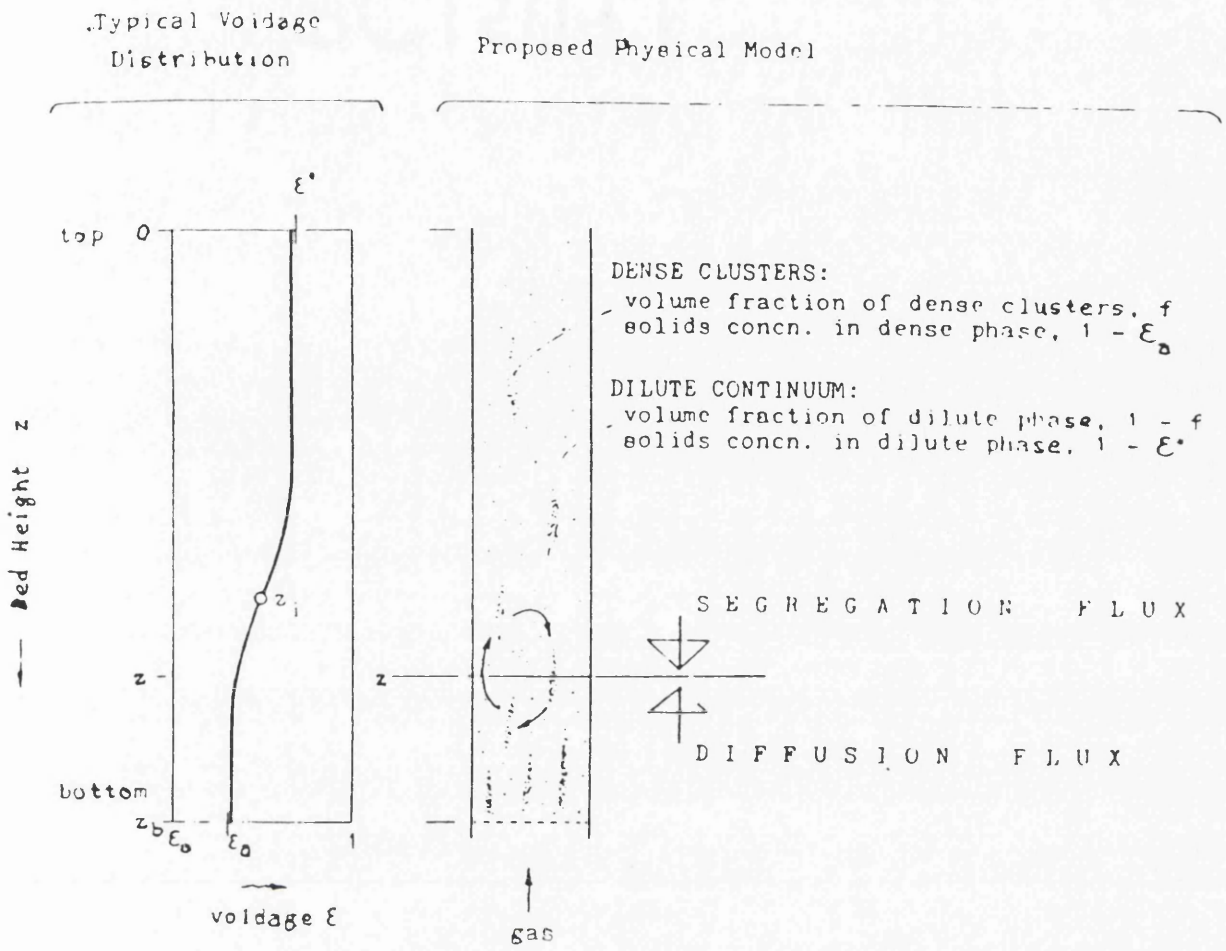

Figure 2.3 Modelling for fast fluidisation (Kwauk et al., 1985).

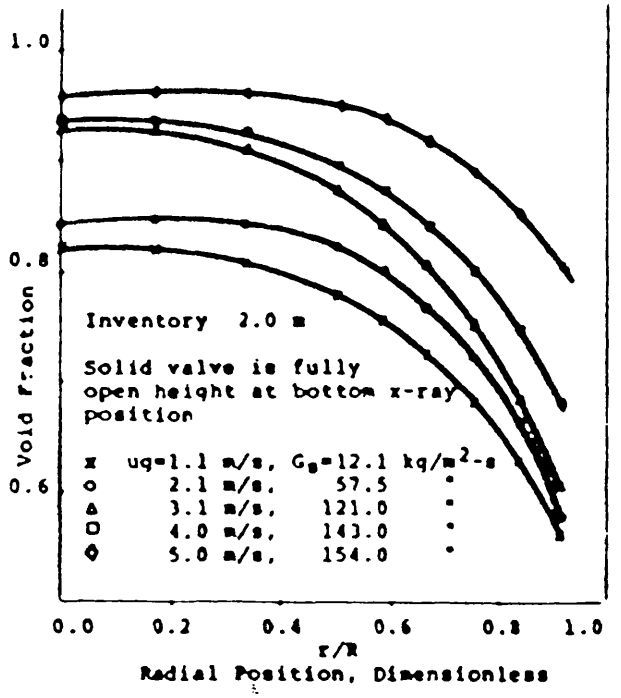

Figure 2.4A Radial variation of void fraction at different velocities, open valve (Weinstein et al., 1985)

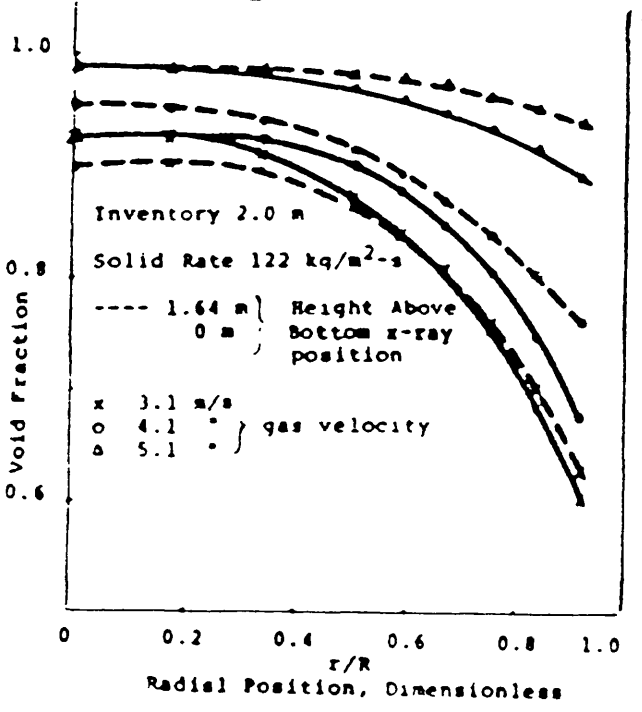

Figure 2.4B Radial variation of void fraction, constant solids rate (Weinstein et al., 1985).

CHAPTER 3

MATHEMATICAL MODELLING

In this chapter a model is presented which relates pressure drop along the axis of a circulating fluidised bed (CFB) riser to two of the main operating variables. These are;

(1) superficial gas velocity, u_g and

(2) solid circulation rate; R_c for dilute core and R_{CD} for the downflow region.

The model takes into account the effect of physical properties of particles and the gas.

With the CFB used for this study (see Chapter 4 for further details), visual observations indicated two distinct regions in the riser. Within the central core of the riser, particles are entrained by the upward flowing gas. This core is characterised by a low particle concentration (high voidage). The second region found in the immediate vicinity of the riser wall (forming an annulus) is characterised by a relatively high concentration of particles (low voidage) which fall downwards in the opposite direction to that of the gas flow. These observations have also been noted by other researchers [Bierl et al.,1980, Weinstein et al., 1984].

As a consquence of these visual observations made during the operation of a CFB, the development of the proposed model proceeds by examining each region in turn. The forces on single particles and clusters in both regions are examined. This is then followed by the

examination of the pressure drops in each region and finally the total pressure drop for the riser is considered.

3.1 FORCES ON A SINGLE PARTICLE

Consider a spherical particle at some axial distance x from the base of the riser (Figure 3.1). Neglecting the effect of bouyancy, there are two forces that will influence the motion of the particle: (i) the force of gravity, mg, acting downwards, and (ii) the drag force F_D, acting upwards caused by the relative speed between the air and the particle.

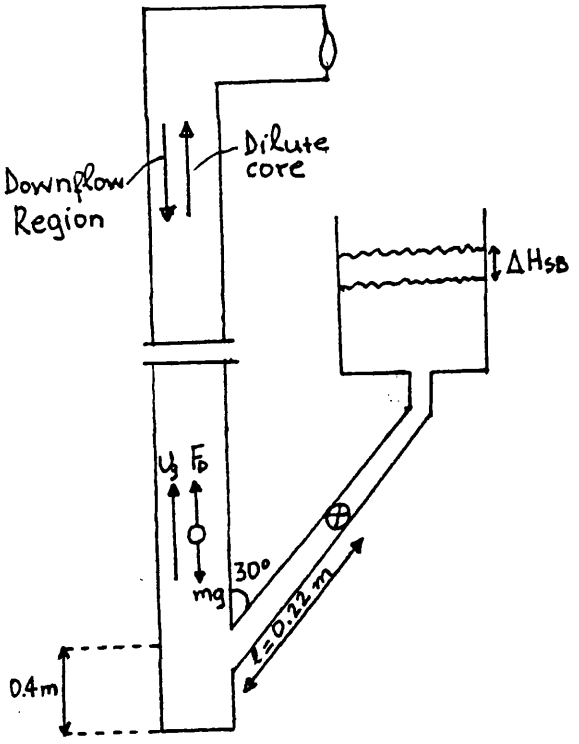

FIGURE 3.1 FORCES ON A SINGLE PARTICLE

At a distance x ,

$$m\left[\frac{d^2x}{dt^2}\right] = mg - F_D \qquad 3.1.1$$

taking the convention that downwards is the positive x-direction. In eqn. 3.1.1, m is the mass of the particle. The drag force may be written in terms of a drag coefficient, c_D. Thus,

$$F_D = \frac{1}{2}\pi \left[\frac{d_p}{2}\right]^2 u^2 c_D \rho_g \qquad 3.1.2$$

where: u is the slip velocity

d_p is the particle diameter

c_D is the drag coefficient, and

ρ_g is the gas density

$$u = -(u_g/\varepsilon - u_p)$$

$$c_D = f(Re_p) \qquad 3.1.3$$

For small particles, c_D can be approximated by its value in the Stoke's regime, calculated from:

$$c_D = \frac{24}{Re_p} \qquad 3.1.4$$

where:

$$Re_p = \frac{\rho_f u d_p}{\mu_f} \qquad 3.1.5$$

For particles of the order of 100μm in diameter and slip velocity of the order of 1m/s in air, the particle Reynolds number is about 1.

Substituting for Re_p in eqn. 3.1.4 from eqn. 3.1.5, then

$$c_D = \frac{24 \mu_f}{\rho_f \, u \, d_p} \qquad 3.1.6$$

Replacing c_D in eqn. 3.1.2 using eqn. 3.1.6 gives:

$$F_D = 3 \pi \, d_p \, \mu_f \, u \qquad 3.1.7$$

Substituting for F_D into eqn. 3.1.1

$$m \frac{d^2x}{dt^2} = mg - 3 \pi \, d_p \, \mu_f \, u \qquad 3.1.8$$

Dividing by m

$$\frac{d^2x}{dt^2} = g - \frac{3\pi d_p \mu_f u}{m} \qquad 3.1.9$$

Noting that

$$m = \pi \frac{d_p^3}{6} \rho_p \qquad 3.1.10$$

and substituting into eqn. 3.1.9 for m using eqn. 3.1.10 and replacing the slip velocity u, with eqn. 3.1.3 and

rearranging, gives

$$\frac{d^2x}{dt^2} = g - \frac{18\mu_f(u_g - u_p)}{d_p^2 \rho_p} \qquad 3.1.11$$

Noting that $u_p = \frac{dx}{dt}$

Hence,

$$\frac{d^2x}{dt^2} + \left[\frac{18\mu_f}{d_p^2 \rho_p}\right] \frac{dx}{dt} - \left[\left[\frac{18\mu_f u_g}{d_p^2 \rho_p}\right] + g\right] = 0 \qquad 3.1.12$$

Letting $A = \frac{18\ \mu_f}{d_p^2\ \rho_p}$, 3.1.12a

eqn. 3.1.12 reduces to

$$\frac{d^2x}{dt^2} = - A \frac{dx}{dt} + (A u_g + g) \qquad 3.1.13$$

Eqn. 3.1.13 is applicable both in the bulk of the riser where the particles are entrained by the air stream and in the region of the riser immediately adjacent to the vertical walls where the solids are flowing downwards. The differences between the solutions for the two regions are due to the initial conditions. Knowing the initial boundary conditions and u_g, eqn. 3.1.13 can be solved for each region using a numerical method, outlined below.

To solve eqn. 3.1.13 for the bulk of the riser it is necessary to calculate the initial particle velocity at t=0 and x=0(see Fig. 3.1). This was assumed to be equal to the terminal velocity of the particles i.e u_p= 0.2 m/s.

Additionally, it is also assumed that $\Delta x/\Delta t \rightarrow dx/dt$ as $\Delta x \rightarrow 0$. In this case Δt will be incremented by steps of 0.01s. Using smaller increments of time would increase the accuracy of the prediction at the expense of computational time.

The general algorithm for the Solution of eqn. 3.1.13 is as follows:

1. Set u_g, ρ_p, μ_f, d_p and D_T
2. Calculate A from eqn. 3.1.12a
3. Set initial value for dx/dt at t=0, x=0 (u_p= 0.2 m/s)
4. Calculate d^2x/dt^2 from eqn. 3.1.13
5. Calculate Δx (dx/dt x Δt) i.e.(dx/dt)0.01
6. Calculate the new value of $dx/dt=\Delta x/n\Delta t$ where n=2,3,4...
7. Hence, go to 4

The results of this numerical solution are shown in Fig. 3.2 for the FCC powder and for u_g of 3 m/s.
At first the particles appear to fall by a small distance before rising upwards with the gas. After about 0.1 s, corresponding to a distance of about 0.12 m, the particles appear to reach its terminal slip velocity u_{ts}; u_{ts}=0.2m/s, calculated from standard correlations:

$$u_t = \frac{d_p^2 g(\rho_p - \rho_f)}{18\mu}$$ (Shamlou, 1988).

3.2 FORCES ON A PARTICLE IN AN ASSEMBLY

The presence of other particles will modify the effective drag coefficient for a single particle in the gas flow. Work by Wen and Yu (1966) and Wen and Galli (1971) has indicated that this modification can be adequetly described by:

$$C_D' = C_D \, \varepsilon^{-4.7} \qquad 3.2.1$$

where C_D is the single particle drag coefficient predicted by eqn. 3.1.4. Combining eqns. 3.1.4, 3.1.12a and 3.2.1 it can be shown that:

$$\frac{d^2x}{dt^2} = - A \, \varepsilon^{-4.7} \, \frac{dx}{dt} + (A \, \varepsilon^{-4.7} u_g + g) \qquad 3.2.2$$

ε can be obtained by dividing the solid superficial velocity by its linear velocity. Thus:

$$1-\varepsilon = \frac{V_c}{u_p} = \frac{V_c}{dx/dt} \qquad 3.2.3$$

where V_c is the superficial solid velocity (m/s)

$$V_c = \frac{R_c}{\rho_p A} = \frac{4R_c}{\rho_p \pi D_T^2} \qquad 3.2.4$$

where: D_T is the riser diameter (m)

ρ_p is the particle density (kg/m^3)

In eqn. 3.2.4, R_c is the solid circulation rate.

For the dilute core, R_c is obtained from experimental

measurements of solid flowrate. These measurements indicated that R_c is a function of the gas velocity and the ball valve opening. It was found that R_c varied in the range of 3×10^{-3} kg/s to 30×10^{-3} kg/s for gas velocities in the range 2-4 m/s and ball valve openings between 40° to 70°.

The numerical solution of eqn. 3.2.2 for the dilute core is similar to that described previously for eqn. 3.1.13, except that the values of the solid circulation rate, R_c, and column diameter, D_T, (eqn. 3.2.4) are now part of the input data. The algorithm for the solution of eqn. 3.2.2 is as follows:

1. Set u_g, ρ_p, μ_f, d_p, D_T and R_c
2. Calculate A from eqn. 3.1.12a
3. Set initial values for dx/dt at t=0, x=0 (u_p= 0.2m/s)
4. Calculate d^2x/dt^2 from eqn. 3.1.13
5. Calculate V_c using eqn. 3.2.4
6. Calculate voidage ε using eqn. 3.2.3
7. Calculate Δx (dx/dt x Δt) i.e. (dx/dt)0.01
8. Calculate the new value of $dx/dt = \Delta x/n\Delta t$ where n=2,3,4...
9. Hence go to 4

Figures 3.3 and 3.3A show calculated values of the voidage plotted against riser height with gas velocity and particle diameter as variables. Evidently, the voidage and particle velocity reach their steady state values within the first few centimeters after the point of entry. The voidage appears to be relatively insensitive to the changes in particle diameter. Figure 3.3B shows predicted values of

the voidage plotted against riser height with the gas velocity and particle density as variables.

For the downflow region, the solution of eqn. 3.2.2 is complicated by two factors. Firstly, close to the vertical wall of the riser, calculations (see Appendix C) show that particles are likely to fall not as individual primary grains, but rather as clusters. As far as the solution of eqn. 3.2.2 is concerned, this implies that the magnitude of parameter A (eqn. 3.1.12a) is determined by cluster diameter, D_c, and not by primary particle diameter d_p. Unfortunately, it is not possible at this stage to estimate the size of these clusters and therefore for the purpose of solving eqn. 3.2.2 a trial and error procedure has to be adopted. Secondly, solution of eqn. 3.2.2 for the downflow region requires information about solid circulation rates R_{CD} near the wall. This is obtained as shown below.

Calculation of solid circulation rate in the downflow region

At time, t=0, and for a fixed ball valve opening position, setting the gas velocity to a pre-determined value will cause a change in the height of the material in the slow bed. For a given gas velocity, let the height of material in the slow bed fall by ΔH_{SB} (see Fig. 3.1). This means that during the steady-state operation the mass of solids in motion is gicen by:

$$\Delta M_{SB} = \Delta H_{SB} \frac{\pi D_{SB}^2}{4} \rho_{SB} \qquad 3.2.5$$

where:

$$\rho_{SB} = (1-\varepsilon_{SB})\rho_p + \varepsilon_{SB}\rho_g \qquad 3.2.6$$

ε_{SB} is the voidage corresponding to the point of minimum fluidisation.

If the total volume V_T of the system is known, and the volume of the riser V_R is known then as an approximation the mass of the solids in the riser, M_R, will be:

$$M_R = \frac{V_R}{V_T} \Delta M_{SB} \qquad 3.2.7$$

From a simple mass balance:

$$M_R = M_{DC} + M_D \qquad 3.2.7a$$

where: M_R is the total solid hold-up in the riser

M_{DC} is the solid hold-up in the dilute core

M_D is the solid hold-up in the downflow

If it is also assumed that all the solid initially goes to the dilute core region, then the solid hold-up in that zone is equal to the product of solid circulation rate and its residence time. Since the acceleration zone is relatively short (see Fig. 3.2), the residence time, t_R, may be estimated by using:

$$t_R = \frac{H_R}{u_{slip}} \qquad 3.2.8$$

where: $u_{slip} = u_g - u_t$

Thus, the solids hold-up in the dilute core is given by:

$$M_{DC} = \frac{R_C H_R}{u_{slip}} \qquad 3.2.9$$

Substituting for M_{DC} and M_R in eqn. 3.2.7a using eqns. 3.2.9 and 3.2.8 gives:

$$M_D = M_R - M_{DC} = \frac{V_R}{V_T} \Delta M_{SB} - \frac{R_C H_R}{u_{slip}} \qquad 3.2.10$$

To calculate the mass flowrate of solids, R_{CD}, the residence time of solids in the downflow region must be known. Assuming an estimated mean value of 1m/s based on visual observations (Bolton, 1988) for the solids velocity in the downflow region, the residence time in that zone will be given by (Section 3.4):

$$t_{CD} = \frac{H_R}{1} \qquad 3.2.11$$

and thus R_{CD} is given by:

$$R_{CD} = \frac{M_D}{t_{CD}} = M_D \frac{1}{H_R} = \frac{M_D}{H_R} \qquad 3.2.12$$

The difference between the initial and steady-state height in the slow bed, ΔH_{SB}, has to be known in order to use eqn. 3.2.5. The variation of ΔH_{SB} was measured experimentally as a function of gas velocity and ball valve opening.

Equation 3.2.12 provides the value of the solid

circulation rate in the downflow region. This together with eqn. 3.2.4 and an estimated value of cluster diameter are used to solve eqn. 3.2.2 in order to obtain the voidage and solid velocity profiles in the downflow region. As explained previously, the solution of eqn. 3.2.2 involves a trial and error procedure involving cluster diameter D_c.

The numerical solution adopted involves solving eqn. 3.2.2 for an initial guess of D_c. Having obtained the voidage profile distribution for the downflow as well as for the dilute core, the computer programe then calculates the overall pressure drop profile for the riser (see next section). The predicted pressure is then compared (visually) with the measured pressure distribution for the same operating conditions. If the two profiles do not match then a new value of D_c is used and the whole procedure repeated, until the calculated pressure profile adequetely matches the measured distribution. The voidage profile and solid velocity distribution in the downflow region are then plotted routinely as part of the solution.

Figures 3.4 and 3.5 shows plots of solid velocity and voidage in the downflow region. It is interesting to note that the voidage in the downflow region (Fig.3.5) is lower than that for the dilute core.

3.3 PREDICTION OF PRESSURE DROP IN THE RISER

The pressure losses in the riser have four origins: (1) particle acceleration (2) change in static pressure (3) gas-wall friction and (4) solid-wall friction.

$$\frac{\Delta P_T}{\Delta L} = \frac{\Delta P_{ACC}}{\Delta L} + \frac{\Delta P_{STAT}}{\Delta L} + \frac{\Delta P_{FRIC}}{\Delta L} \qquad 3.3.1$$

$\rho_p(1-\varepsilon)g$ — contribution due to solids

$\rho_g \varepsilon\, g$ — contribution due to gas

$\frac{2f_s\rho_p(1-\varepsilon)u_p^2}{D_T}$ — contribution due to solids

$\frac{2c_f\rho_g u_g^2}{D_T}$ — contribution due to gas

The pressure drop due to particle acceleration, although is calculated by the program, is relatively small compared to the other terms in eqn. 3.3.1

The pressure drop due to the static head of bulk material may be split into the contributions of particles and fluid. Thus

$$\Delta P_{STAT} = \rho_p\ (1-\varepsilon)\ g\ \Delta x + \rho_g\ g\ \varepsilon\ \Delta x \qquad 3.3.2$$

Calculation show that, the extra pressure contribution due to the gas flow alone ($\rho_g g \varepsilon \Delta x$) is significantly smaller than that due to the solid particles. While in practice the contribution due to gas flow alone may be ignored, it was routinely calculated and its contribution was included in this analysis.

Using the Fanning friction factor versus Reynolds number relationship for turbulent flow, the pressure drop due to the gas-wall friction can be calculated in the

standard way (Kay, 1960):

$$\Delta P_{gw} = 2\, c_f\, \rho_g\, \Delta x\, \frac{u_g^2}{D_T} \qquad 3.3.3$$

The pressure drop due to the flow of solids is obtained using a solid-wall friction factor (Zenz and Othmer, 1960):

$$\Delta P_{sw} = 2\, f_s \rho_p (1-\varepsilon)\, \Delta x\, \frac{u_g^2}{D_T} \qquad 3.3.4$$

where: f_s is the solid-wall friction factor similar to gas-wall friction factor. f_s is normally obtained from experimental data. For the purpose of this discussion the following correlation is used (Breault et al.,1989):

$$f_s = 12.2\, \frac{(1-\varepsilon)}{\varepsilon^3\, u_p} \qquad 3.3.5$$

The local values of ε in eqns. 3.3.2 and 3.3.5 and the magnitude of the local particle velocity u_p in eqn. 3.3.5 are obtained from the solution of eqn. 3.2.2. for the dilute core and for the downflow regions.
The total pressure drop is calculated by adding the pressure drops for the dilute core and the downflow region.

$$\Delta P_{TOTAL} = \Delta P_{DILUTE} + \Delta P_{DOWNFLOW} \qquad 3.3.6$$

Both ΔP_{DILUTE} and $\Delta P_{DOWNFLOW}$ are obtained by using eqns. 3.3.2 to 3.3.5. For each region local ε and u_p are obtained by solving eqn. 3.2.2 as described previously.

Figures 3.6 to 3.11 show predicted pressure profiles with an initial solid velocity in the downflow region of 1m/s and for a range of assumed cluster diameters (eqn.3.3.1). Small changes in cluster diameter as shown in

Figs. 3.6 and 3.7 make significant differences for the solution of eqn. 3.2.2 and the subsequent pressure drop calculations.

Typical plots of the pressure distribution in the dilute core, the downflow region and the total pressure for three gas velocities (4, 3.5 and 2.5 m/s) for the FCC powder are presented in Figs. 3.9 to 3.11 for a mean solid velocity of 1m/s. Figure 3.12 shows an example of predicted pressure profiles in the dilute core, downflow region and total pressure with a mean downflow solid velocity of 0.7m/s. This difference (from 1m/s to 0.7m/s) has resulted in lowering the pressure drops in the downflow region by 20%.

Appendix (F) contains the algorithm and listing of the computer program that has been developed for predicting the pressure profile in the riser.

Chapter 4 contains details of experiments conducted in this study. The results of these experiments are discussed in Chapter 5 and also compared with the predictions made using the model developed in this Chapter.

FIGURE 3.2 PLOT OF SOLID VELOCITY VERSUS TIME ACCORDING TO EQ. 3.1.13

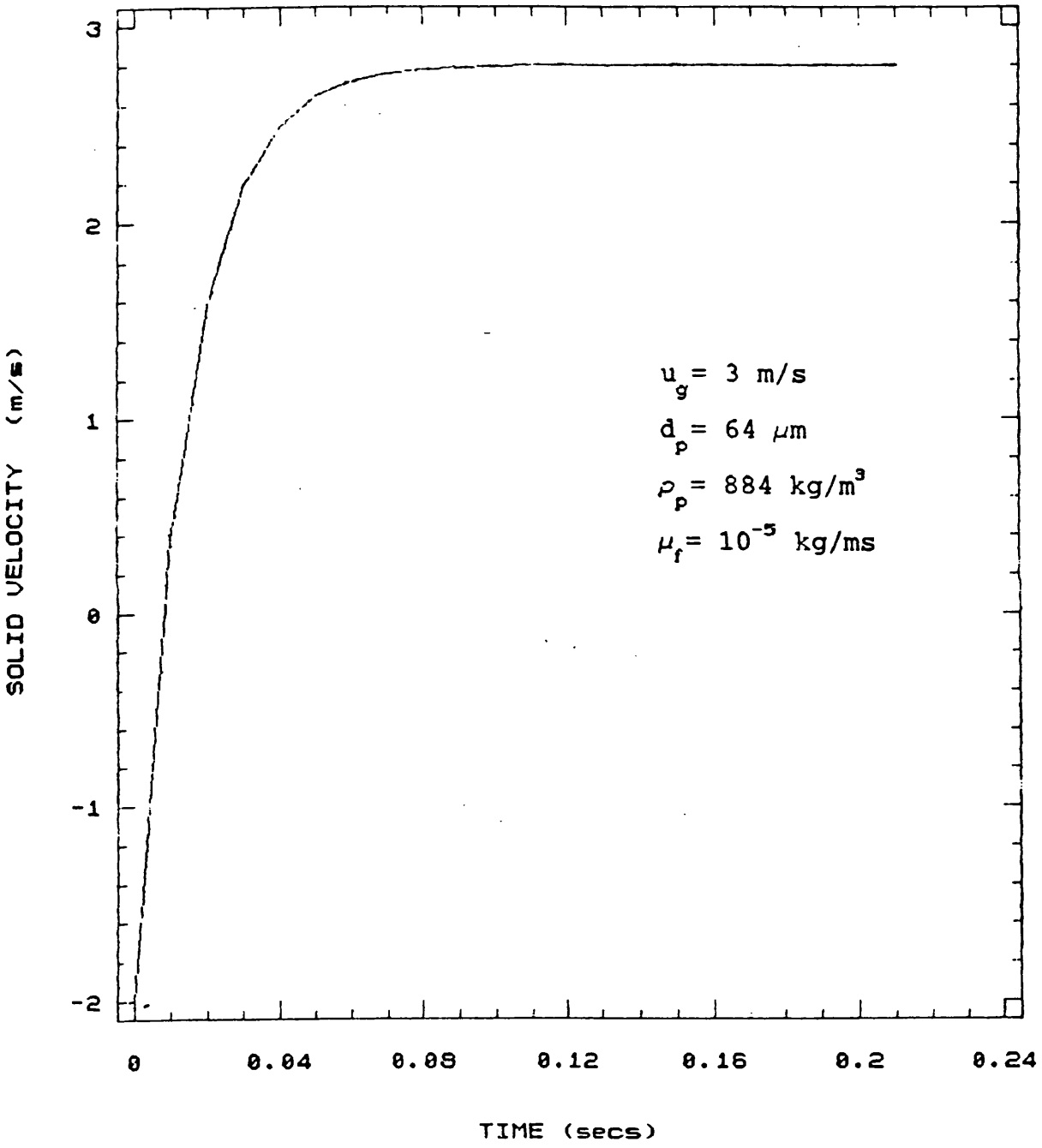

Figure 3.3 Theoretical voidage of dilute core versus riser height

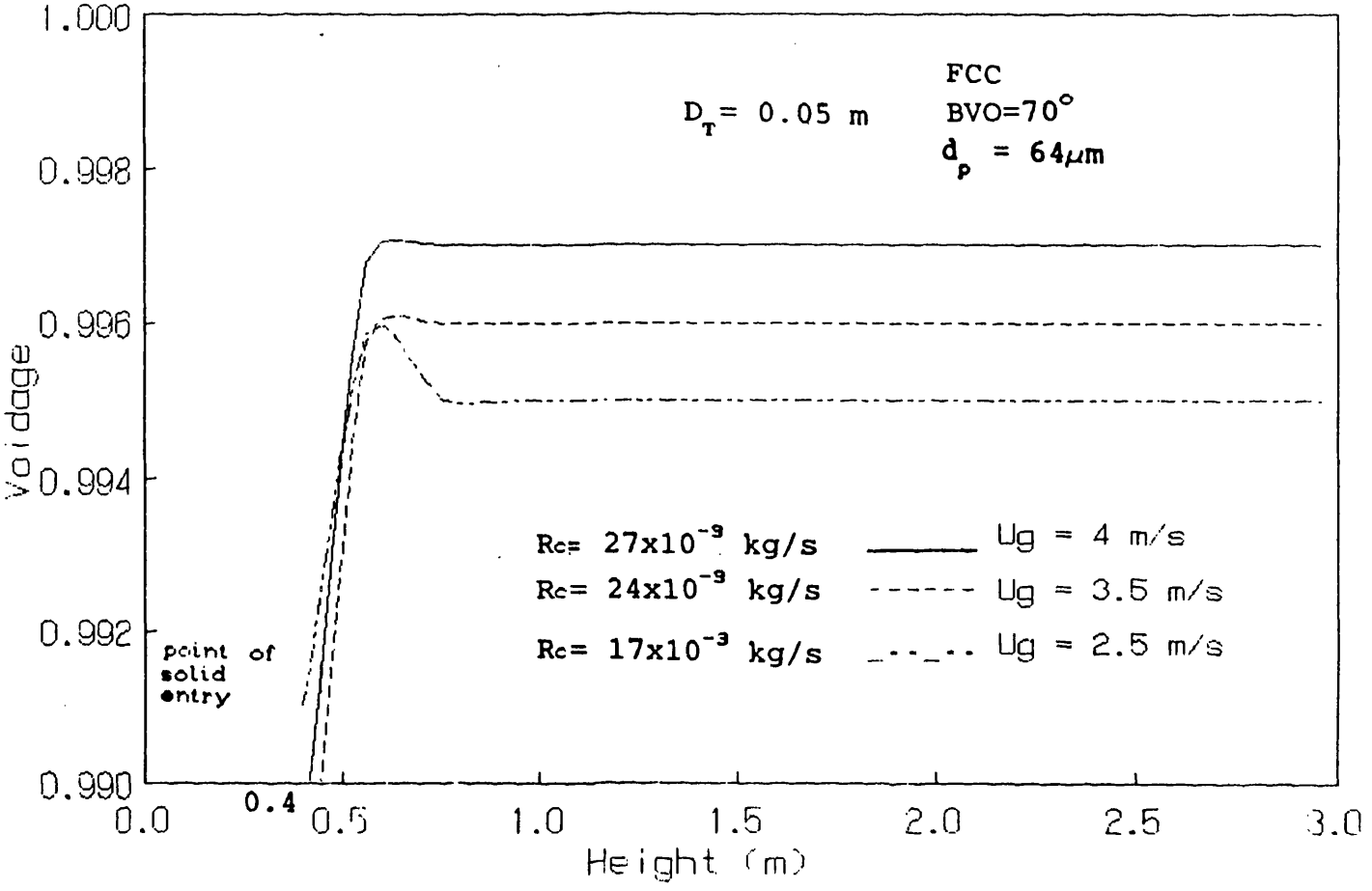

FIGURE 3.3A Theoretical Voidage of dilute core versus riser height

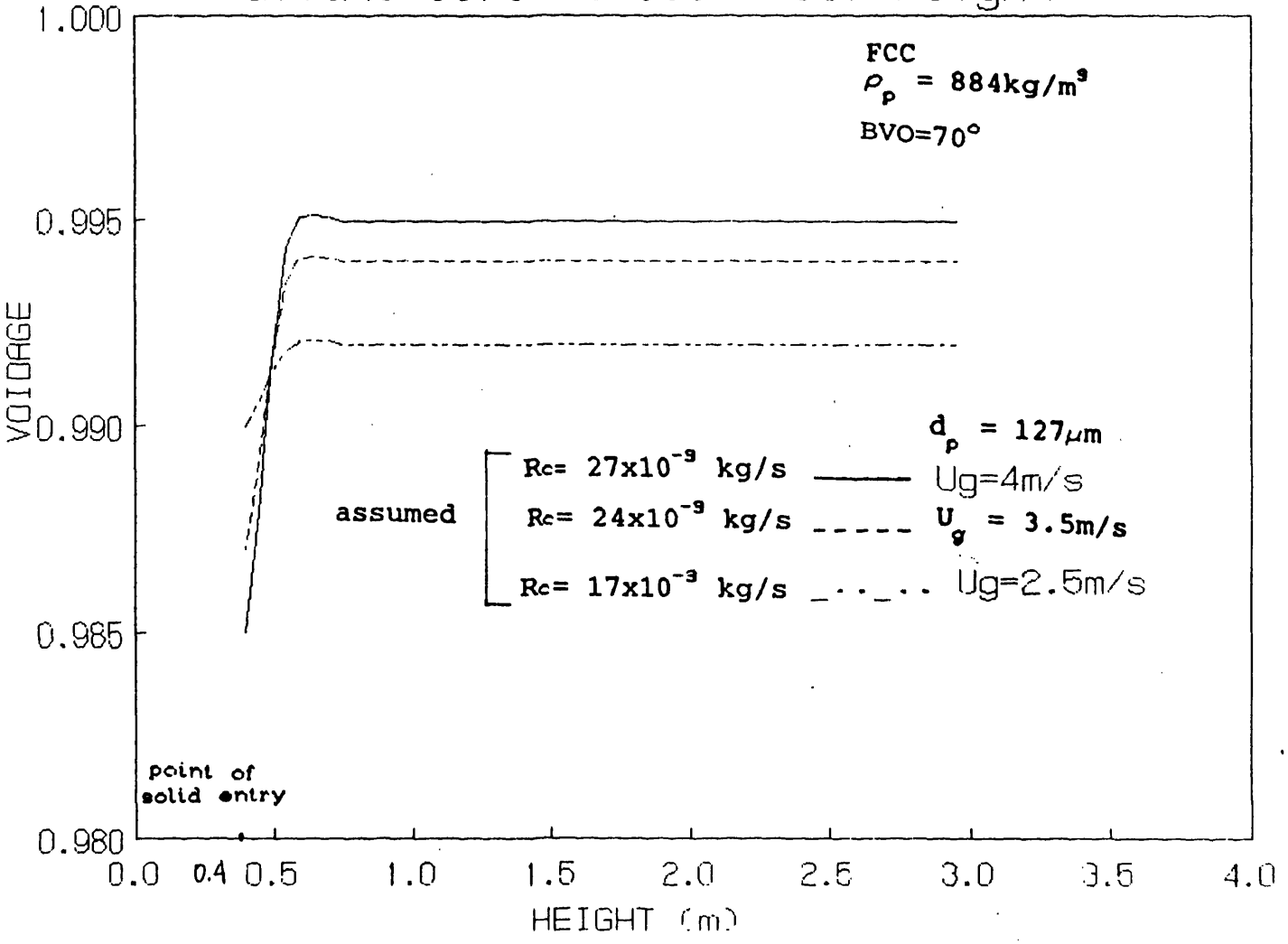

FIGURE 3.3B Theoretical voidage of dilute core versus riser height

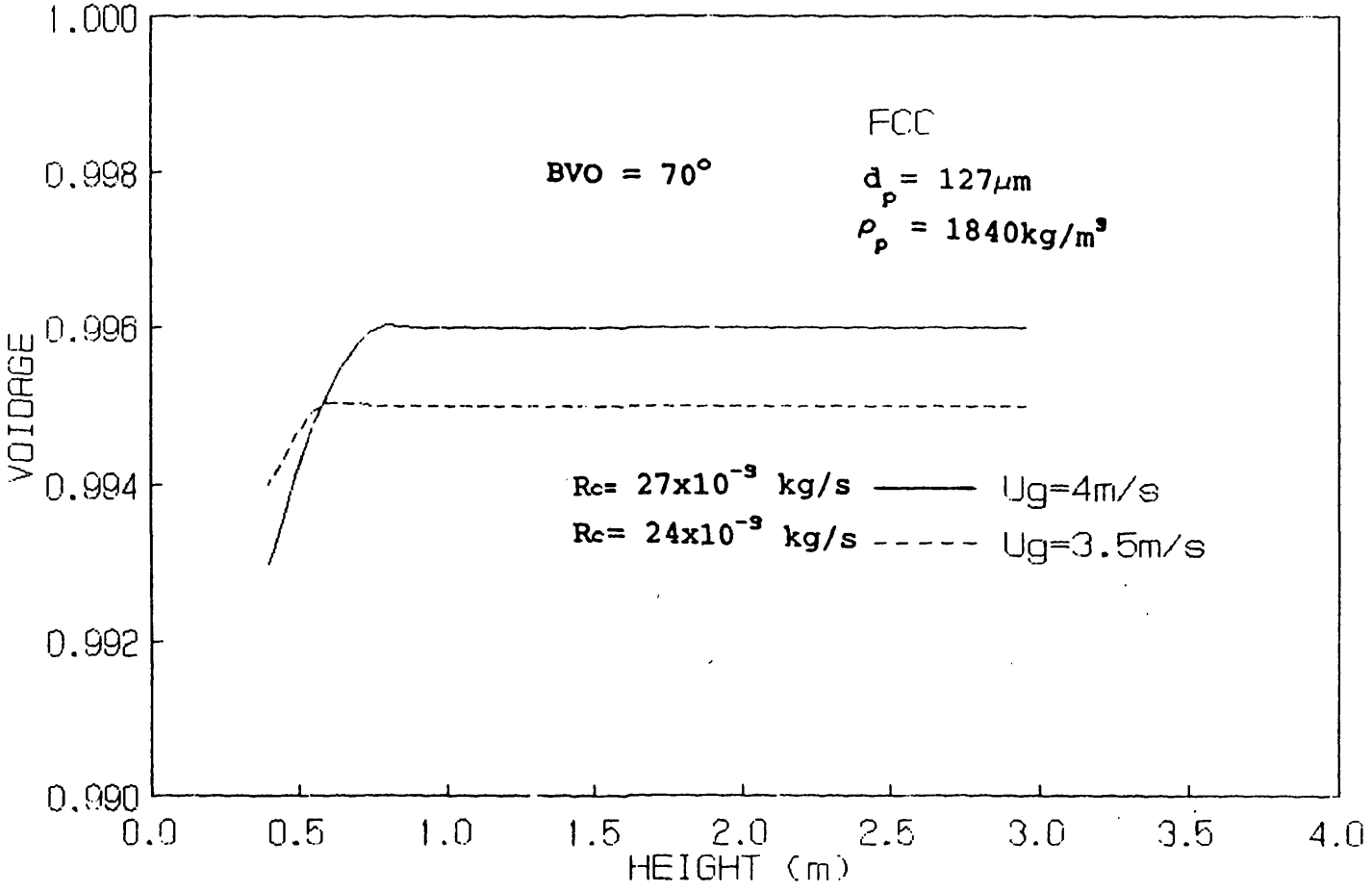

Figure 3.4 Theoretical solid velocity of downflow region versus riser height

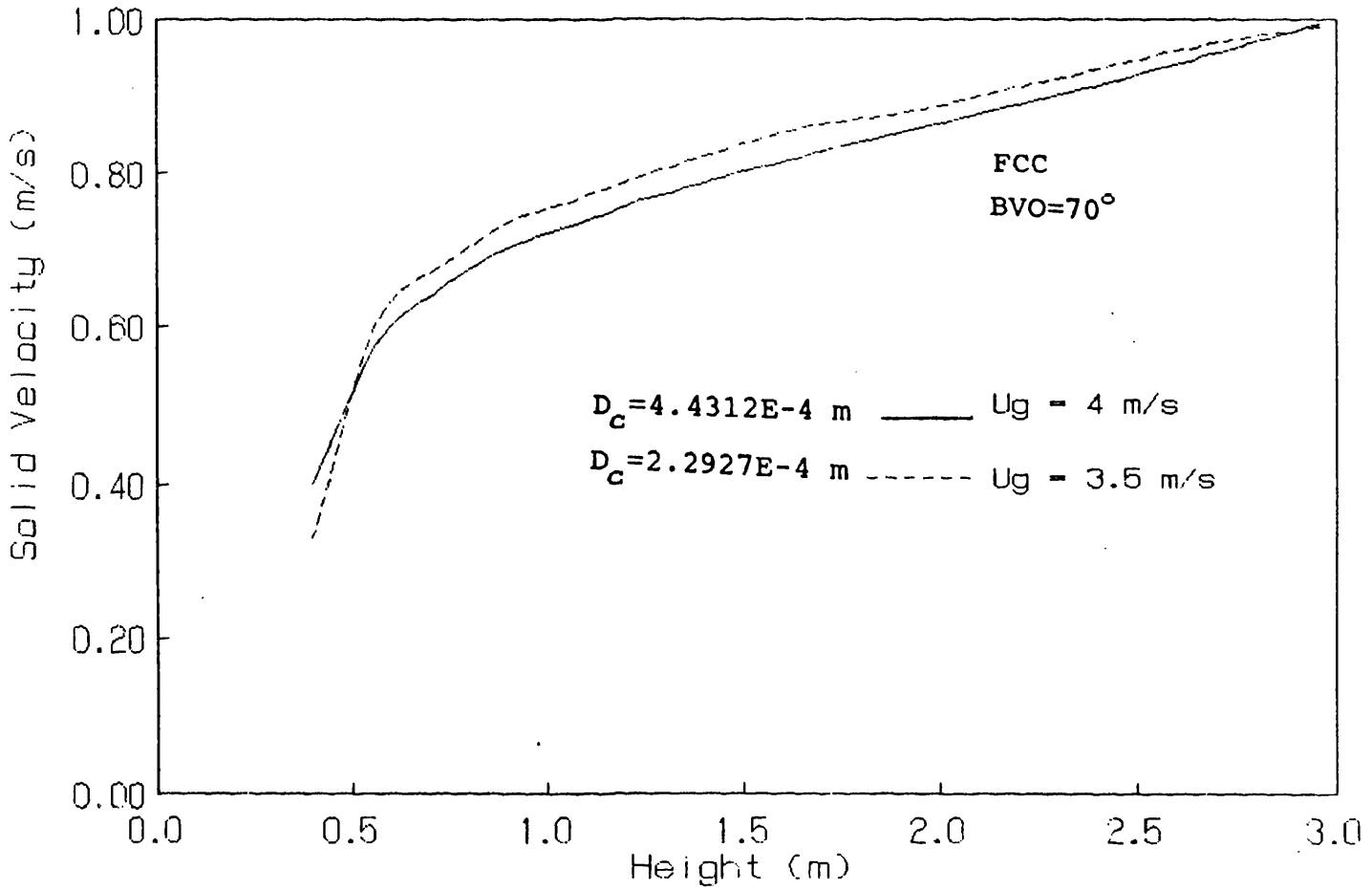

Figure 3.5 Theoretical voidage of downflow region versus riser height

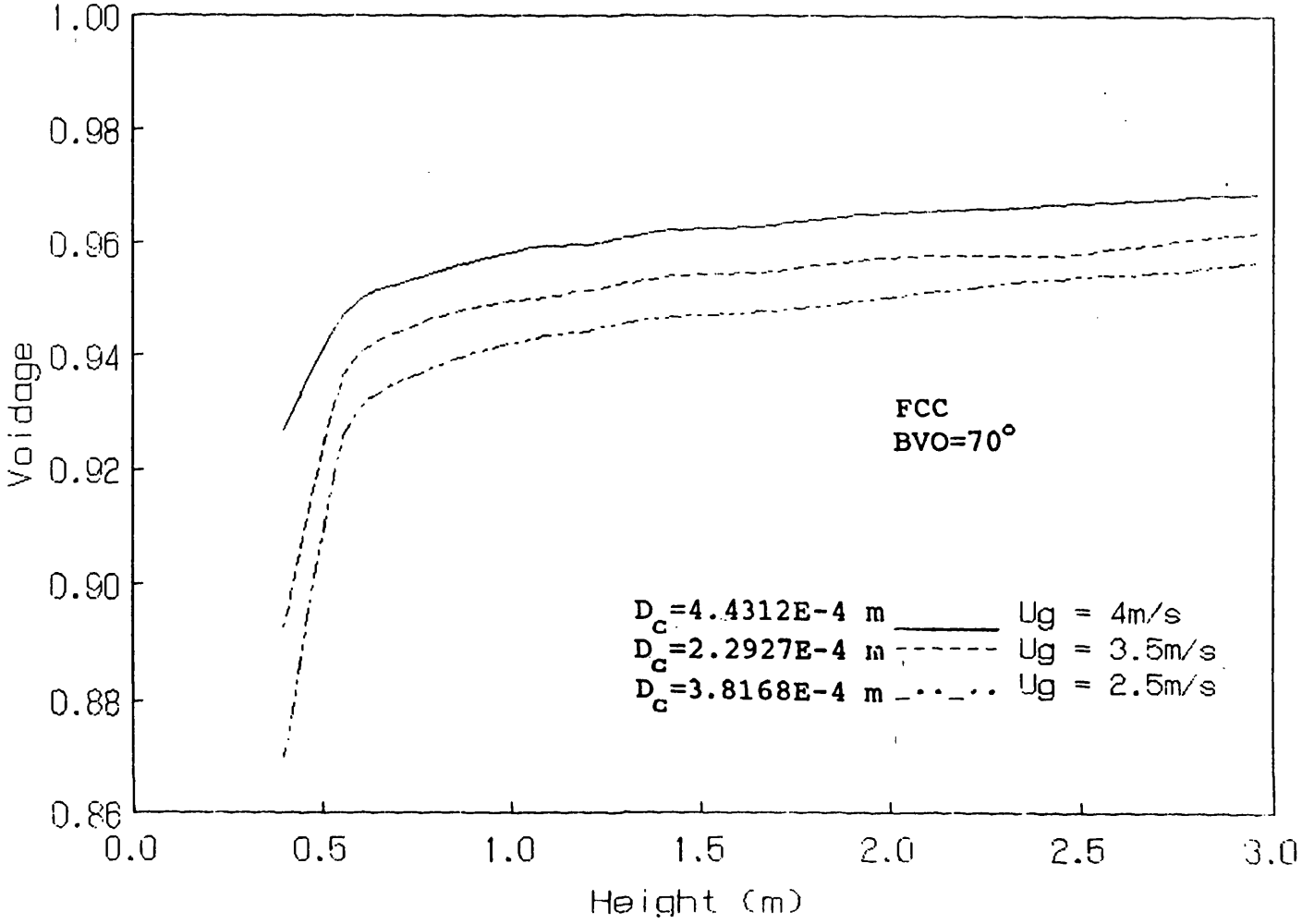

Figure 3.6 Plot of pressure Gradient versus riser height

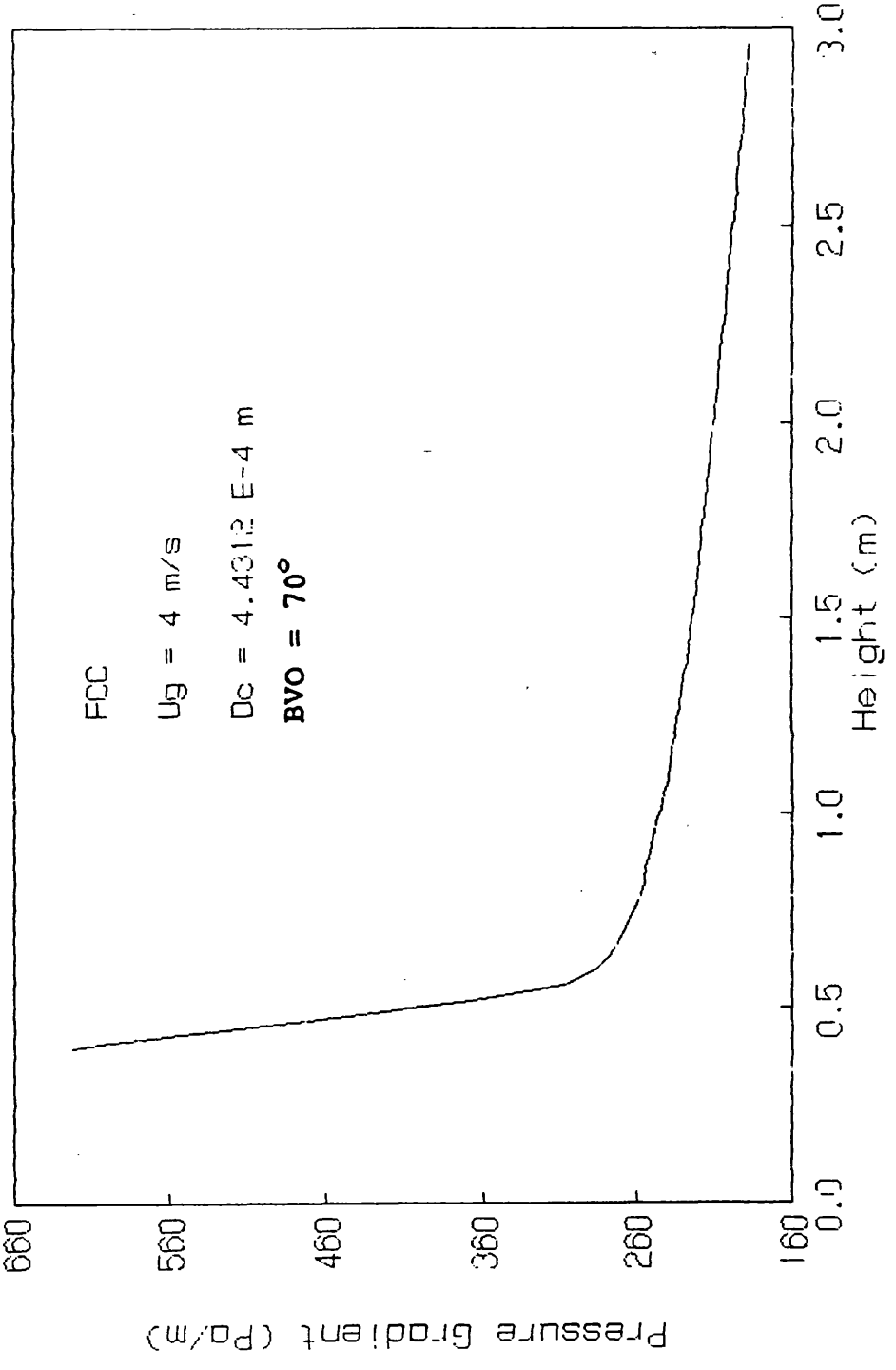

Figure 3.7 Plot of pressure Gradient versus riser height

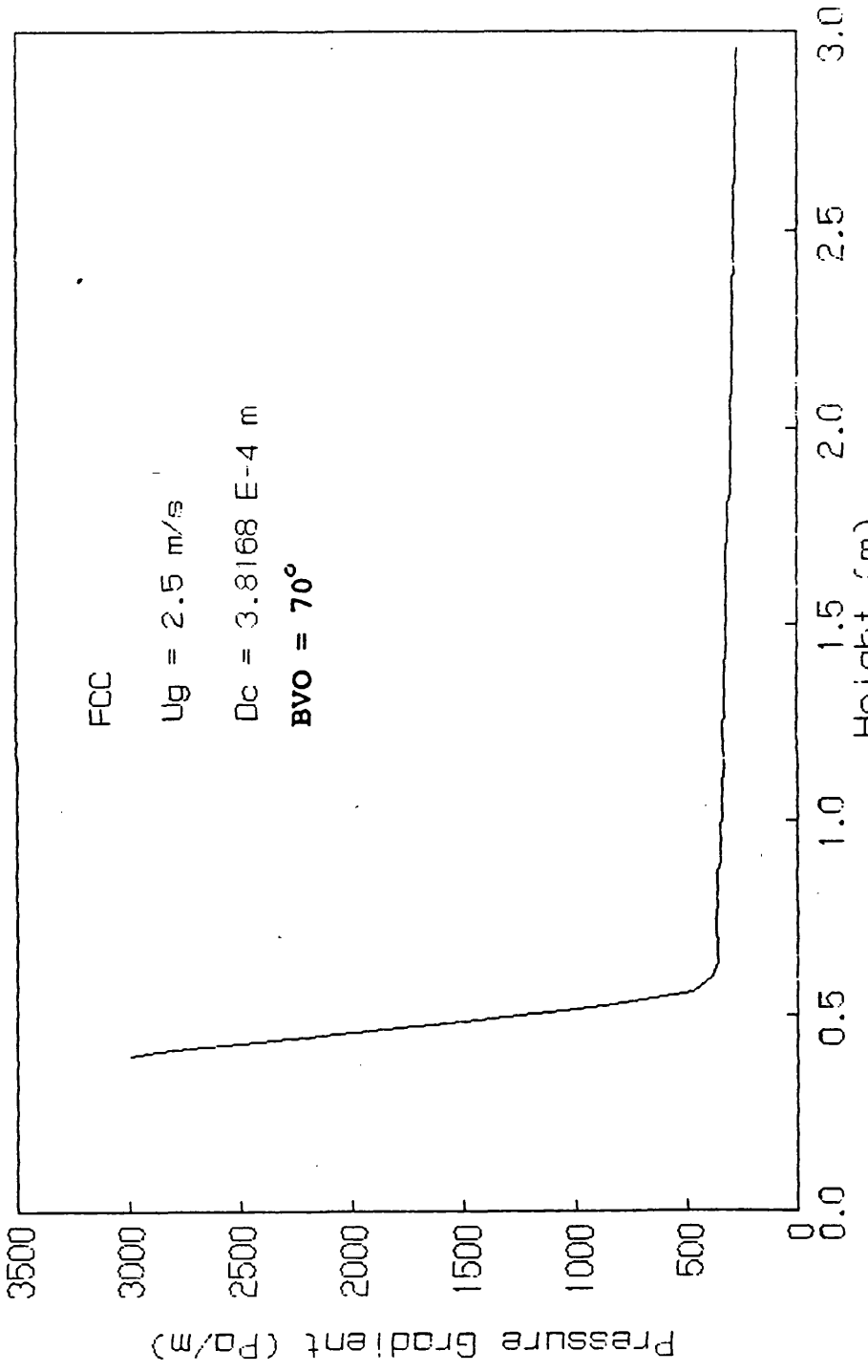

Figure 3.8 Plot of pressure gradient versus riser height

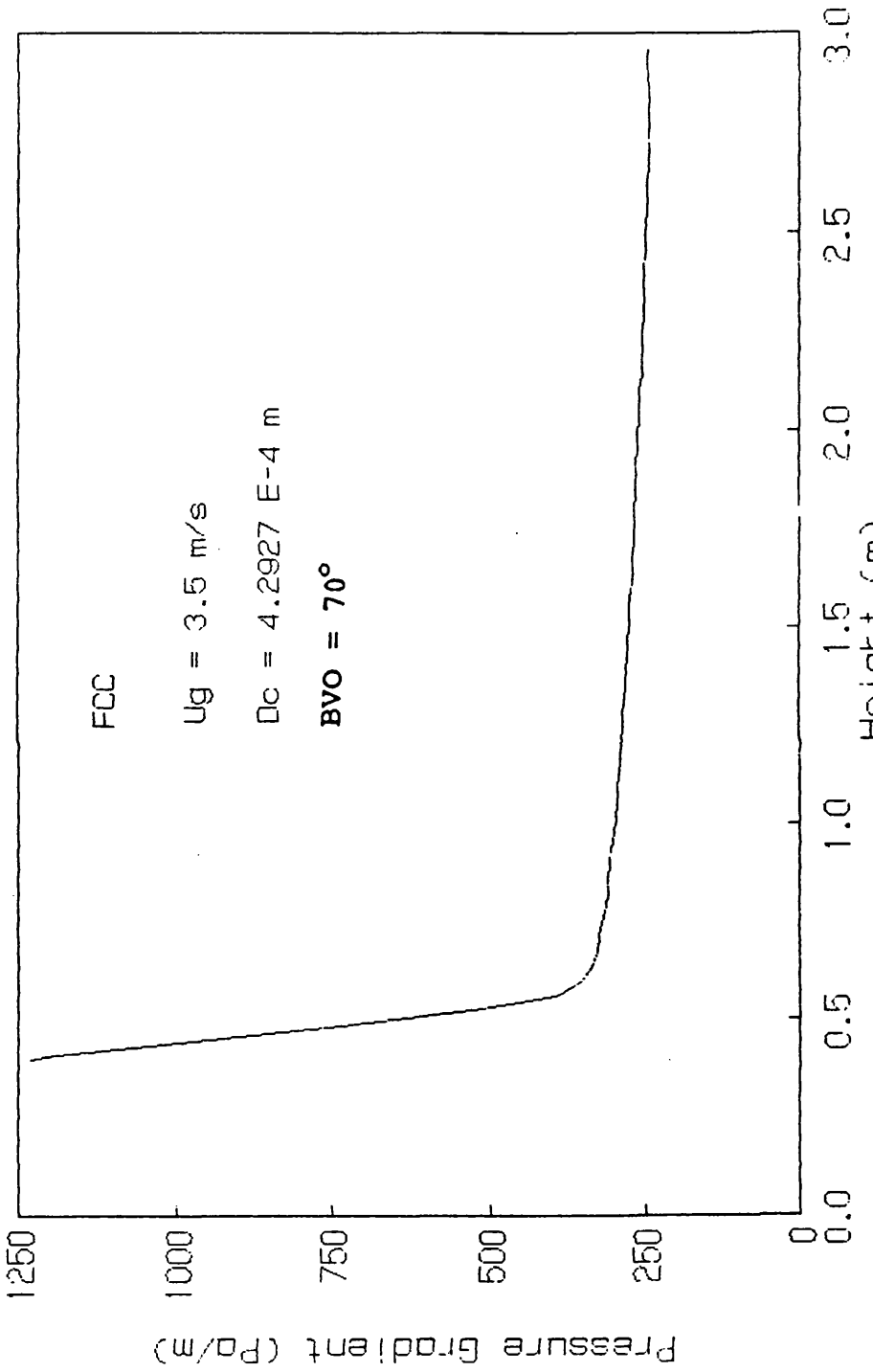

FIGURE 3.9 Pressure gradient versus riser height

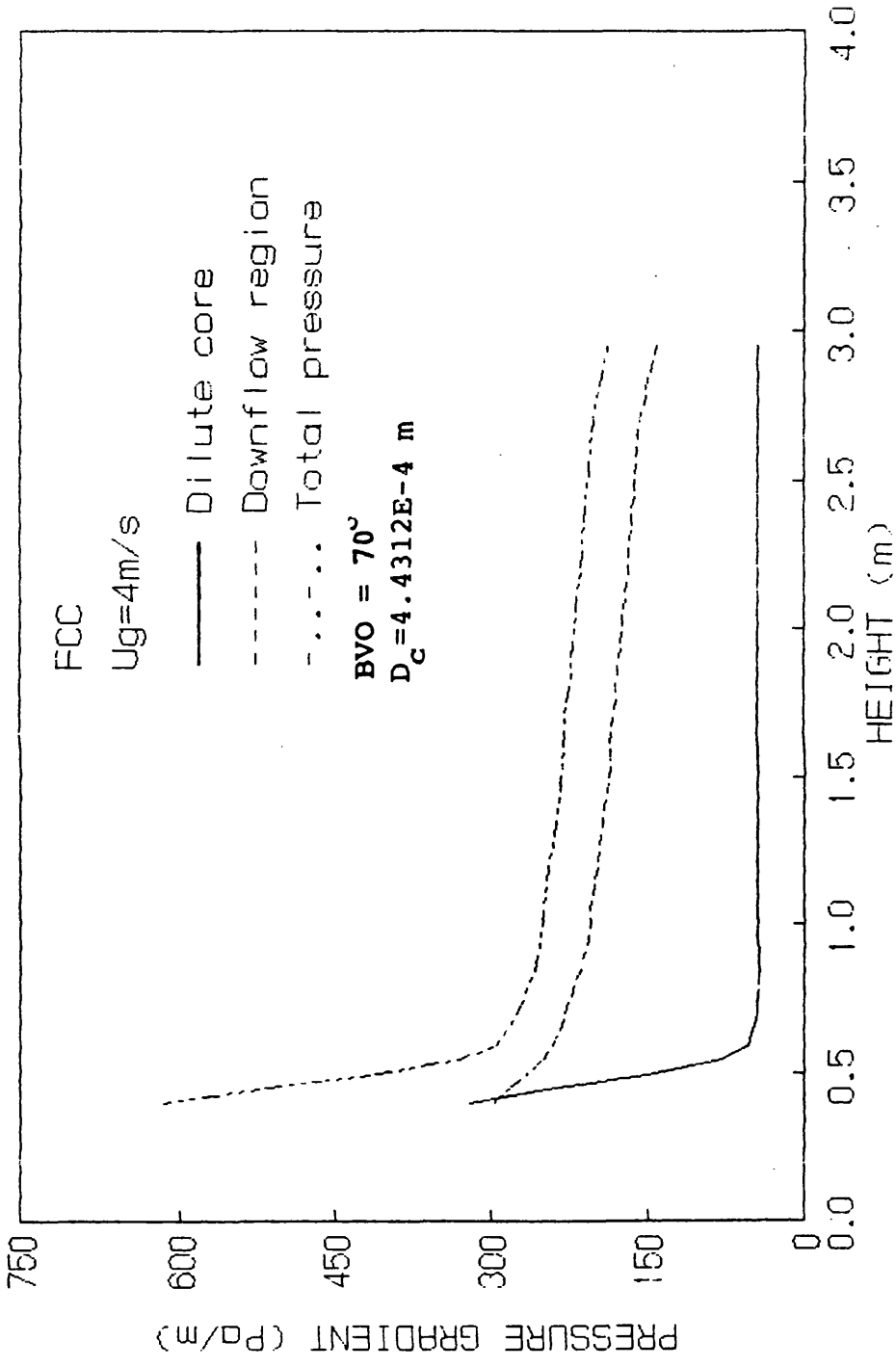

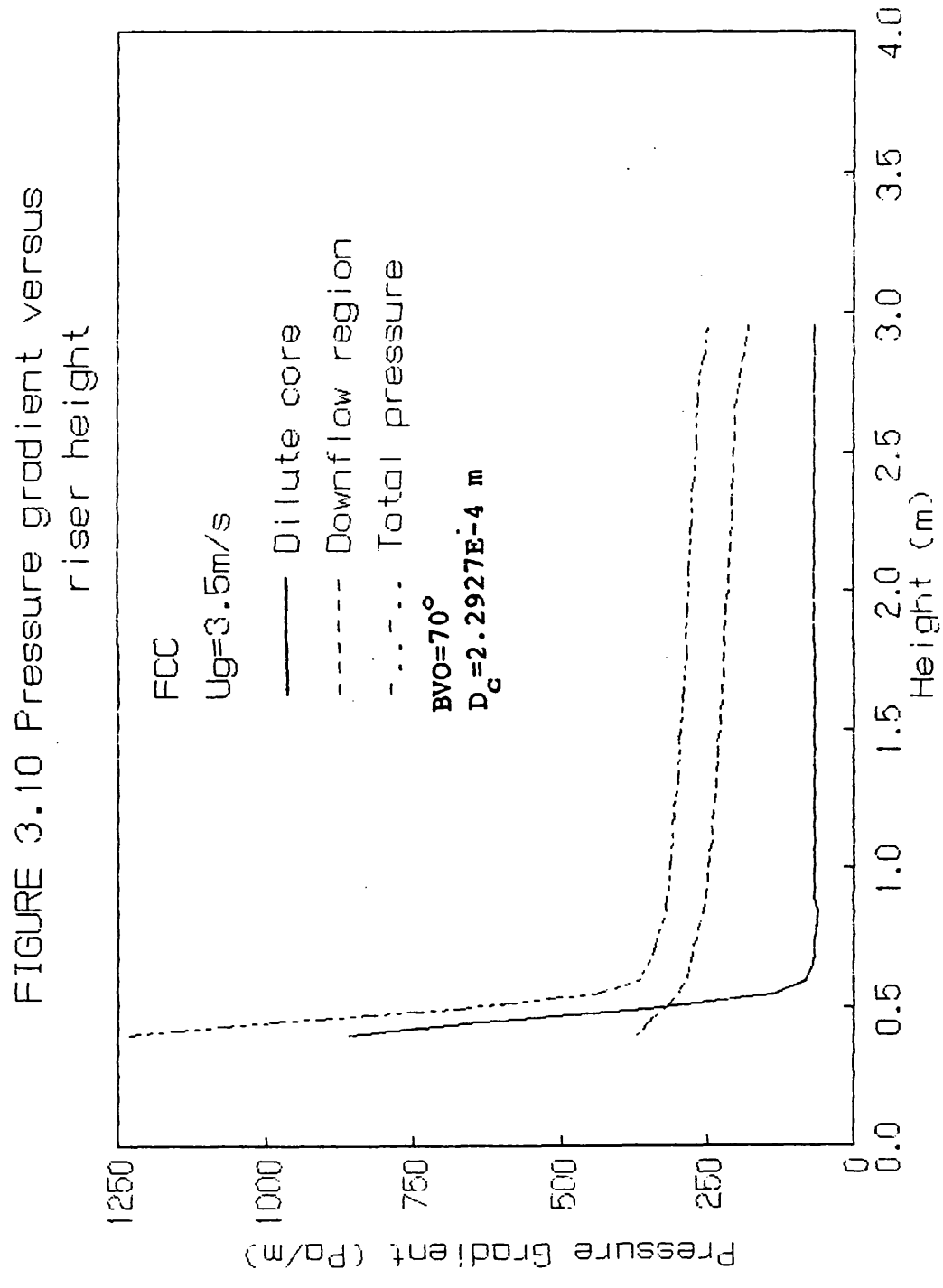

FIGURE 3.10 Pressure gradient versus riser height

FIGURE 3.11 Pressure gradient versus riser height

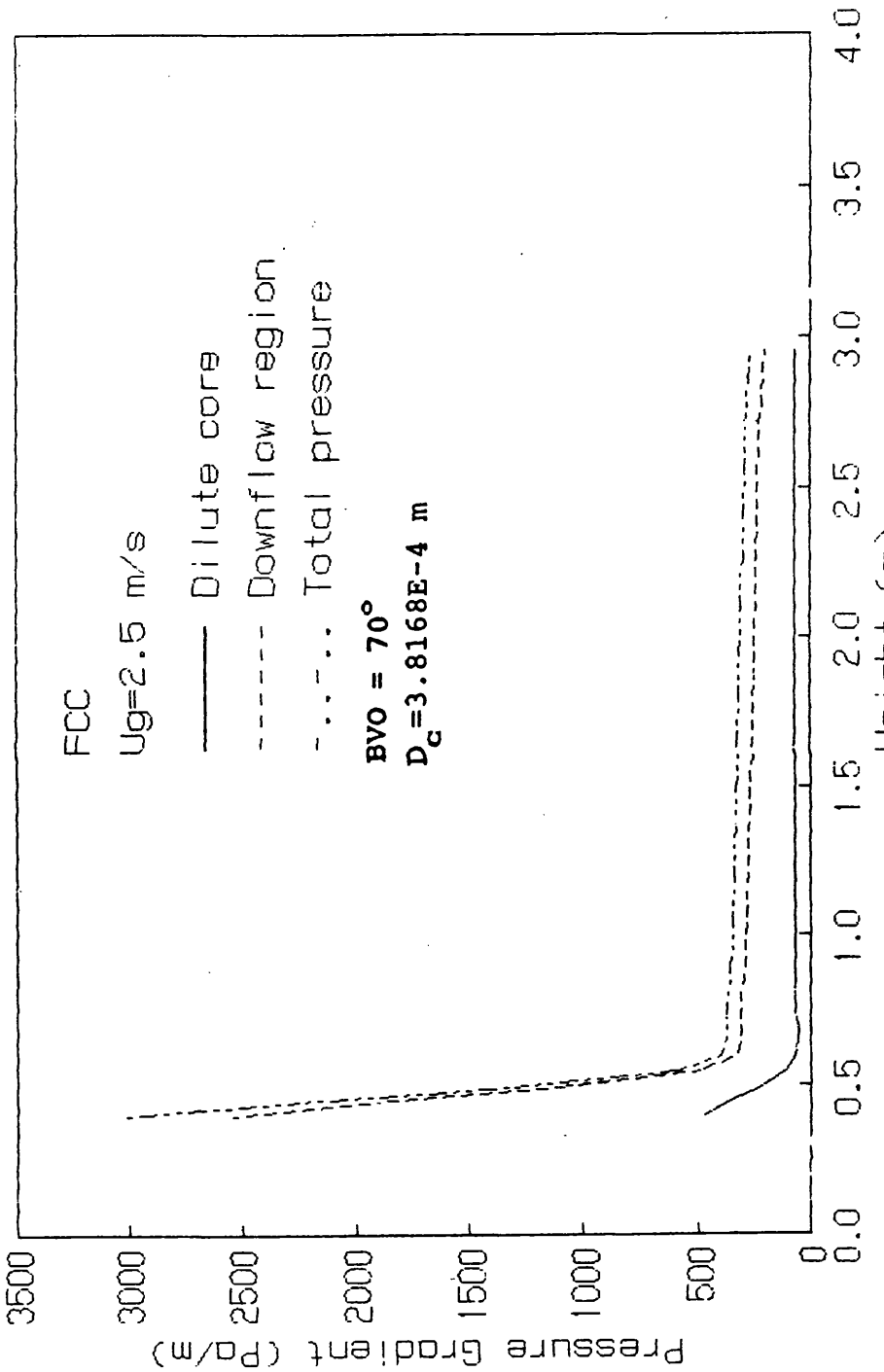

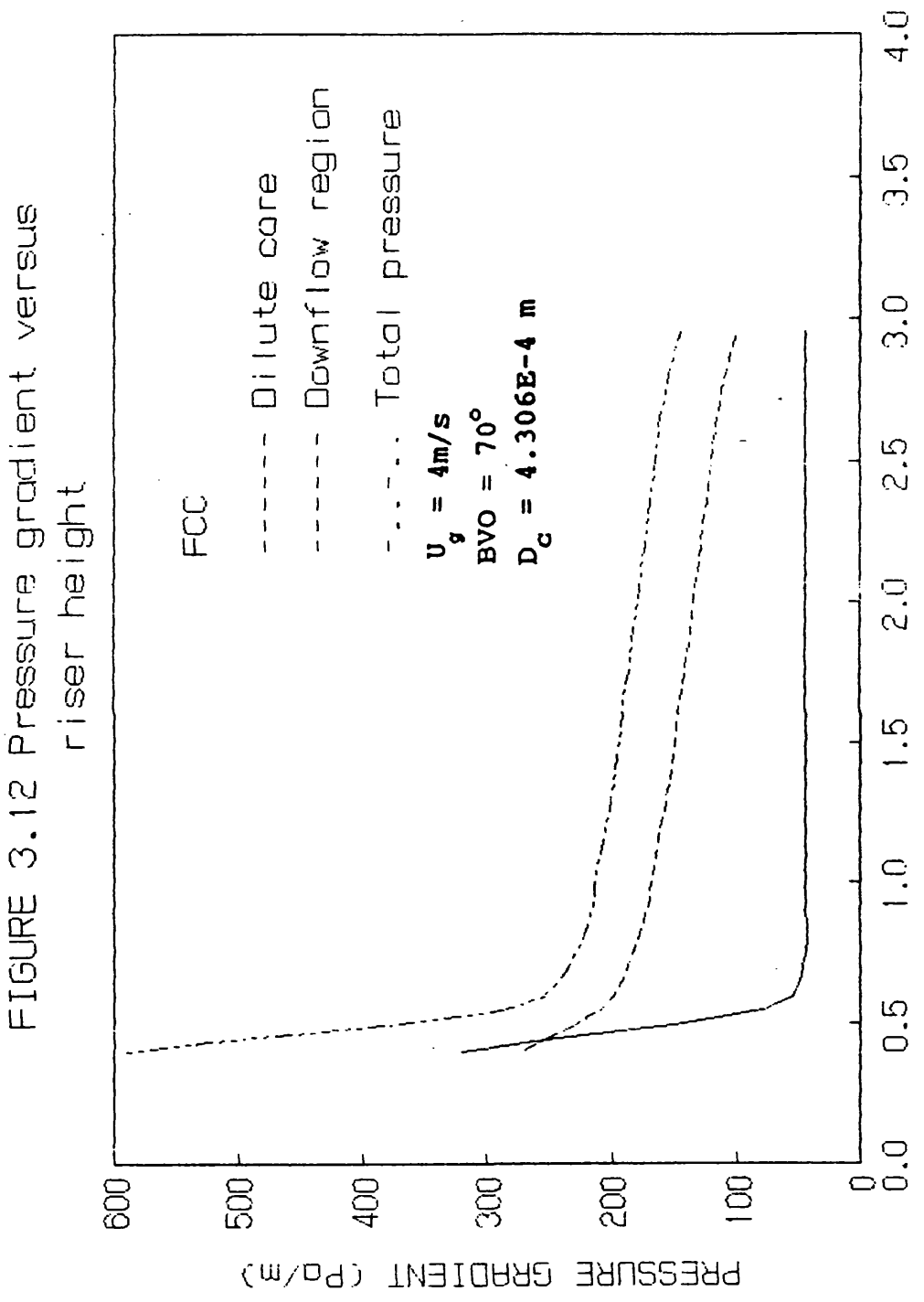

FIGURE 3.12 Pressure gradient versus riser height

CHAPTER 4

EXPERIMENTAL APPARATUS, MATERIALS AND PROCEDURES

Previous research concerning circulating fluidised beds has usually involved gas velocities in the range 1 - 5m/s for Groups A and B powders. The purpose of this experimental study was to extend the range of gas velocity to 4m/s safely entering the fast fluidisation regime, and measure the corresponding pressure profile along the height of the riser.

The pressure drop measurements yielded data that can be used for both qualitative and quantitative comparisons with previous work, as well as providing a means by which to test the "Dense Annulus/Lean Core" model proposed in Chapter Three.

Apart from the gas velocity, the other important independent variable is the opening of the ball valve between the slow bed and the riser. Experiments have been conducted to measure the solid circulation rate, and the changes in the slow bed inventory, as well as the pressure drop for various combinations of gas velocity and ball valve openings.

Data has also been collected to determine the performance of the CFB when using a 50/50 v/v mixture of two different powders.

4.1 THE CIRCULATING FLUIDISED BED SYSTEM

The design of the circulating fluidised bed apparatus is schematically shown in Figure 4.1.1, (front elevation and side elevation).

It consisted of a 50mm diameter, 3m high fast fluidised column, the riser, a solid collecting system and 150mm diameter bubbling bed, the slow bed. The riser was composed of two perspex sections, each 1.5m in height connected to each other by flanges. Pressure tappings located at 0.18m intervals were provided along the riser. The slow bed, also made of perspex, had the purpose of storing solids and providing the force for solid circulation in the system. Fluidised air for the slow bed fed through a porous plate distributor at the side of the bed in order to maintain the solids in the state of minimum fluidisation. Solids fed to the riser by means of a plastic pipe 25 mm in diameter inclined at an angle of 30 degrees. In general the solid circulation rate to the riser was determined by the ball valve installed between the riser and the slow bed as well as by the gas velocity. Three different riser gas distributors were used.

The top of the riser was connected to the inlet of the primary cyclone by a standard elbow. The primary cyclone was designed according to the Stairmand (1959) high efficiency (H.E.) design (see Appendix E) for an operation of 10m/s riser velocity and by assuming that the riser cross-sectional area and the cyclone inlet area are the

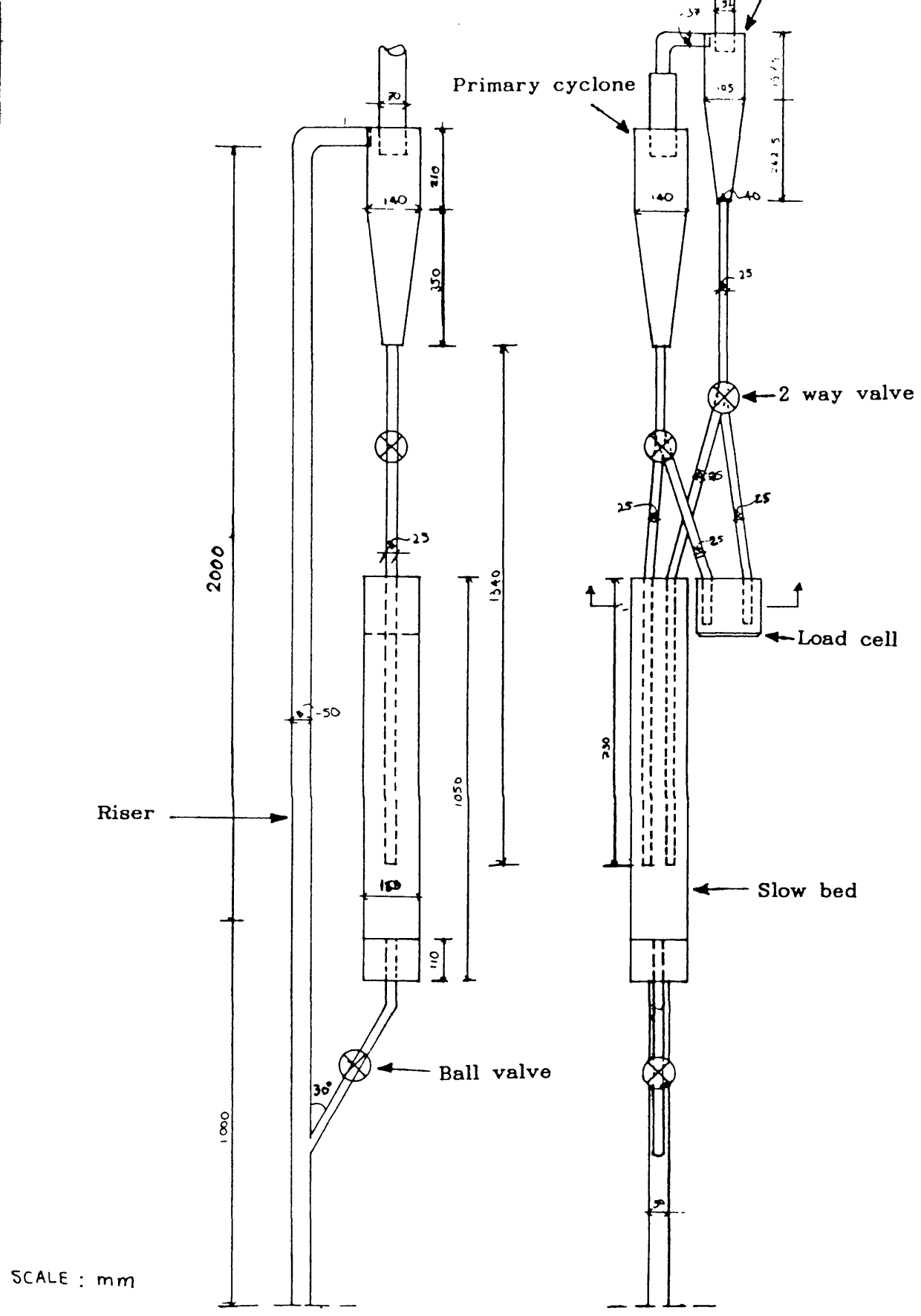

FIGURE 4.1.1 DESIGN OF THE CIRCULATING FLUIDISED BED

same. Solids leaving the primary cyclone were directed either into the slow bed or the load cell system. Diverting two-way valves were placed along the discharge lines of both cyclones to allow accurate solid flowrate measurements to be made. Gas leaving the primary cyclone was fed into the secondary cyclone which was also based on the Stairmand H.E. design by considering that the cyclone efficiency may be improved if the pressure drop inside this cyclone does not exceed the upper pressure drop limit of 1200 N/m^2, as recommended by Svarovsky (1986).

Both cyclones were fabricated from copper. Gas leaving the secondary cyclone was discharged into a duct.

The air was taken from the laboratory compressed air supply and air flowrates were measured using rotameters.

The design of the ball valve (Figure 4.1.2) was such that between 0 and 15 degrees there was no opening and consequently no possible solids flow. There was need to determine the open area of the ball valve at a particular angle ϕ of the stem. The ball valve was fully open at 90 degrees (ϕ_{max}). The minimum opening was 15 degrees (ϕ_{min}). Diameter of ball valve, D_v = 25 mm. Assume that

$$\frac{D_v}{90 - \phi_{min}} = 2x$$

Then 25/75 = 2x = 0.33 mm/degree

Hence x = 0.167 mm/degree

CASE I 2x < R

For an angle $\phi > \phi_{min}$

1) Find 2x

2) Find distance y = R - 2x

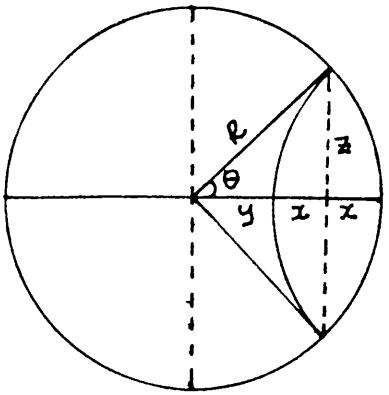

3) Find $\cos\theta = \frac{y + x}{R}$

4) Find θ in degrees

5) Calculate sector area $\frac{2\theta}{360}\pi R^2$

6) Calculate $z = (R^2 - (x+y)^2)^{0.5}$

7) Calculate open area

$$A_{op} = 2 \left[\left[\frac{2\theta}{360} \right] \pi R^2 - z\,(x+y) \right] \qquad 4.1$$

CASE II 2x > R

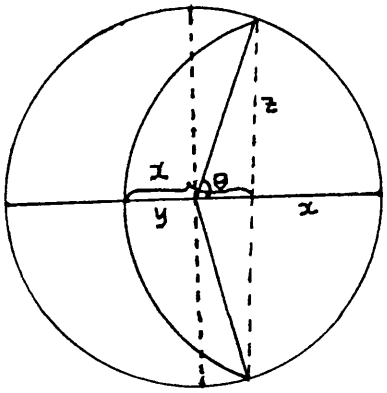

Radius of ball always constant.

Symmetry applicable.

x = 0.167 mm/degree

y = 2x - R

Use the same algorithm to determine the open area.

For an angle $\phi > \phi_{min}$, $\phi > 15$

(1) Find 2x

(2) Calculate $y = 2x-R$

(3) Calculate $z = R^2-(x-y)^2$

(4) Find $\sin\theta = z/R$

(5) Find θ in degrees

(6) Calculate the sector area $\frac{2\theta}{360}\pi R^2$

(7) Calculate the open area

$$A_{op} = 2 \left[\frac{2\theta}{360}\pi R^2 - z(x-y) \right] \qquad 4.2$$

$$2x = \frac{0.167}{90-\phi}$$

The open area of the valve, A_v is related to the angle ϕ,

from equations 4.1 and 4.2. A non-linear regression of the calculated values of A_v, gives the following expression:

$$A_v = 1.29\ (\phi)^{1.38} \qquad 4.3$$

Above 15 degrees the area of the opening can be calculated from equation 4.3. For the range of gas velocities used in this study, operation of the CFB with a ball valve opening greater than 70 degrees, led to an unstable situation caused by flow reversal of solids through the ball valve.

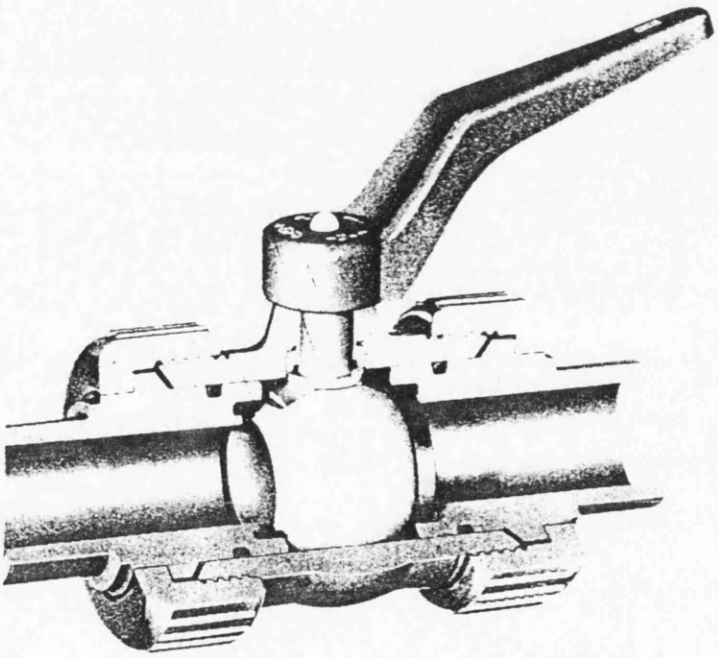

FIGURE 4.1.2 DESIGN OF THE BALL VALVE

4.2 POWDERS USED

The powders used in the 50mm diameter riser of the circulating fluidised bed were; calcined FCC silica alumina, Paralox and a 50/50 v/v mixture of the two. The mean particle sizes were determined by using a sieve analysis. The densities of particles were measured using mercury pychnometry. This method involved the following steps: a) cells were filled with mercury and weighted b) cells were emptied and cleaned and a known weight of sample was introduced to the cell c) the cell with the sample was placed under vaccuum to exclude all the air d) mercury was introduced into the cell by releasing the vaccuum e) the cells were then re-weighted and f) the density of the sample ρ_s was estimated as following:

$$\rho_s = \frac{W_s}{W_s - (W_{sHg} - W_{Hg})}$$

where: W_s is the weight of the sample

W_{sHg} is the weight of the sample and mercury

W_{Hg} is the weight of mercury.

Values of relevant particle properties are given in TABLE 4.2.1.

	FCC	PORALOX
d_p (μm)	64	127
ρ_p (kg/m^3)	884	1850
U_{mf} (m/s)	1.36E-2	1.6E-2

TABLE 4.2.1.
Properties of powder used

4.3 PRESSURE DROP EXPERIMENTS

4.4.1 APPARATUS

For this series of experiments, the circulating fluidised bed described in section 4.1, was used.

4.4.2 MATERIALS

The pressure drop experiments were conducted with three different powders all of them belonging to Group A according to Geldart's classification. The properties of these powders are shown in Table 4.2.1

4.4.3 PROCEDURE

The riser was first emptied of solids by conveying any remaining powder into the slow bed by suppling a large air velocity. The required air velocity, U_g, for the experiment was then set constant using one of the rotameter valves, and the ball valve was set to a particular angular opening. This allowed a flow of solids to run into riser. The system was then allowed to settle to a steady state which deemed to exist when the solid height in the slow bed shows no variation with time.

Normally, when making any change to the operation of the CFB (either by altering U_g or ball valve opening), approximately half an hour was required before the system approached steady state.

While the system approached a new steady state, pressures within the riser cause backpressures on the piping upstream of the distributor, causing fluctuations to the rotameter reading. This required slight adjustments to be made to ensure that the desired flowrate of air was admitted to the riser.

Confirmation that the steady state been achieved came from monitoring manometer levels and the height of the slow bed. After steady state achieved, the pressure profile determined by recording each of the 15 pressure tappings along the riser.

The pressures were detected using U-tube manometers filled with water dyed with rhodamine. The difference in the water levels in each arm of the U-tube was measured with a graduated scale with measurements made to the nearest millimeter.

4.4 SOLID CIRCULATION RATE EXPERIMENTS

4.4.1 APPARATUS

For this series of experiments, the circulating fluidised bed described in section 4.1, together with the load cell system used.

4.4.2 MATERIALS

The solids used for these sets of experiments are shown in Table 4.2.1.

4.4.3 PROCEDURE

With a desired gas velocity U_g, and ball valve opening ϕ_{BVO}, the CFB allowed to achieve steady state. The two-way valves (see Figure 4.1.1) manipulated to divert the solids through flexible tubing to a vessel supported by a platform which in turn formed part of the load cell apparatus, shown in Figure 4.4.1.

The deflection caused by the weight on the load cell measured by a chart-recorder. This recorder was previously calibrated using the procedure explained in section 4.5. Knowing the weight on the load cell and the time that had ellapsed since the solids were diverted then the rate at which the solids circulated through the CFB was estimated. It should be noted that the weight recorded by the load cell was also a function of the distance between the cell and the pivot. This means that the weight has to be divided by 5.

The diversion of solids via the two-way valve disrupted the steady state operation of the CFB, because of the intrusive nature of the sampling technique. This means that a balance had to be achieved so that the diversion of solids took place for a long enough period to record a reproducible deflection on the chart-recorder, but whilst also ensuring that the diversion should not continue for so long that the CFB allowed to deviate marketly from its original steady state condition. In practice, this

diversion of solids was allowed for approximately 15 seconds.

4.5 CALIBRATION OF LOAD CELL

The load cell was connected to the chart-recorder. The chart-recorder was set up to 10mV and 30mm/min. In order to obtain a direct calibration of the load cell, a known weight was added periodically on top of the vessel, and the deflection caused by the additional weight was recorded on paper.

Readings of the chart-recorder paper produce the deflection of weight in terms of mV, mm of paper and time.

A graph of the chart-recorder readings in millivolts is plotted against the known weight in grams. The staight line equation is given by:

$$(mV) = A\ (Weight) + C$$

A is the slope of the line

$A = 2.91E\text{-}3\ mV/g$

C is the intercept, set to zero by adjusting the chart-recorder and corresponds to the value of the vessel weight.

SPECIFICATION OF THE LOAD CELL

The load cell made within the Chemical Engineering Department. It contained strain guages which respond to changes in the electrical resistance of the metal within the load cell.

The maximum load of the load cell was estimated to

correspond to 16mV equivalent to 0.9 kg weight.

4.6 RISER DISTRIBUTOR DESIGNS

Three different designs of riser distributor were used with the same fraction of free open area of 4%, but with a variable number of orifices.

Riser Distributor No.1: 1 nozzle centrally located of id=10mm.

Riser Distributor No.2: 7 orifices,each one of id=3.8mm, arranged in a triangular pitch.

Riser Distributor No.3: 13 orifices, each one of id=2.8mm, arranged in atriangular pitch.

Designs of the riser distributors 1, 2 & 3 are presented in Figure 4.6.1.

correspond to 16mV equivalent to 0.9 kg weight.

4.6 RISER DISTRIBUTOR DESIGNS

Three different designs of riser distributor were used with the same fraction of free open area of 4%, but with a variable number of orifices.

Riser Distributor No.1: 1 nozzle centrally located of id=10mm.

Riser Distributor No.2: 7 orifices,each one of id=3.8mm, arranged in a triangular pitch.

Riser Distributor No.3: 13 orifices, each one of id=2.8mm, arranged in atriangular pitch.

Designs of the riser distributors 1, 2 & 3 are presented in Figure 4.6.1.

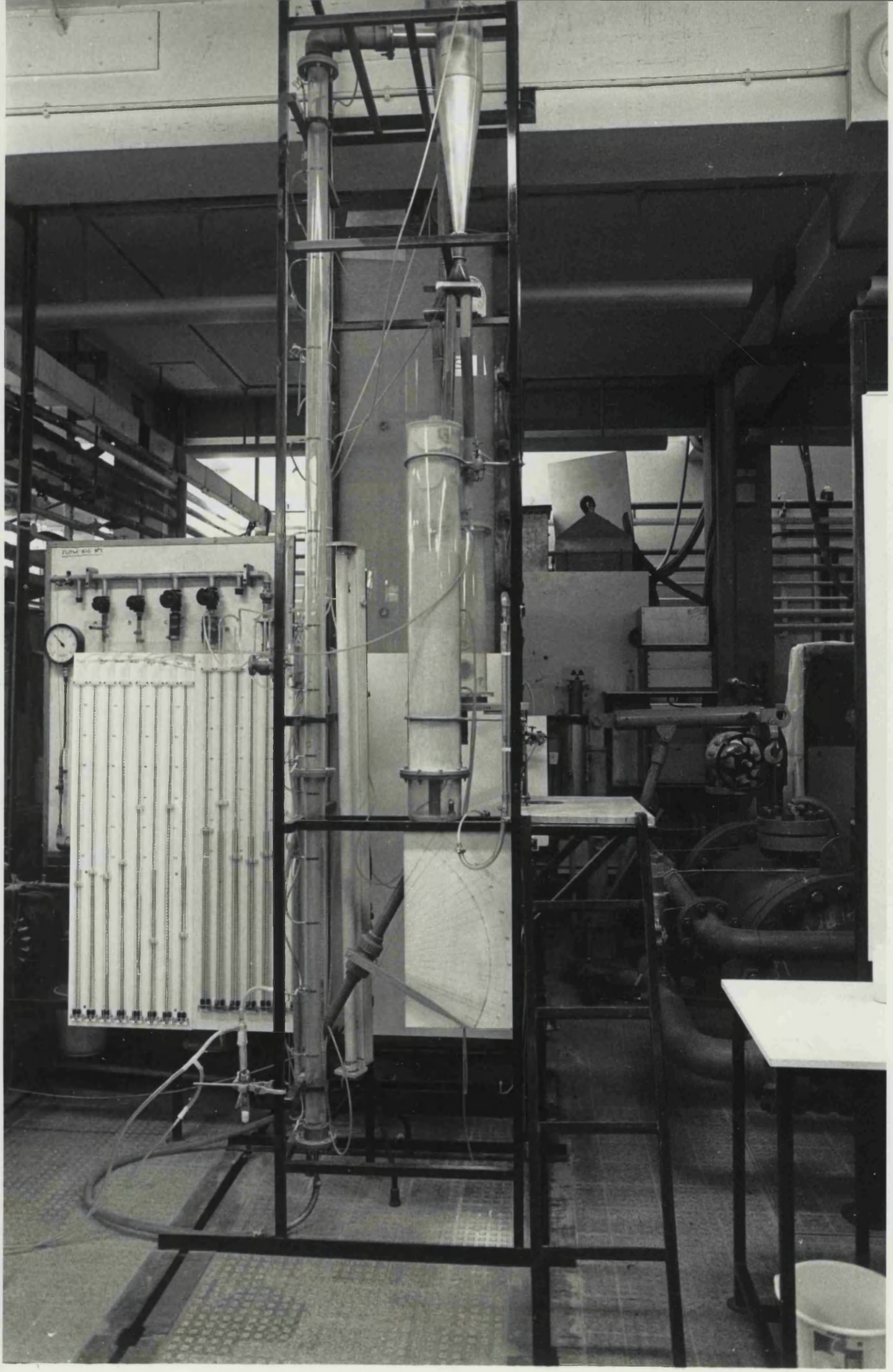

CHAPTER 5

RESULTS AND DISCUSSION

5.1 INTRODUCTION

This chapter describes experiments carried out in a circulating fluidised bed to investigate (1) the effect of the inventory on the solid circulation rate, slow bed height, pressure profiles and voidage and (2) the effect on riser pressure drop and the solid circulation rate of the four main design variables of the system:

a) Distributor Design

b) Gas Velocity

c) Ball Valve Opening and

d) Particle Properties.

The results of these experiments are then compared with the "Dense Annulus/Lean Core" model developed in Chapter Three to test its accuracy and predictions. The model is then applied to the case in which a first order reaction is taking place in the riser of a CFB.

5.1.1 Effect of bed inventory on solids circulation rates and slow bed height.

The solids circulation rates and slow bed heights measured at each of the five ball valve openings are plotted in Figures 5.1.1.1 and 5.1.1.2. Four bed inventory levels in the range of 21 to 60 cm were used and for each inventory and constant gas velocity, the solids circulation rates and slow bed heights were measured.

FIGURE 5.1.1.1 SOLID CIRCULATION RATE VERSUS BALL VALVE OPENING

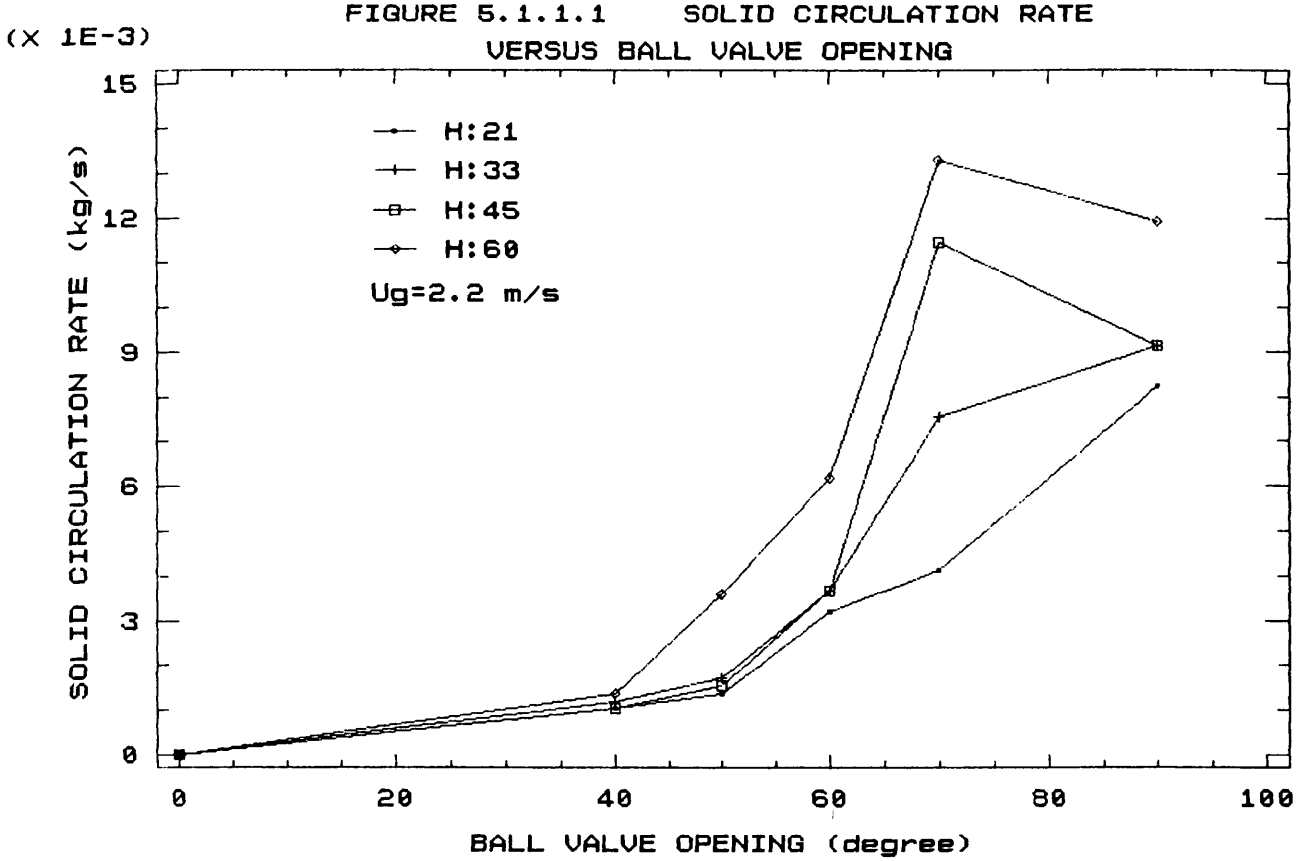

FIGURE 5.1.1.2 SLOW BED HEIGHT VERSUS BALL VALVE OPENING

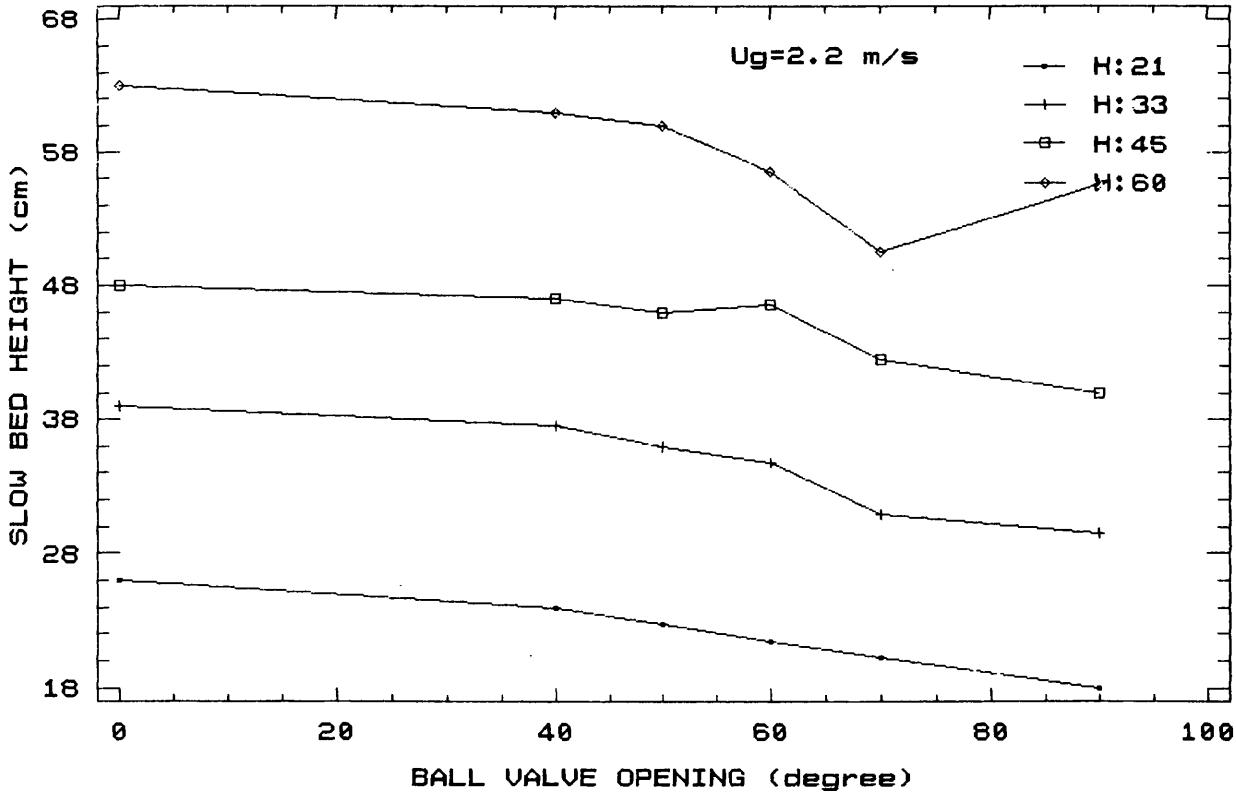

At constant slow bed inventory level as the opening of the ball valve increases the solid circulation rate (SCR) also increases. This increase of SCR is significantly higher at the inventory levels of 45 and 60 cm.

The slow bed height at a constant inventory level decreases slowly by increasing the ball valve opening. The change in the slow bed height, from its initial position, has a mean average value of 0.1 cm/degree for the four different inventory levels. Although the decrease of the slow bed height is small for the four different inventory levels, at a nearly constant value, the inventory levels clearly affect the flow in the riser and increase the solid circulation rate.

5.1.2 Effect of inventory and ball valve opening (BVO) on pressure profiles around the system

The pressure profiles around the fluidisation system may be generalised into three diagrams as shown in Figures 5.1.2.1 a-c.

Three different slow bed inventories were chosen in the range of 33 to 60 cm and four openings of the ball valve, at a constant gas velocity of 2.2 m/s.

When the ball valve is fully opened (BVO=90) the pressure profiles around the system for the three different inventories are of the same form as is shown in Figure 5.1.2.1b.

The higher pressure drop is located just below the ball valve due to acceleration effects that are present at the

bottom of the column. On the other hand, the pressure drop in the exit section of the bed decreases with the increase of inventory. Hence the bed height in the riser increases. If however, the gas velocity in the riser is increased to higher values at constant BVO and inventory this height will reduce to zero not only because of the flow conditions but also because of the constraints of the equipment.

A completely different picture is now presented, Figure 5.1.2.1a and 5.1.2.1c, if the solid flow is restricted by means of the ball valve.

At the lower inventory levels (33 or 45 cm) and low openings of the ball valve (50 or 60) the system behaves as shown in Figure 5.1.2.1c. The pressure drop values above and below the ball valve are lower than those corresponding to the riser side. This means that the gas entering the riser at high velocity has two paths; an upward movement through the riser and a diverted upward movement through the valve. This is not desirable because it prevents the solids flow in the riser and disturbs the equilibrium of the system.

For the highest inventory level of 60 cm and all restrictions to the solid flow due to the ball valve, Figure 5.1.2.2a represents the pressure balance around the system. Because of the pressure drop across the valve, the maximum pressure is located above the valve. The bed height in the riser increases by increasing the BVO and obviously it will decrease if higher gas velocities are used.

The pressures at the lowest part are identical which

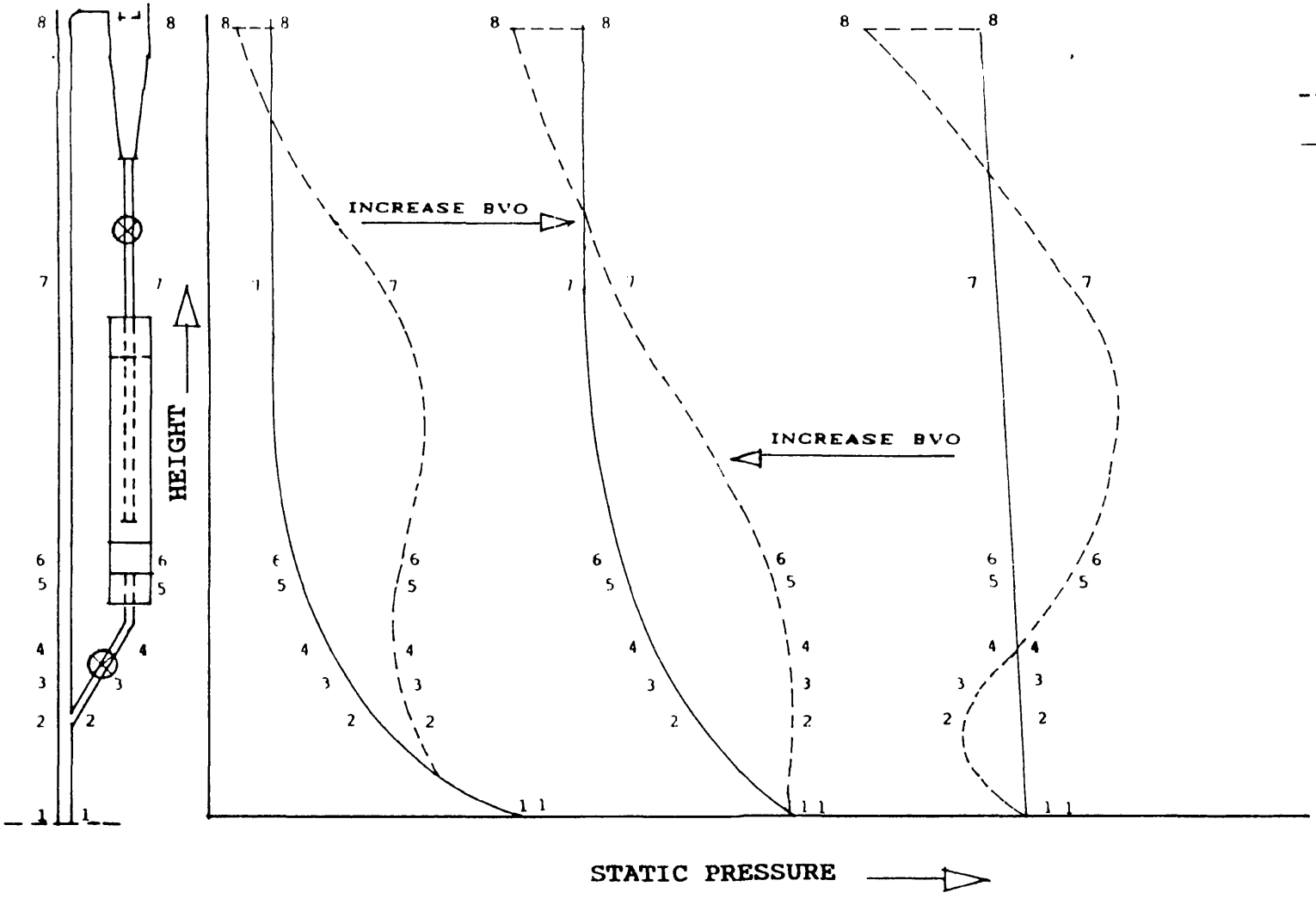

FIGURE 5.1.2.1 PRESSURE PROFILE AROUND THE CFB

means that the solid is falling in free fall from the ball valve to the riser.

Therefore, for safe operation of the riser reactors, the pressure profiles shown in Figure 5.1.2.1c should be avoided at all costs.

Based upon the above information, for the safe operation of the riser of a circulating fluidised bed, it was decided to operate the riser at a slow bed inventory of 60 cm.

5.1.3 Effect of the inventory and ball valve opening (BVO) on the voidage profiles

The pressure drop measurements are converted into voidage ε by assuming no acceleration or frictional effects and by using the equation:

$$\frac{\Delta P}{\Delta L} = (1-\varepsilon)\rho_s \, g$$

ΔP is the pressure difference between succesive pressure tappings and ΔL the distance apart.

The voidage profiles along the riser, for constant superficial gas velocity of 2.2 m/s, constant opening of the ball valve and various slow bed inventory levels in the range of 21 to 60 cm are shown in Figures 5.1.3.1a-b.

Each plot presents the axial profiles for 4 different inventory levels of the slow bed at constant gas velocity and BVO.

At the lower BVO of 60 only the highest inventory shows an inflection point and the presence of both dense and dilute phases. At this BVO, the voidage profiles of the lower inventory levels (ie 21, 33 and 45 cm) are constant

FIGURE 5.1.3.1a
VOIDAGE VERSUS RISER HEIGHT

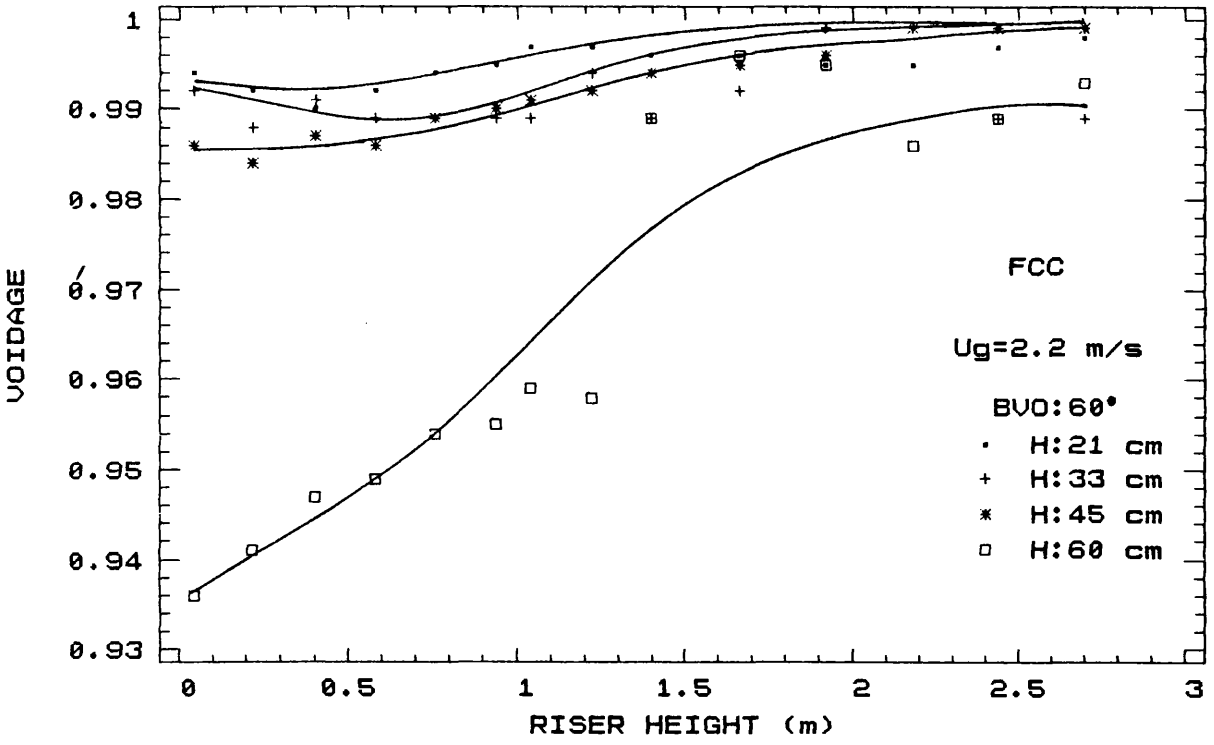

FIGURE 5.1.3.1b
VOIDAGE VERSUS RISER HEIGHT

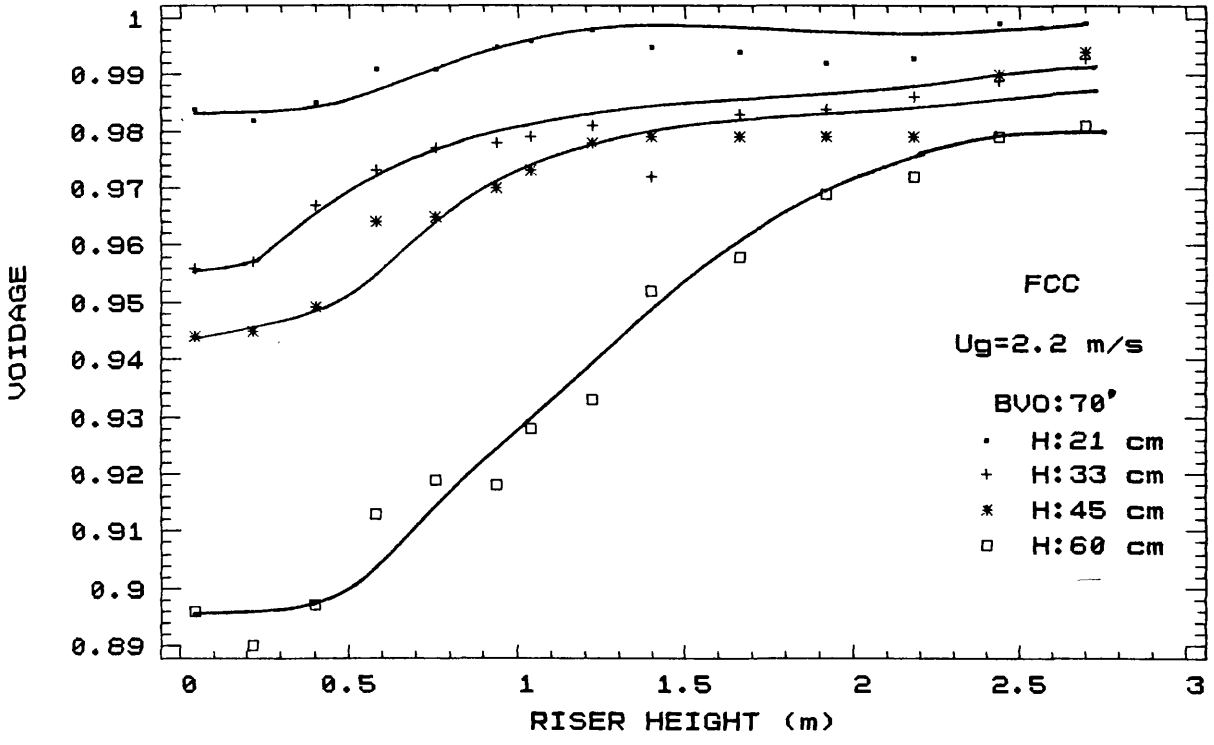

along the riser which operates in the dilute phase transport regime Figure 5.1.3.1a. The higher the BVO, and hence the higher the solids circulation rate, the higher the position of the inflection point, Figure 5.1.3.1b. The increased inventory imposed a greater pressure drop on the riser which was shown by the bed filling with dense phase. The dense phase regions in the riser have solids fractions of 0.15-0.05 characteristic of the fast fluidisation regime while the dilute phase region has solid fractions of about 0.03.

This finding is in contradiction to that of Rhodes et al. (1987) ie the inventory of solids has no effect on the axial profiles in the riser at constant values of U_g and solid circulation rate (SCR). The reason for such a difference might be due to the ball valve used in this work to control the solid rate. Weinstein et al. (1984) reported that the axial solids profiles are independent of the solids inventory but are dependent on solids rate and gas velocity.

As we already reported, at constant U_g, the solid circulation rate increases with the BVO and slow bed inventory level. Since the axial solids profiles are dependent on solids rate and the solids circulation rates are increased with the increase of the slow bed inventory therefore it would seem that the axial solids profiles in the riser will be affected by the inventory level of the slow bed.

5.2 EFFECT OF DISTRIBUTOR DESIGN ON PRESSURE DROP AND SOLID CIRCULATION RATE

The effect on pressure drop and solid circulation rate of the different design of distributors mentioned in Chapter 4 will now be discussed.

5.2.1 EFFECT ON PRESSURE DROP

The pressures recorded at each of the 13 pressure tappings, above the solids inlet, along the riser are plotted in Figures 5.2.1 to 5.2.18. Six gas velocities in the range 1.5 to 4 m/s were used and at each velocity four openings of the ball valve (BVO), shown as the parameter BVO on the plots, in the range 40 to 70 degrees were studied for the FCC powder. From these observations the following conclusions may be drawn:

(a) For a given gas velocity as the ball valve opening is increased the pressure drop between adjacent pressure tapping in the riser also increases for all three designs of distributor.

(b) The rate of change of pressure drop decreases with riser height, at constant gas velocity, for each one of the three riser distributors.

(c) At low values of the ball valve openings (BVO<60), the pressure profile is relatively flat along the entire height of the riser and decreases slightly with the riser height. This is demonstrated very clearly for all distributor designs in Figures 5.2.1 to 5.2.18.

(d) Visual observations indicate that the relatively flat pressure profile corresponds to the fact that the riser is

operating in the dilute phase mode. In this mode, the particles are moving upwards in relatively straight lines with the absence of any significant downflow.

(e) As the ball valve opening increases (BVO>60), there is a marked increase in the pressure drop at the bottom part of the riser and a levelling off near the top. Under these conditions a dense slugging phase is formed in the lower part of the riser and strong fluctuations are observed in the pressure drops. Further up the riser the solid particles appear to be divided into two phases, a dense phase near the riser wall where particles are falling downwards and a dilute core in the centre of the column where particles are transported upwards.

(f) At higher gas velocities a large increase of solid circulation and hence concentration by increasing the ball valve opening is required to bring the riser into the dense phase transport regime. This dense phase region which occupies the lower part of the riser remains nearly constant for values of the ball valve openings greater than 60 degrees.

By increasing the gas velocity from 1.5 to 4 m/s each pressure profile plot consists of two regimes, a lower regime at low ball valve openings where the pressure profile is flat and decreases only slightly with the height, and an upper regime where there is an initial sharp decrease of pressure drop with the height.

The axial pressure profile measurements have been performed along the riser for several operation conditions.

For the air gas velocities of 1.5 and 2m/s and the seven hole distributor, the profiles are shown in Figures 5.2.7 and 5.2.8. From these curves the existence of three different sections, according to Monceaux et al. (1985), can be present: a) the acceleration section at the bottom of the riser b) a section of constant pressure gradient which is characteristic of a fully-developed pipe flow and c) a disengagement section where the pressure gradient is lower than that in fully-developed flow section, and appears only for high loading ratios.

The shape of the pressure profile changes slightly with the ball valve opening and hence with solid flowrates. Although Monceaux et al. (1985) presented a linear pressure profile at Ug=2.7m/s, the profiles showing in Figures 5.2.7 and 5.2.8 are not linear. They explained the non-linearity due to the increase of the lengths of acceleration and disengagement regions as the solid flowrate increases. They also claimed the disappearance of the fully-developed region at sufficiently high solid flowrates.

The axial pressure profiles are in agreement with those reported by Yerushalmi et al.(1976), Weinstein et al. (1982). Li et al. (1980) observed a transition from a high concentration at the bottom of the riser to a low concentration at the top with an inflection point in between the two regions. Monceaux et al. explained the inflection point as being due to the fact that the acceleration length becomes very large and even sometimes the fully-developed flow is not obtained.

FIGURE 5.2.1 RISER DISTRIBUTOR:1 NOZZLE
PRESSURE DROP VERSUS RISER HEIGHT

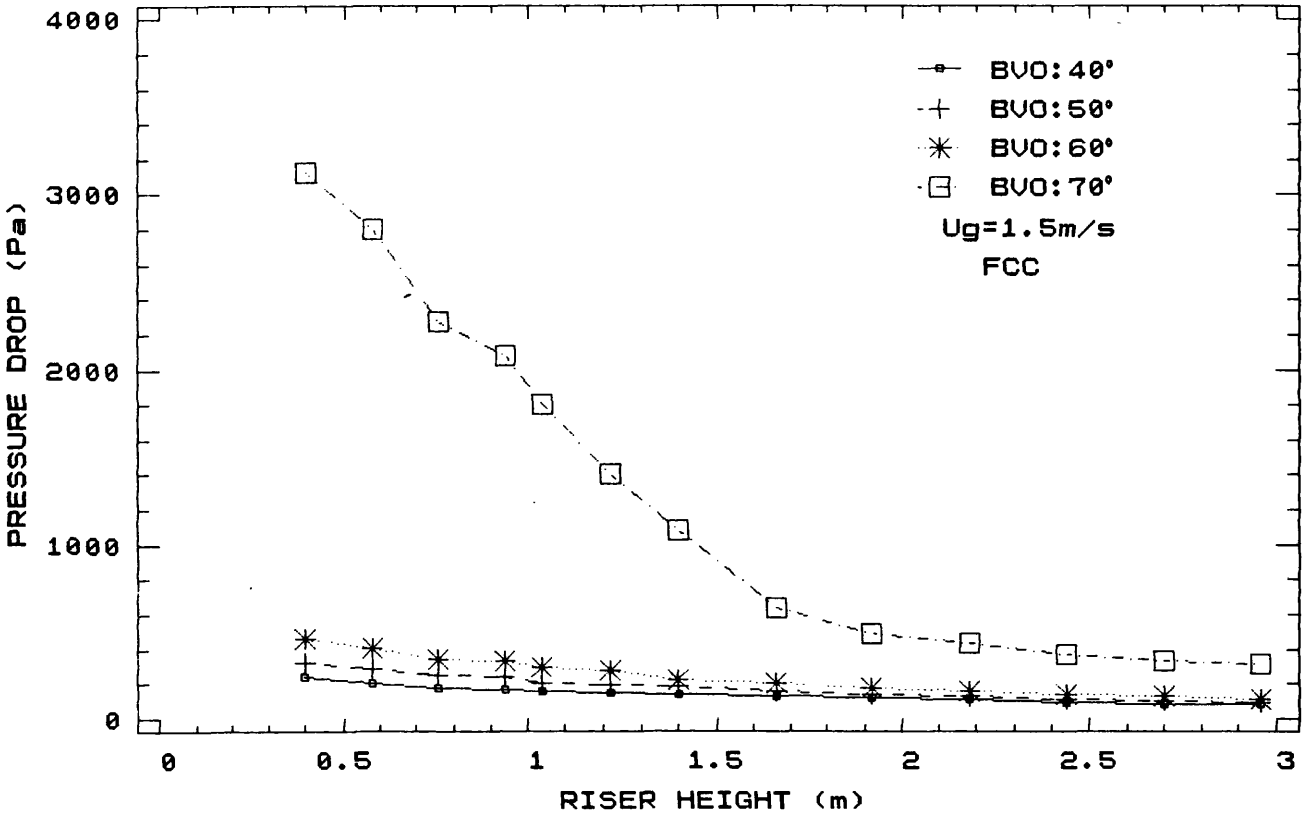

FIGURE 5.2.2 RISER DISTRIBUTOR:1 NOZZLE
PRESSURE DROP VERSUS RISER HEIGHT

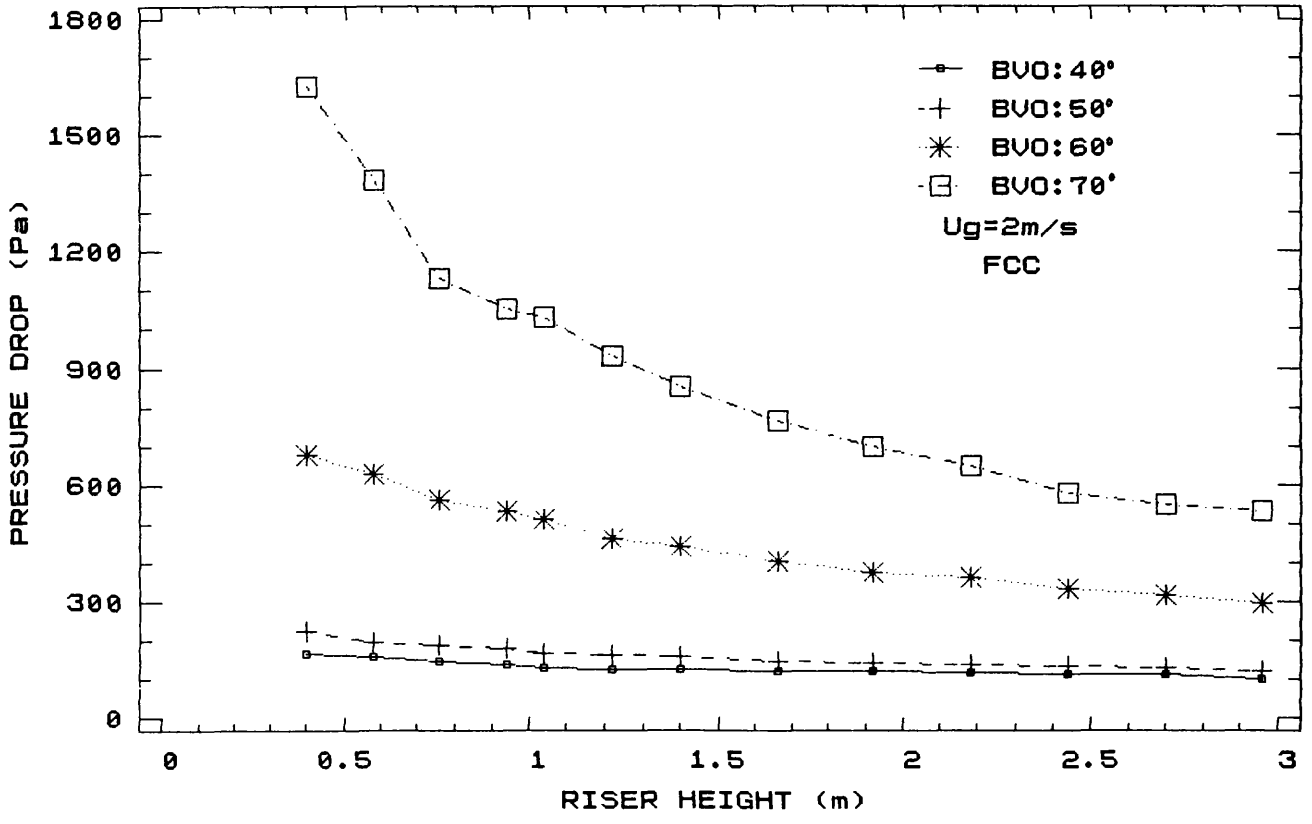

FIGURE 5.2.3 RISER DISTRIBUTOR:1 NOZZLE
PRESSURE DROP VERSUS RISER HEIGHT

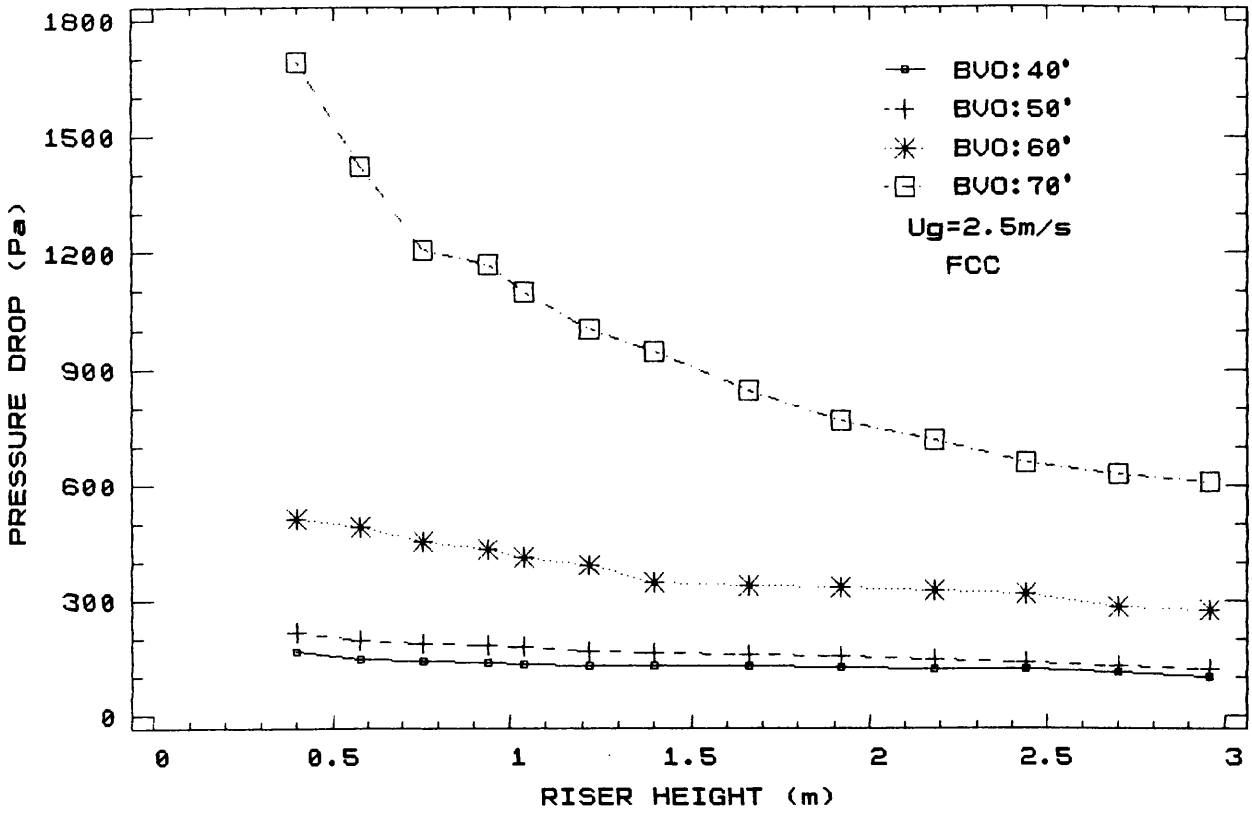

FIGURE 5.2.4 RISER DISTRIBUTOR:1 NOZZLE
PRESSURE DROP VERSUS RISER HEIGHT

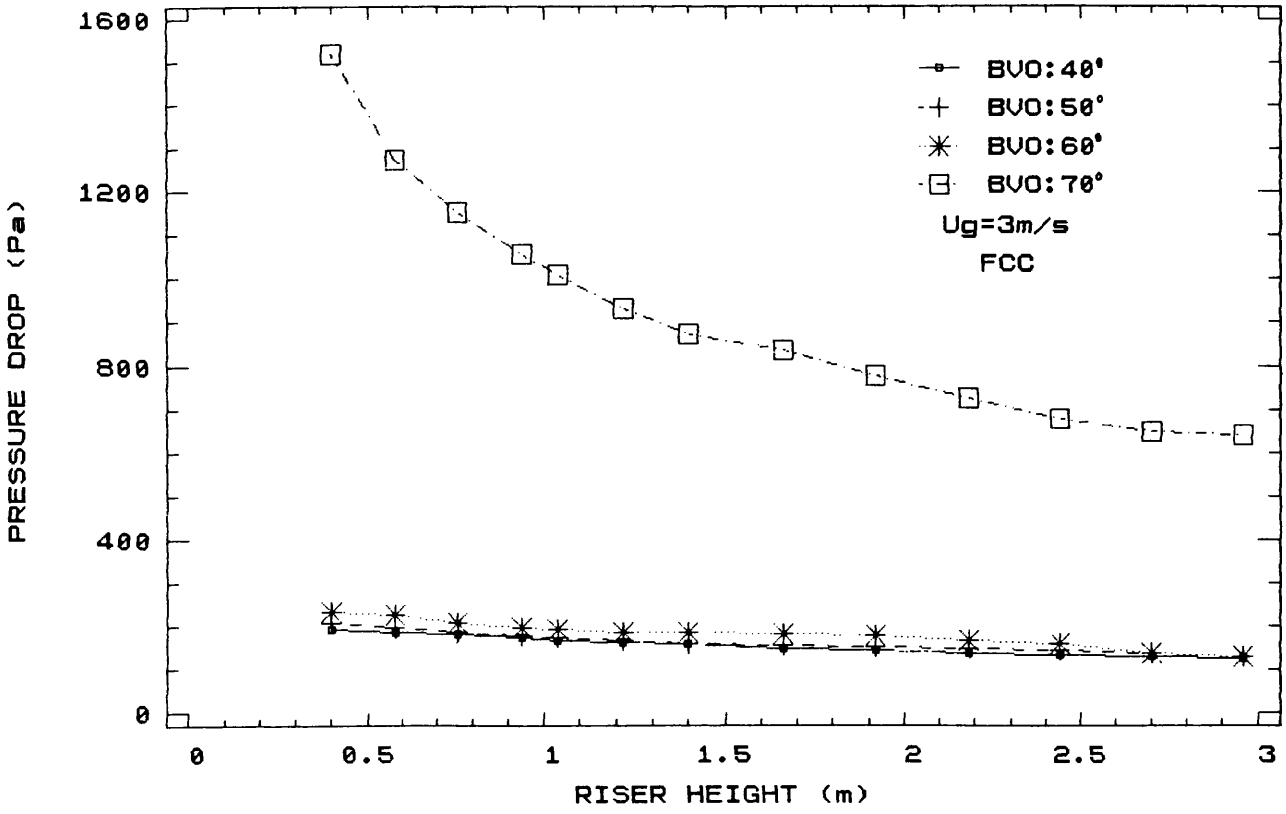

FIGURE 5.2.5 RISER DISTRIBUTOR:1 NOZZLE
PRESSURE DROP VERSUS RISER HEIGHT

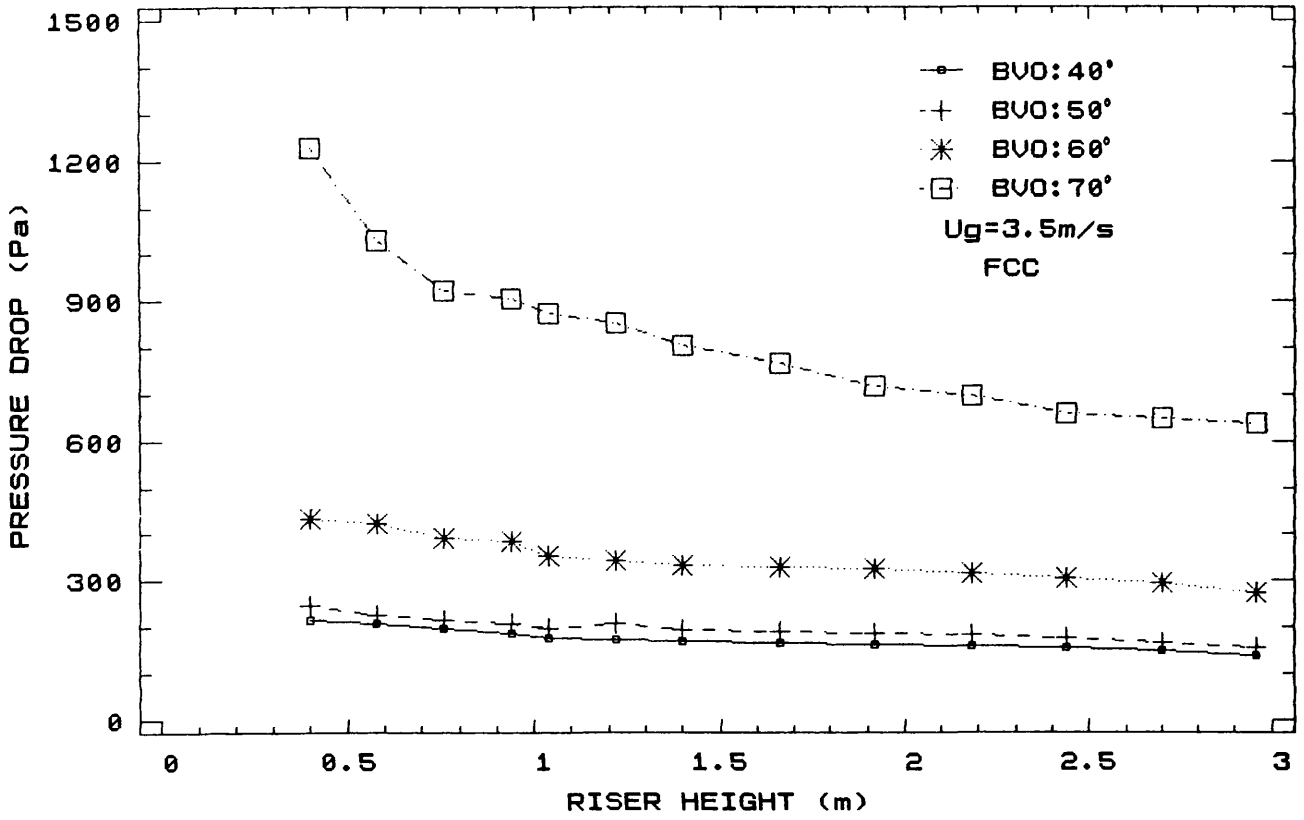

FIGURE 5.2.6 RISER DISTRIBUTOR:1 NOZZLE
PRESSURE DROP VERSUS RISER HEIGHT

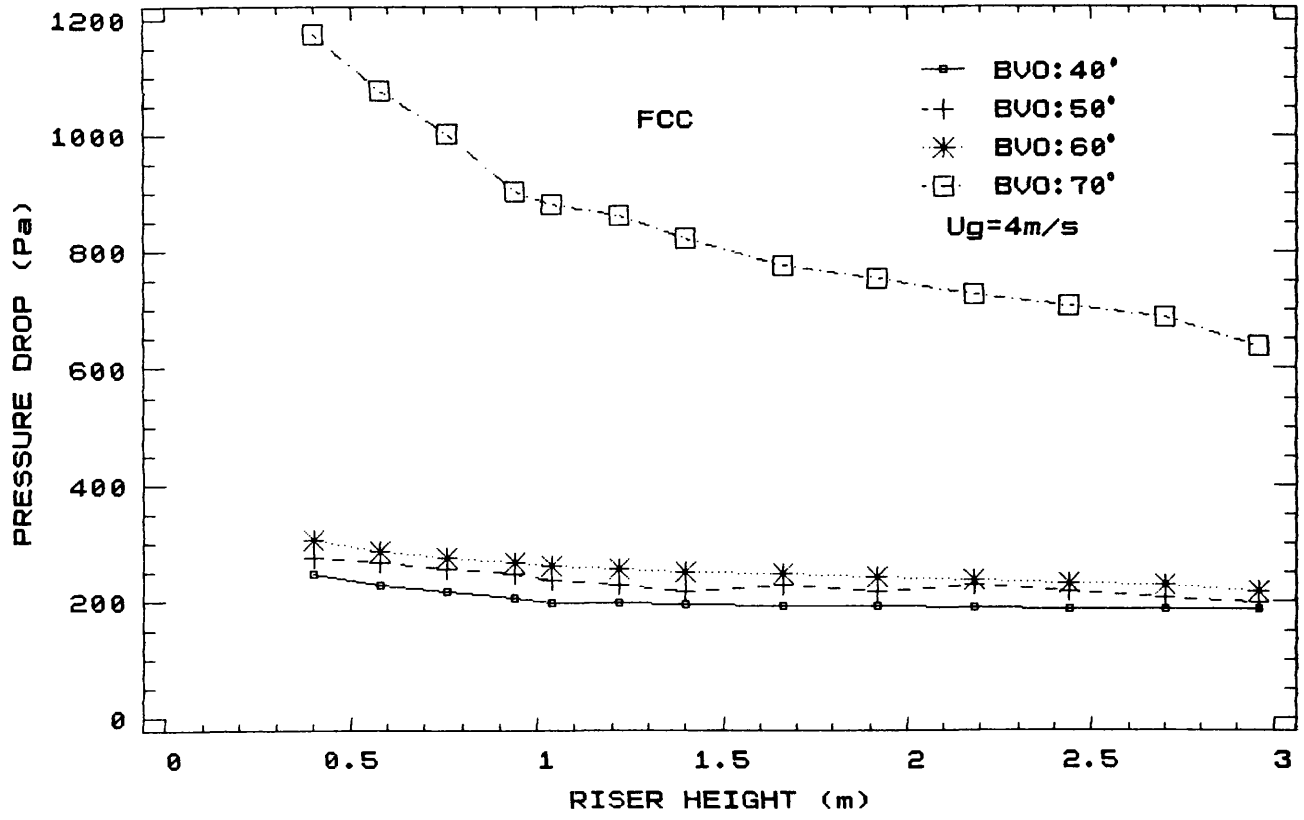

FIGURE 5.2.7 RISER DISTRIBUTOR:7 HOLES
PRESSURE DROP VERSUS RISER HEIGHT

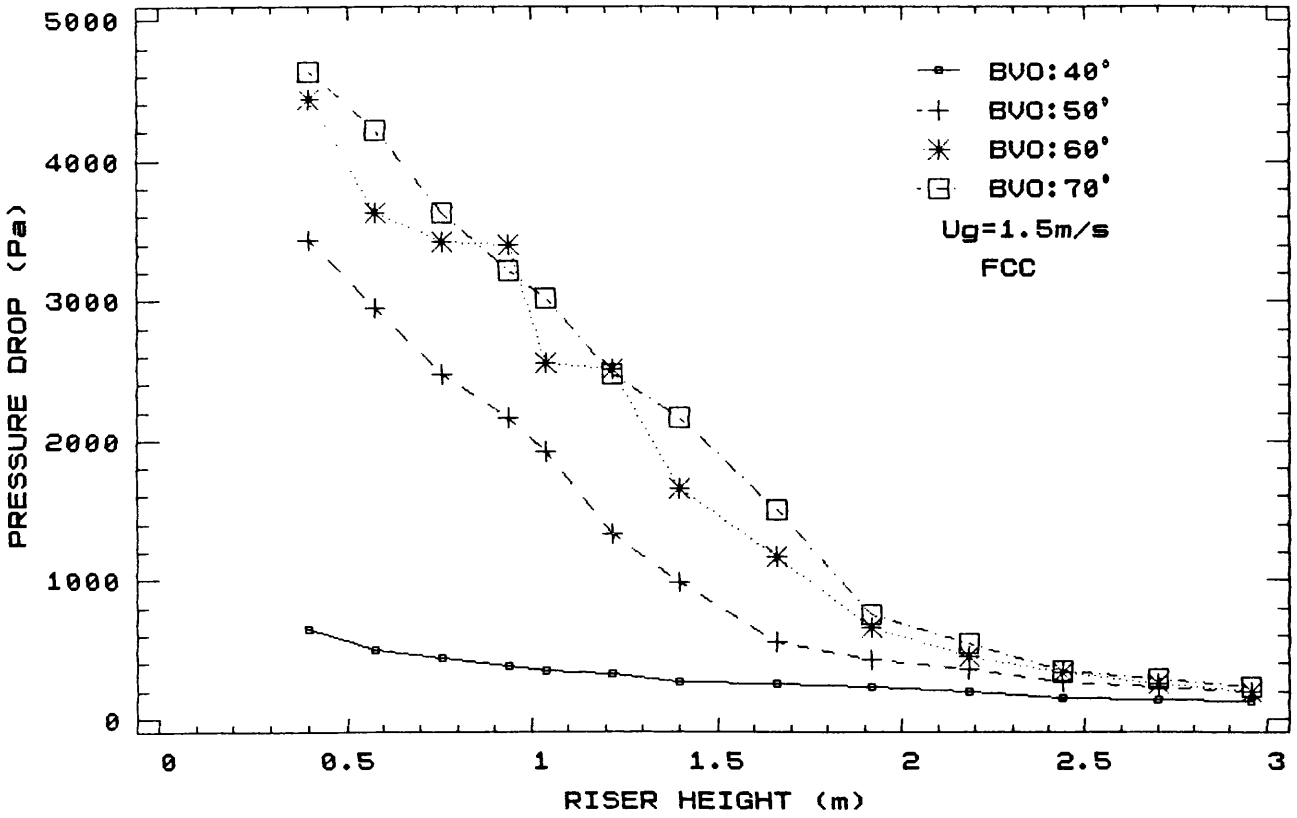

FIGURE 5.2.8 RISER DISTRIBUTOR:7 HOLES
PRESSURE DROP VERSUS RISER HEIGHT

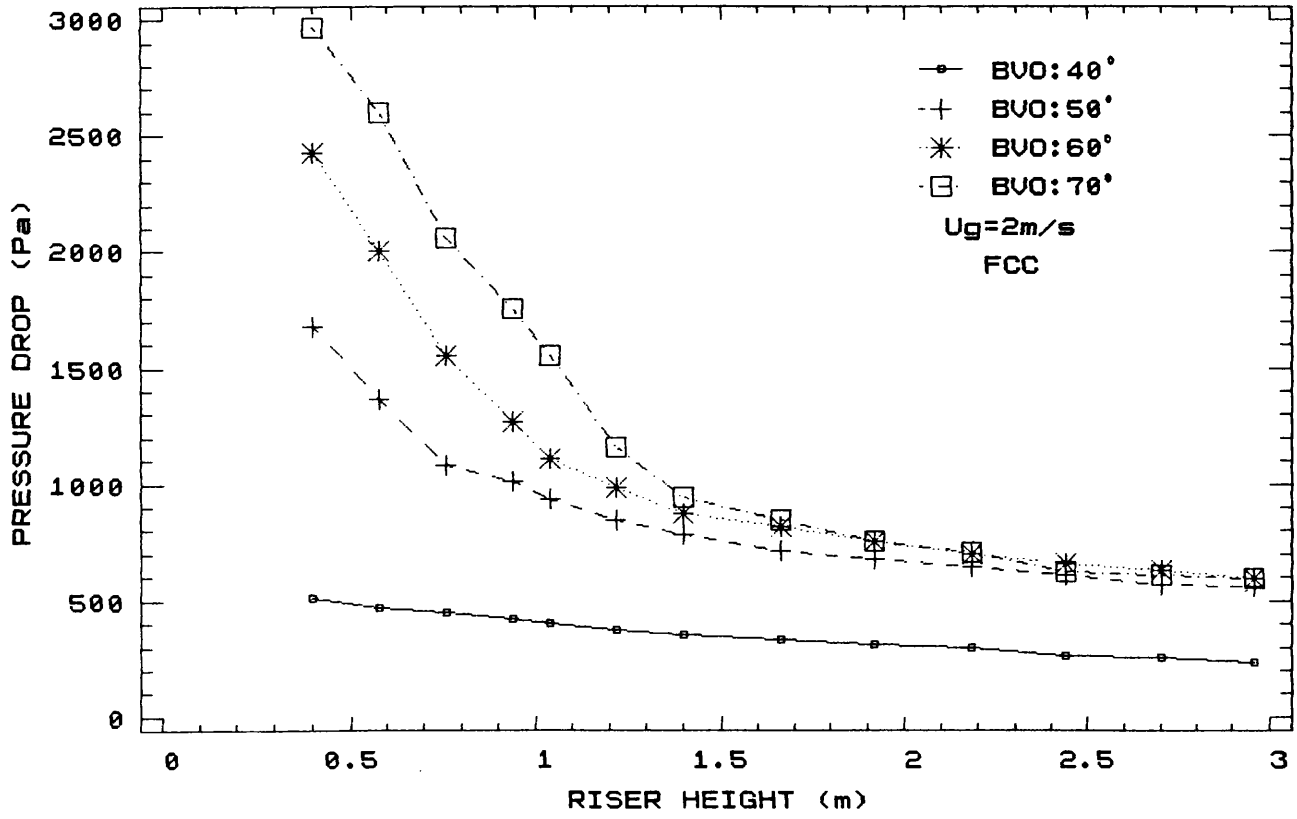

FIGURE 5.2.9 RISER DISTRIBUTOR:7 HOLES
PRESSURE DROP VERSUS RISER HEIGHT

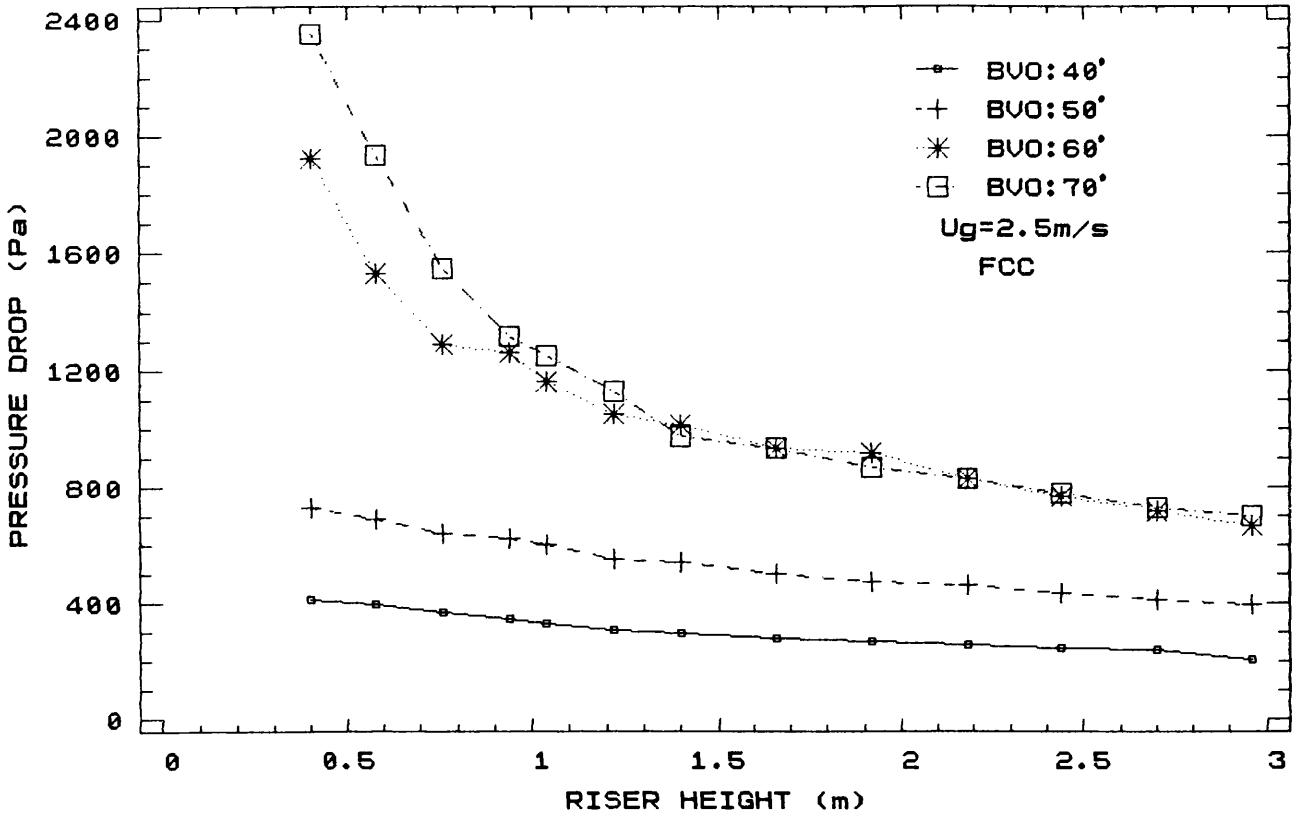

FIGURE 5.2.10 RISER DISTRIBUTOR:7 HOLES
PRESSURE DROP VERSUS RISER HEIGHT

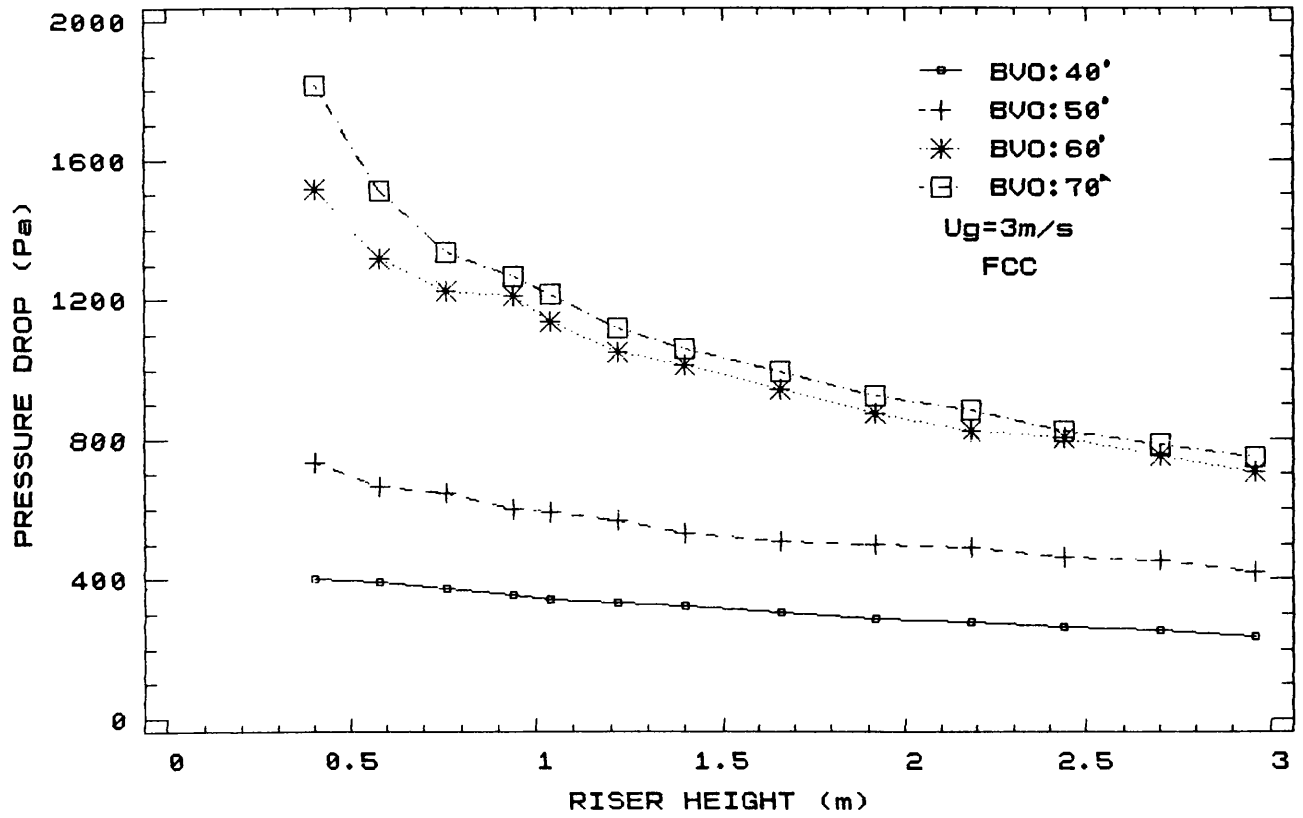

FIGURE 5.2.11 RISER DISTRIBUTOR:7 HOLES
PRESSURE DROP VERSUS RISER HEIGHT

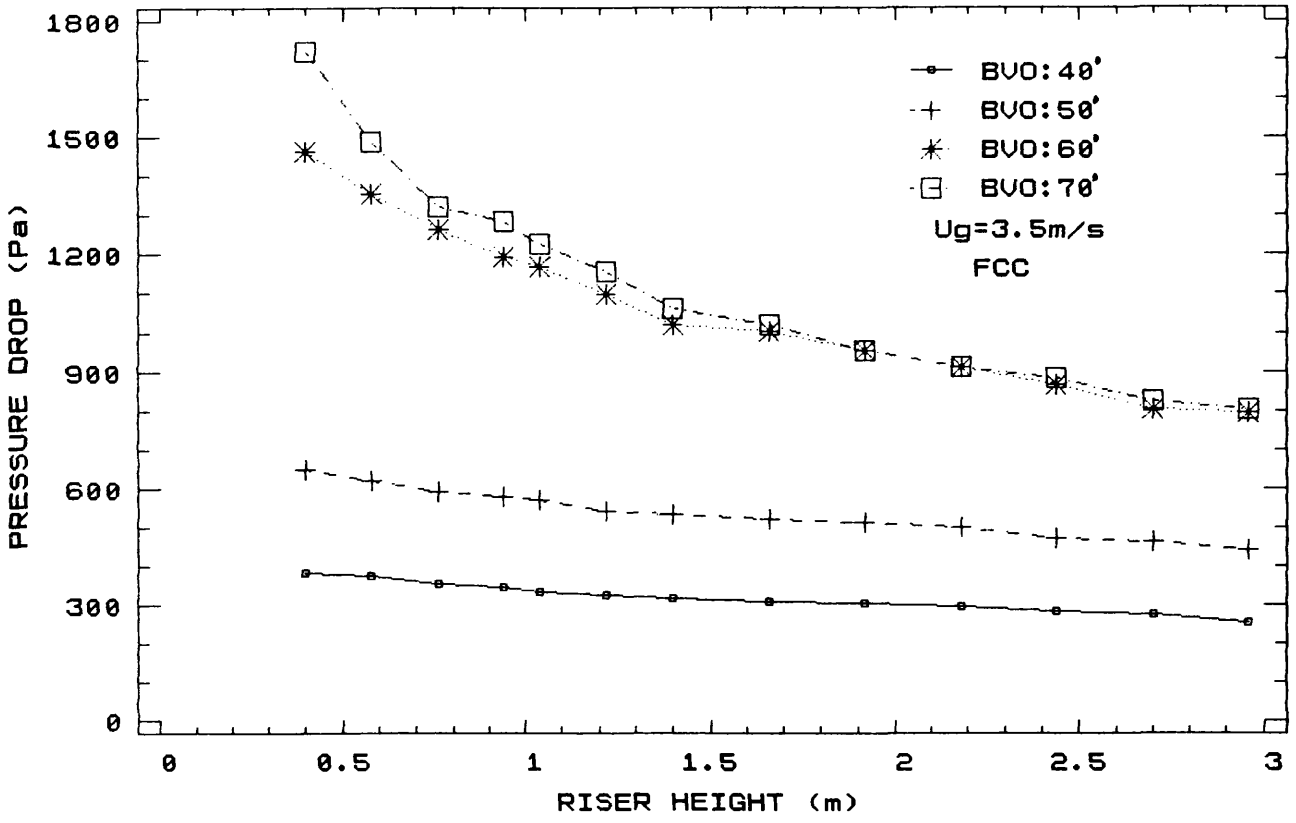

FIGURE 5.2.12 RISER DISTRIBUTOR:7 HOLES
PRESSURE DROP VERSUS RISER HEIGHT

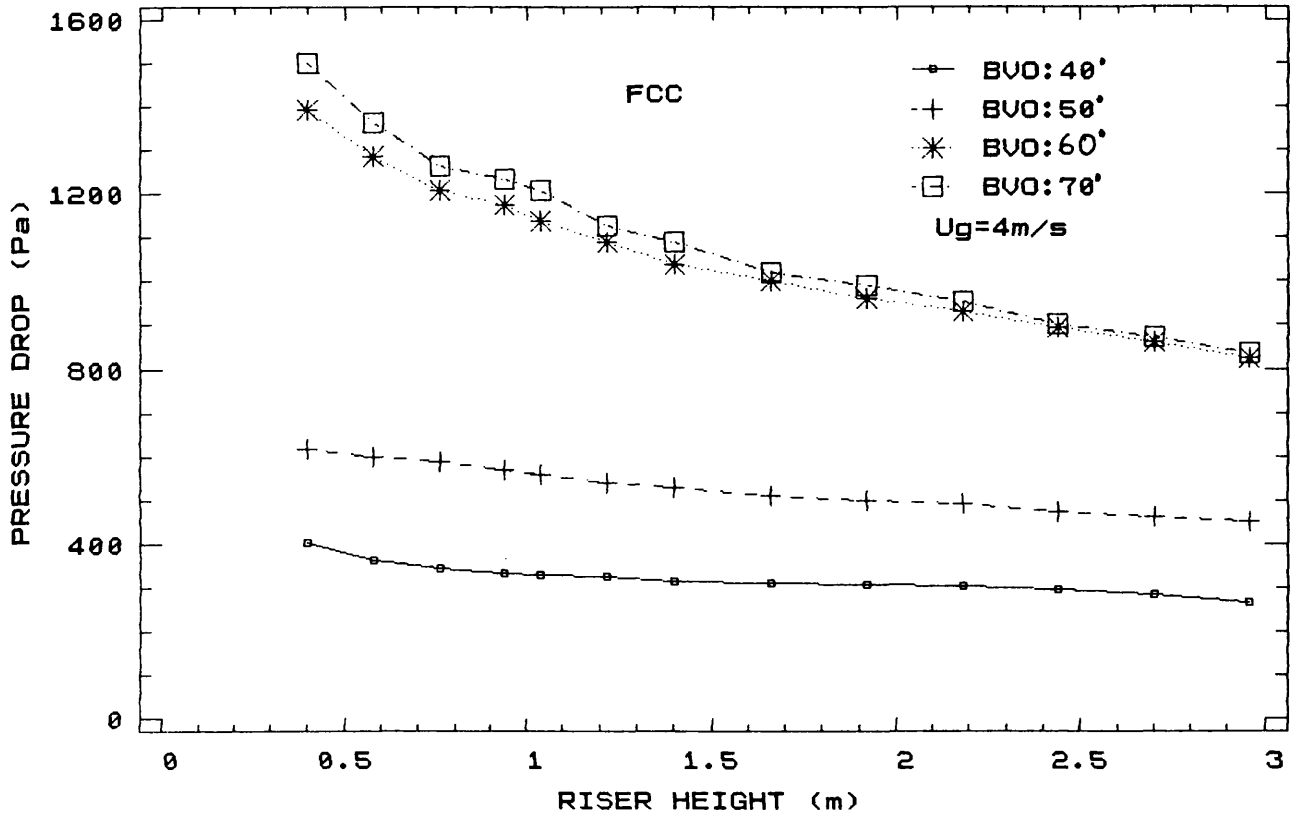

FIGURE 5.2.13 RISER DISTRIBUTOR:13 HOLES
PRESSURE DROP VERSUS RISER HEIGHT

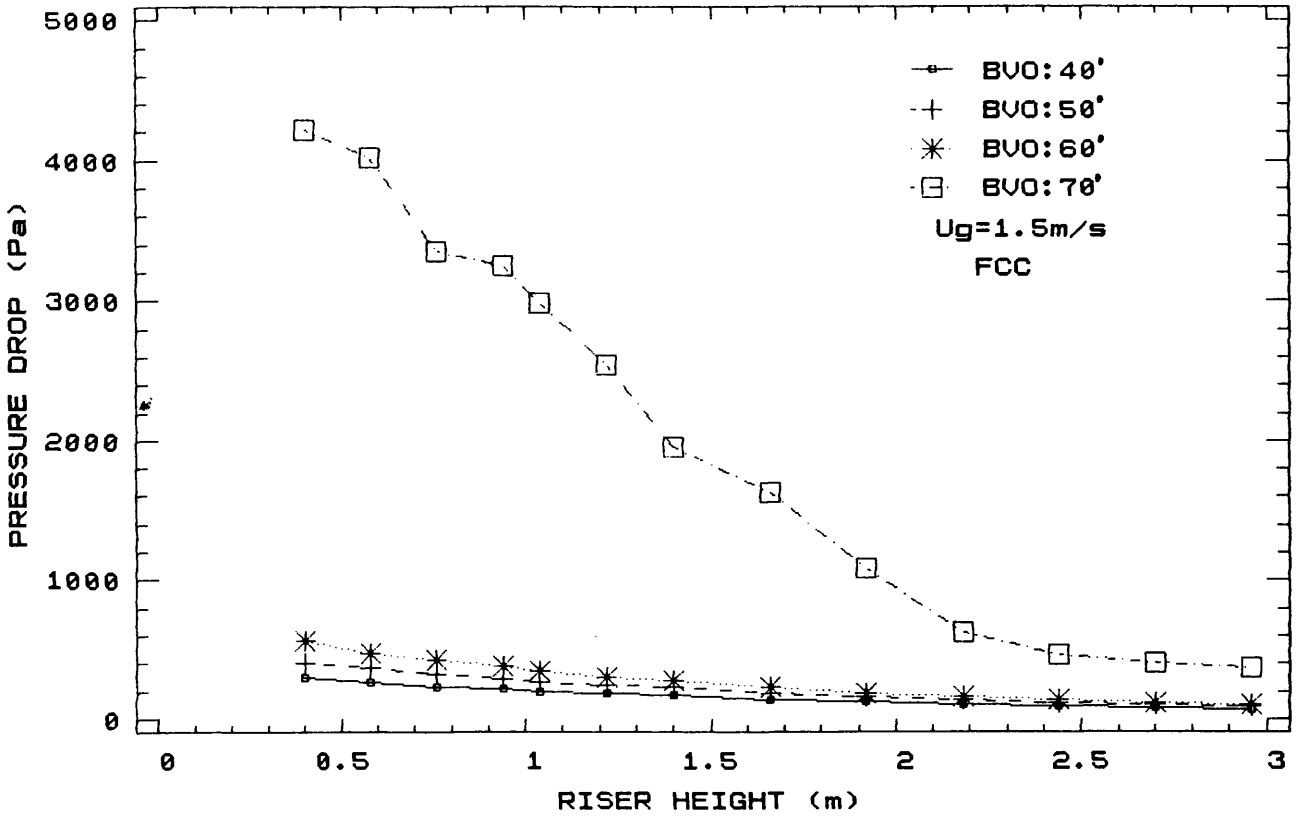

FIGURE 5.2.14 RISER DISTRIBUTOR:13 HOLES
PRESSURE DROP VERSUS RISER HEIGHT

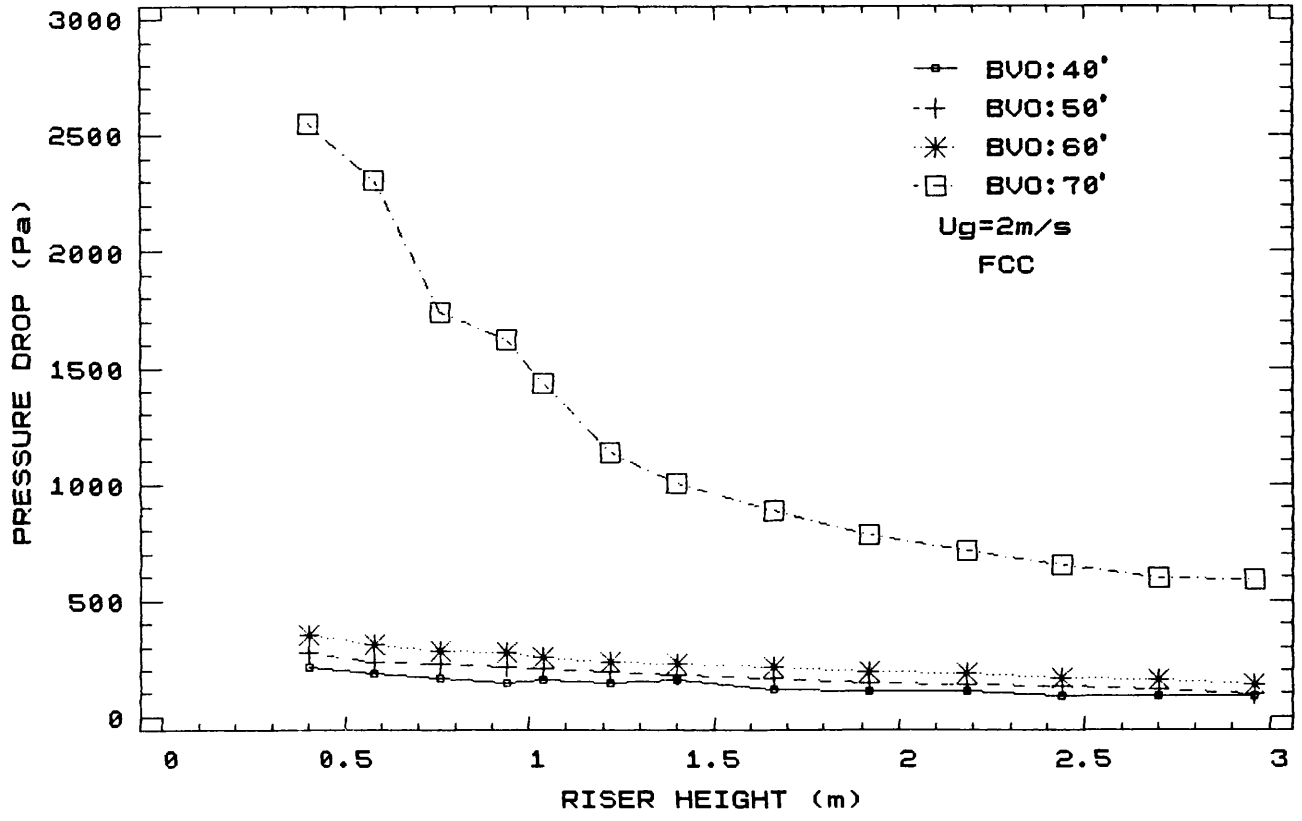

FIGURE 5.2.15 RISER DISTRIBUTOR:13 HOLES
PRESSURE DROP VERSUS RISER HEIGHT

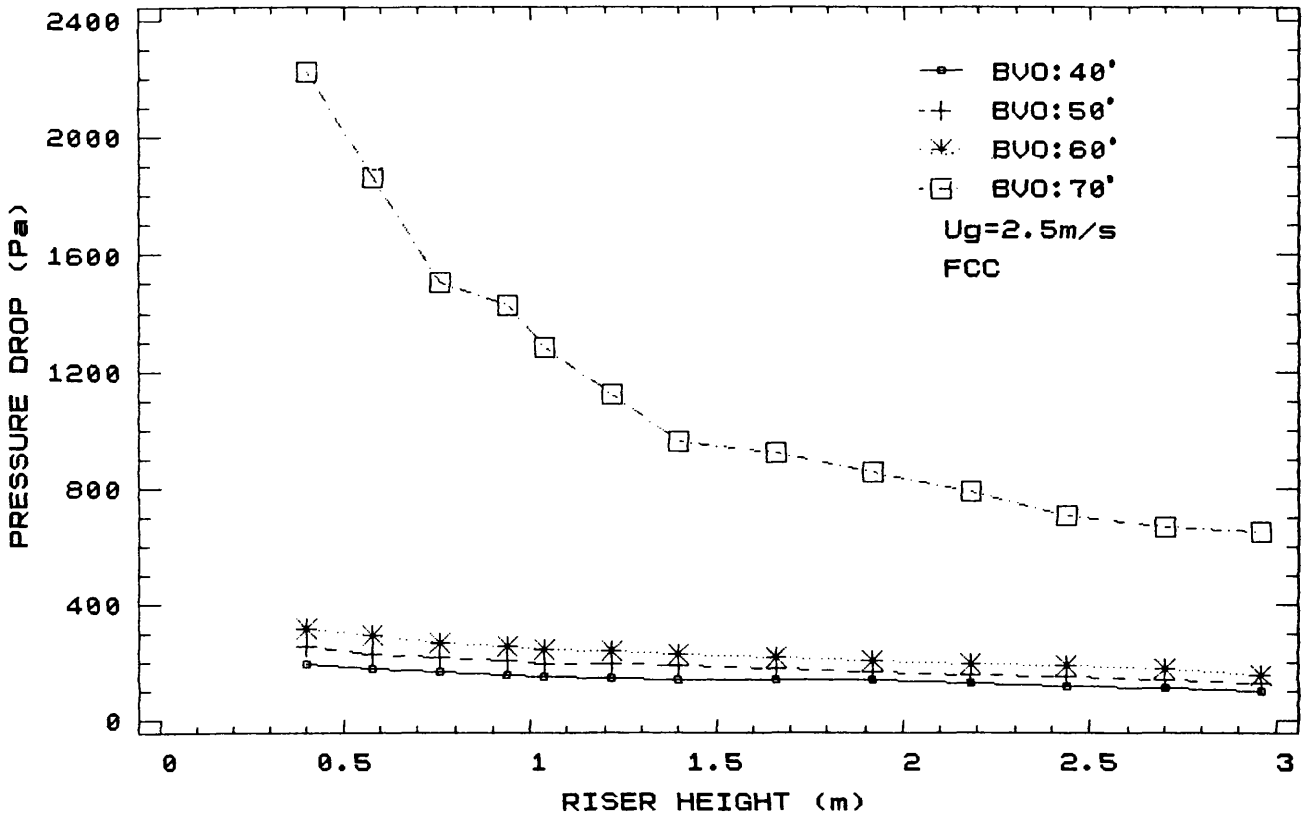

FIGURE 5.2.16 RISER DISTRIBUTOR:13 HOLES
PRESSURE DROP VERSUS RISER HEIGHT

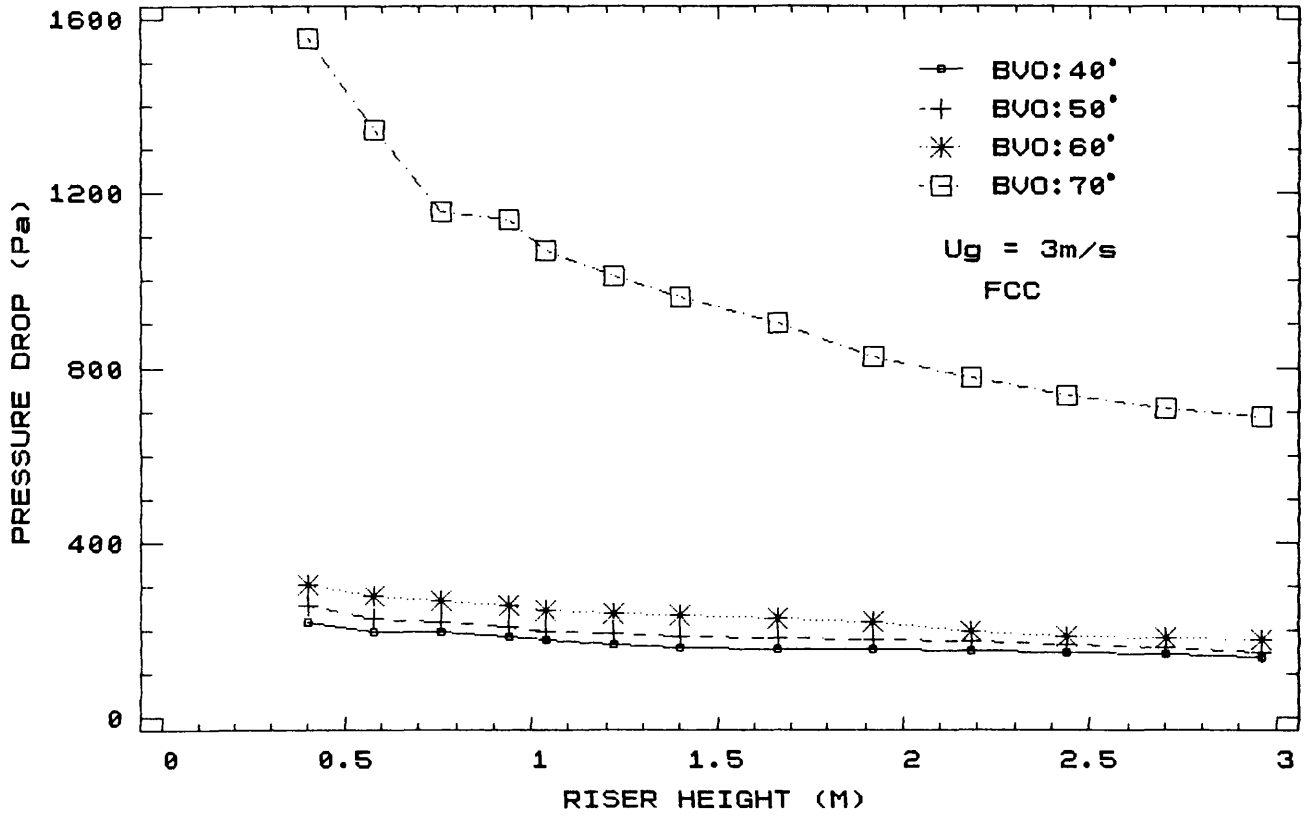

FIGURE 5.2.17 RISER DISTRIBUTOR:13 HOLES
PRESSURE DROP VERSUS RISER HEIGHT

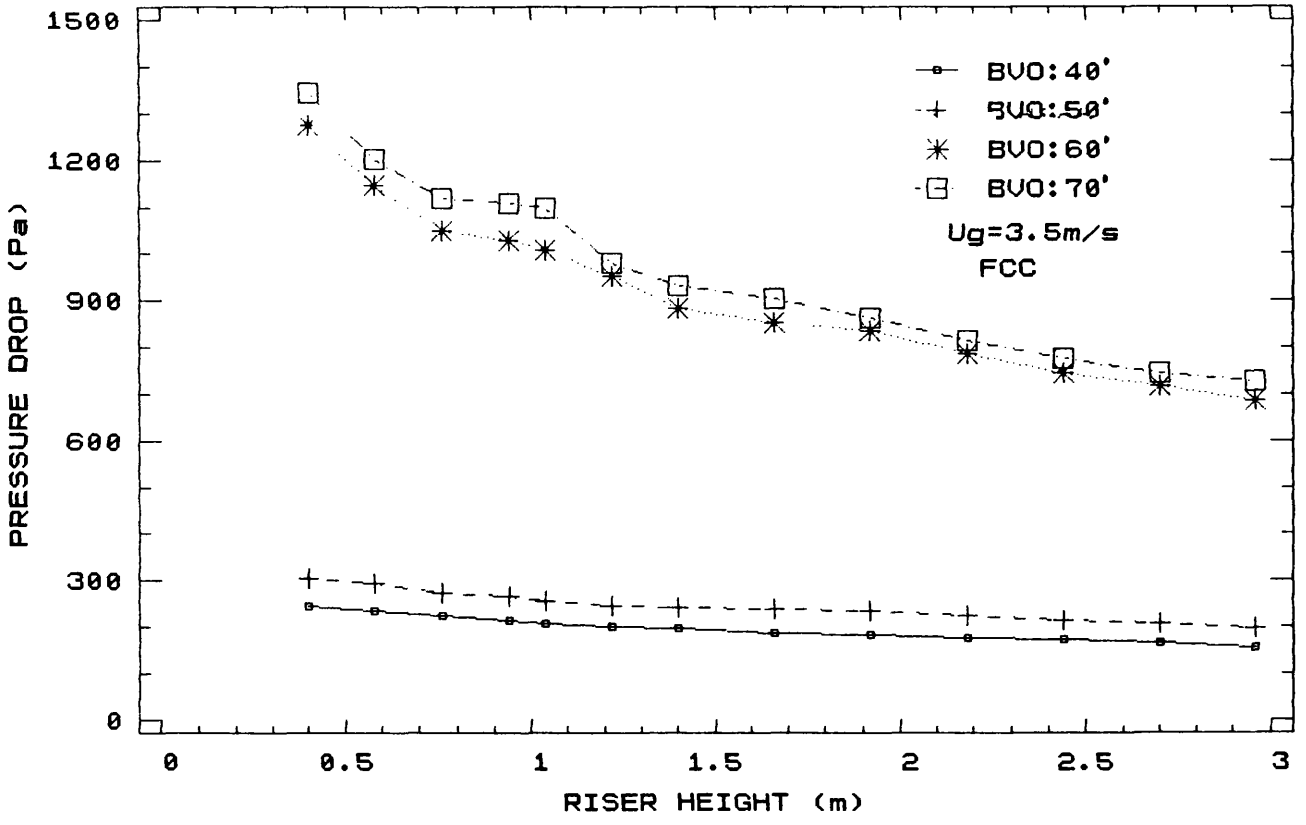

FIGURE 5.2.18 RISER DISTRIBUTOR:13 HOLES
PRESSURE DROP VERSUS RISER HEIGHT

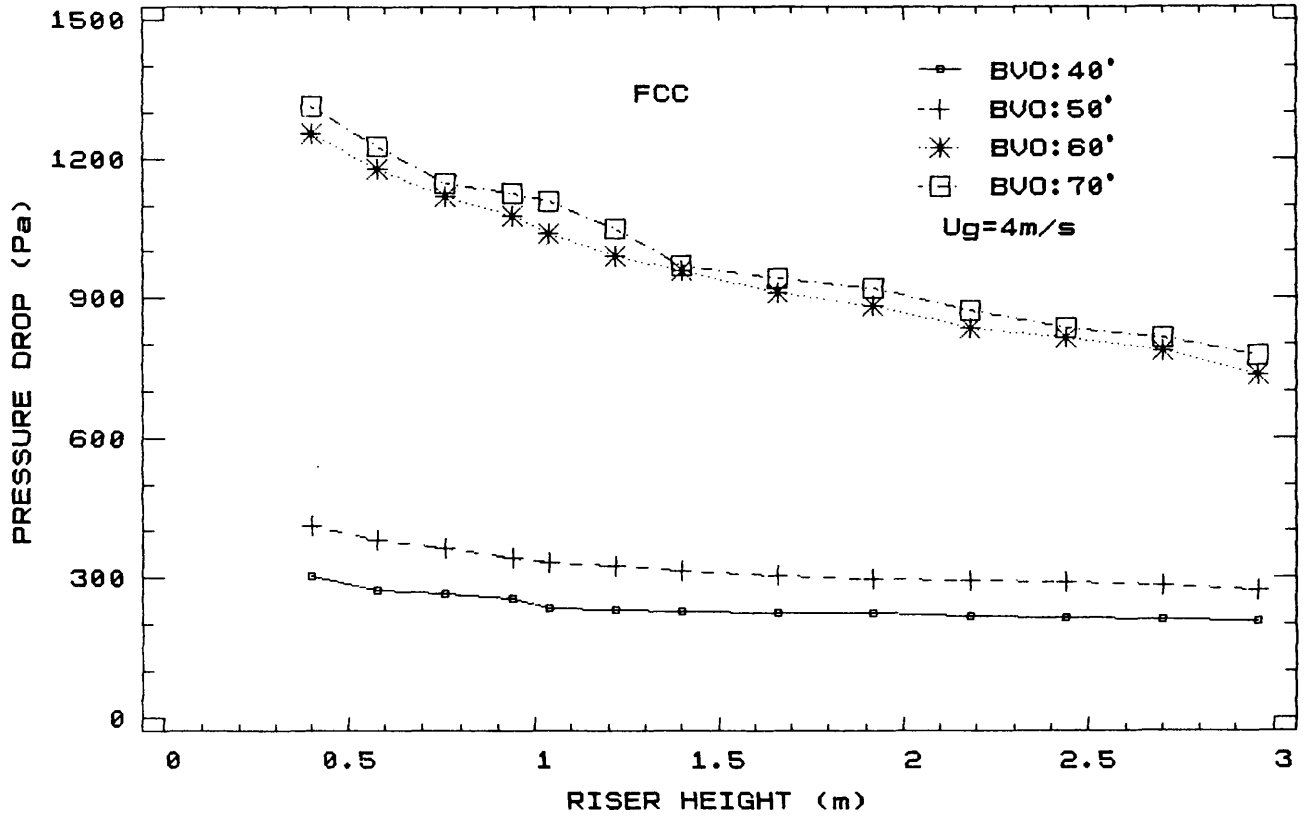

However calculations have showed that the acceleration length of a particle is not more than a few centimeters of riser height before it reaches its steady state (Figure 3.2, Chapter 3).

The pressure drop values for the 7 and 13 holes riser distributors are of the same order of magnitude to each other.

The main difference between the 1 nozzle distributor and the 7 and 13 hole distributors lies in the order of magnitude of pressure drops. The pressure profiles obtained with the 1 nozzle distributor have lower pressure drop values under identical conditions of operation of the system. This means that less solid is present in the riser.

Whether or not there is a high or low pressure drop in the riser is at least partly determined by the solid circulation rate which in turn is influenced by the distributor design. If it is assumed that each hole of the distributor design behaves as a fluid jet, then an introduction to fluid jets is given in Appendix G.
By considering the design of the three distributors used during the experimental work and by assuming that the jet angle is of 14 degrees, then the potential core length can be determined for each orifice diameter of the distributor.

The effect of the distributor design on the pressure profile is shown in Figures 5.2.19 and 5.2.20. From those observations the following conclusions may be drawn:
a) For a given gas velocity and constant ball valve opening, the pressure drop at a particular level in the

FIGURE 5.2.19 PRESSURE DROP PROFILES
AT UG=3M/S & BVO=40'

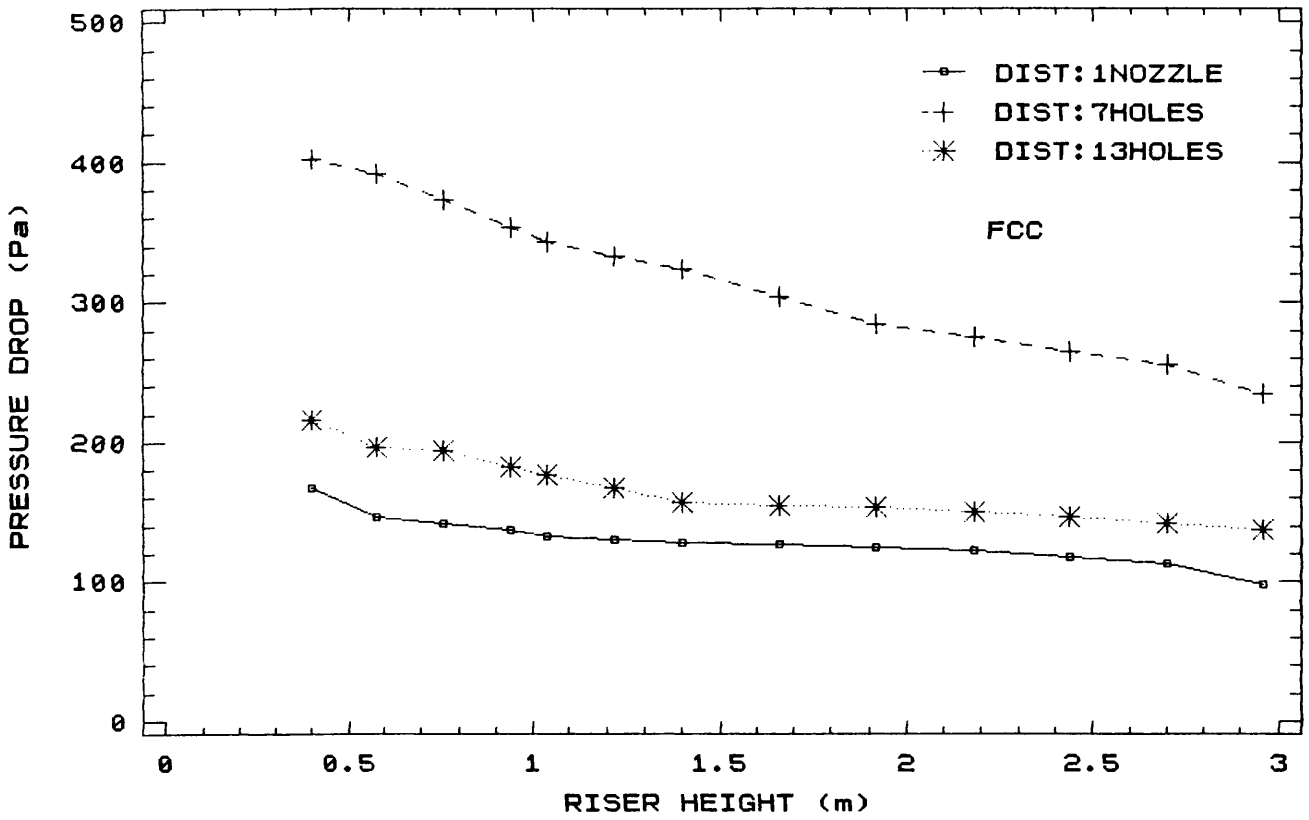

FIGURE 5.2.20 PRESSURE DROP PROFILES
AT UG=3.5M/S & BVO=70'

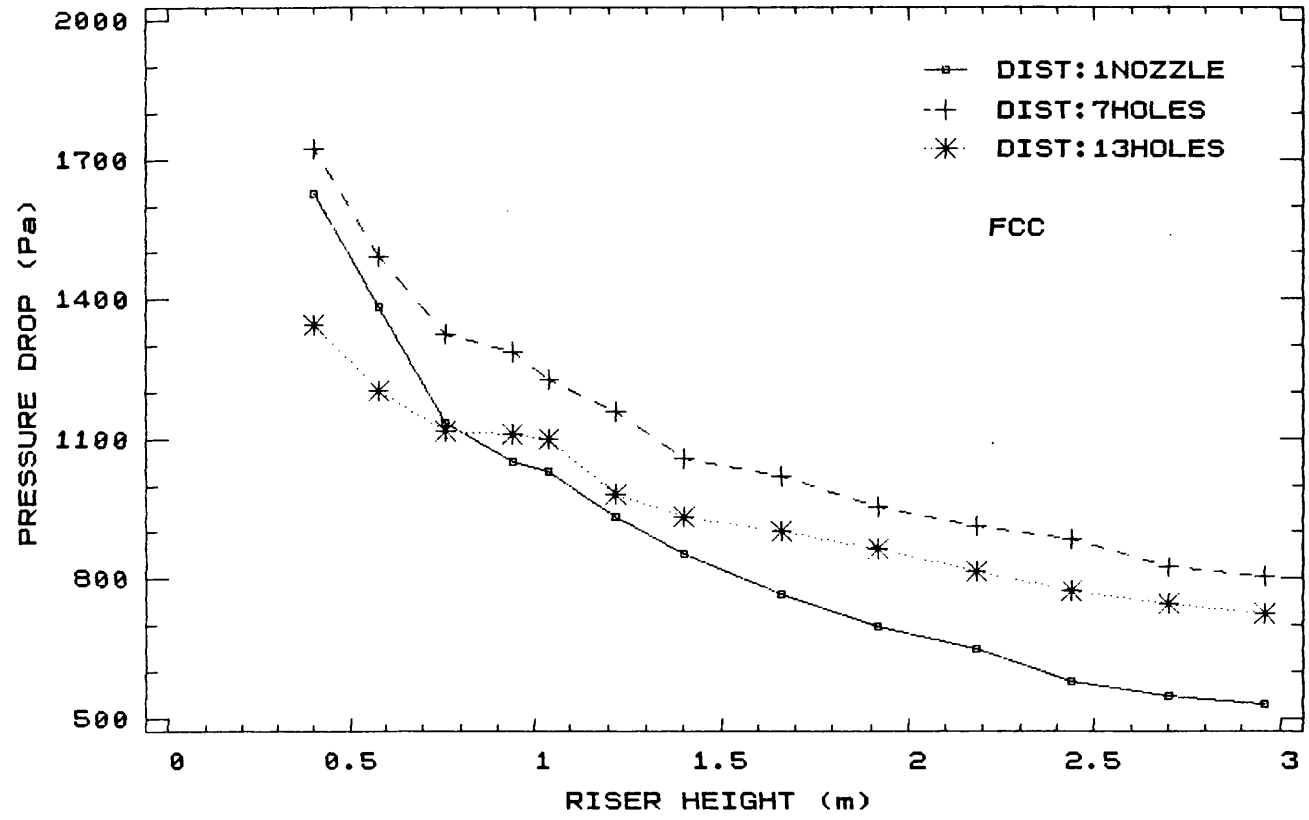

riser increases with the increase of the number of holes of the distributor due to a change in voidage in the riser.
b) At high ball valve openings, Figure 5.2.20, there is a marked increase in pressure drop at the bottom of the riser up to 1m riser height and then a linear decrease at higher levels. This sudden increase of pressure drop is higher for the 7 hole distributor than for the distributors consisting of 1 nozzle and 13 holes.
c) At low ball valve openings, Figure 5.2.19, there is a continuous decrease of pressure drop along the riser height. This decrease is sharper for the 7 hole distributor and rather smoother for the 1 nozzle and 13 hole distributors.
For the case of 1 nozzle, the local radial gas velocity profile is as shown in Figure 5.2.21(a). The air as it passes the 1 nozzle, expands in the upward direction. The local velocity in the centre reaches a maximum value at first and then decreases along the height until it approaches the final turbulent state. This turbulent state is reached at a riser height of 16.3 cm if the jet angle is assumed to be 14 degrees. After that, the radial profile does not change but remains constant along the height. The particles are introduced in the riser and are accelerated until they reach their final linear velocity at a vertical height. The linear velocity is smaller than the linear gas velocity by the value of terminal velocity. According to the local gas profile, as soon as particles are distributed in the region near the

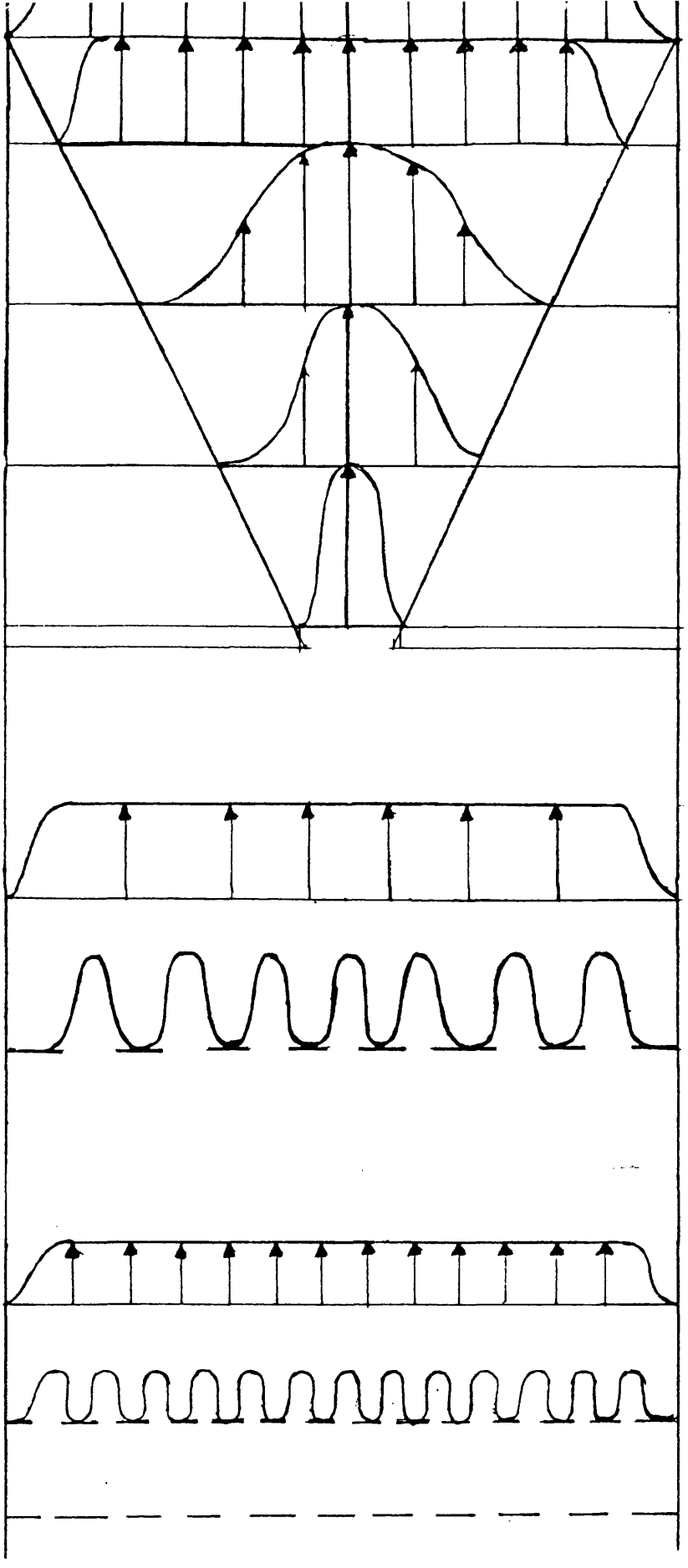

FIGURE 5.2.21 GAS FLOW PATTERNS THROUGH DISTRIBUTOR

wall, they start falling in the opposite direction of the upwards gas movement because the local gas velocity reaches its minimum value near the wall. Hence a stagnant region of particles starts to accumulate in the area above the 1 nozzle distributor. This stagnant region extents about 20cm up from the distributor plate.

In the case of the 7 hole distributor, the local gas velocity profile radially and axially is as shown in Figure 5.2.21(b). The local gas radial profile reaches its final vertical state in a short axial length that is of axial length of 4.6 cm if the jet angle is taken as 14 degrees. As a result the particles when they enter the riser reach their final linear velocity in a shorter vertical distance and time. Because of the minimum value of the local gas profile next to the wall region, a downward movement of particles and some accumulation of particles will occur in the 7 hole distibutor area.

The case of the 13 holes distributor is similar with that of 7 hole distributor, with the only difference that the local gas profile is reached at a riser distance of about 4 cm.

The values of pressure profiles can be explained as being due to the axial and radial gas profile.

For the 7 hole distributor, the pressure values are of higher order in comparison to the 13 hole and 1 nozzle distributors. These high values are due to the higher solid concentration present in the riser. For the 1 nozzle distributor the low pressure values might be due to the

stagnant areas of particles present in the flat area next to the nozzle, which limits the gas distribution.

5.2.1.1 Solid concentration

Graphs 5.2.1.1 to 5.2.1.14 are plots of the variation of solid concentration fraction ($1-\varepsilon$) along the riser height at constant gas velocity, for the three different gas distributors.

Graphs 5.2.1.4, 5.2.1.5 and 5.2.1.6 of the 1 nozzle gas distributor , 5.2.1.9 and 5.2.1.10 of the 7 hole gas distributor and 5.2.1.13 and 5.2.1.14 of the 13 hole gas distributor show a common trend with respect to the shape of the graph, 'an exponential decay', that is a sharp decrease of solid concentration fraction up to a riser height of about 1m and then a constant value of solid concentration fraction along the rest of the riser height.

Comparison of the graphs 5.2.1.4, 5.2.1.9 and 5.2.1.13 at the same gas velocity of 3 m/s reveals that for the three gas distributors the solid concentration fraction along the riser varies from 18% at the bottom part of the riser to 2% at the top part of the riser, for all three distributors, although the solid circulation flux achieved varies from 6 kg/m^2s to 10 kg/m^2s.The measured axial profiles of solids fraction within the 5cm riser for the FCC powder are in agreement to the axial solids fraction

FIGURE 5.2.1.1 SOLID CONCENTRATION FRACTION VERSUS RISER HEIGHT

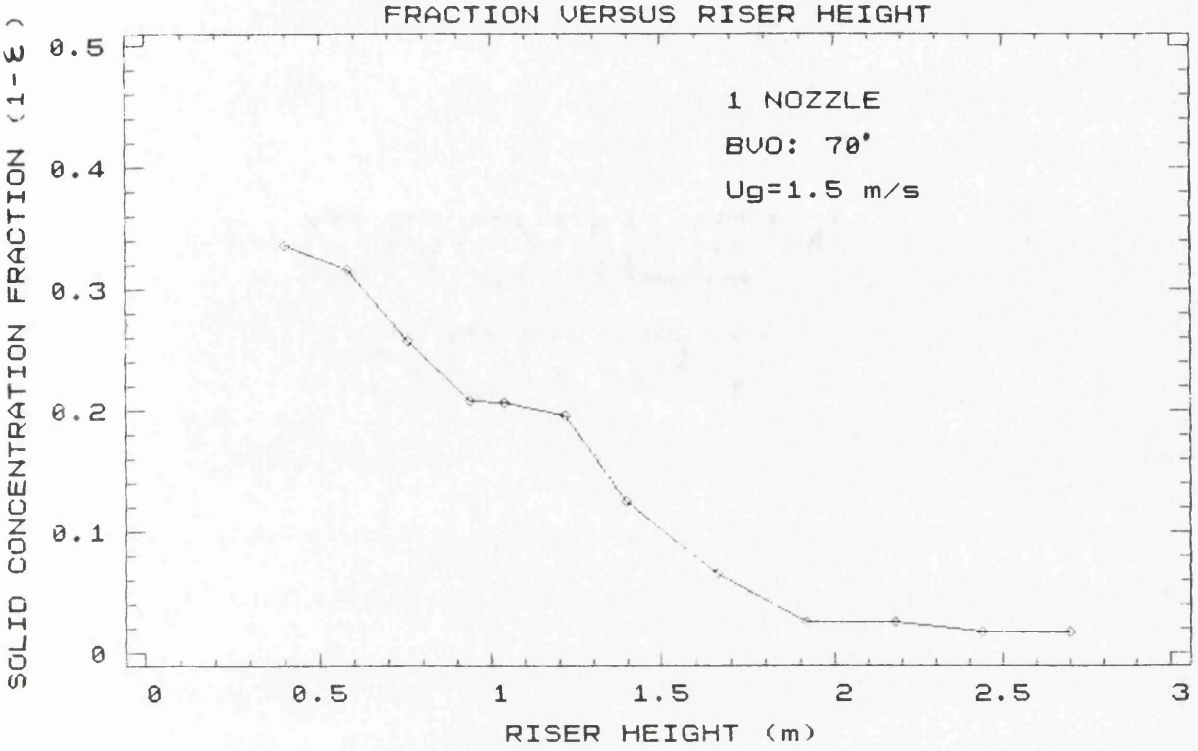

FIGURE 5.2.1.2 SOLID CONCENTRATION FRACTION VERSUS RISER HEIGHT

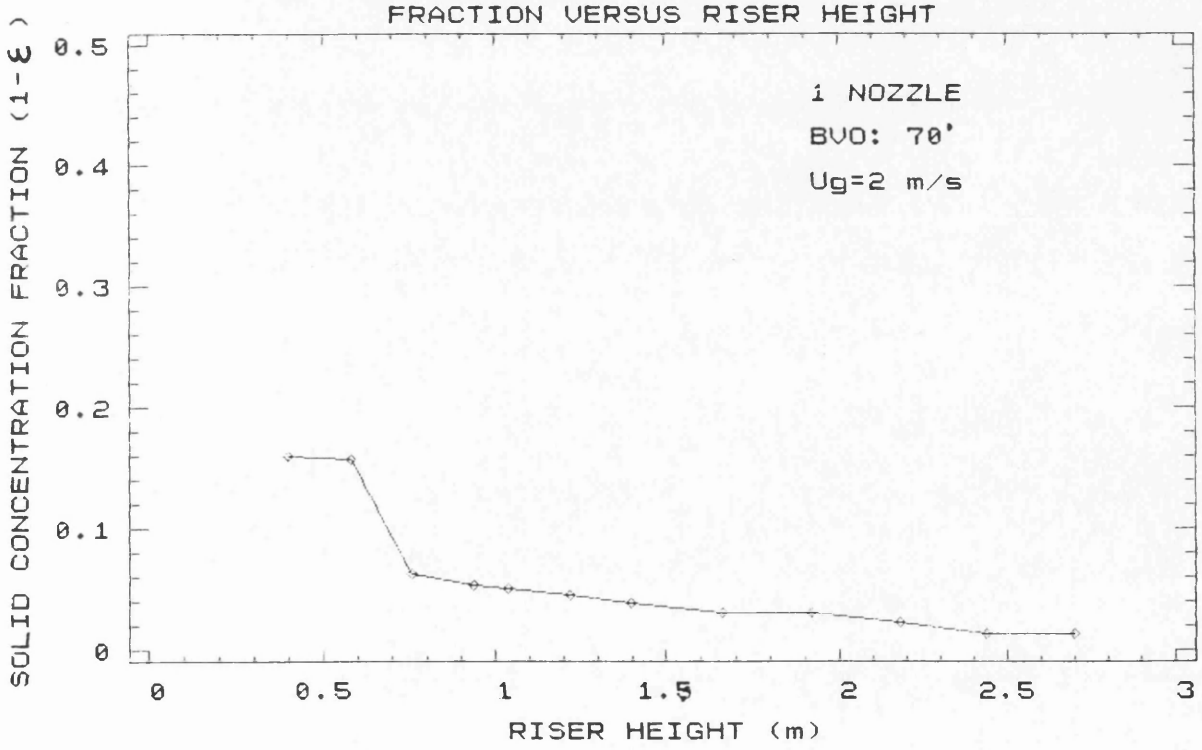

FIGURE 5.2.1.3 SOLID CONCENTRATION FRACTION VERSUS RISER HEIGHT

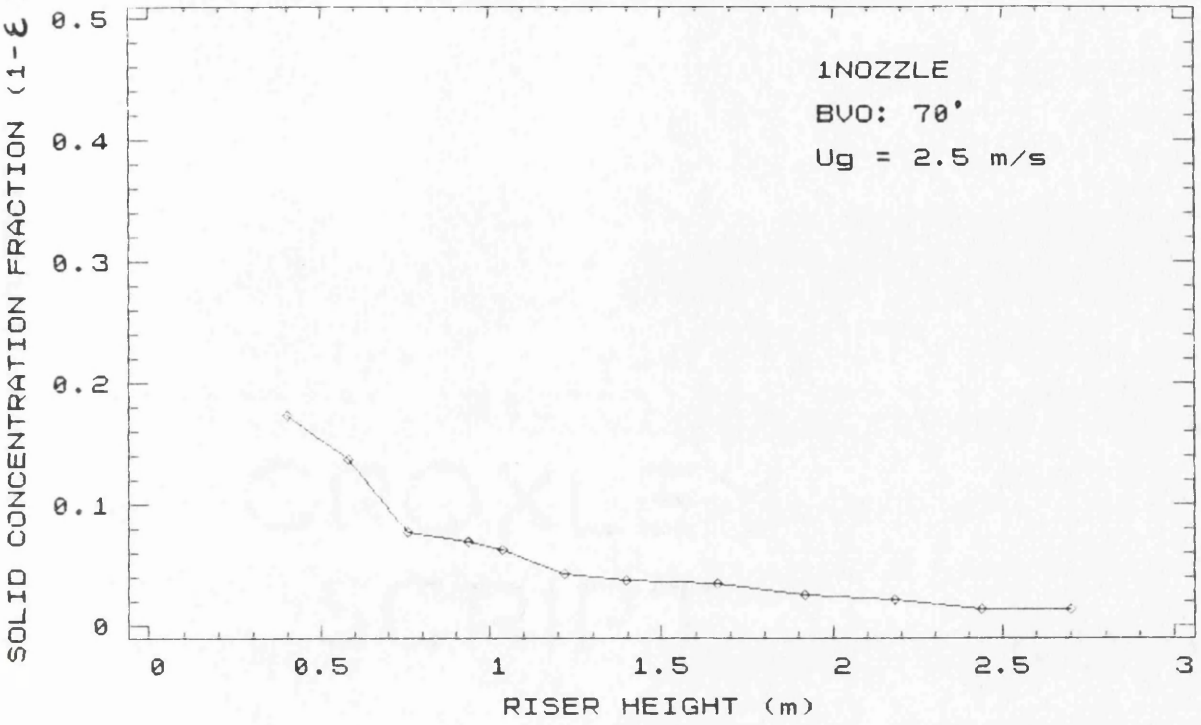

FIGURE 5.2.1.4 SOLID CONCENTRATION FRACTION VERSUS RISER HEIGHT

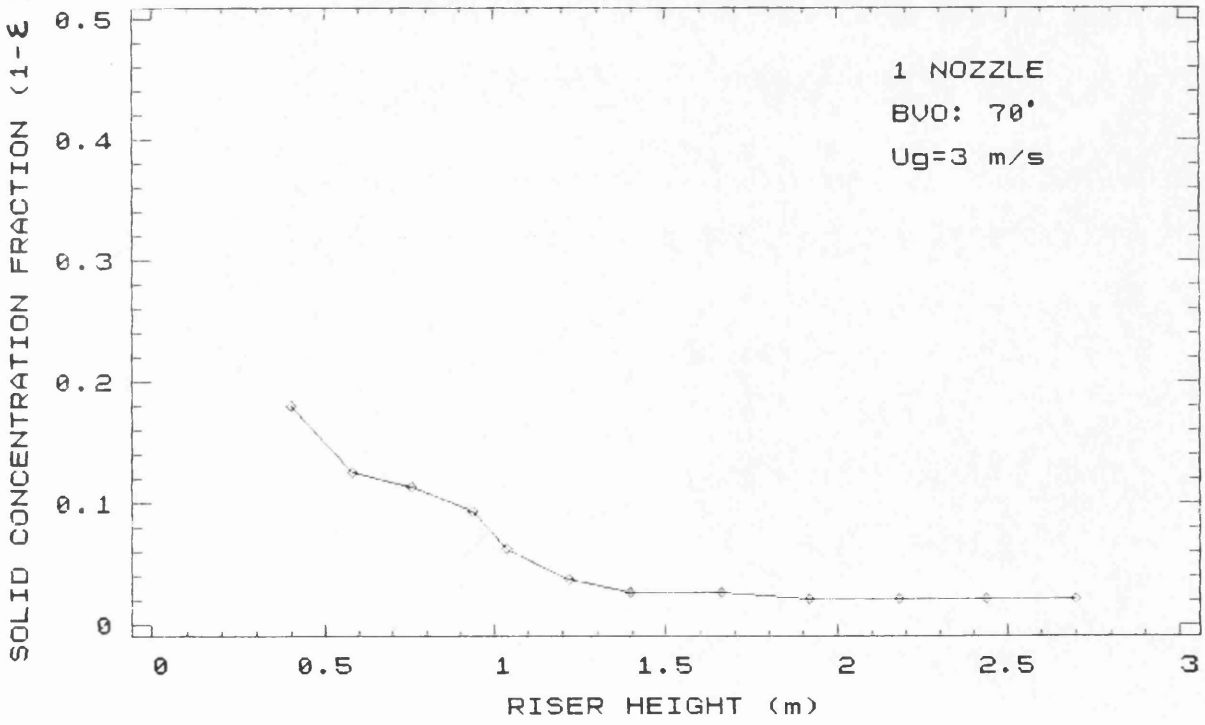

FIGURE 5.2.1.5 SOLID CONCENTRATION FRACTION VERSUS RISER HEIGHT

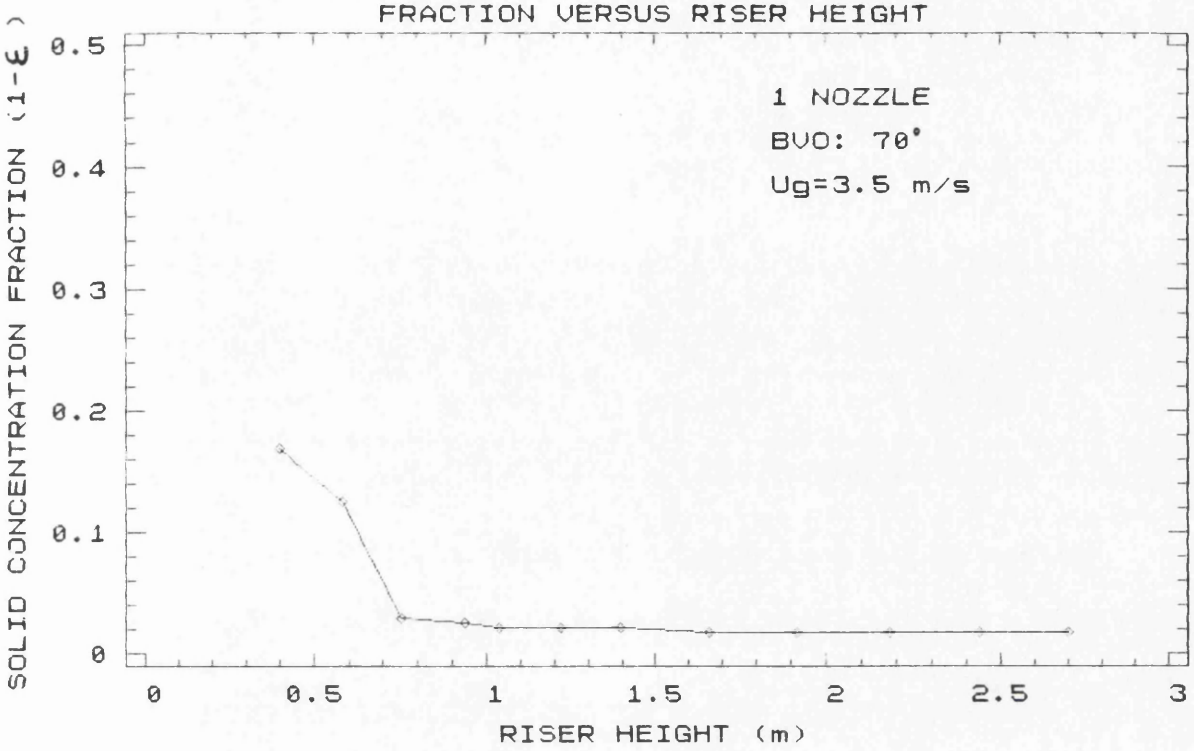

FIGURE 5.2.1.6 SOLID CONCENTRATION FRACTION VERSUS RISER HEIGHT

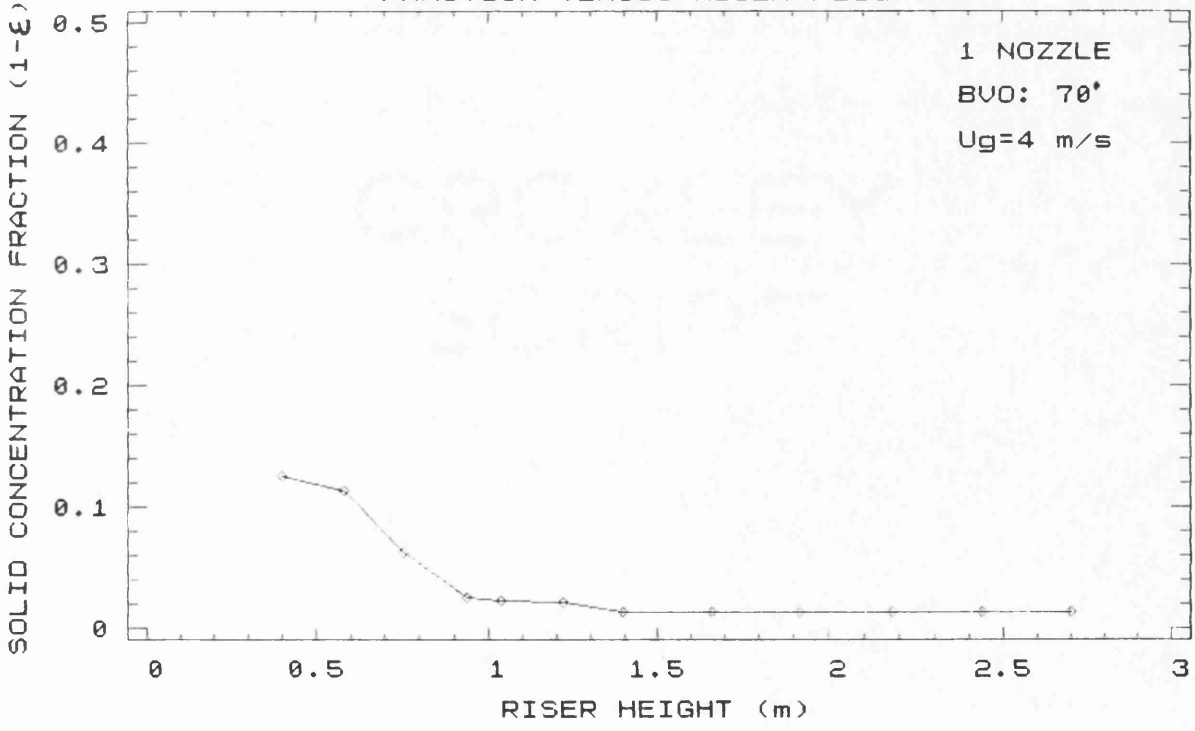

FIGURE 5.2.1.7 SOLID CONCENTRATION FRACTION VERSUS RISER HEIGHT

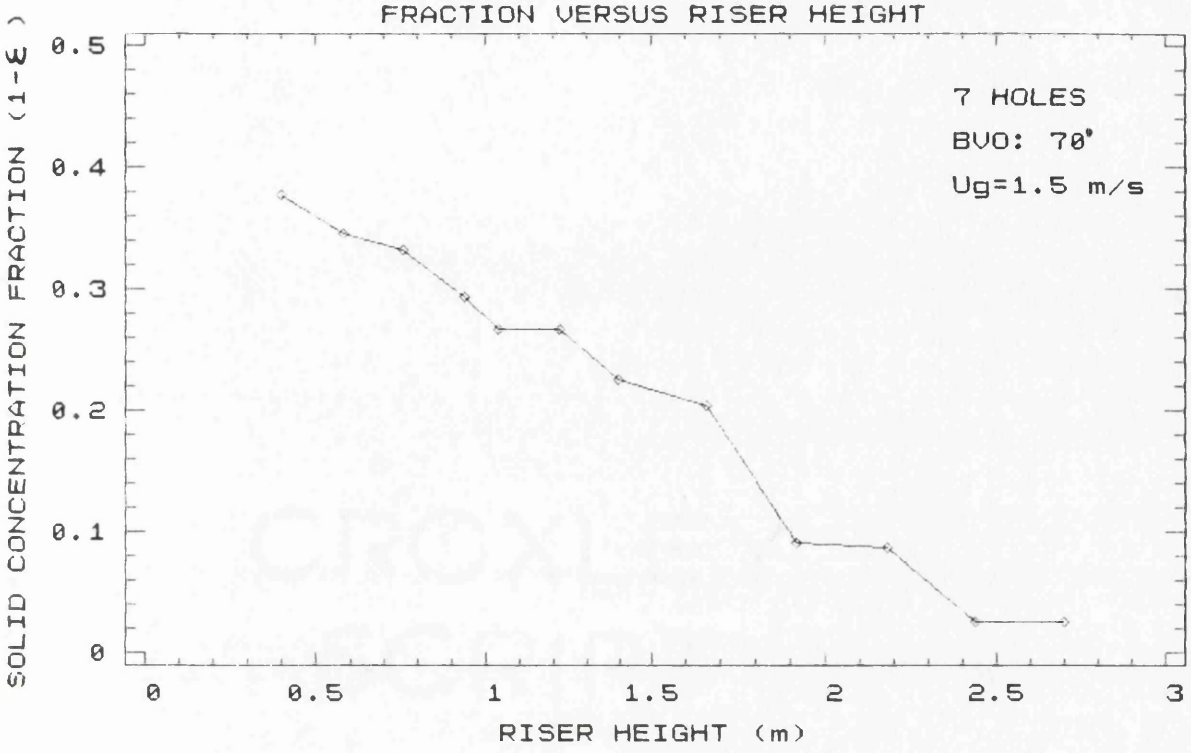

FIGURE 5.2.1.8 SOLID CONCENTRATION FRACTION VERSUS RISER HEIGHT

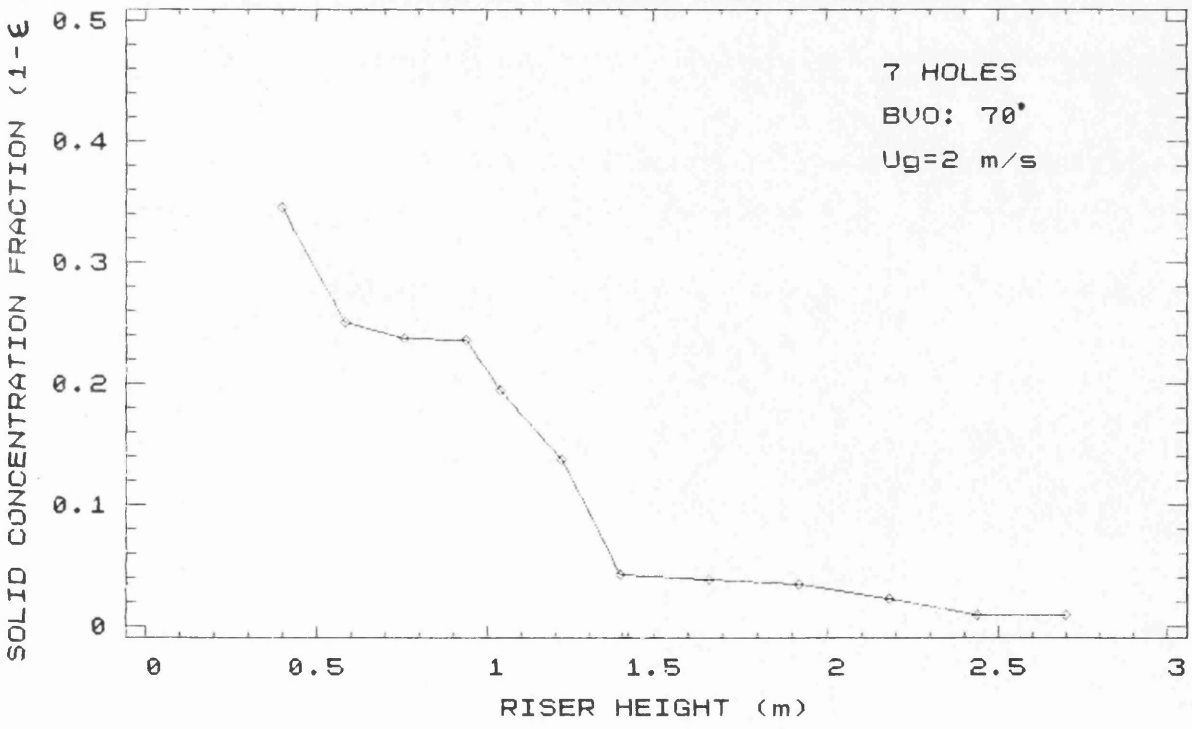

FIGURE 5.2.1.9 SOLID CONCENTRATION FRACTION VERSUS RISER HEIGHT

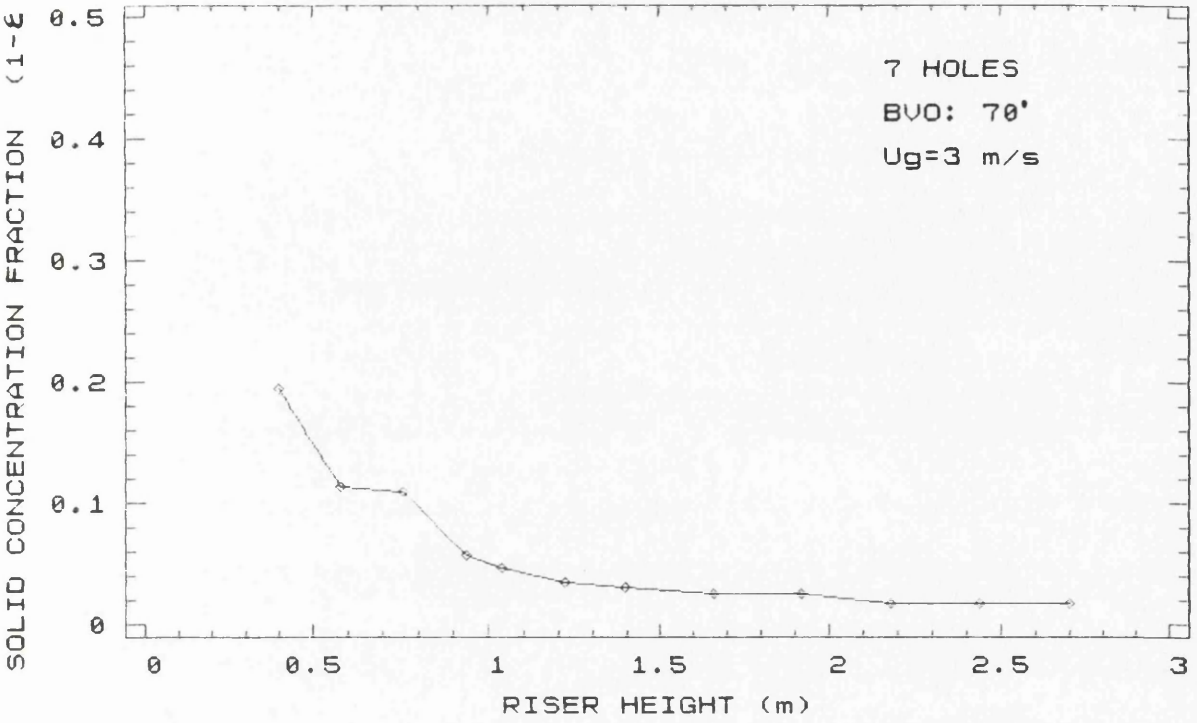

FIGURE 5.2.1.10 SOLID CONCENTRATION FRACTION VERSUS RISER HEIGHT

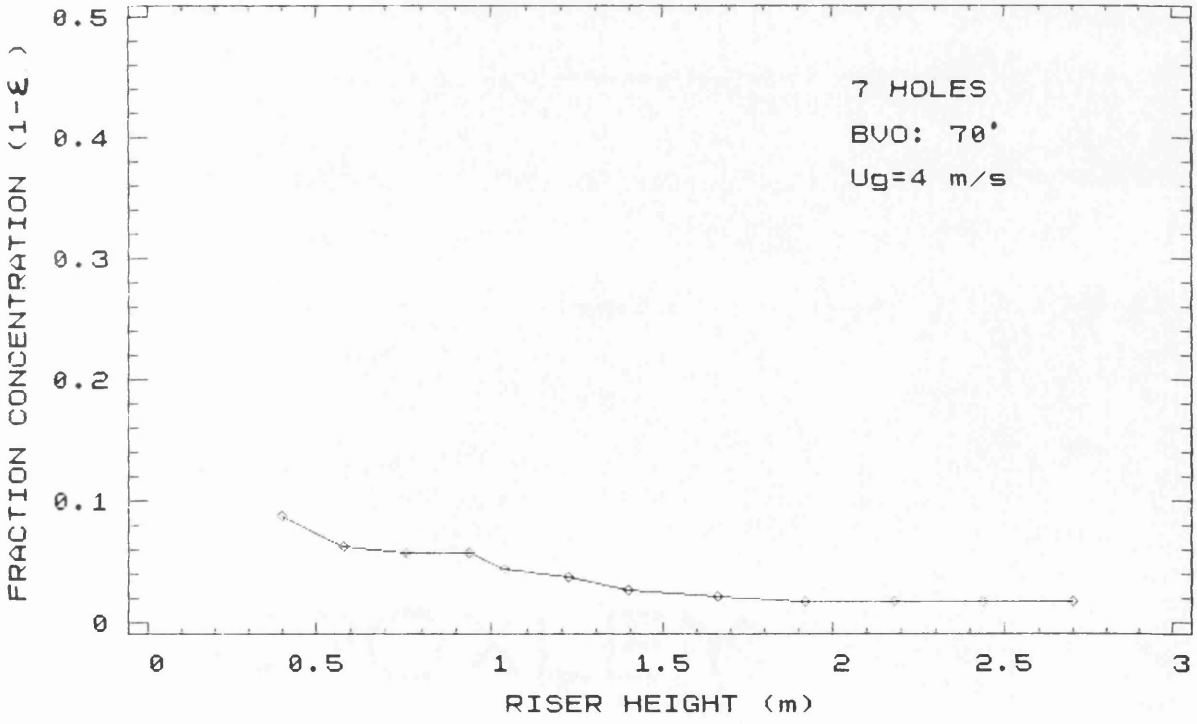

FIGURE 5.2.1.11 SOLID CONCENTRATION FRACTION VERSUS RISER HEIGHT

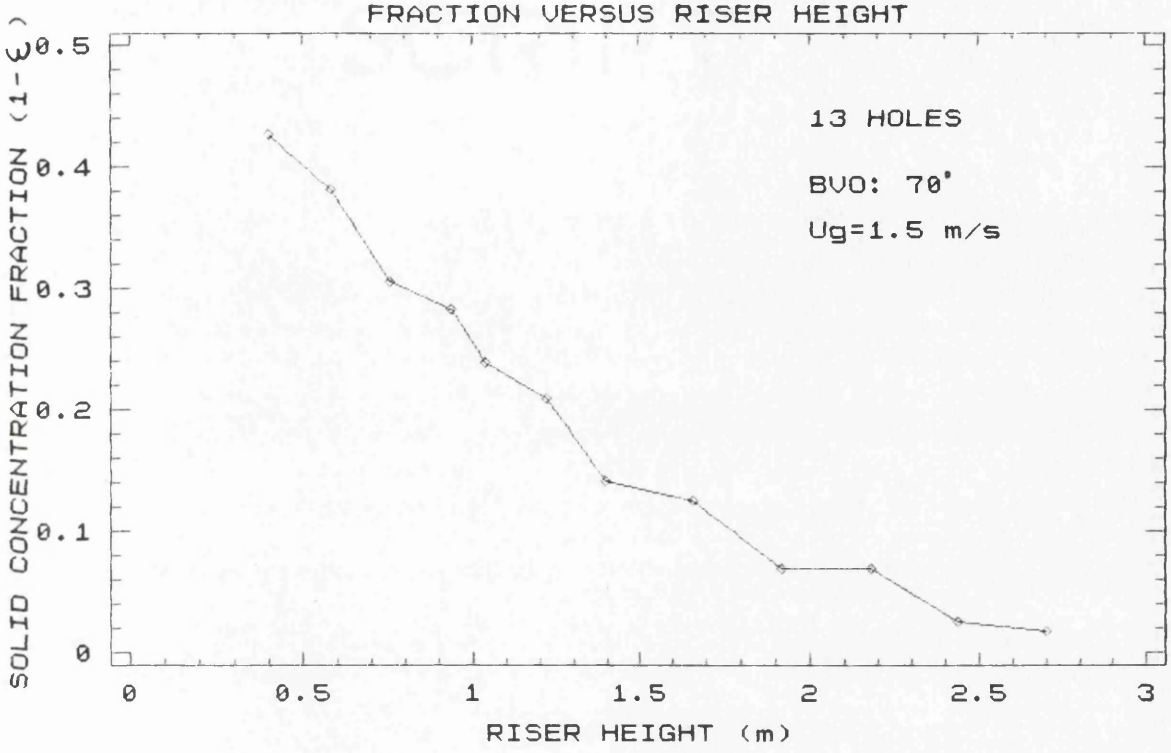

FIGURE 5.2.1.12 SOLID CONCENTRATION FRACTION VERSUS RISER HEIGHT

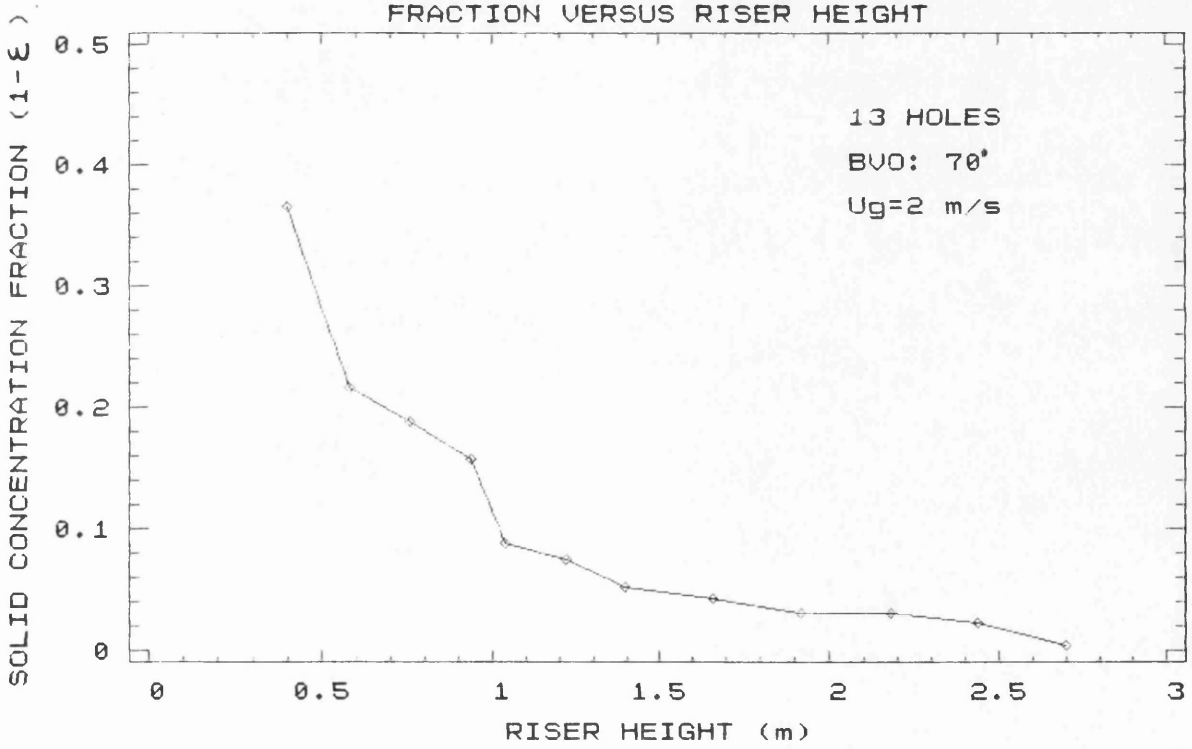

FIGURE 5.2.1.13 SOLID CONCENTRATION FRACTION VERSUS RISER HEIGHT

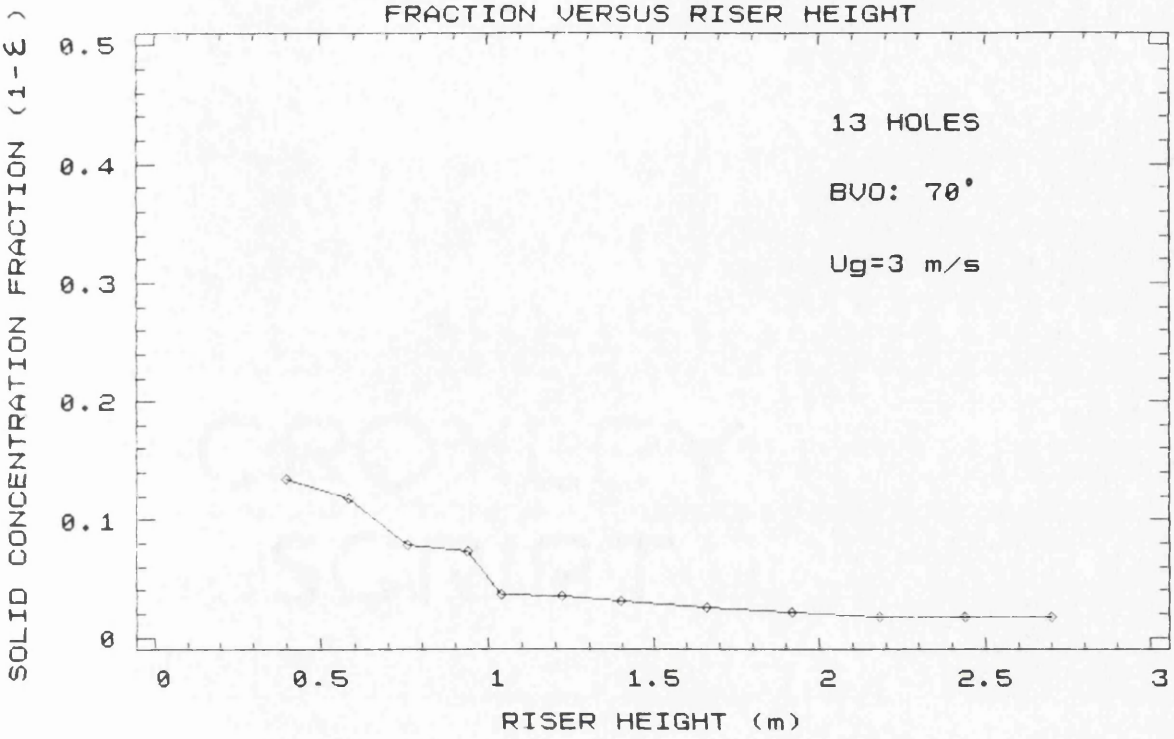

FIGURE 5.2.14 SOLID CONCENTRATION FRACTION VERSUS RISER HEIGHT

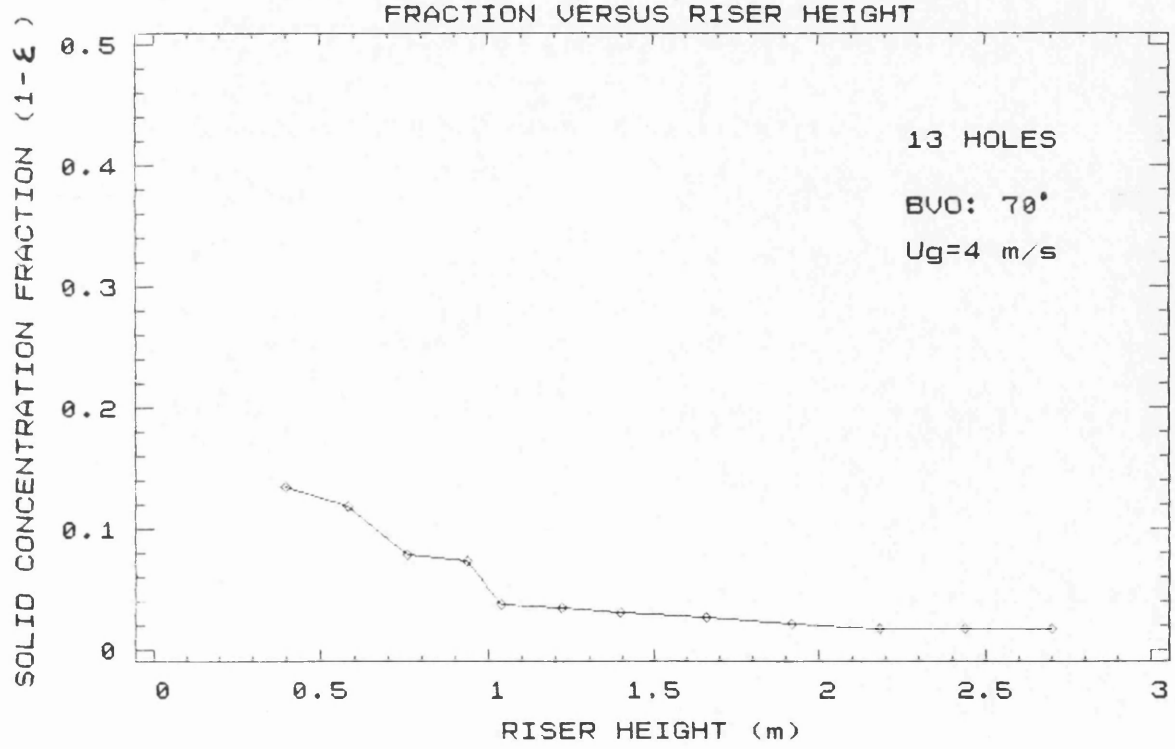

profiles presented by Rhodes and Geldart (1987) with respect to the shape of the graph and magnitude although much higher solid circulation fluxes of the order 10 to 80 kg/m^2s were achieved by using a denser powder (1800 kg/m^3 compared to 884 kg/m^3) within a riser of 15.2 cm diameter.

Work presented by Youchou and Kwauk (1980) and Weinstein et al. (1983) using pressure data reveals the presence of the inflection point between the dense region and the dilute region of the riser. The fact that such inflection point is not present in the concentration profiles presented in Figures 5.2.1.4, 5.2.1.5 and 5.2.1.6, 5.2.1.9 and 5.2.1.10 and 5.2.1.13 and 5.2.1.14 might be related to Youchou and Kwauk (1980) observation that its location is displaced towards the top of the column as the gas velocity decreases.

Graphs 5.2.1.1, 5.2.1.7 and 5.2.1.11 are the corresponding axial solid concentration profiles at a gas velocity of 1.5m/s for the gas distributors with 1 nozzle, 7 holes and 13 holes respectively. The three graphs show a continuous decrease of solid concentration fraction along the riser height. Since the solid fraction varies from 42% to 1%, well above the normal operation of the riser of a CFB system (25%-1%), this particular gas velocity might be either the choking velocity or the transition velocity from turbulent to fast regime.

During the experimental procedure, it was observed that the riser was in the dense form and slugs were travelling upwards within the riser height. Strong fluctuations of the

water manometers were recorded. The values recorded in the graph are averaged ($1-\varepsilon$) values between a maximum and minimum amplitude of the water manometers.

CHOKING

Leung and Wiles(1976) have identified two types of transition from dilute phase flow to dense-phase flow in vertical transport. In the first type, the choking condition is approached as the gas velocity is reduced at a fixed solid rate, the uniform dilute phase flow is replaced by a dense-slugging flow. In the secind type a gradual increase in suspension density is observed before the dense-phase flow is obtained.

There is a degree of confusion in literature over the state of choking. In vertical pneumatic transport, choking is the transition from the dilute-phase flow to the dense-phase flow with increase in solid concentration and pressure fluctuations. With coarse or heave particles slugging occurs while with small light particles a large amount of internal recirculation at the walls of the column take place.

Correlations are available in the literature to classify a system as choking or non-choking. Two well known are those of Yousfi and Gau (1974) and Yang (1976). Yousfi and Gau proposed the following criterion for choking: $\frac{V_t^2}{gd_p} > 140$

For the FCC powder used during the experiments $\frac{V_t^2}{gd_p} = 64$

the above criterion does not exhibit the characteristic of choking.

Yang proposed that choking is avoided provided the following criterion is met: $\frac{V_t^2}{gD} < 0.35$

For the FCC powder $\frac{V_t^2}{gD} = 0.082$

Yousfi and Gau criterion does not take into account the effect of pipe diameter. Neither of the above two criteria take into account the effect of the gas velocity for the transition from dilute to dense phase flow.

TRANSPORT VELOCITY

According to Yerushalmi and Cankurt (1979), the transport velocity is regarded as the boundary which divides vertical gas-solid flow regimes into two groups. Below it lie the bubbling and turbulent fluidised bed and above it lies the transport regime which includes a wide range of stages from dilute-phase flow to the fast bed condition. For the FCC the transport velocity was estimated to be in the range of 1.2 to 1.5 m/s. The approach of transport velocity is characterised by a sharp increase in the rate of particle carryover.

The transport velocity, according to the above authors, might be determined from the plots of $\Delta P/\Delta L$ along a section of the riser as a function of the solid rate at different gas velocities.

It is not clearly defined how the transport velocity can be determined. The above plots indicate that at transport velocity a further increase in the solid rate results to a constant $\Delta P/\Delta L$ value across a section of the riser of a circulating fluidised bed.

For the FCC powder used during the experiments it is observed that above 2m/s, the solid rate is increased considerably. If it is assumed that the transport velocity lies between 1.5 to 2 m/s, close enough tothe values suggested by the above authors, then this velocity might it represent the transport velocity as well as the choking phenomenon.

5.2.2 EFFECT ON SOLID CIRCULATION RATE

The solid circulation rate (SCR) is measured using a load cell system, as is reported in Chapter 4. The solid circulation rate is defined as the weight of solids recirculated around the circulating fluidised bed during a time interval. Since it is assumed that the system reaches a steady state condition, after it is operated for half an hour, each SCR is constant and reproducible. Graphs of solid circulation rates versus superficial gas velocities are plotted for a range of ball valve openings (30-70) in Figures 5.2.22, 5.2.23 and 5.2.24, for the three different distributors.

Riser Distributor No.1 **(1 nozzle)**

The SCR does not seem to be affected by the increase of

FIGURE 5.2.22 PLOT OF GAS VELOCITY VERSUS SOLID CIRCULATION RATE

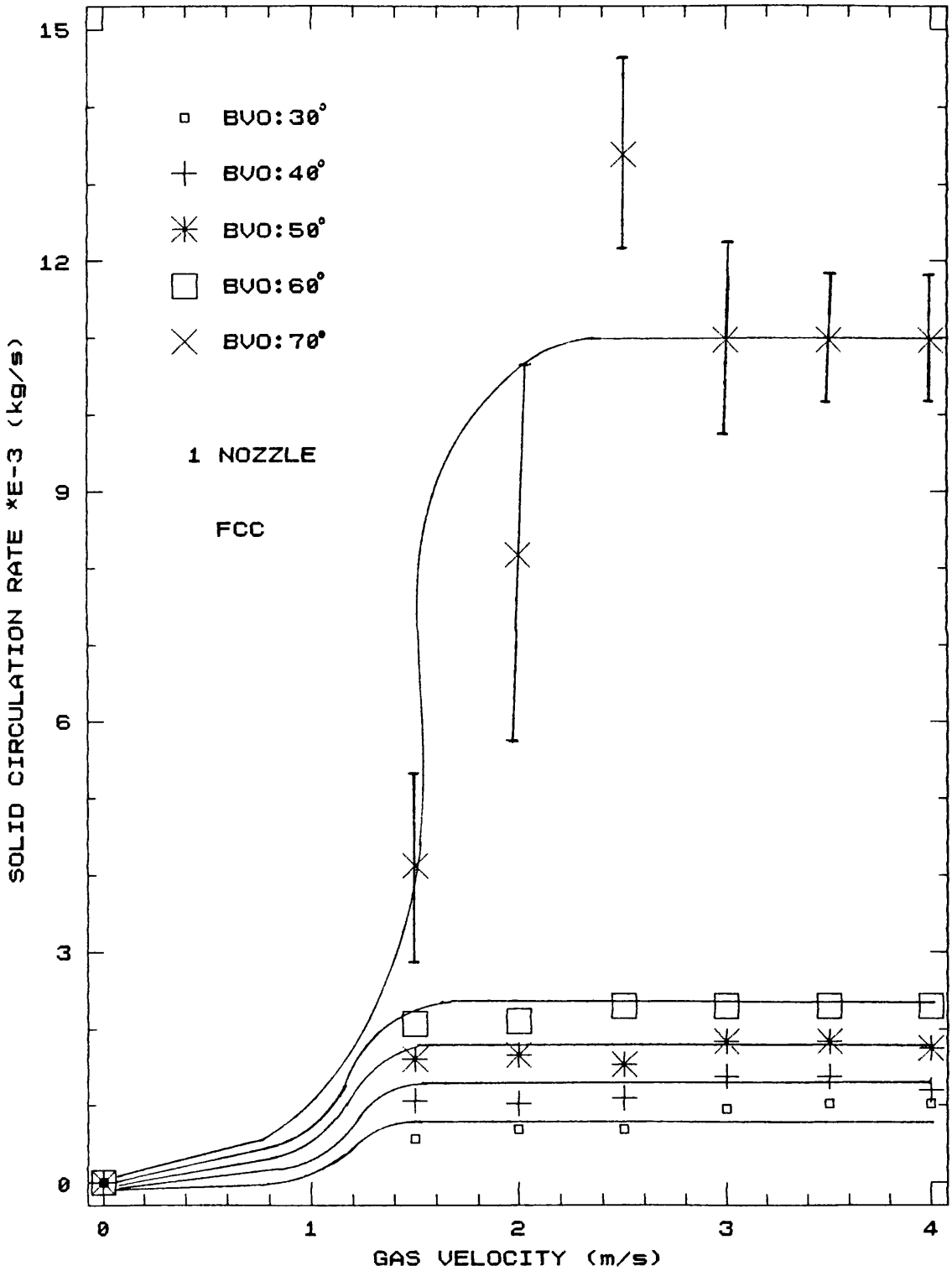

FIGURE 5.2.23 PLOT OF GAS VELOCITY VERSUS SOLID CIRCULATION RATE

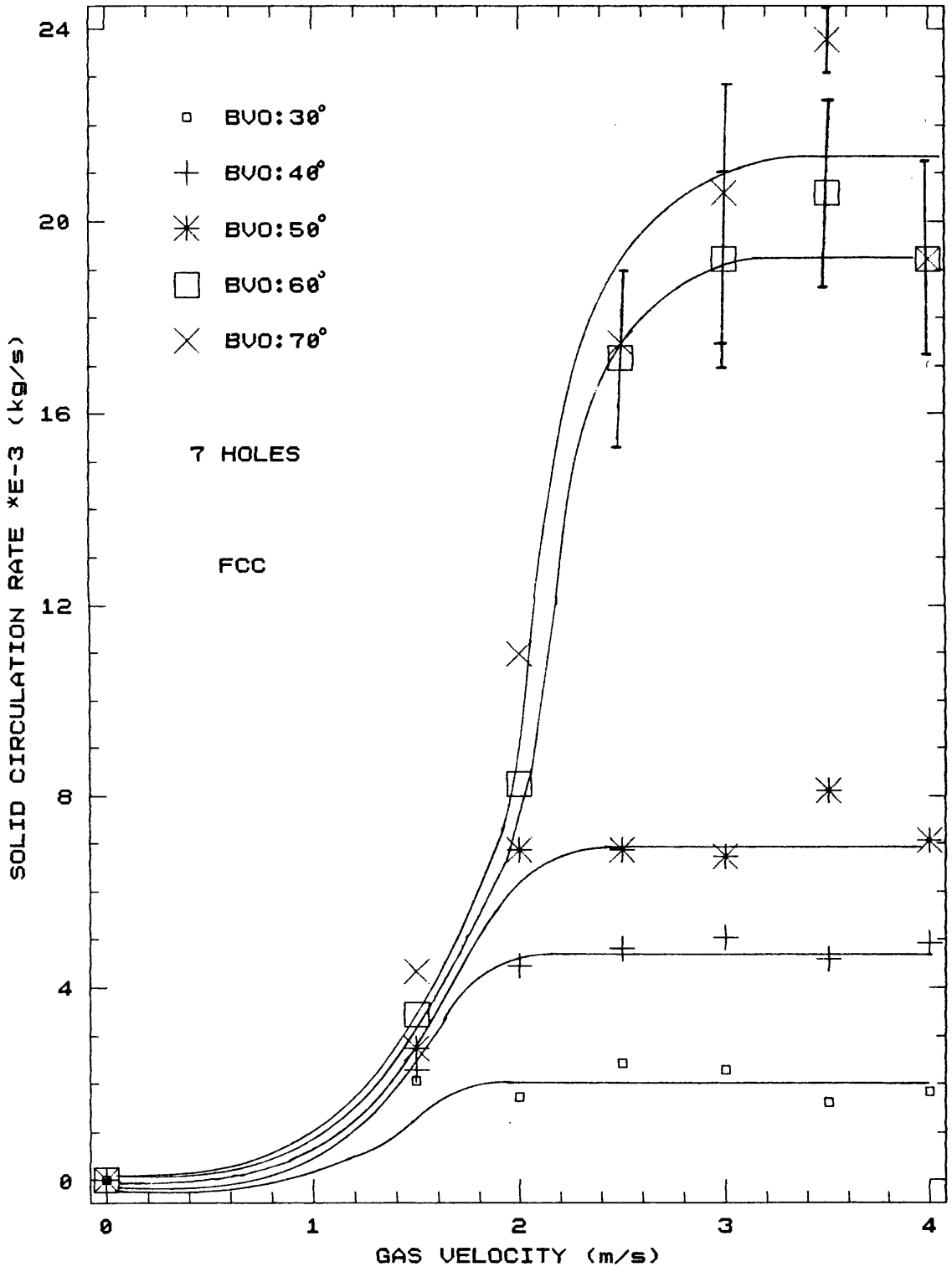

FIGURE 5.2.24 PLOT OF GAS VELOCITY VERSUS SOLID CIRCULATION RATE

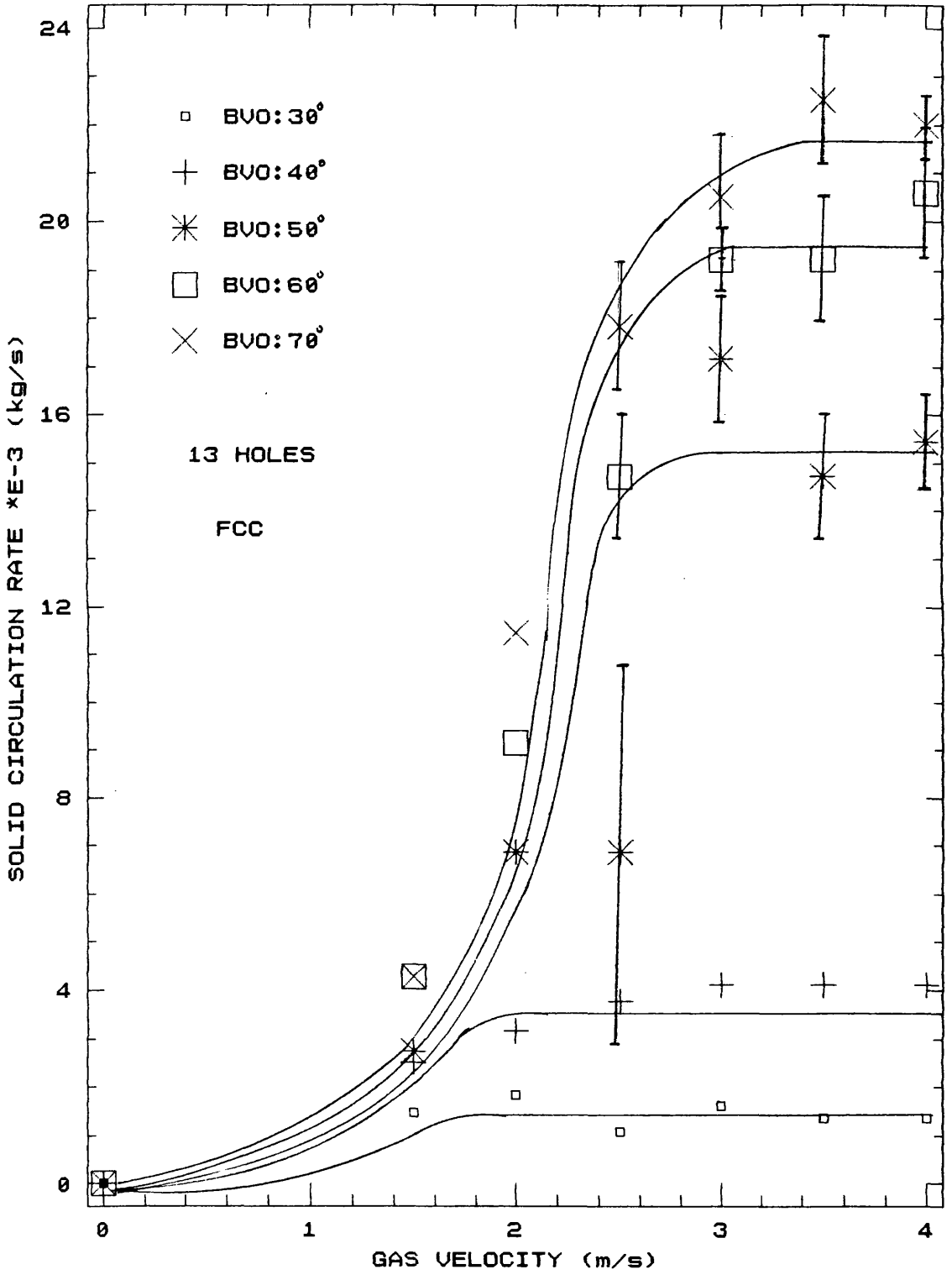

the superficial gas velocity, Ug, for the values of Ug greater than 1.5m/s at constant opening of the valve of 30,40,50 and 60 degrees. However on increasing the opening of the solid-rate control valve above 60 degrees, the SCR for a constant value of Ug does slightly increases.

Riser Distributor No.2 **(7 holes)**

The SCR increases with Ug up to a value of 1.5m/s and then remains constant for constant valve openings of 30,40 and 50 degrees. The general trend of increasing SCR with the increase of Ug is obtainable for the valve openings of 60 and 70 degrees up to a gas velocity of 2.5m/s. Above this value of Ug, the SCR is constant for all values of Ug and is only affected by the opening of the ball valve.

Riser Distributor No.3 **(13 holes)**

The SCR increases with Ug up to a value of 1.5m/s and then remains constant even if Ug is further increased to a value of 4m/s, at the valve openings of 30 and 40 degrees. For the cases of constant valve openings of 50,60 and 70 degrees an increase of SCR with Ug exists up to 2.5m/s. Above that for each valve opening the SCR remains constant but increases with the opening of the ball valve.

5.3 EFFECT OF GAS VELOCITY ON PRESSURE DROP AND SOLID CIRCULATION RATE

5.3.1 EFFECT ON PRESSURE DROP

For Figures 5.3.4, 5.3.5 and 5.3.6 the shapes of the curves at each gas velocity were generally such that the

FIGURE 5.3.4 PRESSURE DROP VERSUS RISER HEIGHT

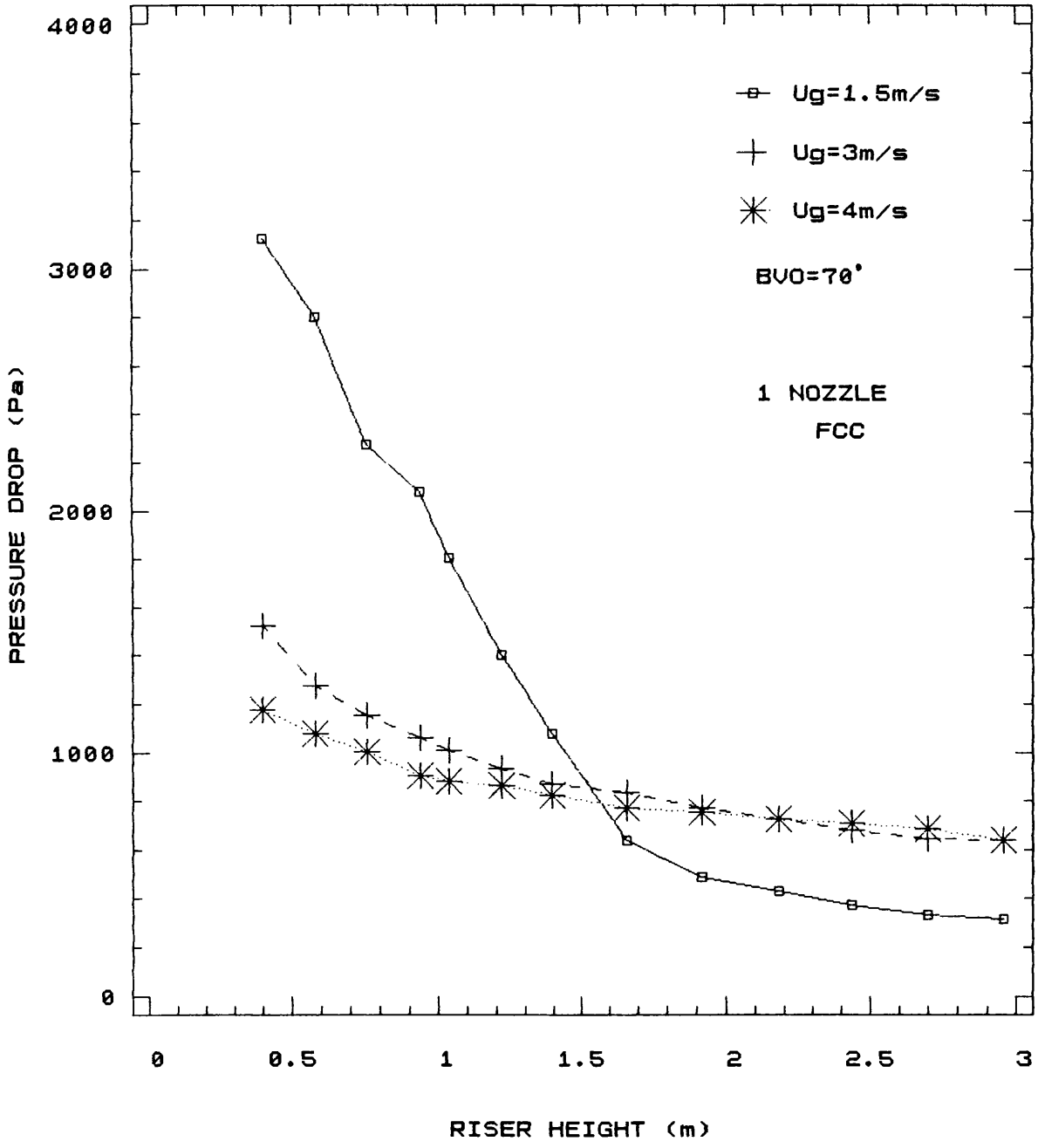

FIGURE 5.3.5 PRESSURE DROP VERSUS RISER HEIGHT

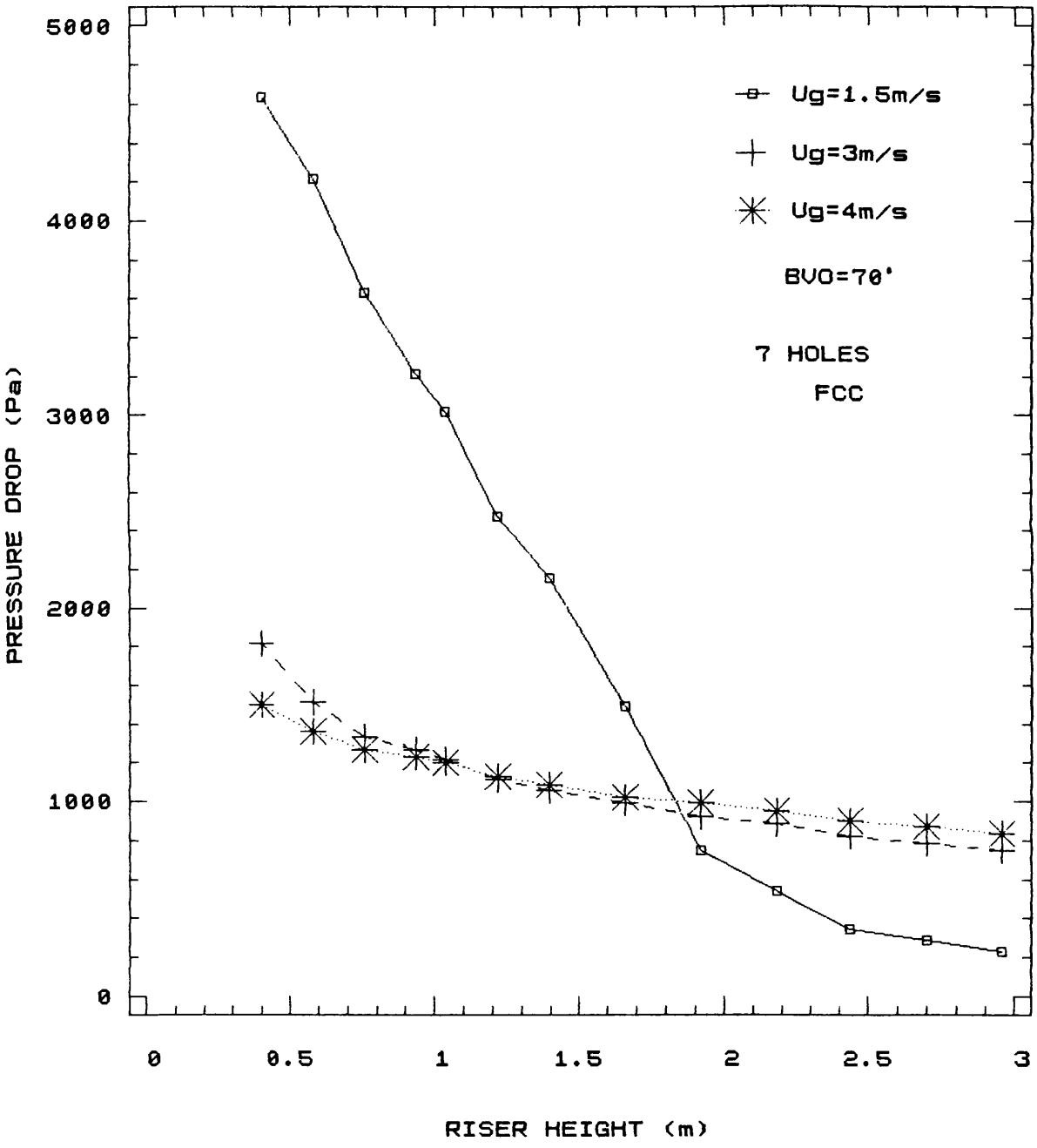

FIGURE 5.3.6 PRESSURE DROP VERSUS RISER HEIGHT

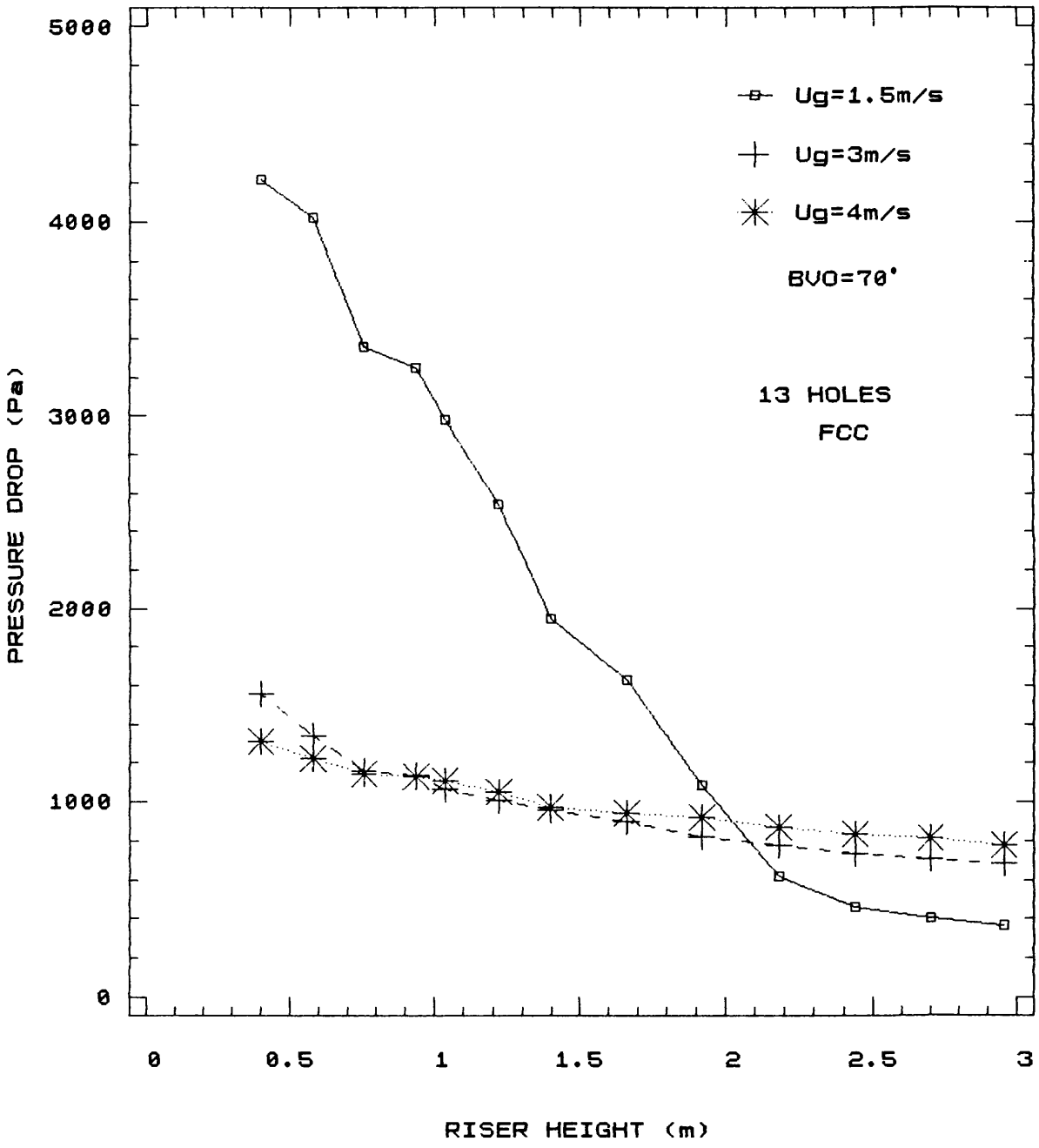

rate of change of pressure drop with height decreases as the top of the riser is approached.

For all three distributor designs, a common pattern emerges. At heights below about 1m, the greatest pressure drops occur at the lowest gas velocities. The variation at the lowest pressure tappings can exceed 2000 Pa when comparing the pressure drop curves for the 1.5 and 4 m/s gas velocities (a factor of about 3).

There is a height of approximately 1 to 1.5 m common to all three design of distributors, at which there is a convergence of all three pressure profiles. The relationship between pressure drop and gas velocity is reversed at this point of convergence. Visual observations made during the course of the experiments showed that below a height of approximately 1 m the riser appeared to contain a relatively dense phase. Above the point of convergence the voidage will be close to unity with the result that the hydrodynamics of the riser will be dominated by the properties of the gas alone. This explains why the pressure drops will be greater for the higher values of gas velocities.

Figures 5.3.1, 5.3.2 and 5.3.3 show the variation of pressure drop with riser height for the three distributor designs at a ball valve opening of 40 degrees. As with a ball valve opening of 70 degrees, the general shape of the pressure profile is such that the rate of change of pressure drop with height is greater in the lower half of the riser as compared with the top half of the riser.

FIGURE 5.3.1 PRESSURE DROP VERSUS RISER HEIGHT

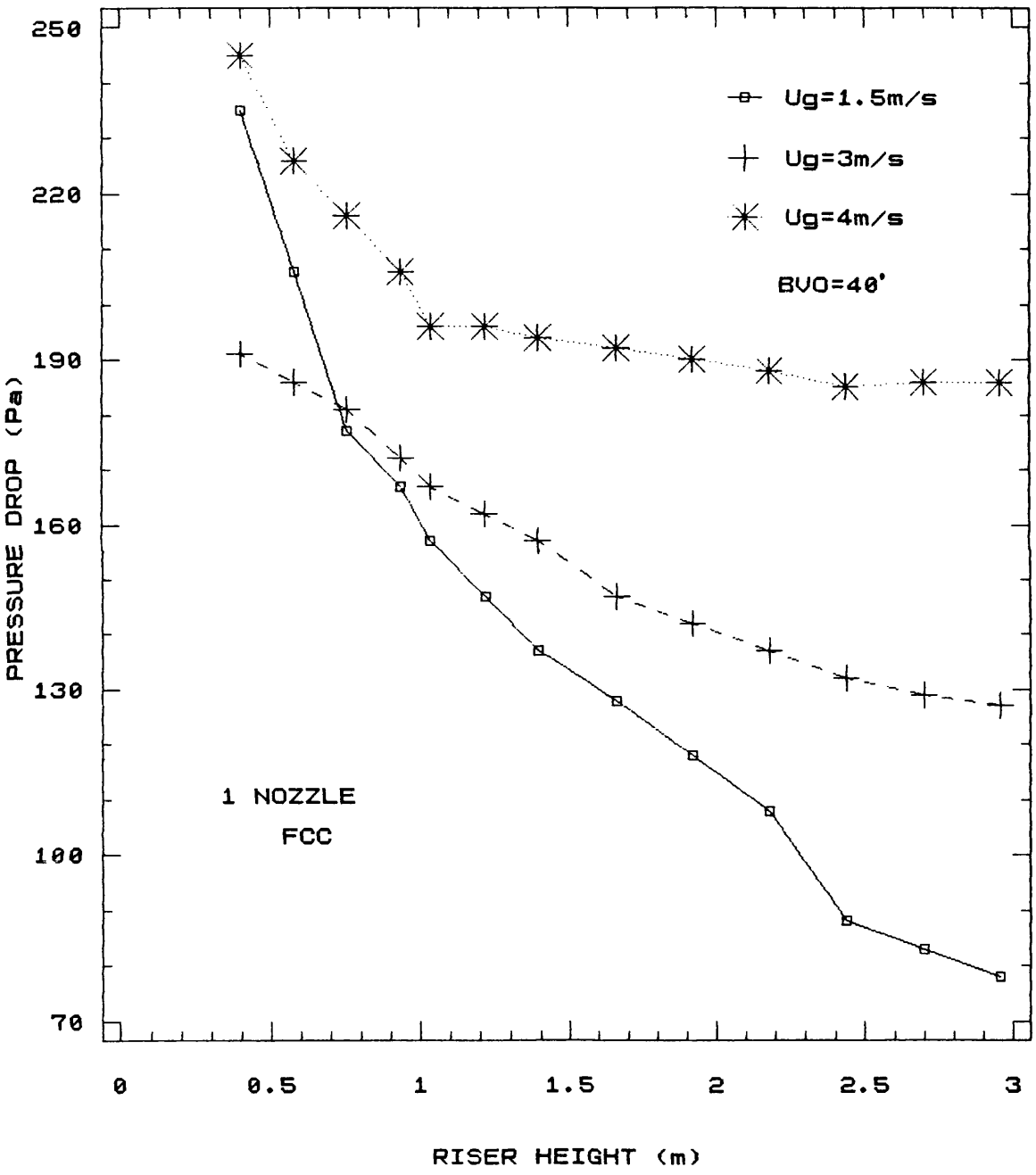

FIGURE 5.3.2 PRESSURE DROP VERSUS RISER HEIGHT

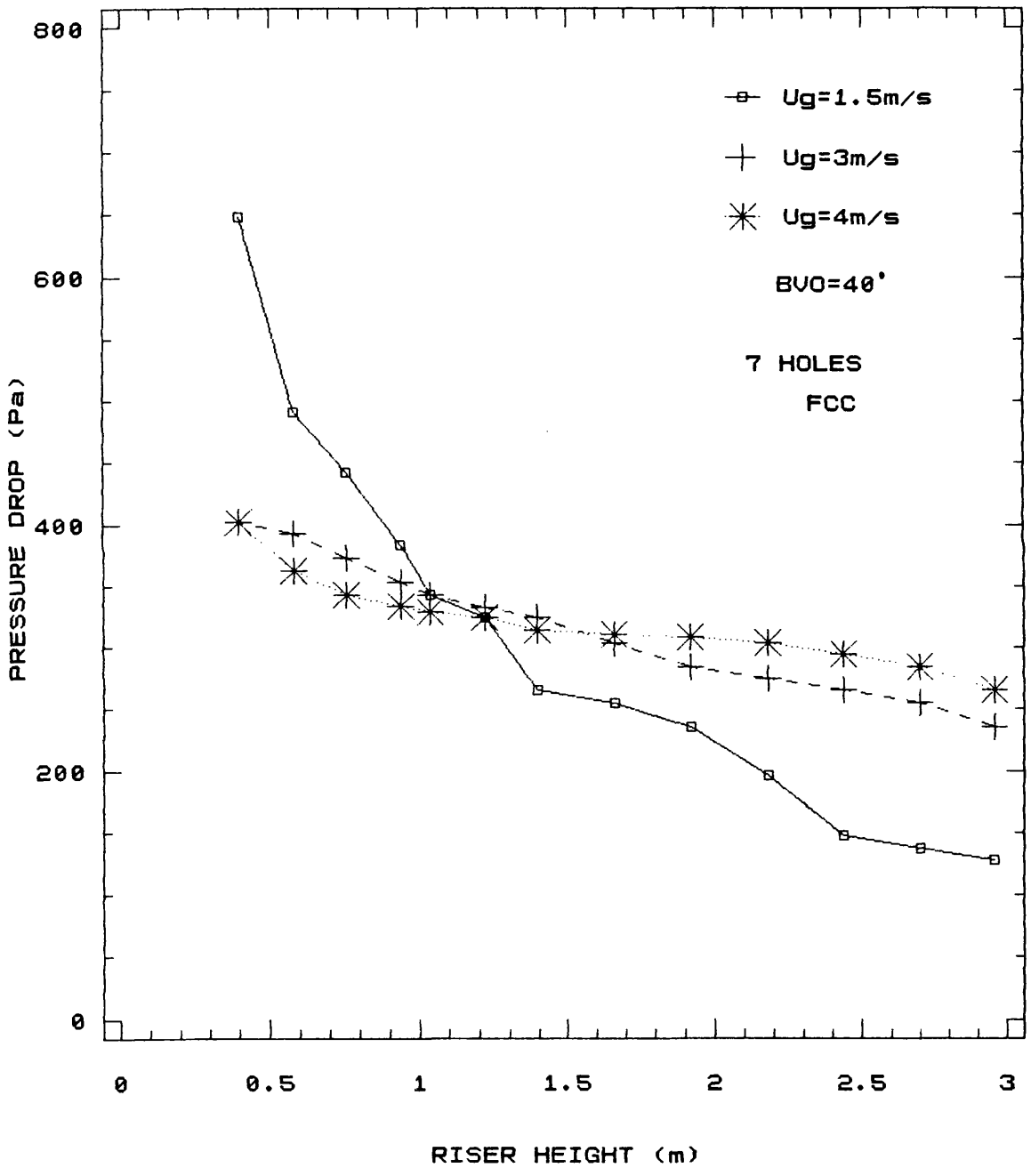

FIGURE 5.3.3 PRESSURE DROP VERSUS RISER HEIGHT

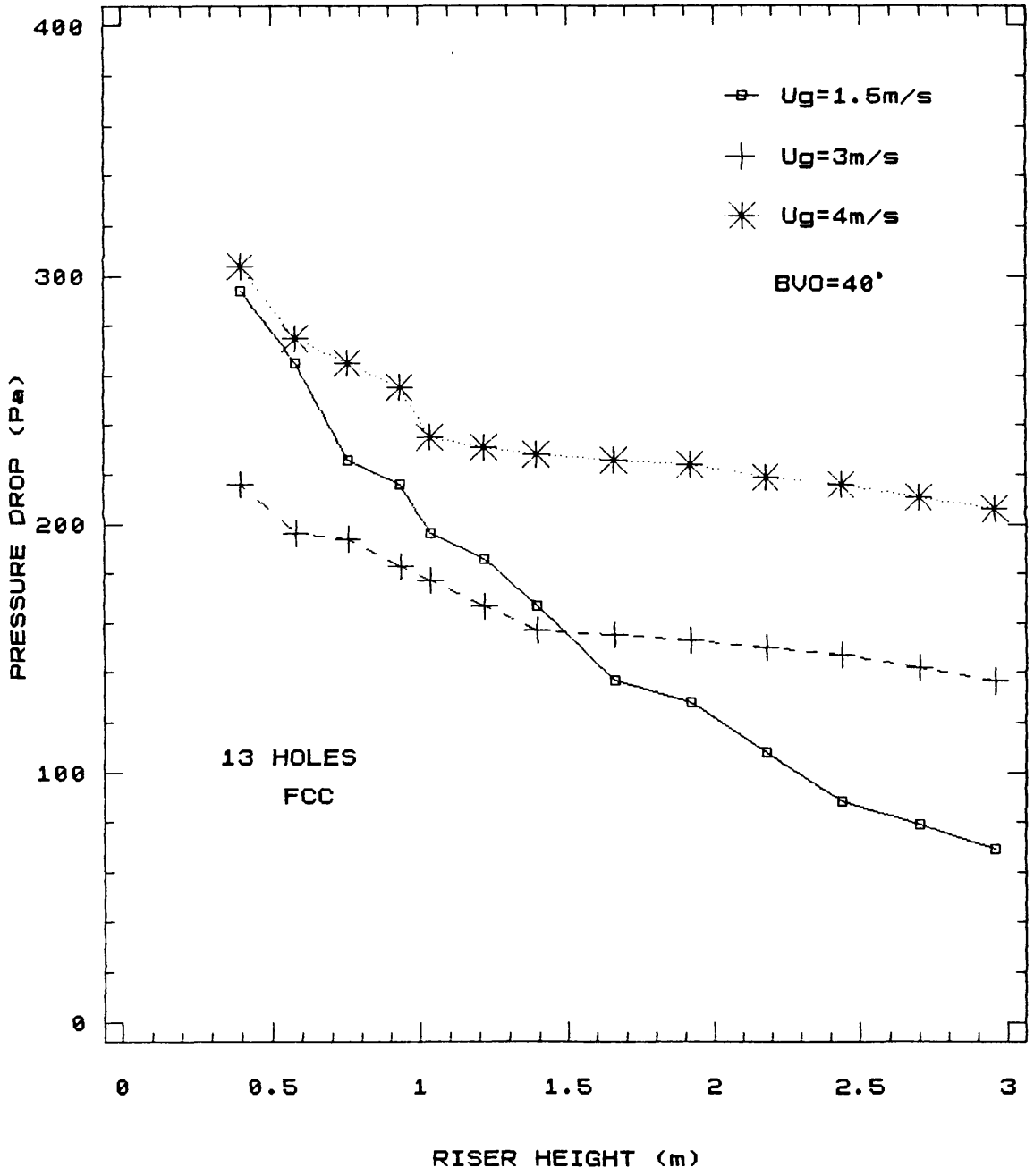

For the gas velocities investigated, the variation in pressure drops, that corresponds to each gas velocity, is much less than when the ball valve opening was at 70 degrees. The pressure drops themselves are almost an order of magnitude less than the pressure drops shown in Figures 5.3.4, 5.3.5 and 5.3.6.

Unlike the curves presented in Figures 5.3.4, 5.3.5 and 5.3.6, no clear trends emerge to characterise the relationship between each pressure profile and the gas velocity. Allowing for some degree of experimental uncertainty it might be appropriate to conclude that at low ball valve opening of 40 degrees the gas velocity has little influence on pressure drop.

5.3.2 EFFECT ON SOLID CIRCULATION RATE

The comparison of solid circulation rates (SCR) versus gas velocity plots of the riser distributors No.1, No.2 and No.3 shows that the SCRs using the distributor No.1 have much lower values than those of distributors No.2 and No.3, for all the cases of constant valve opening. A typical SCR-Ug plot is shown in Figure 5.3.7.

At low flowrates of air, the limiting condition is the energy contained within the air stream that can be transfered to the solid in the riser as it is being forced upwards, line AB of Figure 5.3.7.

At high air flowrates, ie point B of Figure 5.3.7, the air has now sufficient energy to impart to the solids so that the rate at which the solids are forced upwards

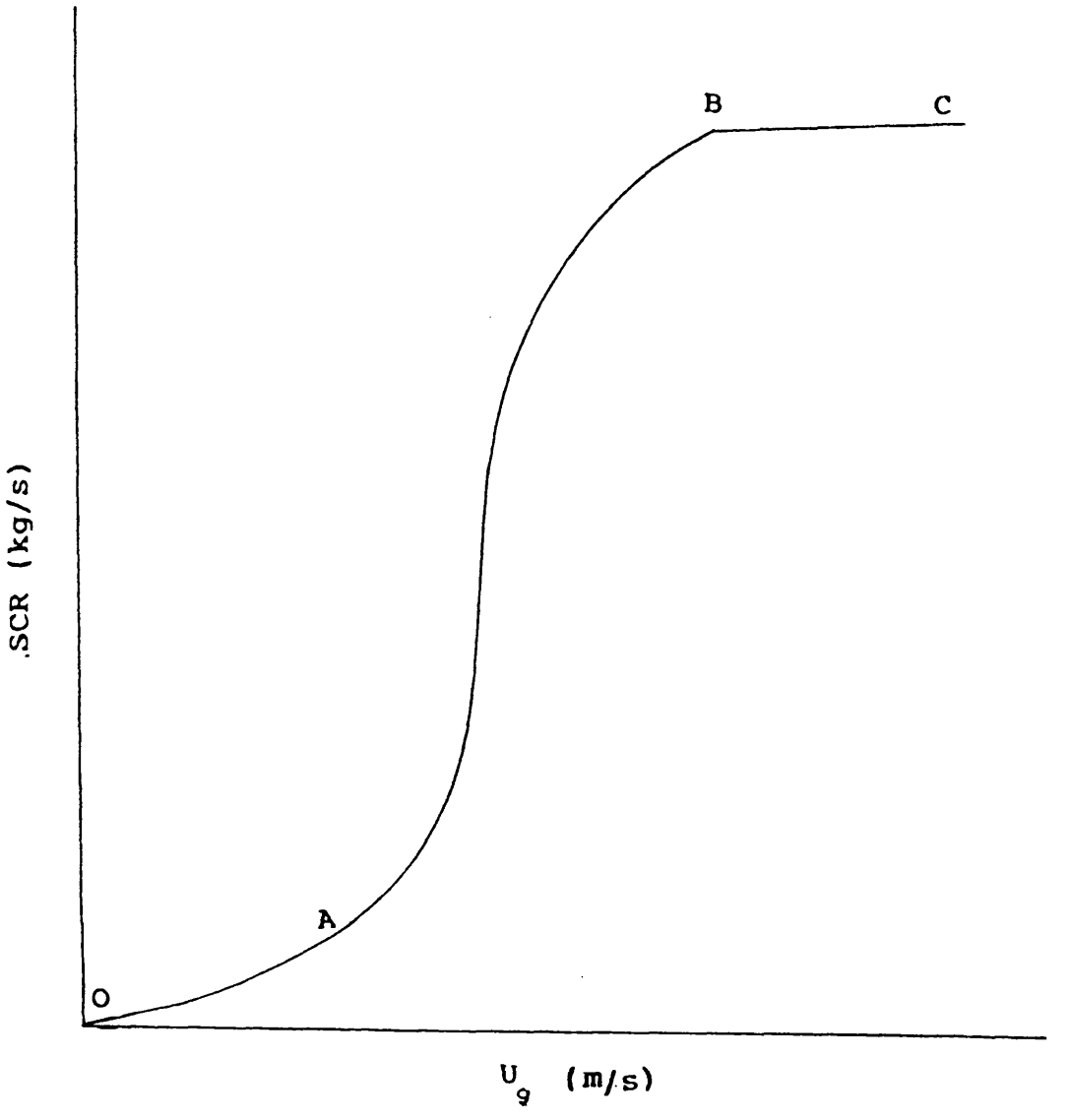

FIGURE 5.3.7 TYPICAL PLOT OF SOLID CIRCULATION RATE VERSUS GAS VELOCITY

matches the rate at which solids can pass through the ball valve. Increasing the air flowrate beyond point B will not increase the solid circulation rate because although the air stream has more energy out the rate at which the solids pass into the air stream does not change because this rate is determined solely by the ball valve.

The influence of the air in the riser is more confined radially causing a region of relative stagnation between the air stream and the wall of the riser immediately above the plane of the nozzle.

Increasing the number of holes in the distributor is likely to improve the radial gas distribution and minimise the stagnant regions especially near the base of the riser where the solids from the ball valve first come into contact with the air stream. Therefore there is more chance that the solid will come into contact with a fast moving air velocity from which it can gain energy in order to move upwards. Hence by improving the radial distribution of air one is likely to increase the solid circulation rate.

At very low gas flowrates, ie Region OA, the solid circulation rate is negligible because the air has insufficient energy to entrain the solids. This means that at low flowrates, Region AB, it is the rate at which the air has a capacity to entrain the solids, so as to carry them up the riser, which will determine, at steady-state, how much solid can pass through a given cross-section of the circulated bed, ie the solid circulation rate.

From the shape of the graph shown in Figure 5.3.7, it

is apparent that within this region AB the solid circulation rate is a very sensitive function of gas velocity. However for the region BC, the solid circulation rate is independent of gas velocity. If the system is operated at such gas velocity greater than B, the air flowrate will have sufficient capacity to entrain more solids, but the opening of the ball valve is such that it is already allowing the maximum possible flowrate for the dynamic equilibrium of the system. Therefore, the extra capacity of the air stream will not be utilised. It can be said that under these conditions the ball valve opening, (BVO), is determining the solid circulation rate. Hence the plateau BC shown in graph Figure 1. Increasing the BVO rather than increasing the gas flowrate will lead to a faster solid circulation rate.

5.4 EFFECT OF BALL VALVE OPENING ON SOLID CIRCULATION RATE

Figures 5.4.1, 5.4.2 and 5.4.3 show graphs of solid circulation rate (SCR) against ball valve opening (BVO) for the three design distributors. Not unexpectedly, an increase in gas velocity leads to an increase in SCR at a given BVO (see previous discussion in Section 5.3.2). Again at a given gas velocity, increasing the BVO leads to an increase in SCR. As with the graphs of SCR versus Ug (Figures 5.2.22 to 5.2.24), each curve resembles an S-shape with three distinct regimes. At low BVO (below 50 degrees) the rate at which the SCR increases with the BVO is

FIGURE 5.4.1 SOLID CIRCULATION RATE VERSUS BALL VALVE OPENING

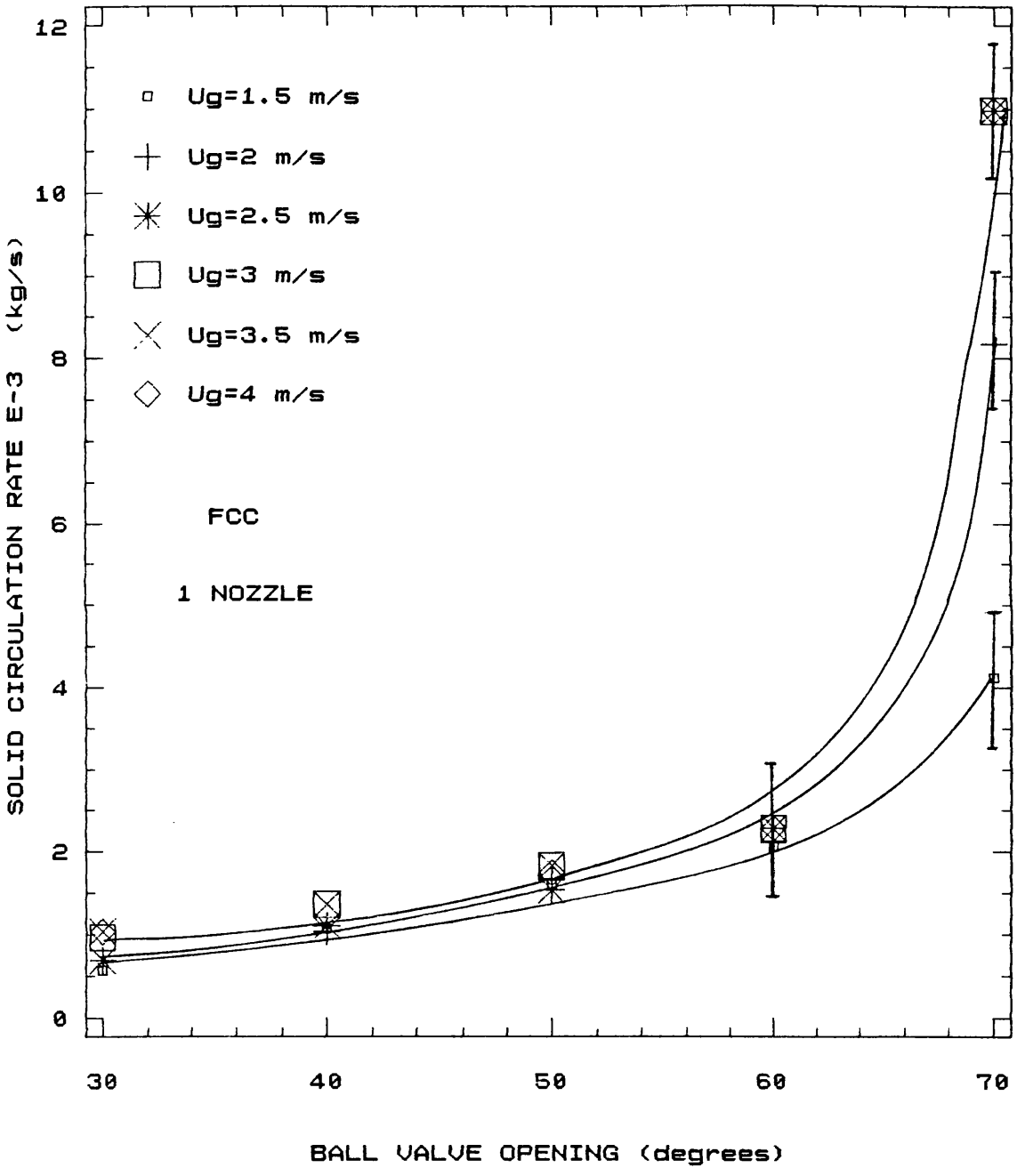

FIGURE 5.4.2 SOLID CIRCULATION RATE VERSUS BALL VALVE OPENING

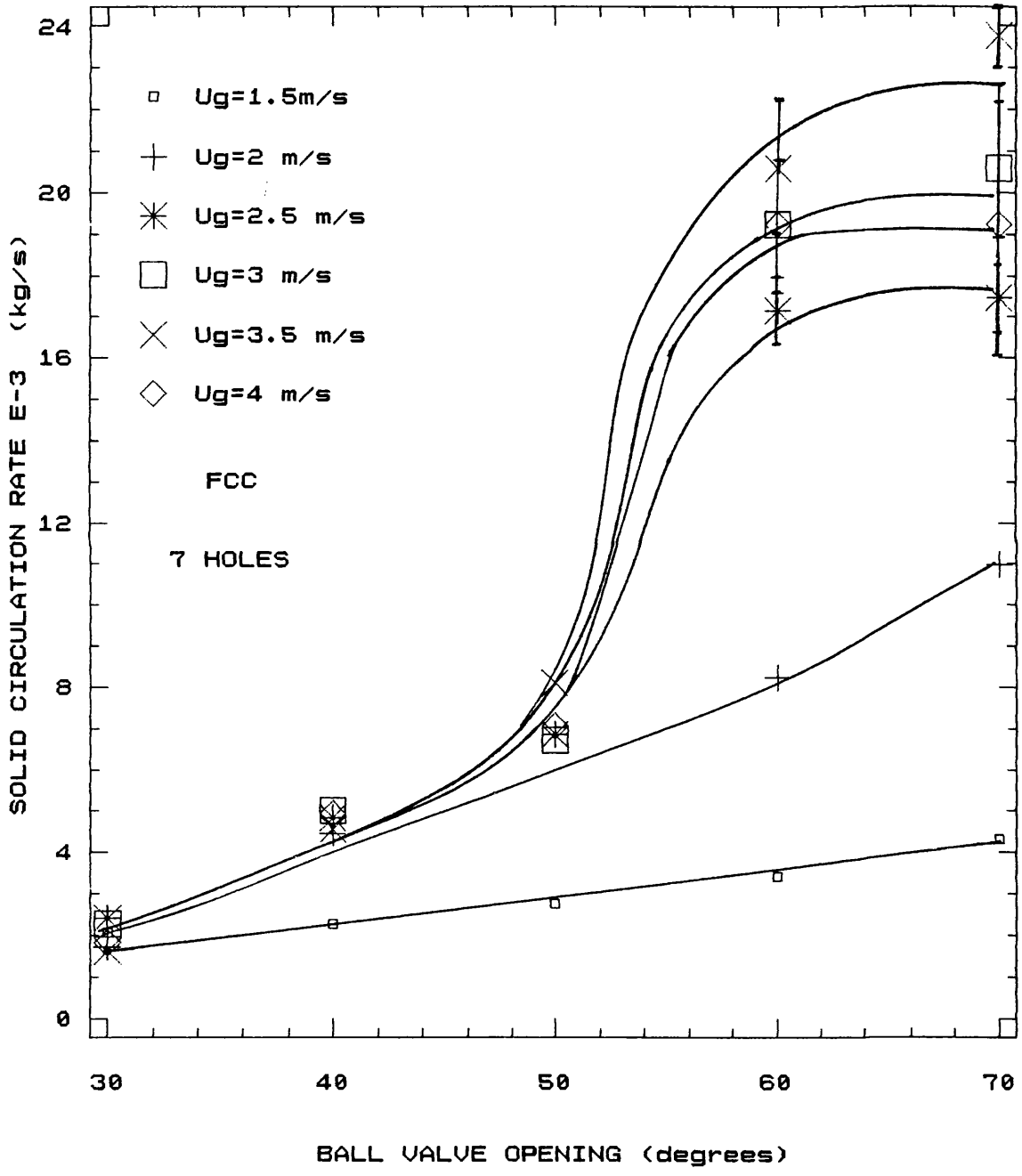

FIGURE 5.4.3 SOLID CIRCULATION RATE

VERSUS BALL VALVE OPENING

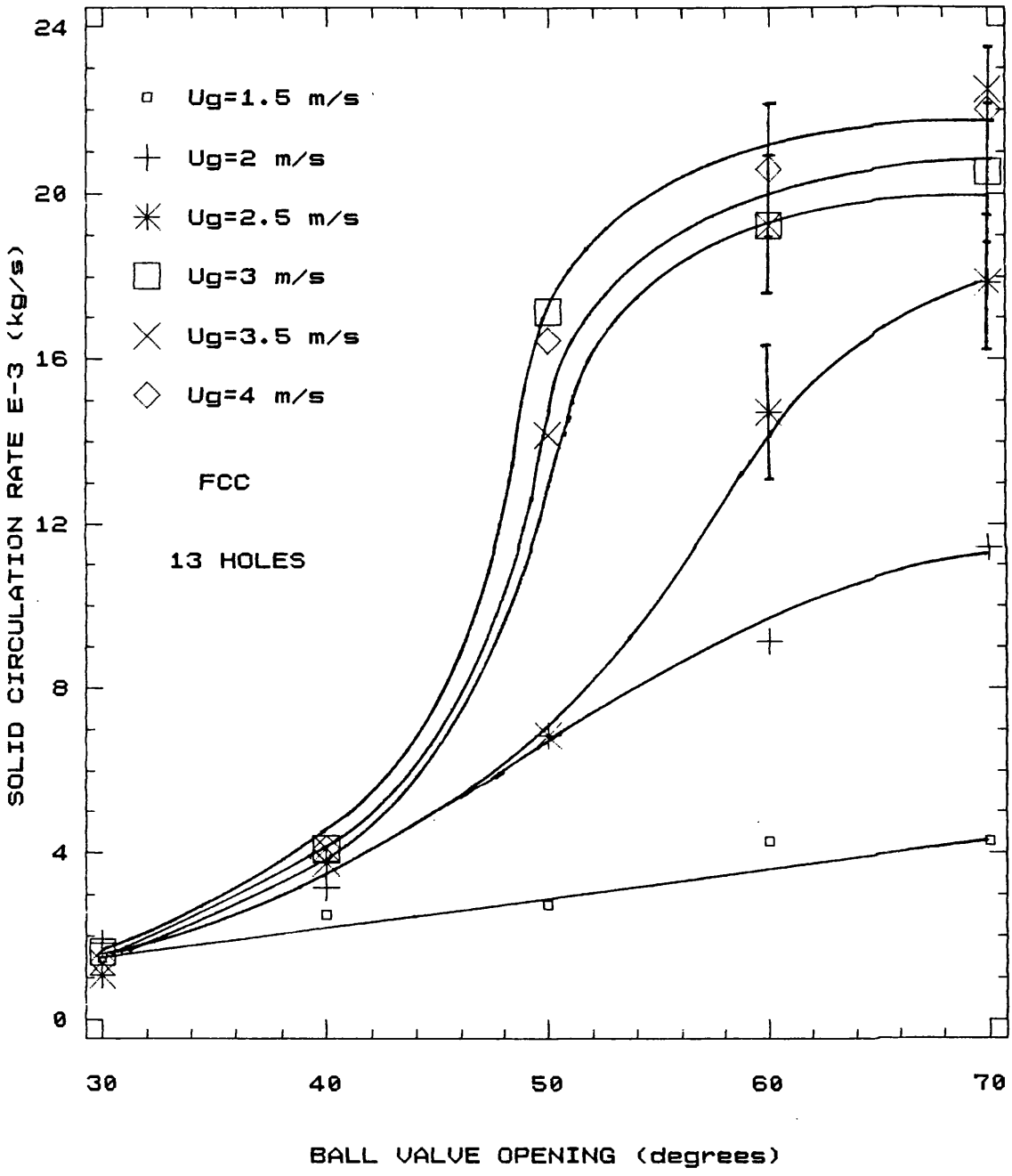

relatively low, whilst between 50 and 60 degrees (between 60 and 70 degrees in the case of 1 nozzle distributor), the slope of the curve dramatically increases, before reaching some plateau. The reasons why the curves follow this characteristic S-shape are very similar to the arguments discussed in Section 5.3.2.

The main differences in the performance of the three distributors manifest themselves at the higher gas velocities (above 2.5m/s). For the 7 and 13 hole distributors both the shape of the graphs and the actual solid circulation rates measured are very similar. However for the 1 nozzle distributor the curves at each gas velocity do not appear to display the emergence of a plateau. Futhermore, the solid circulation rates are significantly lower (above half) than the solid circulation rates achieved with the 7 and 13 hole distributors.

5.5 EFFECT OF PARTICLE PROPERTIES ON PRESSURE DROP AND SOLID CIRCULATION RATES

5.5.1 EFFECT ON PRESSURE DROP

Two different types of particles were used for the experimental investigation of the hydrodynamics of the riser when using a 1 nozzle distributor. The properties of these particles are shown in Table 5.5.1.

Particle Type	Density kg/m^3	Particle diameter μm
FCC	884	64
PORALOX	1840	127

TABLE 5.5.1

Experiments were conducted using only the Poralox powder as well as with a 50/50 v/v mixture with FCC powder.

Figure 5.5.1 shows the pressure drops with riser height for pure Poralox, pure FCC and a 50/50 v/v mixture, at a ball valve opening of 70 degrees and a gas velocity of 3 m/s. The shape of the graphs are similar to those presented in Figures 5.2.1 to 5.2.18. For all riser heights and especially near to the base the pressure drops measured with Poralox are much higher than the pressure drops using pure FCC powder. Not suprisingly, a mixture of the two powders gives rise to a pressure drop curve between the two pure powder curves.

At a riser height of 40 cm the Poralox pressure drop is well over twice the FCC pressure drop (3600 compared to 1500 Pa). When the pressures are measured near to the top of the riser the variation in pressure drop has narrowed considerably (1100 compared with 650 Pa).

The explanation for the larger pressure drops measured when using Poralox lies in the increased density and diameter of the Poralox particles. As mentioned before (see Section 5.4.1), the lower part of the riser will experience lower voidages and therefore higher particle concentrations especially at high ball valve openings. If the voidages at the base of the riser are similar for the FCC and Poralox

FIGURE 5.5.1 RISER DISTRIBUTOR:1 NOZZLE

PRESSURE DROP VERSUS RISER HEIGHT

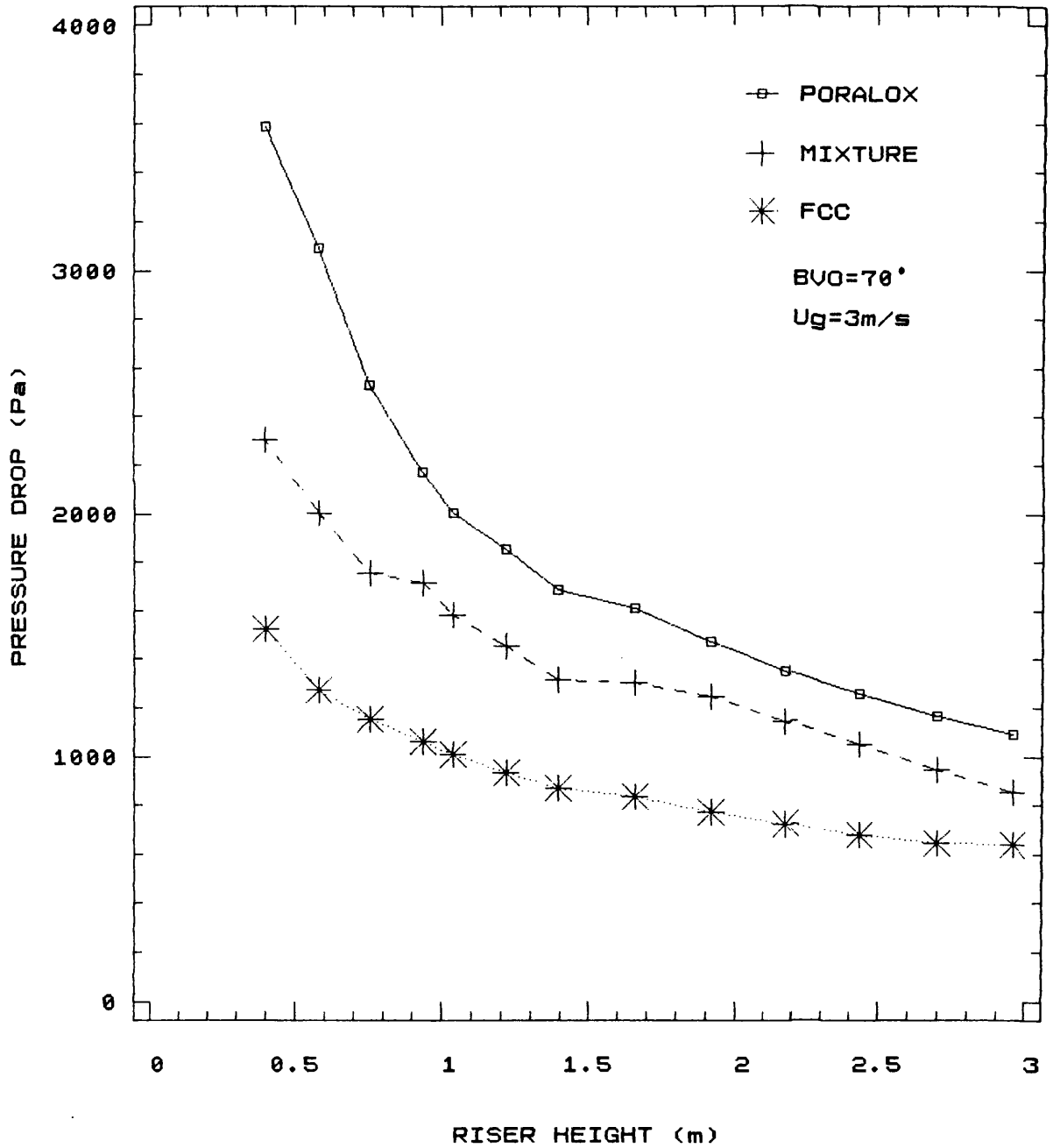

powder, then the increased density of the Poralox powder will imply a greater static pressure.

Figure 5.5.2 shows the variation of cummulative pressure difference with the ball valve opening (gas velocity of 3 m/s), for the pure Poralox, pure FCC and the mixture of the two. As the ball valve opening is increased the variation in cummulative pressure drop increases marketly for the three curves. At a ball valve opening of 40 degrees the variation between the Poralox curve and the FCC curve is about 1050 Pa but at a ball valve opening of 70 degrees this variation has increased to 1400 Pa.

Figures 5.5.3 and 5.5.4 show pressure drops along the height of the riser with Poralox at gas velocities of 2 and 4 m/s.

Comparison with the equivalent graphs for FCC presented in Figures 5.2.2 and 5.2.6 show that for the same ball valve opening and gas velocity the fluidisation of Poralox lead to much greater pressure drops.

At a gas velocity of 2 m/s and a ball valve opening of 60 degrees the Poralox pressure drop was nearly ten times greater than the FCC pressure drop (5000 compared with 700 Pa).

At a gas velocity of 4 m/s and a ball valve opening of 70 degrees the Poralox pressure drop was about twice the equivalent FCC pressure drop (2700 compared with 1200 Pa).

Using Poralox powder it was found that instabilities occured when the ball valve opening was increased beyond 60 degrees at low gas velocities ie 2 and 2.5 m/s.

FIGURE 5.5.2 PRESSURE DIFFERENCE VERSUS BALL VALVE OPENING

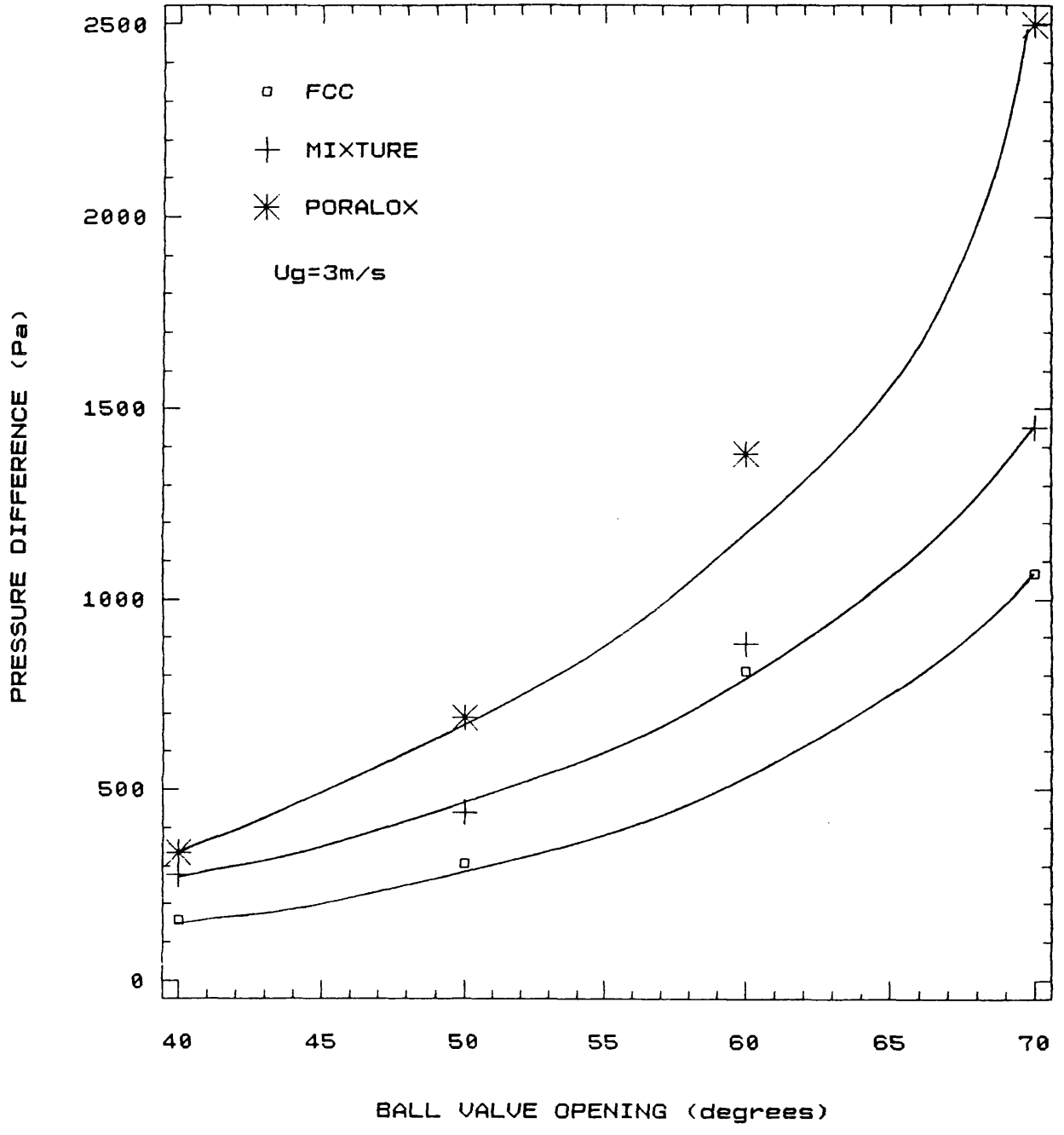

FIGURE 5.5.3 RISER DISTRIBUTOR:1 NOZZLE
PRESSURE DROP VERSUS RISER HEIGHT

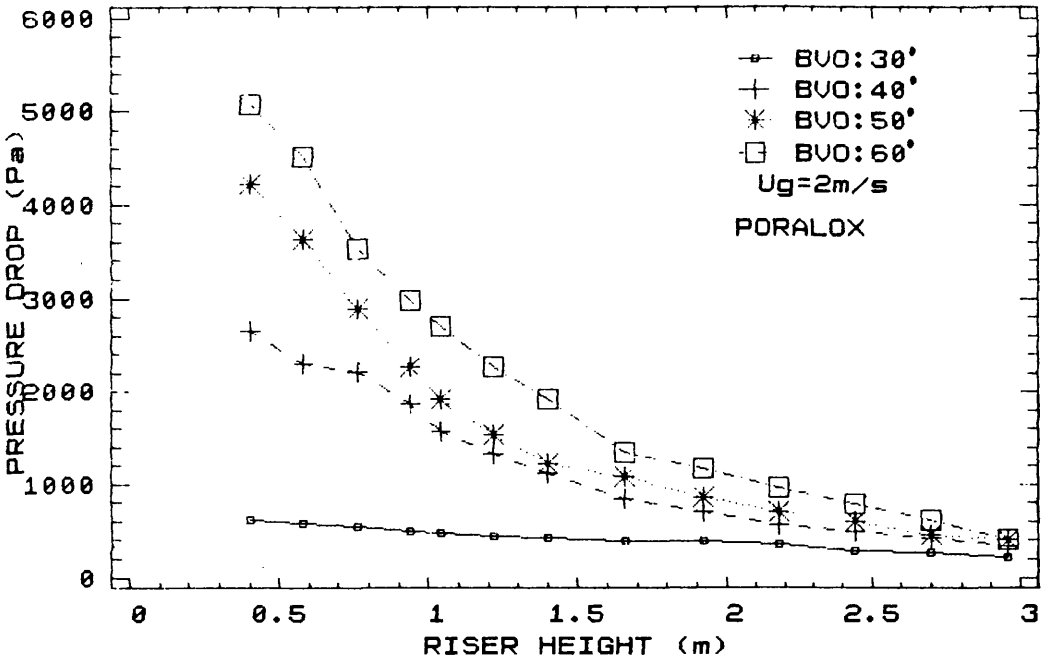

FIGURE 5.5.4 RISER DISTRIBUTOR:1 NOZZLE
PRESSURE DROP VERSUS RISER HEIGHT

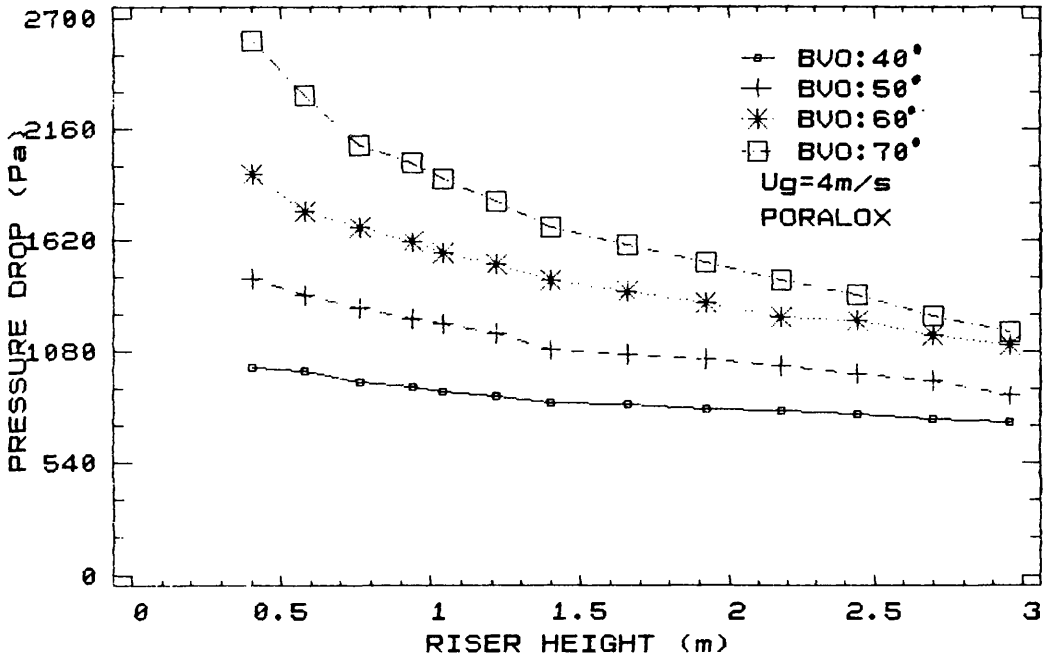

This unstable condition corresponds to a situation when a very dense phase appears at the base of the riser promoting a flow reversal of solids through the ball valve at ball valve openings greater than 60 degrees.

5.5.2 EFFECT ON SOLID CIRCULATION RATE

Figure 5.5.5 shows the variation of solid circulation rate with gas velocity at different ball valve openings using pure Poralox powder. As in Section 5.5.1 the circulating fluidised bed was operated using a 1 nozzle distributor. The curves at each ball valve opening are similar to the S shape curves presented in Figure 5.2.22 to 5.2.24, so that at high gas velocities the solid circulation rate reaches some plateau value. This has already been discussed and explained in Section 5.3.2.

Figure 5.5.6 shows a comparison of the solid circulation rate versus ball valve opening for the pure Poralox, pure FCC and 50/50 v/v mixture, at a gas velocity of 3 m/s. Generally, the solid circulation rates are higher with the pure Poralox powder as compared with the pure FCC powder. Whilst the experimental data for the pure Poralox and the 50/50 v/v mixture are well fitted to a single straight line, the FCC data might be better described by a curve, whose slope increases dramatically when the ball valve opening is greater than 60 degrees.

Figure 5.5.7 shows the variation of solid circulation rate with gas velocity using pure FCC powder and pure

FIGURE 5.5.5 SOLID CIRCULATION RATE VERSUS GAS VELOCITY FOR PORALOX

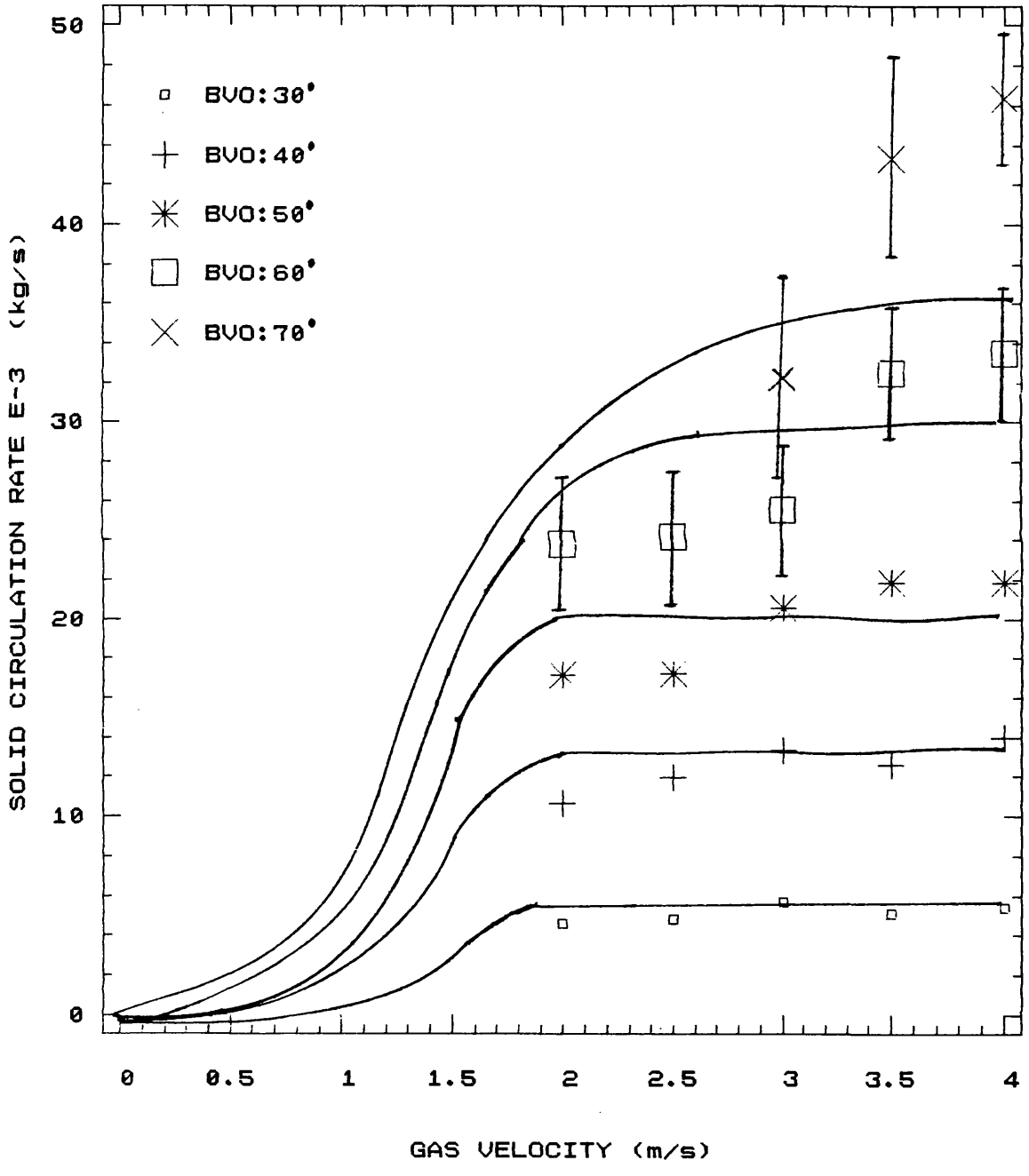

FIGURE 5.5.6 SOLID CIRCULATION RATE

VERSUS BALL VALVE OPENING

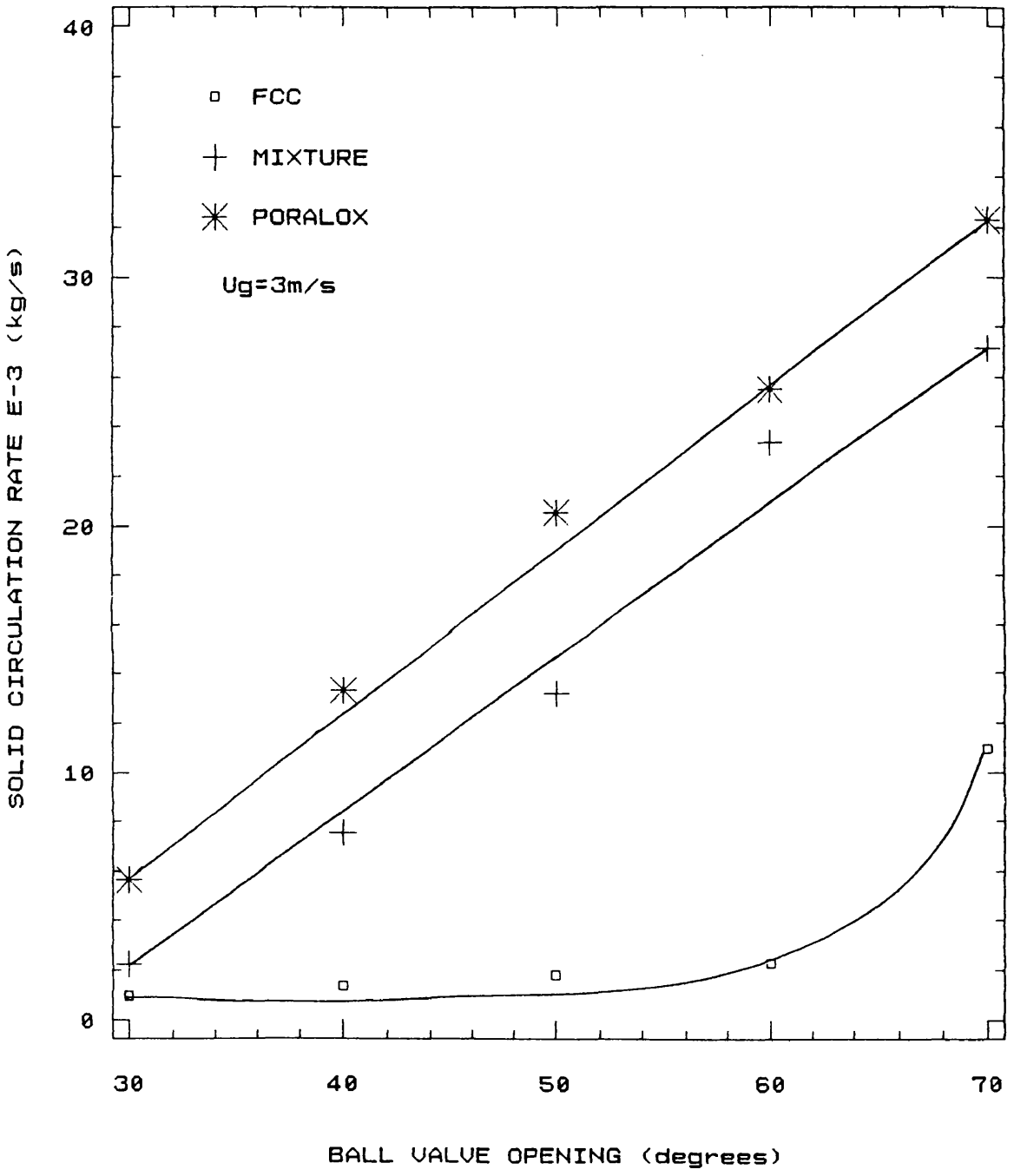

FIGURE 5.5.7 PLOT OF SOLID CIRCULATION RATE VERSUS GAS VELOCITY

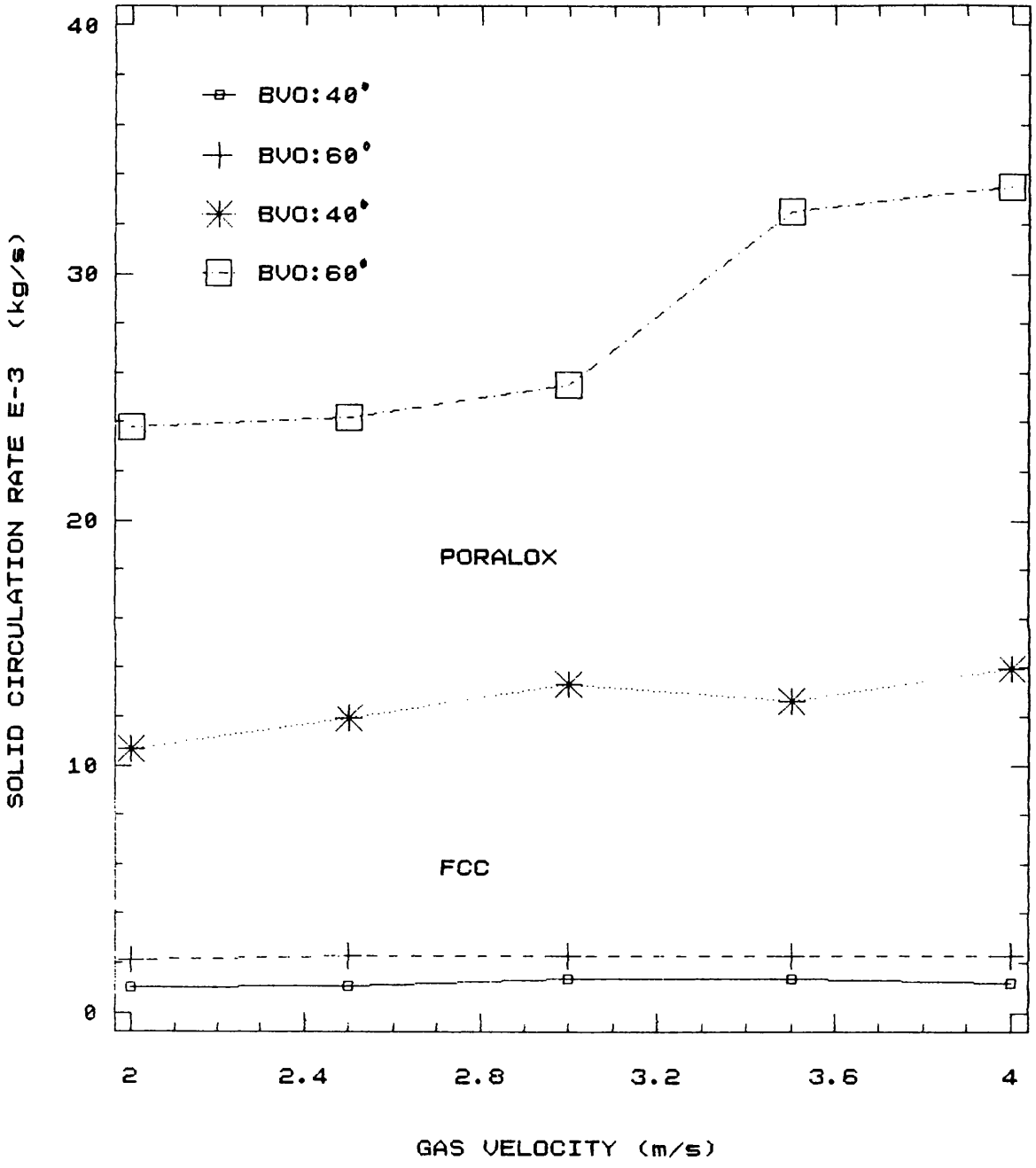

Poralox powder. For the pure FCC powder at ball valve openings between 40 and 60 degrees there is very little variation in solid circulation rate as the gas velocity is increased. At a ball valve opening of 40 degrees the solid circulation rate of FCC powder was barely more than 1 g/s for the range of gas velocities investigated. At a ball valve opening of 60 degrees the solid circulation rate stayed at about 2 g/s.

Operating the circulating fluidised bed using Poralox powder ment much higher solid circulation rates, and greater variation in solid circulation rate with increasing gas velocity. At higher gas velocities the solid circulation rates at ball valve openings of 40 and 60 degrees appear to reach a plateau. At a ball valve opening of 60 degrees the plateau is about 34 g/s. This can be compared with a value of 2 g/s measured for pure FCC powder at the same ball valve opening of 60 degrees.

5.6 COMPARISONS OF PRESSURE DROP DATA WITH PREDICTIONS MADE WITH MODEL

Figures 5.6.1 to 5.6.6 show the pressure drop per unit length at different heights in the riser. The graphs represented can be used to show a comparison between the experimentally measured pressure gradients and the theoretical predictions made using the model developed in Chapter 3.

Figure 5.6.1 is an example of where prediction and measurement are closely matched. For the range of gas

FIGURE 5.6.1 PRESSURE GRADIENT VERSUS RISER HEIGHT AT Ug=4m/s & BVO=70°

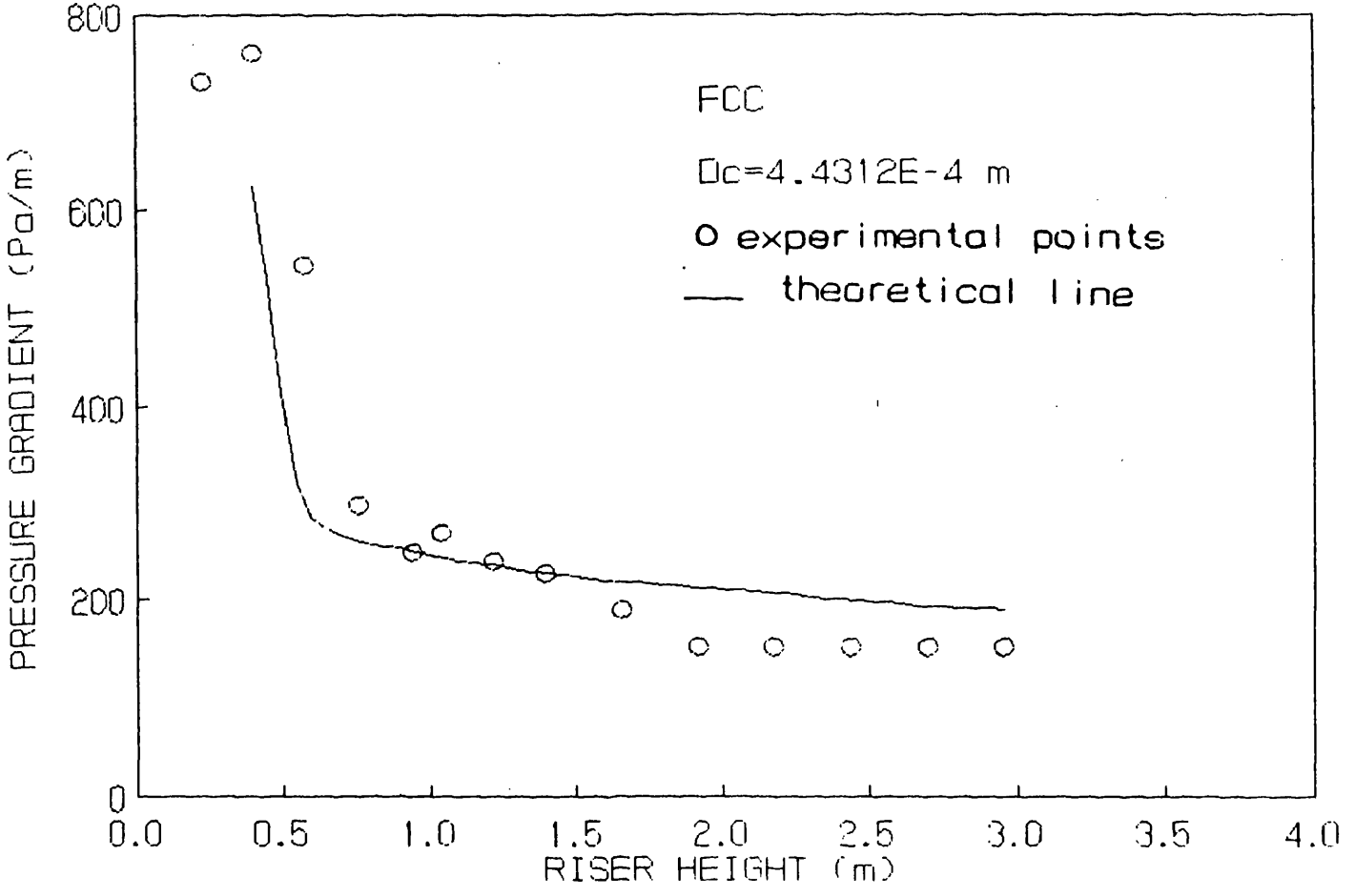

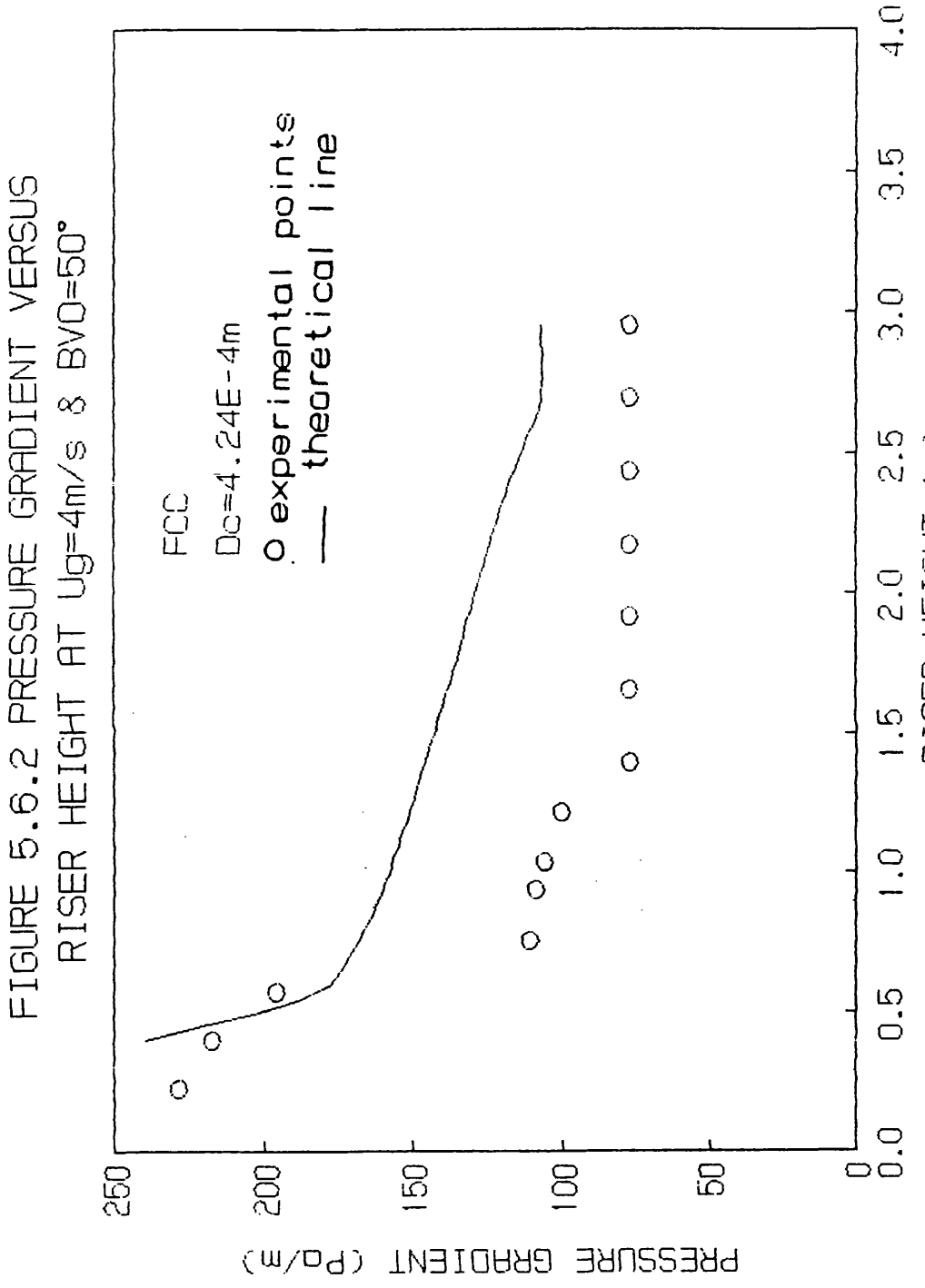

FIGURE 5.6.2 PRESSURE GRADIENT VERSUS RISER HEIGHT AT Ug=4m/s & BVO=50°

FIGURE 5.6.3 PRESSURE GRADIENT VERSUS RISER HEIGHT AT Ug=4m/s & BVO=70°

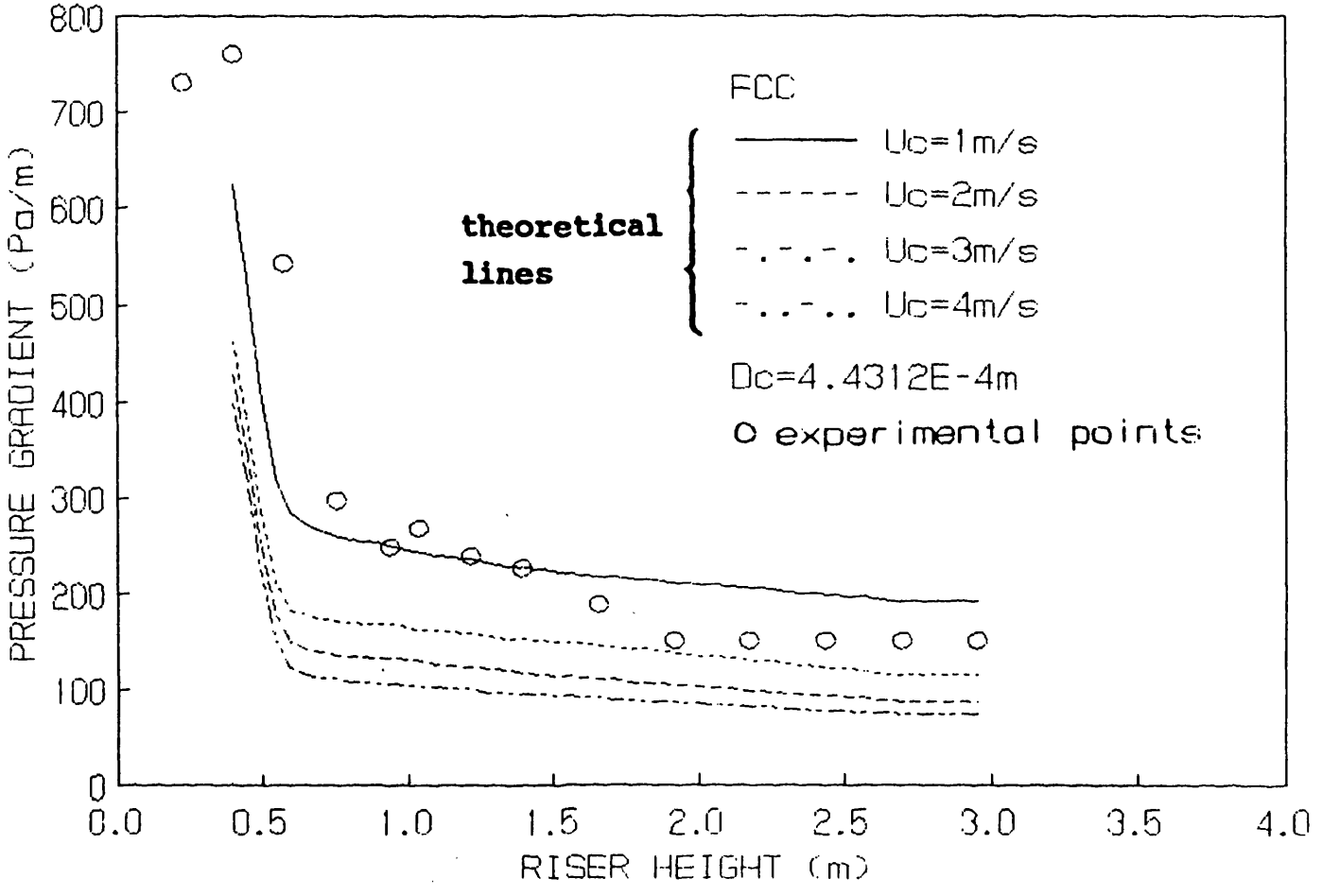

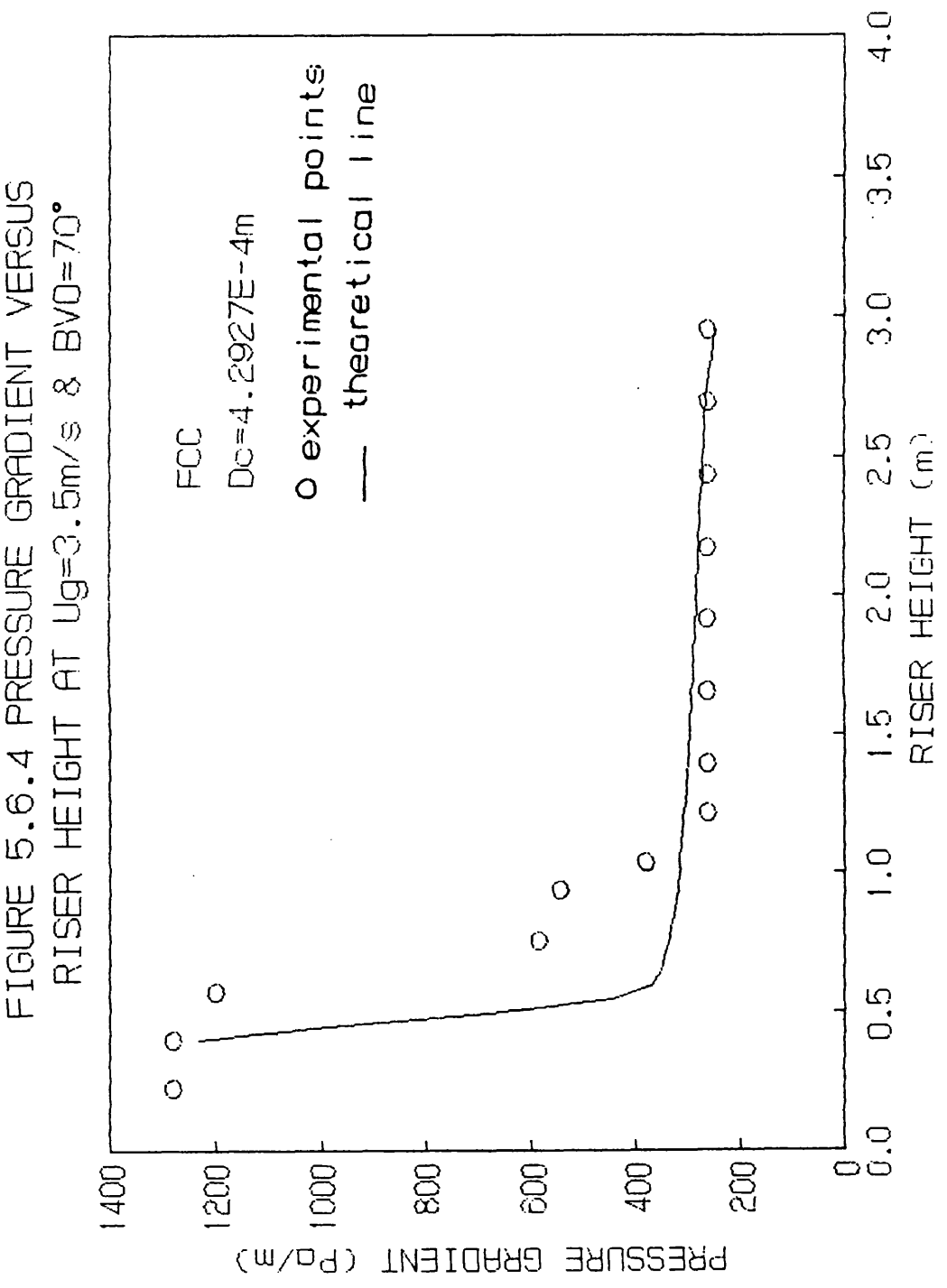

FIGURE 5.6.4 PRESSURE GRADIENT VERSUS RISER HEIGHT AT Ug=3.5m/s & BVO=70°

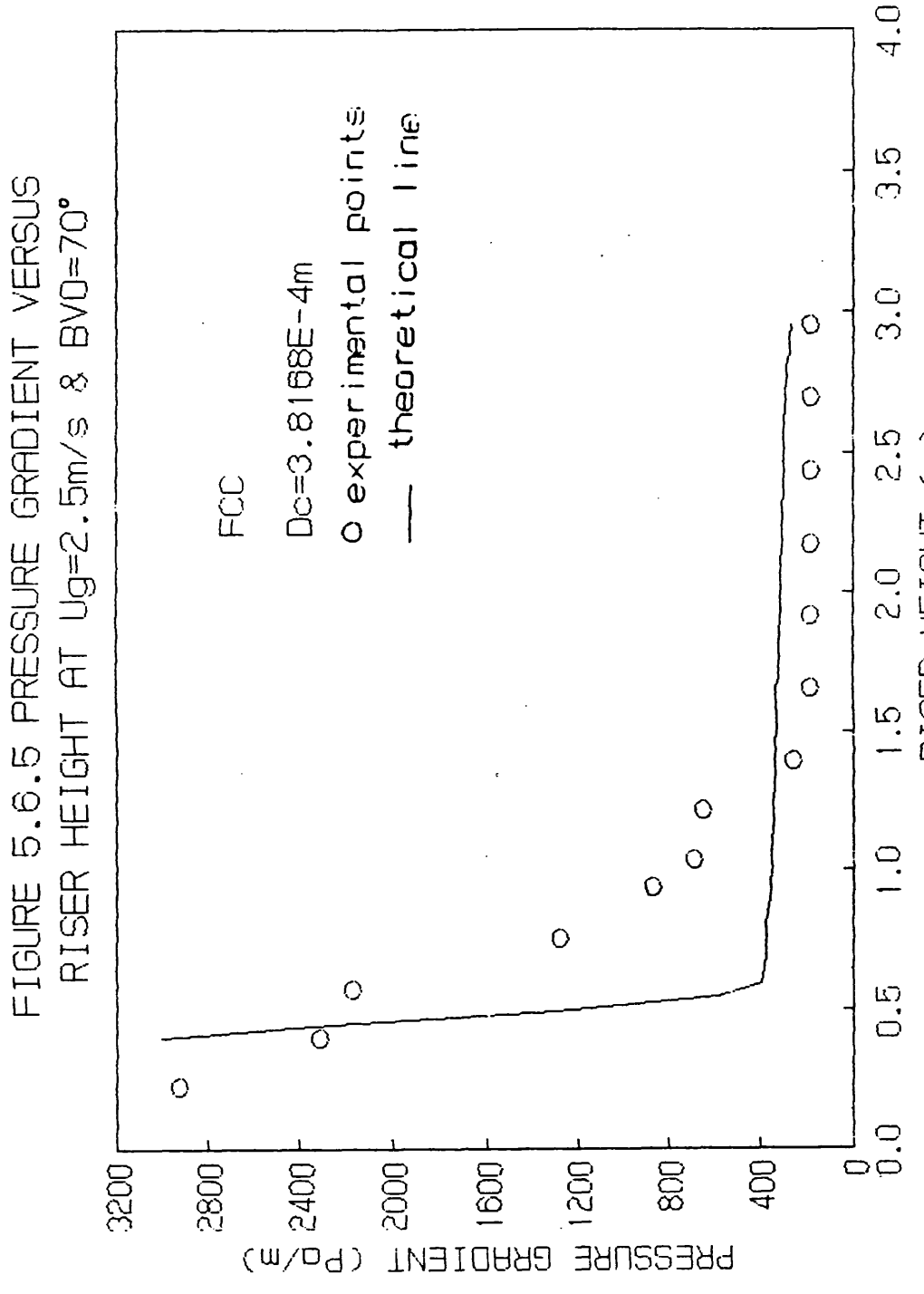
FIGURE 5.6.5 PRESSURE GRADIENT VERSUS
RISER HEIGHT AT Ug=2.5m/s & BVO=70°
FCC
Dc=3.8168E-4m
o experimental points
— theoretical line
PRESSURE GRADIENT (Pa/m)
RISER HEIGHT (m)
3200
2800
2400
2000
1600
1200
800
400
0
0.0
0.5
1.0
1.5
2.0
2.5
3.0
3.5
4.0

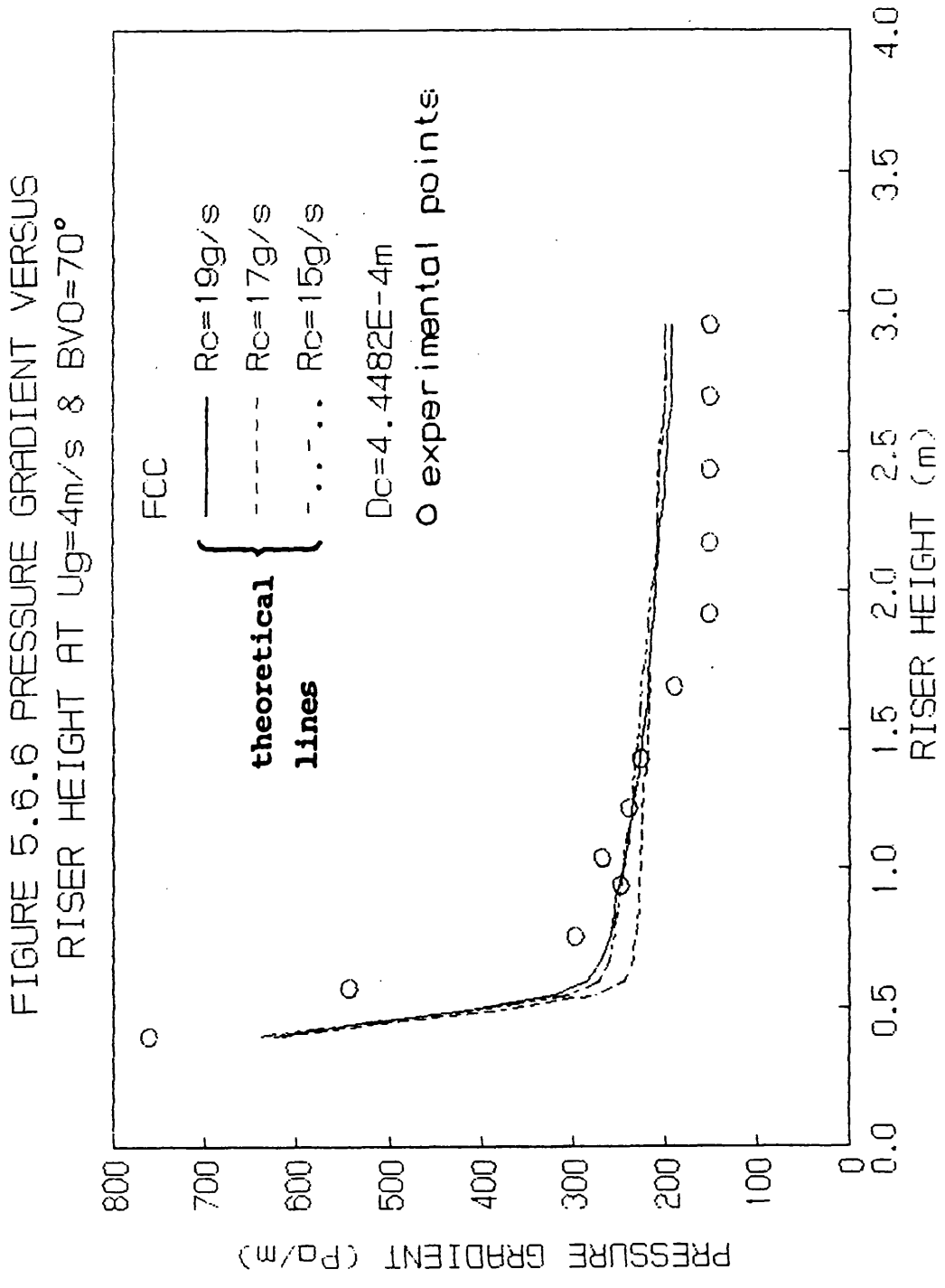
FIGURE 5.6.6 PRESSURE GRADIENT VERSUS
RISER HEIGHT AT Ug=4m/s & BVO=70°
FCC
Rc=19g/s
Rc=17g/s
Rc=15g/s
theoretical
lines
Dc=4.4482E-4m
o experimental points
PRESSURE GRADIENT (Pa/m)
RISER HEIGHT (m)
800
700
600
500
400
300
200
100
0
0.0
0.5
1.0
1.5
2.0
2.5
3.0
3.5
4.0

velocities and ball valve openings experimentally investigated, the predicted curve always followed the same "exponential decay" type graphs as those that arise from plotting the experimental data.

There is a good qualitative comparison between model and experiment in terms of graphical shape and order of magnitude. However, at low ball valve openings and gas velocities (ie those conditions that give rise to a low solid circulation rate), there is a wider quantitative divergence between model and experiment (see Figure 5.6.2).

During the development of the proposed Dense Annulus Lean Core (DALC) model many assumptions and approximations were required.

Figures 5.6.3 and 5.6.4 show experimental data points superimposed on to the curves representing DALC predictions at different initial cluster velocities. The accuracy of prediction does not appear to vary widely when the initial (downward) cluster velocity, Uc, is varied from 1 to 4 m/s. In general however using lower Uc will lead to a lesser divergence between experiment and model.

Figure 5.6.5 shows experimental data superimposed on the curves representing DALC predictions at a U_g = 2.5m/s BVO = 70^o. There is a good agreement between experimental points and the theoretical line.

Figure 5.6.6 shows the sensitivity of predicted pressure profiles with changing solid circulation rates. The actual measured solid circulation rate under the experimental conditions described in Figure 5.6.6 is 19.22 g/s. The other two predicted curves represent calculated pressure profiles that correspond to using solid circulation rates 10 and then 20 % less than the measured solid circulation rate. The three predicted curves are very similar with a maximum deviation of 10 % between the curves representing a solid circulation rate of 19.22 and 14.79 g/s.

5.7 IMPLICATIONS OF THE HYDRODYNAMIC MODELLING

The hydrodynamic model described in Chapter 3 is now applied to the case in which the riser of the CFB is used as a reactor. Suppose a first-order catalytic reaction of the form $A \xrightarrow{k} B$ takes place in the riser reactor at 400 C and that the fluidising gas velocity u is many multiples of u_{mf}. By considering the model of Yates and Rowe (1977) and assuming the reactant gas to be in plug flow, the rate of change of concentration of A within the cell of gas surrounding a particle will be determined by the mass transfer coefficient h_m, the surface area of the particle A_p and the concentration driving force $C_{Ah} - C_{Ap}$. Thus

$$-\frac{dC_A}{dt} = \frac{h_m A_p}{V_c} (C_{Ah} - C_{Ap})$$

The rate of change of concentration of A at the particle surface will be determined by the chemical reaction rate which is assumed to be of the first-order with respect to A:

$$\frac{dC_{Ap}}{dt} = k\, C_{Ap} \left[\frac{1-\varepsilon_b}{1-\varepsilon_m} \right]$$

where: ε_m is the fixed bed voidage on which the value of k is based

k is the fixed bed rate constant

Let $$\varepsilon_1 = \frac{1-\varepsilon_b}{1-\varepsilon_m}$$

then $$-\frac{dC_{Ap}}{dt} = k\, C_{Ap}\, \varepsilon_1$$

At any height h above the bed surface

$$\frac{dC_A}{dt} = \frac{dC_{Ap}}{dt} = \frac{dC_{Ah}}{dt}$$

Hence: $$-\frac{dC_{Ah}}{C_{Ah}} = \frac{dt}{\frac{V_c}{h_m A_p} + \frac{1}{k\, \varepsilon_1}}$$

The above equation may be integrated with boundary condition that at t=0, $C_{Ah}=C_{As}$ where C_{As} is the concentration of A at the surface of the fluid bed.

Thus $$\frac{C_{Ah}}{C_{As}} = \exp - \left[\frac{t}{\frac{V_c}{h_m A_p} + \frac{1}{k\, \varepsilon_1}} \right] \quad (5.7.1)$$

where: $$V_c = \frac{V_p}{1-\varepsilon_b}$$

Equation 5.7.1 enables conversions in the dilute core and downflow region to be calculated for the case of plug flow of the reactant gas.

Figures 5.7.1, 5.7.2 and 5.7.3 are the results of the calculations for the three values of the rate constant, k, 0.5 s^{-1}, 5 s^{-1} and 15 s^{-1} at a gas velocity of 4 m/s and by using the 7 hole distributor. It is clear from the results that the conversion in the downflow region is higher than the conversion in the dilute core and that this mainly depended on the value of reaction rate constant. The most extreme example is shown in Figure 5.7.3 for $k=15s^{-1}$ where the model indicates a conversion of 55 % in the downflow region within a distance of less than 3m of the riser height, although the correspondant conversion in the dilute core is less than 1 %. This is explained due to the fact the particle concentration in the dilute core is very low in comparison to that in the downflow region. In both regions the particle concentration decreases with increasing riser height. In the model described, the particles are assumed to be of uniform size but in practice there will be a distribution of small and large particles. Certainly some of the assumptions on which the model is based represent over-simplifications. But it is worth mentioning here that this model takes into consideration that the solid concentration fraction decreases along the riser height. Measurements of other workers agree well with

FIGURE 5.7.1
Ca/Cao VERSUS RISER HEIGHT

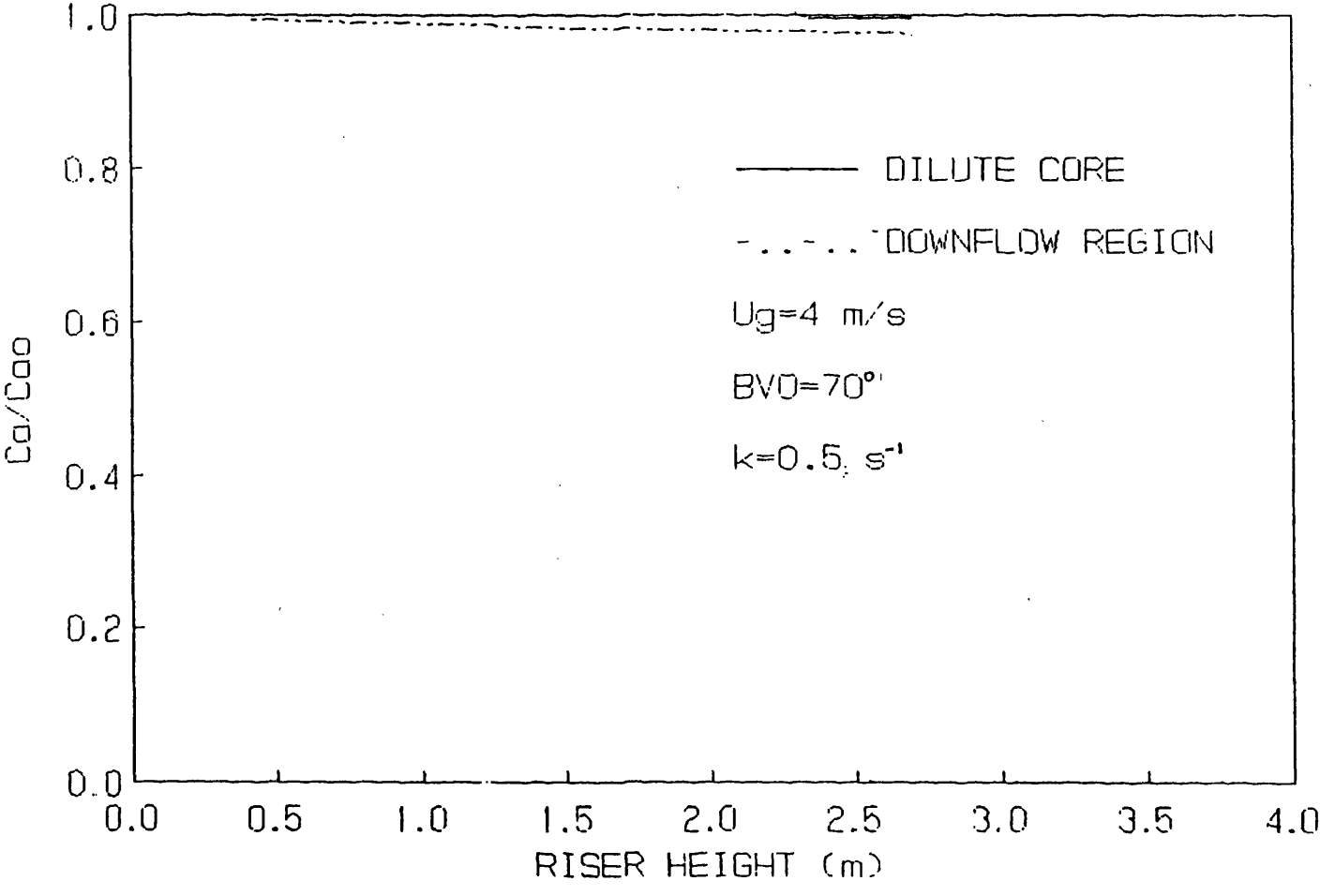

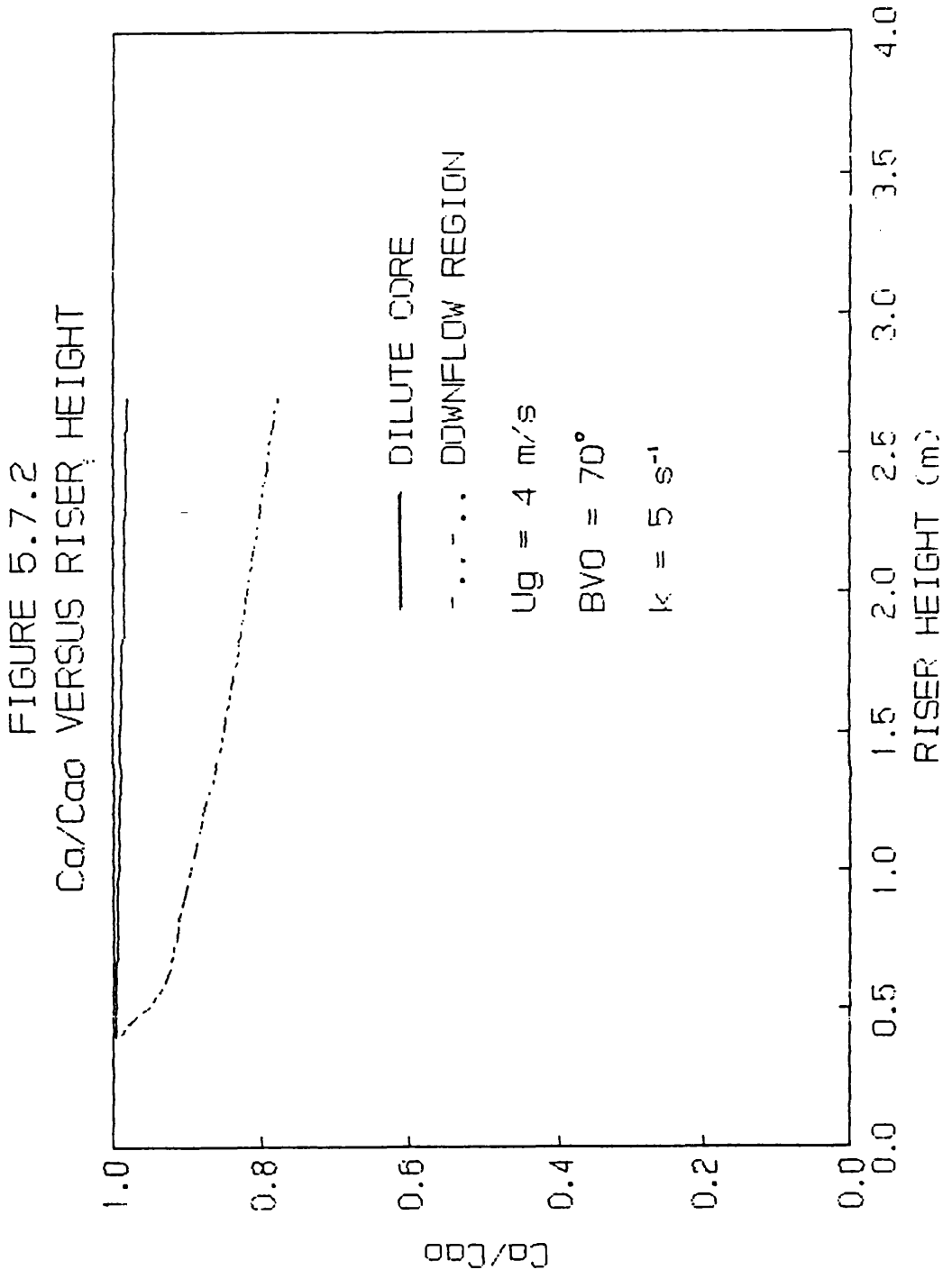
FIGURE 5.7.2
Ca/Cao VERSUS RISER HEIGHT
DILUTE CORE
DOWNFLOW REGION
Ug = 4 m/s
BVO = 70°
k = 5 s⁻¹
Ca/Cao
RISER HEIGHT (m)
0.0
0.2
0.4
0.6
0.8
1.0
0.0
0.5
1.0
1.5
2.0
2.5
3.0
3.5
4.0

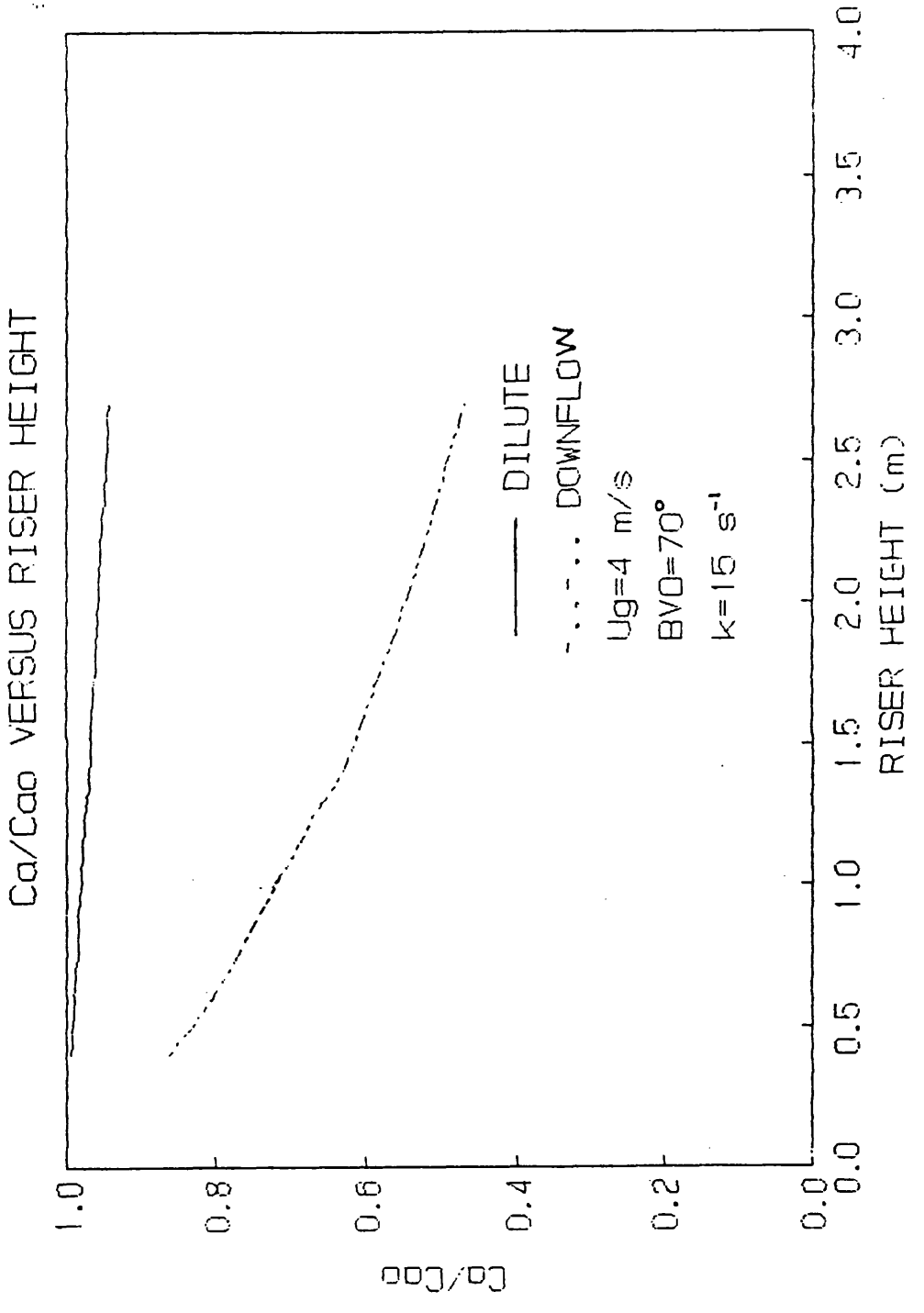
FIGURE 5.7.3
Ca/Cao VERSUS RISER HEIGHT
Ca/Cao
RISER HEIGHT (m)
0.0
0.2
0.4
0.6
0.8
1.0
0.0
0.5
1.0
1.5
2.0
2.5
3.0
3.5
4.0
DILUTE
DOWNFLOW
Ug=4 m/s
BVO=70°
k=15 s⁻¹

this fact. This is the main difference between this model which calculates the variation of voidage with the riser height and the model presented by Yates and Rowe (1977). It is clear from the results that the downflow region next to the riser wall, exerts a considerable influence on the course of the reaction compared with that of the dilute core.

Figures 5.7.4, 5.7.5 and 5.7.6 are the results of calculation when the 1 nozzle distributor is used at a constant value of the reaction rate constant ($k=15s^{-1}$) and at constant value of the solid circulation rate (10.98g/s),and only the gas velocity is varried for 3 to 4 m/s. The effect of increasing the gas velocity from 3 to 4 m/s , in the dilute core, is small since the conversion in this region of the riser has varried from 0.5 to 0.3 % respectively. However, the effect of increasing gas velocity is very significant for the 'Downflow Region', where the conversion at the top of the riser ie at a height of 2.7 m reaches a value of 85% at a gas velocity of 3 m/s and this value decreases to 70 % at a gas velocity of 4 m/s. The results show that the conversion of a 1st order reaction decreases by increasing gas velocity.
This is explained that under the above mentioned conditions by increasing the gas velocity the solid concentration within the riser decreases and hence the voidage increases. Since the conversion is inversely proportional to voidage, an increase in gas velocity will result to a decrease of the conversion.

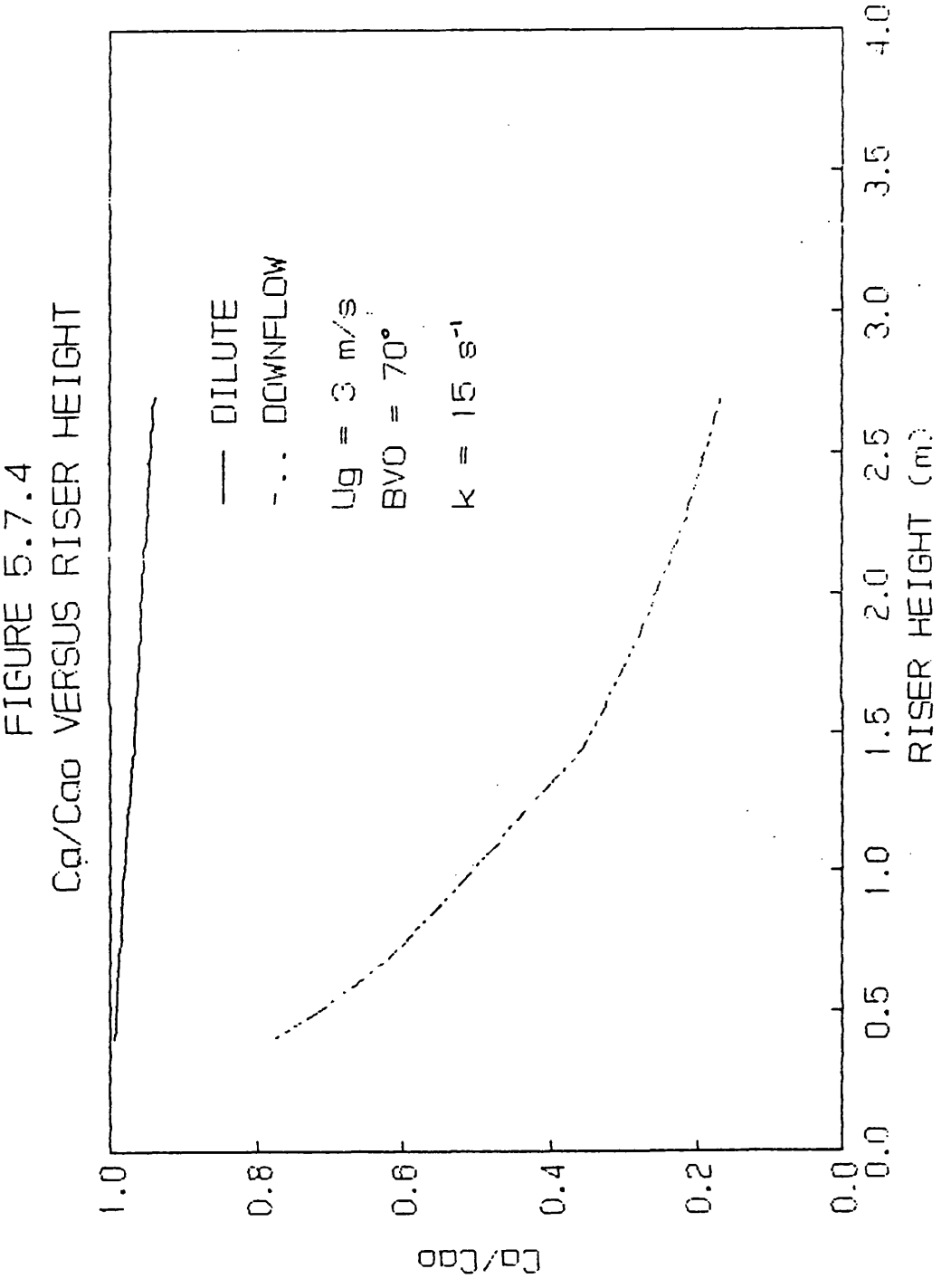
FIGURE 5.7.4
Ca/Cao VERSUS RISER HEIGHT
DILUTE
DOWNFLOW
Ug = 3 m/s
BVO = 70°
k = 15 s⁻¹
Ca/Cao
RISER HEIGHT (m)
0.0
0.2
0.4
0.6
0.8
1.0
0.0
0.5
1.0
1.5
2.0
2.5
3.0
3.5
4.0

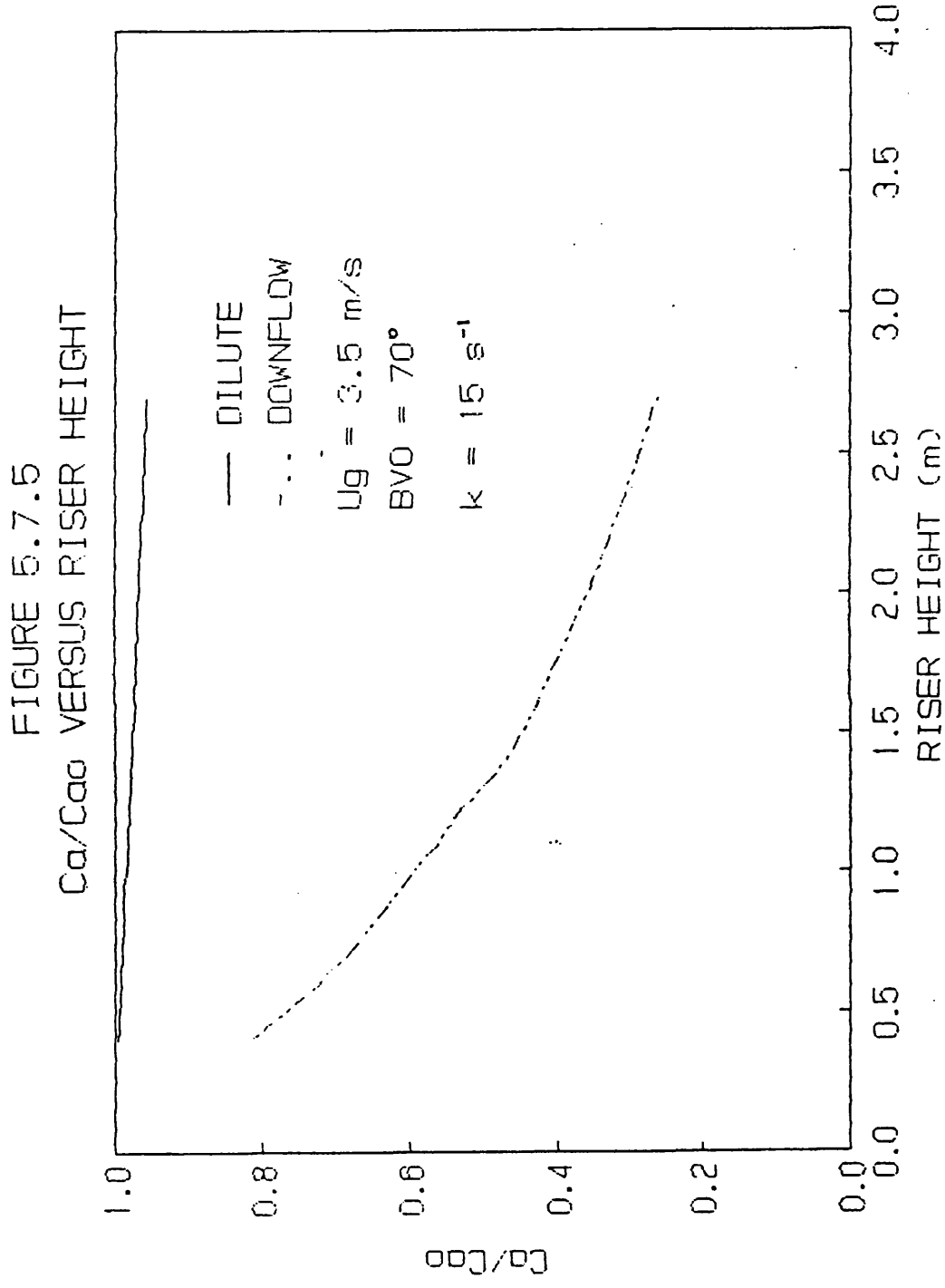
FIGURE 5.7.5
Ca/Cao VERSUS RISER HEIGHT
DILUTE
DOWNFLOW
Ug = 3.5 m/s
BVO = 70°
k = 15 s⁻¹
Ca/Cao
RISER HEIGHT (m)
0.0
0.2
0.4
0.6
0.8
1.0
0.0
0.5
1.0
1.5
2.0
2.5
3.0
3.5
4.0

FIGURE 5.7.6
Ca/Cao VERSUS RISER HEIGHT

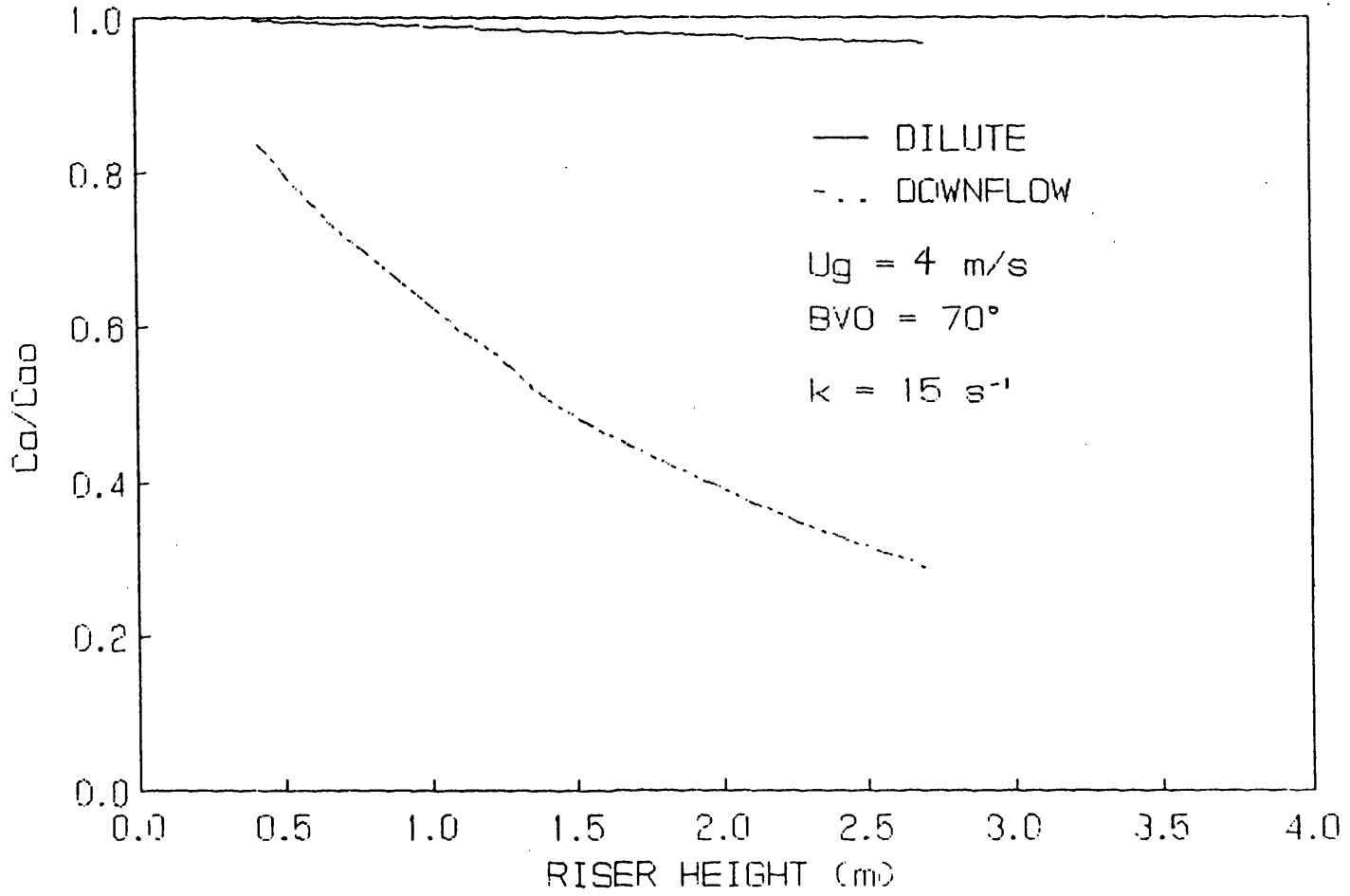

Up to date, there is no literature available to compare these results with respect to the variation of conversion with height. In a recent publication, Kunni and Levenspiel (1990), reported that a fast fluidised bed reactor can be treated as having a) a lower dense zone where ε_{bed}= 0.75-0.85 and this behaves as a bubbling bed where similar conversion equations are applicable and b) the upper freeboard zone, the freeboard model applies for the extra conversion. Hence this model determines one conversion in the dense bed and an extra conversion at the exit of the reactor, without taking into account the variation of conversion along the reactor height due to the voidage variation, which was the main objective of this exersize.

CHAPTER 6

Conclusions and Recommendations for Further Work

6.1 CONCLUSIONS

Pressure drop and solid circulation rate measurements have been made during the operation of the circulating fluidised bed. The riser of the circulating fluidised bed was made of transparent perspex with a height of 3m and internal diameter of 50mm. Most of the experiments have been conducted with FCC powder of average particle diameter of 64μm and particle density of 884 kg/m^3. Some further experiments were conducted with either pure Poralox powder of particle diameter of 127μm and density of 1850 kg/m^3 or a 50/50 v/v mixture of Poralox and FCC. The fluidising medium was compressed air directed through the base of the riser using three designs of distributor plates. The gas velocities were varied between 1.5 to 4 m/s. The three distributor plates had the same free percentage of open area; divided into 1 nozzle, 7 and 13 holes.

Analysis of the experimental data leads to the following conclusions:

(1) The design of the distributor plate can effect the performance of the circulating fluidised bed. For the same operating conditions using the 7 and 13 hole distributors lead to much higher solid circulation rates in comparison with the 1 nozzle distributor. These increased solid circulation rates corresponded with an increased pressure

drops for the 7 and the 13 hole distributors.

(2) Increasing the solid circulation rate can only be achieved at the expense of higher pressure drop. For reactive systems, a high solid circulation rate is often desirable to improve conversion. The benefits of improved conversion must be weighted against the economic costs of a greater pressure drop.

(3) Increasing the density and size of particle (from FCC to Poralox) will lead to higher solid circulation rate but also higher pressure drop.

(4) Operating the circulating fluidised bed at high ball valve openings (above 60 degrees) will normally lead to a downflow of solids. This downflow region is confined to an annulus adjacent to the riser wall.

(5) If the ball valve opening is greater than 70 degrees then the circulating fluidised bed cannot be operated without instabilities. These instabilities manifest themselves by fluctuations, sometimes vigorous, of the levels in the water manometers; and also by the periodic reversal of solid flow through the ball valve.

Observations made during the operation of the circulating fluidised bed confirm that the riser consists of a dense phase, close to the base of the riser with a much leaner phase above it.

In Chapter 3 a model has been proposed (DALC) which aims to relate the pressure drop along the axis of the riser to particle and fluid properties. The DALC model has showing itself able to give good predictions, both

quantitatively and qualitatively when the circulating fluidised bed is operated so as to achieve high solid circulation rates. However at the model's present stage of development it has not been possible to predict the experimentally measured values of pressure drop with a satisfactory degree of accuracy under all conditions.

The DALC model is applied to the case in which a first order catalytic reaction takes place in the riser of a CFB. By increasing the reaction rate constant to 15 s^{-1} the model indicates a conversion of 55 % in the downflow region within a distance of less than 3m above the distributor. By increasing the gas velocity in the riser the model predicts that the conversion of a first order reaction decreases.

6.2 RECOMMENTATIONS FOR FURTHER WORK

The pressure measurements for this study were made with pressure tappings flash with the wall of the riser. It is not clear that these pressure tappings accurately reflect the pressure across the whole cross-section of the riser, at that tapping height, or, as it has been suggested in this study, the region immediately adjacent to the riser wall. For this reason experimental equipment should be designed to allow the measurement of any radial pressure profile, at a given height in the riser.

A more accurate measurement of the solid circulation

rate can only be achieved with a non-intrusive technique.

More sensitive measurements of pressure can be achieved by using pressure transducers. If the output from these transducers is fed to appropriate computer software a time average value of pressure drop can be calculated to deal with any fluctuations.

An explanation for the origin of the downflow has been proposed during the development of the DALC model. However more work is required to investigate this phenomenon. This might be accomplished using X-ray photography.

A wider range of powders should be used in order to more fully investigate the effect of particle diameter and density on the operation of the circulating fluidised bed.

NOMENCLATURE

SYMBOLS

A	cross-section area of riser m^2
a	cross-section area of downcomer m^2
α	constant in eqn. 2.17
a	constant in eqn. 2.20
a	constant in eqn. 2.22
Ar	Archimedes number
b	constant in eqn. 2.23
BVO	angle of the ball valve, degree
C	equal to $(dP_v+dP_c)/\rho_s$ eqn. 2.16
C	constant in eqn. 2.24
c_D	drag coefficient of a single particle
c_D'	drag coefficient of particles in assembly
c_{dp}	drag coefficient of particles in assembly
c_{ds}	drag coefficient of a single particle
c_f	Fanning friction factor
D	riser diameter m
Dc	cluster diameter m
D_t	tube diameter m
d_p	particle diameter m
D_{SB}	diameter of slow bed m
D_T	riser diameter m
dx	length m
dP	pressure drop N
dh	riser length m
d_p	particle diameter m

dP_v	pressure drop due to solid valve N
dP_d	pressure drop in the downcomer N
dP_f	pressure drop in fast bed N
dP_c	pressure drop in cyclone N
dW	constant in eqn. fitted to wall flow rate
E	entrainment flux kg/m^2s
E^*	entrainment flux above TDH kg/m^2s
E_o	entrainment flux at bed surface kg/m^2s
F_D	drag force N
f_s	solid friction factor
g	acceleration due to gravity m/s^2
G	mass flux of solid kg/m^2s
G_S	mass flowrate of air kg/s
G_s	solid mass flux kg/m^2s
h	distance above the dense phase of riser m
H_R	riser height m
I	total solid inventory kg
k	exponential decay coefficient
L	length of riser m
m	mass of a particle kg
M_D	solid hold-up in the annular region kg
M_R	total solid hold-up in the riser kg
M_s	solid flux kg/m^2s
M_{DC}	solid hold-up in the dilute core kg
m_c	mass of cluster kg
N	number of clusters in length dL
N_P	number of particles per unit length

R_C	solid circulation rate in dilute core	kg/s
R_{CD}	solid circulation rate in downflow	kg/s
Re_p	particle Reynolds number	
Re_t	terminal Reynolds number	
t_o	average particle residence time	s
t_R	residence time	s
t_{CD}	residence time of solids in the downflow	s
u	slip velocity	m/s
U_g	superficial velocity	m/s
Ug	superficial gas velocity	m/s
Up	linear particle velocity	m/s
u_g	superficial gas velocity	m/s
u_p	linear particle velocity	m/s
U	superficial gas velocity	m/s
Umf	gas velocity at minimum fluidisation	m/s
U_a	superficial gas velocity	m/s
U_{sl}	slip velocity	m/s
U_p	linear solid velocity	m/s
U_t	terminal solid velocity	m/s
u_{ts}	terminal slip velocity	m/s
V_C	superficial solid velocity	m/s
V	solid velocity	m/s
Vt	terminal velocity	m/s
V_T	total volume of system	m^3
V_R	riser volume	m^3
Vp	particle velocity	m/s
W	flowrate of particles	kg/s

W_o	flowrate of solids down the wall	kg/s
Z	height of fast bed	m
z	height	m
z_i	position of inflection point	m
z_o	characteristic length	m
z	riser height	m

GREEK SYMBOLS

ρ_b	bed density	kg/m^3
ρ_g	density of gas	kg/m^3
ρ_f	density of fluid	kg/m^3
ρ_p	density of particle	kg/m^3
ρ_{SB}	slow bed density	kg/m^3
ε	voidage	
ε_{mf}	voidage at point of minimum fluidisation	
ε^*	voidage for dilute phase-section	
ε_a	voidage for dense phase - section	
ε_i	dilute phase voidage	
ε_{SB}	voidage value at u_{mf}	
ΔP	pressure drop	N
ΔP_{STAT}	static pressure drop	N
ΔP_{GW}	pressure drop due to gas-wall friction	N
ΔP_{SW}	pressure drop due to solid-wall friction	N
ΔH_{SB}	change of slow bed height	m
ΔM_{SB}	mass of solids in motion	kg
μ	gas viscosity	kg/ms

REFERENCES

Adams C.K. (1988), "Gas mixing if fast fluidised beds", 2nd International Conference on CFBs, France, March 1988.

Arena U., Cammarota A., Massimilla L. and Pirozzi D. (1988), "The hydrodynamic behavior of two circulating fluidised bed units of different sizes", 2nd International Conference on CFBs, France, March 1988.

Avidan A.A. (1980), "Bed expansion and solids mixing in high velocity fluidised beds", PhD Dissertation, City College, New York.

Avidan A.A. and Yerushalmi J. (1982), "Bed expansion in high velocity fluidization", Powd. Techn., 32 , p.223.

Bierl T.W., Gajdos L.J., McIver A.E. and MacGovern J.J. (1980), D.O.E. Report No. EE2449-11.

Bolton L.W. and Davidson J.F. (1988), "Recirculation of particles in fast fluidised risers", 2nd International Conference on CFBs, France, March 1988.

Breault R.W. and Mathur V.K. (1989), "High-velocity bed hydrodynamic modelling.1. Fundamental studies of pressure drop", Ind. Eng. Chem. Res., 28 , No. 6, p.684.

Brereton C. and Stromberg L. (1985), "Some aspects of the fluid dynamic behavior of fast fluidised beds", 1st International Conference on CFBs, Halifax, Nova Scotia, Canada, November 1985.

Burkell J.J., Grace J.R., Zhao J. and Lim C.J. (1988), "Measurement of solid circulation rates in circulating fluidised beds", 2nd International Conference on CFBs, France, March 1988.

Cankurt N.T. and Yerushalmi J. (1978), "Gas backmixing in high velocity fluidised beds" in Fluidization, Davidson J.F. and Kearins D.L., Cambridge Univ. Press, Cambridge, p.387.

Carlson H.M., Frazier P.M. and Engdahl R.B. (1948), Trans. ASME, 70 , p. 65.

Cooke M.J. (1989), "Principles of fluidisation" course notes, University College London.

Do H., Grace J.R. and Clift R. (1972), "Particle ejection and entrainment from fluidised beds", Pow. Techn., 6 , p.195.

Donald M.B. and Singer H. (1959), Trans. Instn. Chem. Engrs., 36 , p.255.

Farbar L. (1953), Trans. ASME, 75 , p. 943.

Gajdos L.J. and Bierl T.W. (1978), Topical report submitted to U.S. Deptm. of Energy, NTIS No. FE-2449-6.

Geldart D. (1973), "Types of gas fluidisation", Powder Techn., 7 , p. 285.

Geldart D. (1979), Pow. Tech., 19 , p. 133.

George S.E. and Grace J.R. (1981), "Entrainment of particles from a pilot scale fluidised bed", Can. J. Chem. Eng., 59 , p.279.

Grace J.R. (1986), "Contacting modes and behaviour classification of gas-solid and other two-phase suspensions", Can. J. Chem. Eng., 64 , p.353.

Gugnoni R.J. and Zenz F.A. (1980), "Particle entrainment from bubbling fluidised beds", Fluidisation, J.R. Grace and M.J. Matsen (Ed.), Plenum Press, New York, p.501.

Hartge E.U., Li Y. and Werther J. (1985), "Analysis of the local structure of the two-phase flow in a fast fluidised bed", 1st International Conference on CFBs, Halifax, Nova Scotia, Canada, November 1985.

Horio M., Taki A., Hsieh Y.S. and Muchi I. (1980),

"Elutriation and particle tranport through the freeboard of a gas-solid fluidised bed", in J.R. Grace and J.M. Matsen (Eds), Fluidisation, Plenum Press, New York, p.509.

Horio M., Nonaka A., Hoshiba M., Kobukai Y., Naito J., Tochibana O., Watanabe K. and Yoshida N. (1985), "Coal combustion in a transparent circulating fluidised bed", 1st International Conference on CFBs, Halifax, Nova Scotia, Canada, November 1985.

Horio M., Morishita K., Tachibana O. and Hurata N. (1988), "Solid distribution and movement in circulating fluidised beds", 2nd International Conference on CFBs, France, March 1988.

Ishii H., Nakajima T. and Horio M. (1989), "The clustering annular flow model of circulating fluidised beds", J. Chem. Eng. Japan, 22 , No.5, p.484.

Kato K., Shibasaki H., Tamura K., Arita S., Wang C. and Takarada T. (1989), "Particle hold up in a fast fluidised bed", J. Chem. Eng. Japan, 22 , No.2, p.130.

Kay J.M. (1963), "An introduction to fluid mechanics and heat transfer", 2nd Edition, Cambridge univ. press.

Kefa C., Jianren F., Zhongyang L., Jianhua Y. and Mingjiang N. (1988), "The prediction and measurement of particle

behavior in circulating fluidised beds", 2nd International Conference on CFBs, France, March 1988.

Kehoe P.W.K. and Davidson J.F. (1971), "Continuously slugging fluidised beds", Inst. Chem. Engrs, (London), Symp. Series, 33 , p.97.

Kobro H. and Brereton C. (1985), "Control and flexibility of CFBs", 1st International Conference on CFBs, Halifax, Nova Scotia, Canada, November 1985.

Kunii D. and Levenspiel O. (1990), "Fluidised reactor models. 1. For bubbling beds of fine, intermediate, and large particles. 2. For the lean phase: freeboard and fast fluidisation", Ind. Eng. Chem. Res., 29, p. 1226.

Kunii D. and Levenspiel O. (1969), "Fluidization Engineering", Ch. 12 Circulating Systems, p.396.

Kwauk M., Ningde W., Youchu L., Bingyu C. and Zhiyuan S. (1985), "Fast fluidisation at ICM", 1st International Conference on CFBs, Halifax, Nova Scotia, Canada, Nov.1985.

Lanneau K.I. (1980), "Gas-solids contacting in fluidised beds", Trans. Inst. Chem. Engrs., 38 , p.125.

Li Y. and Kwauk M. (1980), "The dynamics of fast fluidisation", in Fluidisation, Grace J.R. and Matsen J.M.,

Plenum Press, New York, London, p.537.

Li Y., Chen B., Wang F. and Wang Y. (1982), "Hydrodynamic correlations for fast fluidisation", Fluid. Scie. and Techn. Conference, China-Japan Symposium, 1982.

Louge M. and Chang H. (1990), "Pressure and voidage gradients in vertical gas-solid risers", Powd. Techn., 60 , p.197.

Monceaux L., Azzi M., Molodtsof Y. and Large J.F. (1985), "Overal and local characterisation of flow regimes in circulating fluidised bed", 1st International Conference on CFBs, Halifax, Nova Scotia, Canada, Nov.1985.

Nakamura K. and Capes C.E. (1973), Can. J. Chem. Eng., 51 , p. 39.

Pemberton S.T. and Davidson J.F. (1983), "Elutriation of fine particles from bubbling fluidised beds", Fluidisation, D.Kunii and R. Tsei, Engineering Foundation, New York, p.275.

Rhodes M.J. and Geldart D. (1985), "The hydrodynamics of re-circulating fluidised beds", 1st International Conference on CFBs, Halifax, Nova Scotia, Canada, Nov.1985.

Rhodes M.J. and Geldart D. (1987), "A model for the

circulating fluidised bed", Powd.Techn., 53 , p.155.

Rhodes M.J., Laussmann P., Villain F. and Geldart D. (1988), "Measurement of radial and axial solids flux variations in the riser of a circulating fluidised bed", 2nd International Conference on CFBs, France , March 1988.

Rhodes M.J. (1990), "Modelling the flow structure of upward-flowing gas-solids suspensions", Powd.Techn., 60 , p.197.

Richardson J.F.and Zaki W.N. (1954), Trans. Instn. Chem. Engrs., 32 , p.35.

Ruden P. (1933), Naturwissenschaften, 21 , p.375.

Son J.E., Choi J.H. and Lee C.K. (1988), "Hydrodynamics in a large circulating fluidised bed", 2nd International Conference on CFBs, France, March 1988.

Schnitzlein M.G. and Weinstein H. (1988), "Flow characterization in high velocity fluidised beds using pressure fluctuations", Chem.Eng.Scie., 43 , No.10, p.2605.

Shamlou P.A. (1988), "Handling of bulk solids, theory and practice", Butterworths.

Squires A.M., Kwauk M. and Avidan A.A. (1985), "Fluid beds:

at last, challenging two entrenched practices", Science, 230 , p.1329.

Stairmand C.J. (1951), "The design and performance of cyclone separators", Trans. Instn. Chem. Engrs. 29 , p.356.

Svarovsky (1986),"Gas Fluidisation Technology", Chapter 8, Solid-Gas Separation, Edited by D. Geldart.

Takeuchi H., Hirama T., Chiba T. and Leung L.S. (1986), "On the regime of fast fluidisation", Fluidization, World Congress III of Chem.Engr., Tokyo 1986.

Tollmien W.Z. (1926), Math. Mech., 6 , p.468.

Wen C.Y. and Galli A.F. (1971), In Fluidisation, Davidson J.F. and Harrison D.(Eds), Academic Press, New York, p.677.

Wen C.Y. and Yu Y.H. (1966), Chem. Eng. Prog., Symp. Ser., 62, p. 100.

Wenstein H., Graff R.A., Meller M. and Shao M.J. (1983), "The influence of the imposed pressure drop across a fast fluidised bed", Proc.of the 4th International Conference on Fluidisation, Japan 1983, p.299.

Weinstein H., Meller M., Shao M.J. and Parisi R.J. (1984), "The effect of particle densuty on hold-up in a fast fluid

bed", AIChE, Symp.Series, 80 , No.234, p.53.

Weinstein H., Shao M. and Wasserzug L. (1984), "Radial solid density variation in a fast fluidised bed", AIChE, Symp.Series, 80 , No. 234, p.53.

Weinstein H., Shao M. and Schnitlein M. (1985), "Radial variation in solid density in high velocity fluidisation", 1st International Conference on CFBs, Halifax, Nova Scotia, Canada, NOV. 1985.

Wen C.Y. and Chen L.H. (1982), A.I.Ch.E.J., 28 , p.117.

Yang W.C. (1983), Pow. Techn., 35 , p.143

Yang W.C. (1988), "A model for the dynamics of a circulating fluidised bed loop", 2nd International Conference on CFBs, France, March 1988.

Yang W.C. (1977), J. Powder and Bulk Solids Tech., 1 , p.89.

Yates J.G.and Rowe P.(1977), "A model for chemical reaction in the freeboard region above a fluidised bed", Trans. Inst. Chem. Eng., 55, p. 137.

Yerushalmi J., Turner D.H. and Squires A.M. (1976), "The fast fluidised bed", Ind.Eng.Chem., Process Des. Dev., 15 ,

No.1, p.47.

Yerushalmi J., Cankurt N.T., Geldart D. and Liss B. (1978), "Flow regimes in vertical gas-solid contact systems", A.I.Ch.E. Sympos.Ser., 74 , No.176.

Yousfi and Gau (1974), Chem. Eng. Sci., 29, p. 1939.

Zenz F.A. and Othmer D.F. (1960), "Fluidisation and fluid particle systems", Reinhold publ. Corparation, New York.

APPENDIX A

SUMMARY OF EXPERIMENTAL RESULTS

RISER DISTRIBUTOR:1 NOZZLE

POWDER : FCC

Ug=1.5m/s P: N/m^2

BVO	P_3	P_4	P_5	P_6	P_7	P_8	P_9	P_{10}	P_{11}	P_{12}	P_{13}	P_{14}	P_{15}
40	235	206	177	167	157	147	137	128	118	108	88	83	78
50	324	284	245	235	206	196	186	157	137	128	108	98	88
60	461	402	343	334	294	275	216	206	177	157	137	128	108
70	3124	2801	2276	2079	1805	1403	1079	638	491	432	373	334	314

Ug=2m/s P: N/m^2

BVO	P_3	P_4	P_5	P_6	P_7	P_8	P_9	P_{10}	P_{11}	P_{12}	P_{13}	P_{14}	P_{15}
40	167	157	147	137	127	126	123	121	118	116	113	110	98
50	226	196	186	177	167	162	157	147	142	137	132	128	118
60	677	628	559	530	510	461	441	402	373	363	334	314	294
70	1628	1383	1133	1050	1030	932	853	765	697	647	579	549	530

Ug=2.5m/s P: N/m^2

BVO	P_3	P_4	P_5	P_6	P_7	P_8	P_9	P_{10}	P_{11}	P_{12}	P_{13}	P_{14}	P_{15}
40	167	147	142	137	133	130	128	127	125	122	118	113	98
50	216	196	186	181	177	167	162	157	152	147	137	128	118
60	510	490	451	432	412	392	343	338	334	324	314	284	275
70	1692	1422	1207	1167	1099	1001	942	844	765	716	657	628	608

RISER DISTRIBUTOR: 1 NOZZLE

POWDER:FCC

Ug=3m/s P: N/m^3

BVO	P_3	P_4	P_5	P_6	P_7	P_8	P_9	P_{10}	P_{11}	P_{12}	P_{13}	P_{14}	P_{15}
40	191	186	181	172	167	162	157	147	142	137	132	129	127
50	206	196	186	177	172	167	157	153	150	147	142	137	128
60	231	225	206	196	191	186	183	180	177	167	157	137	128
70	1521	1275	1153	1059	1010	932	873	834	775	726	677	647	638

Ug=3.5m/s P: N/m^2

BVO	P_3	P_4	P_5	P_6	P_7	P_8	P_9	P_{10}	P_{11}	P_{12}	P_{13}	P_{14}	P_{15}
40	216	206	196	186	177	172	169	167	162	158	156	147	137
50	245	226	216	206	196	206	196	190	186	180	177	167	157
60	432	422	392	383	353	343	334	328	324	314	304	294	275
70	1226	1030	922	903	873	853	804	765	716	697	657	647	638

Ug=4m/s P: N/m^2

BVO	P_3	P_4	P_5	P_6	P_7	P_8	P_9	P_{10}	P_{11}	P_{12}	P_{13}	P_{14}	P_{15}
40	245	226	216	206	196	196	196	196	186	196	186	196	186
50	275	265	255	245	235	226	216	226	216	226	216	206	196
60	304	284	275	265	260	255	250	245	240	235	230	226	216
70	1177	1079	1005	903	883	863	824	775	755	726	706	687	638

RISER DISTRIBUTOR: 7 HOLES

POWDER: FCC

Ug=1.5m/s P: N/m^2

BVO	P_3	P_4	P_5	P_6	P_7	P_8	P_9	P_{10}	P_{11}	P_{12}	P_{13}	P_{14}	P_{15}
40	648	491	442	383	343	324	265	255	235	196	147	137	128
50	3434	2943	2477	2158	1913	1324	981	549	422	353	265	235	196
60	4439	3630	3414	3394	2551	2502	1648	1167	662	446	338	250	191
70	4635	4218	3630	3213	3017	2477	2158	1496	746	540	343	285	226

Ug=2m/s P: N/m^2

BVO	P_3	P_4	P_5	P_6	P_7	P_8	P_9	P_{10}	P_{11}	P_{12}	P_{13}	P_{14}	P_{15}
40	510	471	451	422	402	373	353	334	314	294	265	255	235
50	1677	1368	1079	1010	932	844	785	716	677	647	608	569	559
60	2423	2001	1550	1265	1109	981	873	814	755	696	657	628	598
70	2967	2600	2060	1756	1550	1158	942	844	755	706	623	608	598

Ug=2.5m/s P: N/m^2

BVO	P_3	P_4	P_5	P_6	P_7	P_8	P_9	P_{10}	P_{11}	P_{12}	P_{13}	P_{14}	P_{15}
40	412	392	363	343	324	304	294	275	265	255	245	235	226
50	726	687	638	618	598	549	540	500	471	461	432	412	392
60	1923	1530	1285	1256	1157	1050	1010	932	912	824	765	716	667
70	2354	1937	1545	1315	1245	1128	971	932	863	824	775	726	697

RISER DISTRIBUTOR: 7 HOLES

POWDER: FCC

Ug=3m/s P: N/m^2

BVO	P_3	P_4	P_5	P_6	P_7	P_8	P_9	P_{10}	P_{11}	P_{12}	P_{13}	P_{14}	P_{15}
40	402	392	373	353	343	333	324	304	284	275	265	255	245
50	736	667	647	598	589	569	530	510	500	491	461	451	432
60	1516	1315	1226	1212	1138	1050	1010	942	873	824	804	755	706
70	1815	1511	1334	1265	1216	1118	1059	991	922	883	824	785	746

Ug=3.5m/s P: N/m^2

BVO	P_3	P_4	P_5	P_6	P_7	P_8	P_9	P_{10}	P_{11}	P_{12}	P_{13}	P_{14}	P_{15}
40	383	373	353	343	334	324	314	309	304	294	284	275	255
50	647	618	589	579	569	540	530	520	510	500	471	461	441
60	1462	1354	1265	1192	1167	1099	1020	1001	952	912	863	804	795
70	1722	1491	1324	1285	1226	1158	1059	1020	952	912	883	824	804

Ug=4m/s P: N/m^2

BVO	P_3	P_4	P_5	P_6	P_7	P_8	P_9	P_{10}	P_{11}	P_{12}	P_{13}	P_{14}	P_{15}
40	402	363	343	334	329	324	314	311	308	304	294	284	265
50	618	598	589	569	559	539	530	510	500	491	471	461	451
60	1393	1285	1207	1177	1138	1089	1040	1001	961	932	893	863	824
70	1501	1364	1265	1236	1207	1128	1089	1020	991	952	903	873	834

RISER DISTRIBUTOR: 13 HOLES

POWDER: FCC

Ug=1.5m/s P: N/m^2

BVO	P_3	P_4	P_5	P_6	P_7	P_8	P_9	P_{10}	P_{11}	P_{12}	P_{13}	P_{14}	P_{15}
40	294	265	226	216	196	186	167	137	128	108	88	79	69
50	402	373	324	285	265	245	235	186	157	137	118	108	83
60	569	471	422	383	343	304	275	226	186	157	137	118	98
70	4218	4022	3355	3247	2982	2541	1947	1629	1089	618	461	402	363

Ug=2m/s P: N/m^2

BVO	P_3	P_4	P_5	P_6	P_7	P_8	P_9	P_{10}	P_{11}	P_{12}	P_{13}	P_{14}	P_{15}
40	216	186	167	147	157	147	157	118	108	108	88	88	88
50	275	235	226	216	206	196	176	167	147	137	128	118	98
60	353	314	285	274	255	235	226	216	196	186	167	157	137
70	2551	2304	1736	1619	1432	1138	1001	883	785	716	648	598	585

Ug=2.5m/s P: N/m^2

BVO	P_3	P_4	P_5	P_6	P_7	P_8	P_9	P_{10}	P_{11}	P_{12}	P_{13}	P_{14}	P_{15}
40	196	177	216	206	196	196	196	196	186	196	186	196	186
50	275	265	255	245	235	226	216	226	216	226	216	206	196
60	304	284	275	265	260	255	250	245	240	235	230	226	216
70	1177	1079	1005	903	883	863	824	775	755	726	706	687	638

RISER DISTRIBUTOR: 13 HOLES

POWDER: FCC

Ug=3m/s P: N/m^2

BVO	P_3	P_4	P_5	P_6	P_7	P_8	P_9	P_{10}	P_{11}	P_{12}	P_{13}	P_{14}	P_{15}
40	216	196	196	183	177	167	157	155	153	150	147	142	137
50	255	226	216	206	196	191	186	182	177	172	167	157	147
60	304	275	265	255	245	235	231	226	216	196	186	182	177
70	1555	1344	1158	1138	1069	1010	961	903	824	775	736	706	687

Ug=3.5m/s P: N/m^2

BVO	P_3	P_4	P_5	P_6	P_7	P_8	P_9	P_{10}	P_{11}	P_{12}	P_{13}	P_{14}	P_{15}
40	245	235	226	216	206	201	196	186	182	176	172	167	157
50	304	294	275	265	255	245	242	238	235	226	216	206	196
60	1275	1148	1050	1030	1010	952	883	854	834	785	746	716	687
70	1344	1202	1118	1109	1099	981	932	903	863	814	775	746	726

Ug=4m/s P: N/m^2

BVO	P_3	P_4	P_5	P_6	P_7	P_8	P_9	P_{10}	P_{11}	P_{12}	P_{13}	P_{14}	P_{15}
40	304	275	265	255	235	231	228	226	224	219	216	211	206
50	412	383	363	343	334	324	314	304	299	294	289	285	275
60	1256	1177	1118	1079	1040	991	961	912	883	834	814	785	736
70	1315	1226	1148	1128	1109	1050	971	942	922	873	834	814	775

RISER DISTRIBUTOR: 1 NOZZLE

POWDER: PORALOX

Ug=2m/s P: N/m^2

BVO	P_3	P_4	P_5	P_6	P_7	P_8	P_9	P_{10}	P_{11}	P_{12}	P_{13}	P_{14}	P_{15}
30	618	579	540	500	481	451	422	392	383	353	294	265	216
40	2649	2305	2207	1874	1570	1324	1128	834	706	559	491	421	334
50	4218	3630	2894	2256	1913	1530	1226	1089	863	706	594	466	417
60	5069	4513	3527	2972	2698	2256	1913	1349	1177	971	799	613	417

Ug=2.5m/s P:N/m^2

BVO	P_3	P_4	P_5	P_6	P_7	P_8	P_9	P_{10}	P_{11}	P_{12}	P_{13}	P_{14}	P_{15}
30	275	255	235	230	216	216	255	216	206	186	177	167	157
40	1040	961	922	873	853	804	755	745	716	687	628	589	540
50	2403	2031	1746	1599	1510	1412	1305	1236	1148	1069	981	922	853
60	4316	3286	2698	2354	2040	1726	1491	1413	1275	1128	991	863	849

Ug=3m/s P: N/m^2

BVO	P_3	P_4	P_5	P_6	P_7	P_8	P_9	P_{10}	P_{11}	P_{12}	P_{13}	P_{14}	P_{15}
40	932	922	893	863	844	814	765	746	736	706	677	638	598
50	1648	1569	1471	1403	1354	1275	1216	1177	1148	1099	1040	991	961
60	2433	2060	1854	1785	1687	1589	1511	1432	1344	1265	1197	1109	1050
70	3586	3090	2531	2168	2001	1854	1687	1609	1472	1354	1256	1167	1089

RISER DISTRIBUTOR: 1 NOZZLE

POWDER:PORALOX

Ug=3.5m/s P: N/m^2

BVO	P_3	P_4	P_5	P_6	P_7	P_8	P_9	P_{10}	P_{11}	P_{12}	P_{13}	P_{14}	P_{15}
40	961	942	903	893	863	844	814	804	785	775	736	726	706
50	1521	1413	1344	1285	1246	1207	1187	1128	1099	1069	1010	971	942
60	2021	1854	1766	1668	1609	1550	1432	1403	1324	1246	1187	1118	1020
70	2811	2462	2197	2060	1991	1815	1727	1599	1511	1413	1324	1226	1148

Ug=4m/s P: N/m^2

BVO	P_3	P_4	P_5	P_6	P_7	P_8	P_9	P_{10}	P_{11}	P_{12}	P_{13}	P_{14}	P_{15}
40	1001	991	932	912	883	863	834	824	804	795	775	750	736
50	1432	1354	1295	1236	1216	1167	1089	1069	1040	1010	971	942	873
60	1942	1756	1678	1609	1560	1501	1422	1373	1315	1246	1226	1158	1109
70	2585	2320	2080	1991	1913	1805	1678	1599	1511	1422	1354	1256	1177

RISER DISTRIBUTOR: 1 NOZZLE

POWDER: 50/50 v/v MIXTURE

Ug=3m/s P:N/m^2

BVO	P_3	P_4	P_5	P_6	P_7	P_8	P_9	P_{10}	P_{11}	P_{12}	P_{13}	P_{14}	P_{15}
40	697	657	598	559	569	549	540	520	471	461	451	441	422
50	1177	1138	1099	1079	1040	981	922	912	873	834	776	746	736
60	1790	1589	1491	1452	1344	1226	1207	1128	1055	976	961	932	907
70	2305	2001	1756	1712	1579	1452	1315	1305	1246	1148	1050	947	853

Ug=3.5m/s P: N/m^2

BVO	P_3	P_4	P_5	P_6	P_7	P_8	P_9	P_{10}	P_{11}	P_{12}	P_{13}	P_{14}	P_{15}
40	677	638	608	598	559	549	540	520	510	500	481	461	451
50	1089	1050	1001	942	922	903	873	853	834	814	785	765	736
60	1619	1452	1383	1324	1285	1236	1207	1187	1177	1079	1030	942	912
70	2477	2207	1987	1795	1697	1570	1462	1442	1393	1246	1167	1118	1040

Ug=4m/s P: N/m^2

BVO	P_3	P_4	P_5	P_6	P_7	P_8	P_9	P_{10}	P_{11}	P_{12}	P_{13}	P_{14}	P_{15}
40	677	657	638	618	589	579	569	559	540	530	510	500	491
50	1079	1010	952	942	902	873	863	834	804	795	736	716	697
60	1540	1393	1344	1324	1255	1226	1197	1148	1128	1079	1050	1001	952
70	2526	2256	2040	1942	1839	1668	1619	1521	1472	1398	1275	1128	1079

POWDER: FCC

RISER DISTRIBUTOR: 1 NOZZLE

SOLID CIRCULATION RATE

	BVO:30 degrees	BVO:40 degrees	BVO:50 degrees	BVO:60 degrees	BVO:70 degrees
Ug (m/s)	SCR (g/s)	SCR (g/s)	SCR (g/s)	SCR (g/s)	SCR (g/s)
0.0	0.0	0.0	0.0	0.0	0.0
1.5	0.57	1.06	1.60	2.06	4.12
2.0	0.69	1.03	1.65	2.10	8.18
2.5	0.69	1.10	1.53	2.29	13.38
3.0	0.96	1.37	1.83	2.29	10.98
3.5	1.03	1.37	1.83	2.29	10.98
4.0	1.03	1.20	1.74	2.29	10.98

POWDER: FCC

RISER DISTRIBUTOR: 7 HOLES

SOLID CIRCULATION RATE

	BVO:30 degrees	BVO:40 degrees	BVO:50 degrees	BVO:60 degrees	BVO:70 degrees
Ug (m/s)	SCR (g/s)	SCR (g/s)	SCR (g/s)	SCR (g/s)	SCR (g/s)
0.0	0.0	0.0	0.0	0.0	0.0
1.5	2.06	2.29	2.75	3.43	4.33
2.0	1.72	4.46	6.86	8.24	10.98
2.5	2.43	4.83	6.86	17.16	17.48
3.0	2.29	5.03	6.73	19.22	20.59
3.5	1.60	4.58	8.10	20.59	23.78
4.0	1.83	4.94	7.07	19.22	19.22

POWDER: FCC

RISER DISTRIBUTOR: 13 HOLES

SOLID CIRCULATION RATE

	BVO:30 degrees	BVO:40 degrees	BVO:50 degrees	BVO:60 degrees	BVO:70 degrees
Ug (m/s)	SCR (g/s)	SCR (g/s)	SCR (g/s)	SCR (g/s)	SCR (g/s)
0.0	0.0	0.0	0.0	0.0	0.0
1.5	1.47	2.52	2.75	4.29	4.29
2.0	1.83	3.17	6.86	9.15	11.44
2.5	1.07	3.77	6.86	14.71	17.84
3.0	1.60	4.12	17.16	19.22	20.50
3.5	1.37	4.12	14.71	19.22	20.50
4.0	1.37	4.12	15.44	20.60	22.0

RISER DISTRIBUTOR: 1 NOZZLE

POWDER: PORALOX

SOLID CIRCULATION RATES

	Ug: 2m/s	U:2.5m/s	Ug:3 m/s	Ug:3.5m/s	Ug:4 m/s
BVO/deg.	SCR (g/s)	SCR(g/s)	SCR (g/s)	SCR(g/s)	SCR(g/s)
30	4.57	4.84	5.65	5.11	5.38
40	10.65	11.94	13.31	12.63	13.98
50	17.20	17.22	20.56	21.88	21.29
60	23.79	24.20	25.54	32.51	33.47
70	---	---	32.26	43.35	46.37

RISER DISTRIBUTOR: 1 NOZZLE

POWDER: 50/50 v/v MIXTURE

SOLID CIRCULATION RATE

	Ug: 2m/s	U:2.5m/s	Ug:3 m/s	Ug:3.5m/s	Ug:4 m/s
BVO/deg.	SCR (g/s)	SCR(g/s)	SCR (g/s)	SCR(g/s)	SCR(g/s)
30	---	---	2.26	3.52	3.52
40	---	---	7.54	9.05	8.75
50	---	---	13.20	16.35	14.08
60	---	---	23.39	23.84	19.62
70	---	---	27.16	37.72	43.0

APPENDIX B

POWDERS USED

SIEVE ANALYSIS

POWDER: FCC

SIEVE SIZE(μm)	% WEIGHT
> 250	0.80
250-212	1.03
212-180	1.01
180-150	2.47
150-125	6.55
125-90	6.55
90-75	33.03
< 75	48.75

POWDER: PORALOX

SIEVE SIZE(μm)	% WEIGHT
>353	0.16
353-300	1.09
300-250	1.09
250-212	6.37
212-180	14.83
180-150	22.12
150-125	22.0
125-106	10.76
63-53	1.85
53-45	0.93
< 45	0.56

APPENDIX C

HYDRODYNAMICS OF DOWNFLOW REGION WITHOUT CLUSTERING

In chapter three during the development of DALC model it was assumed that the origins of the downflow were caused by aggregation of individual particles into clusters. It is the purpose of this Appendix to consider the hydrodynamics of individual particles in the immediate viscinity (within $10d_p$) of the riser wall.

The universal non-dimensional representation of turbulent boundary layer flow is given by

$$\frac{u_y}{u_*} = \begin{cases} y^* & \text{viscous sublayer } y^* \leq 5 \\ 10\arctan(0.1y^*)+1.2 & \text{buffer layer } 5 \leq y^* \leq 30 \\ 5.5 + 2.5\ \ln y^* & \text{turbulent layer } y^* \geq 30 \end{cases}$$

where u_* is the friction velocity defined by

$$u_* = (\tau_w / \rho_f)^{0.5} = u_g\ (c_f / 2)^{0.5}$$

and the non-dimensional wall distance given by

$$y^* = \frac{y\ u_*}{\nu} = \frac{y\ u_*\ \rho_f}{\mu}$$

For a particle diameter of 64μm in air at room temperature and pressure, the terminal particle settling velocity is 0.2 m/s. The particle will start to fall in the downflow region if the gas velocity is less than 0.2 m/s. For air flowing with a bulk velocity of 3 m/s in a riser of diameter 0.05 m the pipe Reynolds number is 18000 safely in the turbulent regime. Using Fanning friction factor chart the friction factor c_f was estimated as 0.006.

The friction velocity $u_* = 3\ (0.006/2)^{0.5} = 0.164$ m/s

When the dimensionless distance $y^* = 5$ then the velocity

$$u_y = 5\ u_* = 5 \times 0.164 = 0.82 \text{ m/s}$$

When $u_y = 0.2$ m/s $\quad y^* = \frac{0.2}{0.82} \times 5 = 1.22$

This corresponds to a dimensional distance of

$$y = \frac{1.22 \times 10^{-5}}{0.164 \times 1.2} = 6.2 \times 10^{-5} \text{ m} = 62\mu\text{m}$$

Individual particles of diameter of 64μm will only fall if they are within the very small annulus 62μm wide. This would imply that only very few particles could constitude a downflow regime one or at best two particle diameter thick. This does not agree with visual observations which indicate that the downflow involves a large number of particles flowing downwards in an annulus of discernible thickness.

APPENDIX D

GAS VELOCITY MEASUREMENTS

GAS VELOCITY MEASUREMENTS

The laboratory compressed air supply was used at air flowrates less than 1200 lt/min and the flowrates were monitoring using rotameters. The rotameters were piped such that the pressure of air inside them could be held constant. This is done by using a pressure regulator and by positioning of the air control valve downstream of the rotameter. The rotameters were calibrated with the air inside the float chamber held at a constant 10 psig. Mass type gas flowmeters were used for calibration depending on the flowrate.

During the calibration the volumetric flowrate was measured at ambient pressure and temperature. Bed temperature and pressure were monitored and used in calculating the actual gas velocity in the bed from the rotameter reading.

APPENDIX E

CYCLONE DESIGN

MINIMUM AND MAXIMUM CLUSTER DIAMETER

Stairmand high efficiency cyclone is used for the design of the primary cyclone, for an operation of 10m/s riser velocity and by assuming that the riser cross-sectional area and the cyclone inlet duct area are equal.

Area of the inlet duct = $\frac{\pi D^2}{4} = \frac{\pi\ 0.05^2}{4} = 0.002\ m^2$

From figure E1, duct area = $0.5\ D_c$ x $0.2\ D_c$

or $0.002 = 0.10\ D_c^2$

Hence D_c = 140 mm

The design of the secondary cyclone is also based on the Stairmand's high efficiency design, by assuming that the cyclone efficiency may be impoved when the maximum pressure drop inside the cyclone do not exceed 1200 N/m^2.

Area of the inlet duct = $\frac{\pi\ 0.037^2}{4} = 1.075\ E\text{-}3\ m^2$

From Figure E1, duct area = $0.5\ D_c$ x $0.2\ D_c$

or $1.075E\text{-}3 = 0.10\ D_c^2$

Hence D_c = 105 mm.

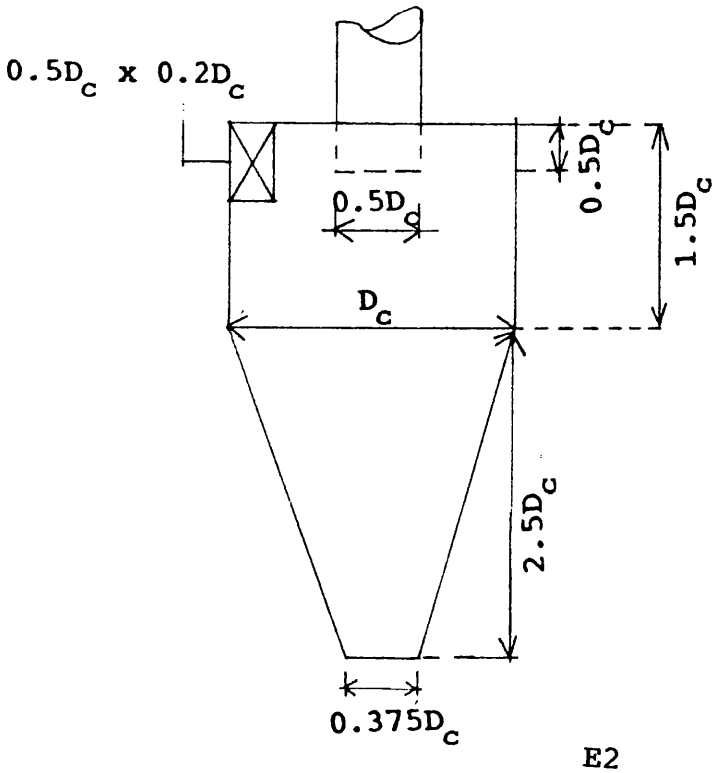

Figure E1

MINIMUM AND MAXIMUM CLUSTER DIAMETER

The minimum and maximum cluster diameters for a range of operation conditions are listed in Table E1, with an initial cluster velocity of 1m/s.

TABLE E1

BVO	U_g m/s	Riser Distributor	Minimum d_c m	Maximum d_c m
70	3	7 HOLES	3.834E-4	3.9E-4
40	3	7 HOLES	3.66E-4	3.81E-4
70	4	7 HOLES	4.43085E-4	4.4655E-4
70	2	7 HOLES	3.82035E-4	3.8276E-4
70	2.5	7 HOLES	3.816865E-4	3.8495E-4
70	3.5	7 HOLES	4.29272E-4	4.31E-4
70	4	13 HOLES	4.6565E-4	4.6658E-4
70	3.5	13 HOLES	4.403E-4	4.4155E-4
70	3	13 HOLES	4.1724E-4	4.1868E-4
70	4	1 NOZZLE	4.82893E-4	4.8316E-4
70	3.5	1 NOZZLE	4.507835E-4	4.51423E-4
70	3	1 NOZZLE	4.364E-4	4.3677E-4

APPENDIX F

COMPUTER PROGRAMMES

FLOW CHART

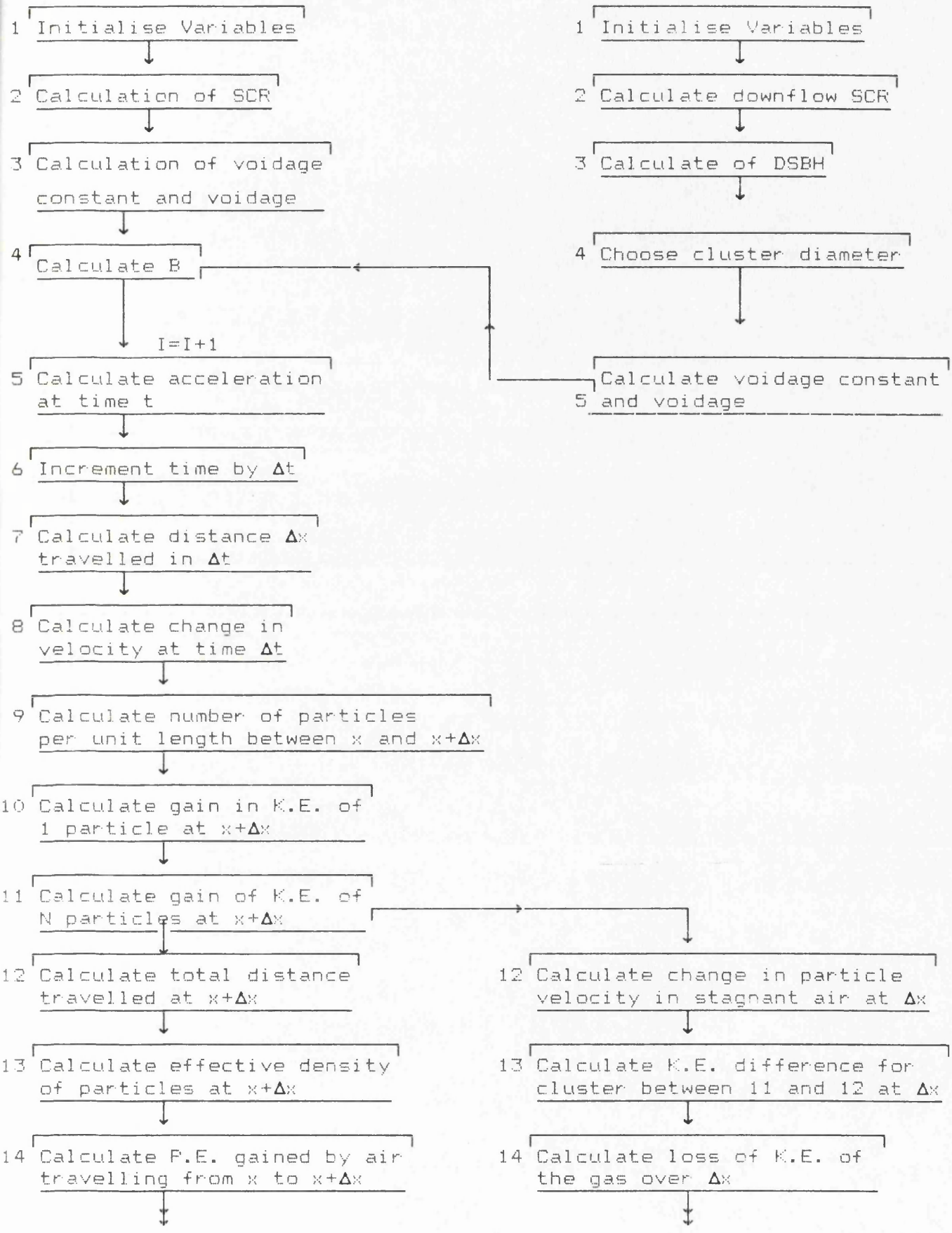
1 Initialise Variables
2 Calculation of SCR
3 Calculation of voidage constant and voidage
4 Calculate B
I=I+1
5 Calculate acceleration at time t
6 Increment time by Δt
7 Calculate distance Δx travelled in Δt
8 Calculate change in velocity at time Δt
9 Calculate number of particles per unit length between x and x+Δx
10 Calculate gain in K.E. of 1 particle at x+Δx
11 Calculate gain of K.E. of N particles at x+Δx
12 Calculate total distance travelled at x+Δx
13 Calculate effective density of particles at x+Δx
14 Calculate P.E. gained by air travelling from x to x+Δx
1 Initialise Variables
2 Calculate downflow SCR
3 Calculate of DSBH
4 Choose cluster diameter
5 Calculate voidage constant and voidage
12 Calculate change in particle velocity in stagnant air at Δx
13 Calculate K.E. difference for cluster between 11 and 12 at Δx
14 Calculate loss of K.E. of the gas over Δx

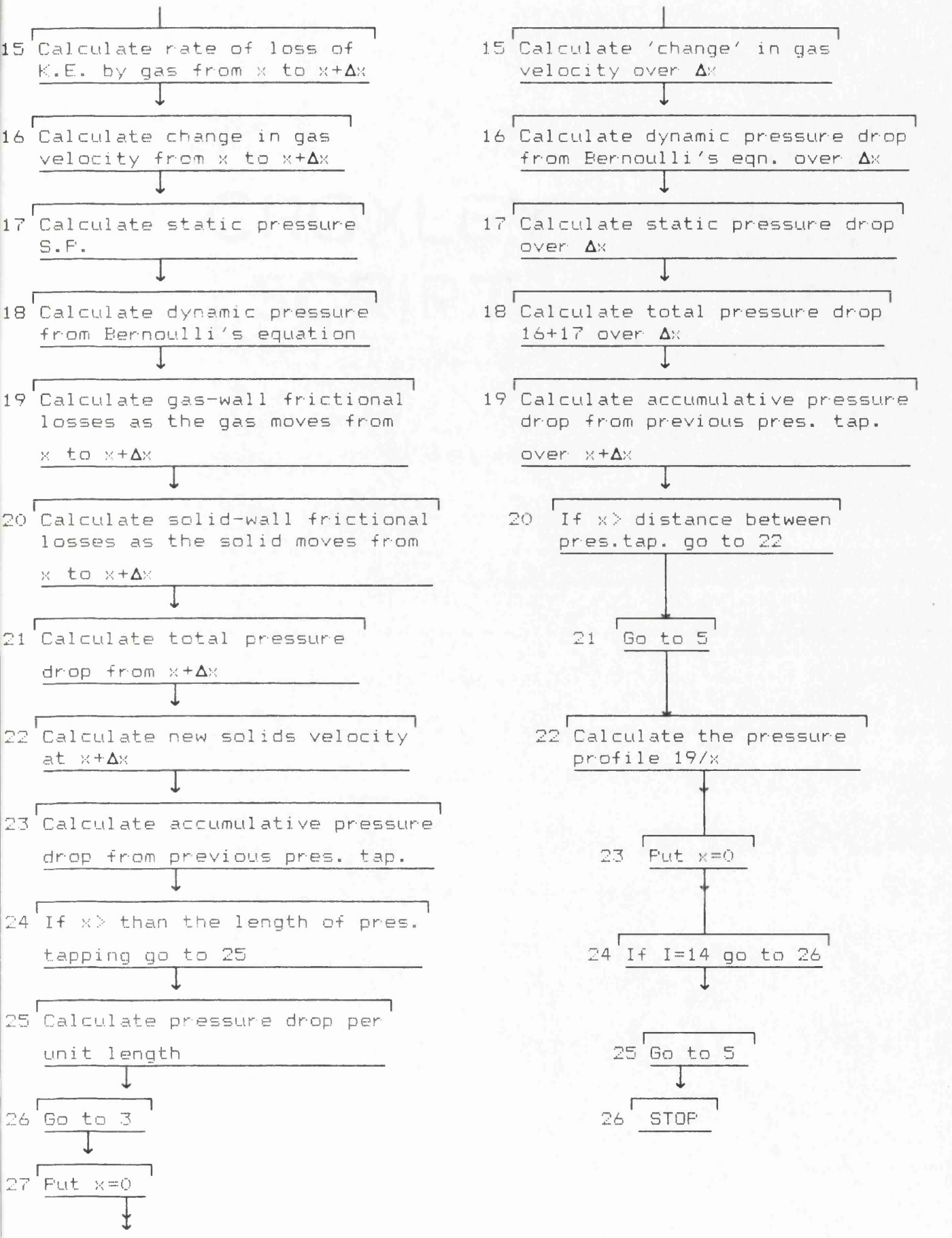
15 Calculate rate of loss of K.E. by gas from x to x+Δx
16 Calculate change in gas velocity from x to x+Δx
17 Calculate static pressure S.P.
18 Calculate dynamic pressure from Bernoulli's equation
19 Calculate gas-wall frictional losses as the gas moves from x to x+Δx
20 Calculate solid-wall frictional losses as the solid moves from x to x+Δx
21 Calculate total pressure drop from x+Δx
22 Calculate new solids velocity at x+Δx
23 Calculate accumulative pressure drop from previous pres. tap.
24 If x> than the length of pres. tapping go to 25
25 Calculate pressure drop per unit length
26 Go to 3
27 Put x=0
15 Calculate 'change' in gas velocity over Δx
16 Calculate dynamic pressure drop from Bernoulli's eqn. over Δx
17 Calculate static pressure drop over Δx
18 Calculate total pressure drop 16+17 over Δx
19 Calculate accumulative pressure drop from previous pres. tap. over x+Δx
20 If x> distance between pres.tap. go to 22
21 Go to 5
22 Calculate the pressure profile 19/x
23 Put x=0
24 If I=14 go to 26
25 Go to 5
26 STOP

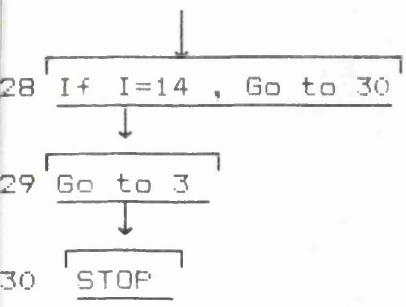
28 If I=14 , Go to 30
29 Go to 3
30 STOP

```
 10PRINT"WHAT IS PARTICLE DIAMETER"
 20INPUT DP
 30PRINT"DENSITY OF PARTICLES"
 40 INPUT ROEP
 50 ROEP=531
 60 MP=3.142*ROEP*DP^3/6
 70  PRINT"PARTICLE MASS",MP
 80PRINT"DENSITY OF GAS"
 90 INPUT ROEG
100 ROEG=1.2
110PRINT"VISCOSITY OF GAS"
120INPUT VIS
130 VIS=1E-5
140  PRINT"WHAT IS INITIAL GAS VELOCITY"
150 INPUT UGAS0
160 PRINT"WHAT IS GAS MASS FLOWRATE"
170 INPUT GS
180 A=(18*VIS)/(DP^2*ROEP)
190PRINT "VALUE OF A", A
200PRINT "WHAT IS INITIAL SOLIDS VELOCITY. DOWNWARDS POSITIVE"
210INPUT VELIN
220 VELIN=1
230 PTOT=0
240VEL=VELIN
250 PRINT"DIAMETER OF RISER"
260 DR=0.05
270 PRINT"SOLID CIRCULATION RATE"
280 INPUT SCR
290 VOIDC=4*SCR/(ROEP*3.142*DR^2)
300 PRINT"VOIDAGE CONSTANT",VOIDC
310 UGAS1=UGAS0
320X=0
330 EPS=1-(VOIDC/VEL)
340 B=A*EPS^(-4.7)
350 PRINT"B",B
360 DEL2=-(B*VEL)+(B*UGAS0+9.81)
370 PRINT"ACCELERATION", DEL2
380 DELTIM=0.01
390DELX= DELTIM*VEL
400X=X+DELX
410 PRINT"DELX",DELX
420 PRINT"DISTANCE", X
430 DVEL=DEL2*DELTIM
440 DVEL2=9.81*DELTIM
450 VEL=DVEL+VEL
460 VEL2=VEL+DVEL2
470 NP=6*(1-EPS)*DR/DP^2
480 H= VEL2^2-VEL^2
490 KE1 =0.5*MP*H
500 PRINT"GAIN OF PARTICLE K.E.",KE1
```

```
510 ENTOT = KE1
520 ENRATE=NP*ENTOT*VEL+(DELX*GS*9.81)
530 PRINT"RATE OF LOSS OF K.E.".ENRATE
540 PRINT"NP".NP
550 PRINT"P.E.GAINED BY AIR".DELX*GS*9.81
560 J=UGAS0^2-(2*ENRATE/GS)
570 UGAS2=-(J^0.5)
580 KELOSS=0.5*GS*(UGAS0^2-UGAS2^2)
590 PRINT"RATE OF LOSS OF K.E".KELOSS
600 PRINT"UGAS2".UGAS2
610 PRINT"VOIDAGE".EPS
620 DELGAS=UGAS0-UGAS2
630 PRINT"DELGAS".DELGAS
640 SP=(1-EPS)*(ROEP-ROEG)*9.81*DELX
650 PRINT"STATIC PRESSURE DROP".SP
660 ROEF=(1-EPS)*ROEP+EPS*ROEG
670 DELP=DELGAS^2*ROEG/2
680 PRINT"ROEF".ROEF
690 DELP=DELP+SP
700 PRINT"PRESSURE DROP".DELP
710 PTOT=PTOT+DELP
720 PRINT"SOLIDS VELOCITY".VEL
730 PL=DELP/DELX
740 PRINT"PRESSURE PROFILE".PL
750 PRINT"TOTAL PRESSURE".PTOT
760 IF X < 2.6 GOTO 330
770 STOP
780 END
```

```
 10 DIM XSTPD(12)
 20 DIM XSTP(12)
 30 DIM PL(20)
 40 DIM PLD(12)
 50 DIM PT(20)
 55 DIM EPS(20)
 60 PRINT"HOW MANY PROBES"
 70 PRINT"IN THE DILUTE CORE"
 80 INPUT NP
 90 NP=13
100 FOR I=1 TO NP
110 PRINT"HOW FAR FROM PREVIOUS PROBE"
120 INPUT XSTPD(I)
130 NEXT I
131 XSTPD(1)=0.0107
132 XSTPD(2)=0.16
133 XSTPD(3)=0.18
134 XSTPD(4)=0.18
135 XSTPD(5)=0.1
136 XSTPD(6)=0.18
137 XSTPD(7)=0.18
138 XSTPD(8)=0.26
139 XSTPD(9)=0.26
140 LSTP=2.57
141 XSTPD(10)=0.26
142 XSTPD(11)=0.26
143 XSTPD(12)=0.26
144 XSTPD(13)=0.26
150 XMIN=0  : XMAX = LSTP
160 YMIN=0  : YMAX = 1000
161 PRINT"WHAT IS GAS DIFFUSIVITY"
162 INPUT DF
163 PRINT"WHAT IS FIXED BED VOIDAGE"
164 INPUT EPSM
165 PRINT"WHAT IS REACTION RATE CONSTANT"
166 INPUT K1
167 PRINT"WHAT IS INLET CONCENTRATION"
168 INPUT CAS
170PRINT"WHAT IS PARTICLE DIAMETER"
180INPUT DP
190 DP=64E-6
200PRINT"DENSITY OF PARTICLES"
210 INPUT ROEP
220 ROEP=884
230 MP=3.142*ROEP*DP^3/6
240  PRINT"PARTICLE MASS",MP
250PRINT"DENSITY OF GAS"
260 INPUT ROEG
270 ROEG=1.2
```

```
280PRINT"VISCOSITY OF GAS"
290INPUT VIS
300 VIS=1E-5
301 SC=VIS/(ROEG*DF)
310  PRINT"WHAT IS INITIAL GAS VELOCITY"
320 INPUT UGAS0
340 PRINT"WHAT IS GAS MASS FLOWRATE"
350 INPUT GS
370 A=(18*VIS)/(DP^2*ROEP)
380PRINT "VALUE OF A", A
390PRINT "WHAT IS INITIAL SOLIDS VELOCITY, DOWNWARDS POSITIVE"
400INPUT VELIN
410  VELIN=-1.08
420 PTOT=0
430VEL=VELIN
440 PRINT"DIAMETER OF RISER"
450 DR=0.05
460 PRINT"SOLID CIRCULATION RATE"
470 INPUT SCR
490 VOIDC=4*SCR/(ROEP*3.142*DR^2)
500 PRINT"VOIDAGE CONSTANT",VOIDC
510 UGAS1=UGAS0
511 CAH=CAS
520 I=0
530 X=0
540 XL=0
550 I=I+1
560 XL = XL + XSTPD(I)
570 PTOT=0
580 X=0
590 DELP=0
600 DELX=0
610 EPS=1+(VOIDC/VEL)
620 B=A*EPS^(-4.7)
630 DEL2=-(B*VEL)+(B*UGAS0+9.81)
640 DELTIM=0.01
650 DELX= DELTIM*VEL
660 X=X+DELX
670 DELVEL=DEL2*DELTIM
680 NP=6*(1-EPS)*DR^2/(4*DP^3)
690 H= (VEL+DELVEL)^2-VEL^2
700 KE1 =0.5*MP*H
710 PE1 = -MP*9.81*DELX
720 ENTOT = KE1 +PE1
730 ENRATE=-NP*ENTOT*VEL-(DELX*GS*9.81)
740 J=UGAS0^2-(2*ENRATE/GS)
750 UGAS2=-(J^0.5)
760 KELOSS=0.5*GS*(UGAS0^2-UGAS2^2)
770 DELGAS=UGAS0-UGAS2
780 SP=-(1-EPS)*(ROEP-ROEG)*9.81*DELX
790 ROEF=(1-EPS)*ROEP+EPS*ROEG
```

```
 800 DELP=DELGAS^2*ROEG/2
 810 FR=2*0.206*(UGAS0^2)
 820 FR=-FR*DELX*ROEG/0.05
 830 FS=-12.2*(1-EPS)/(VEL*EPS^3)
 840 SWF=-2*FS*(1-EPS)*ROEP*DELX*VEL^2/0.05
 850 DELP=DELP+SWF+FR+SP
 860 VEL=VEL+DELVEL
 861 RET=(-UGAS0+VEL)*DP*ROEG/VIS
 862 SH=2+0.69*SC^0.33*RET^0.5
 863 HM=(SH*DF)/DP
 864 EPS1=(1-EPS)/(1-EPSM)
 865 VP=4/3*3.14*(DP/2)^3
 866 VC=VP/(1-EPS)
 867 T=T+DELTIM
 868 AP=3.14*DP^2/4
 869 CAH=CAS*EXP-(T/((VC/(HM*AP))+(1/(K1*EPS1))))
 870 PTOT=PTOT+DELP
 880 IF -X>XSTPD(I) GOTO 910
 890 GOTO 610
 900 STOP
 910 X2=-X
 920 PLD(I)=PTOT/X2
 930 PRINT"PRESSURE PROFILE",  PLD(I)
 931 PRINT"CAH", CAH
 932 PRINT "EPS", EPS
 940 IF XL<LSTP GOTO 550
 950 GOTO 1320
 960 STOP
 970 END
 980
1320 PRINT"HOW MANY PROBES"
1330 PRINT"IN THE DOWNFLOW REGION"
1340 INPUT NP
1350 NP=13
1360 FOR I=1 TO NP
1370 PRINT"HOW FAR FROM PREVIOUS PROBE"
1380 INPUT XSTP(I)
1390 NEXT I
1391 XSTP(1)=0.04
1392 XSTP(2)=0.26
1393 XSTP(3)=0.26
1394 XSTP(4)=0.26
1395 XSTP(5)=0.26
1396 XSTP(6)=0.26
1397 XSTP(7)=0.26
1398 XSTP(8)=0.18
1399 XSTP(9)=0.18
1400 LSTP=2.58
1401 XSTP(10)=0.1
1402 XSTP(11)=0.18
1403 XSTP(12)=0.18
```

```
1404 XSTP(13)=0.1775
1410 PRINT "WHAT IS PARTICLE DIAMETER"
1420 INPUT DP
1430 PRINT"INPUT GAS DIFFUSIVITY"
1431 INPUT DF
1432 PRINT"INPUT FIXED BED VOIDAGE"
1433 INPUT EPSM
1434 PRINT"INPUT REACTION RATE CONSTANT"
1435 INPUT K1
1436 PRINT"INPUT INLET CONCENTRATION"
1437 INPUT CAS
1440 PRINT"DENSITY OF PARTICLES"
1450 INPUT ROEP
1460 ROEP = 531
1470 MP=3.142*ROEP*DP^3/6
1480 PRINT "DENSITY OF GAS"
1490 INPUT ROEG
1500 ROEG=1.2
1510 PRINT"VISCOSITY OF GAS"
1520 INPUT VIS
1530 VIS=1E-5
1531 SC=VIS/(ROEG*DF)
1540 PRINT"WHAT IS GAS MASS FLOWRATE"
1550 INPUT GS
1560
1570 A=(18*VIS)/(DP^2*ROEP)
1580 PRINT"VALUE OF A",  A
1590 PRINT"INITIAL SOLIDS VELOCITY"
1600 INPUT VELIN
1610 VELIN = 1
1620 VEL=VELIN
1630 DR=0.05
1660 GOTO 2170
1670 VOIDC = 4*SCRD/(ROEP*3.142*DR^2)
1680 PRINT"VOIDAGE CONSTANT",  VOIDC
1690 I=0
1700 XL=0
1710 I=I+1
1720 XL=XL+XSTP(I)
1730 PTOT=0
1740 X=0.004
1750 DELP=0
1760 EPS=1-(VOIDC/VEL)
1770 B=A*EPS^(-4.7)
1780 DEL2=-(B*VEL)+(B*UGAS0+9.81)
1790 DELTIM  = 0.01
1800 DELX=DELTIM*VEL
1810 X=X+DELX
1820 DVEL=DEL2*DELTIM
1830 DVEL2=9.81*DELTIM
1840 VEL=VEL+DVEL
1850 VEL2=VEL+DVEL2
1860 NP=6*(1-EPS)*DR/DP^2
```

```
1870 H=VEL2^2-VEL^2
1880 KE=0.5*MP*H
1890 ENRATE=NP*KE*VEL+(DELX*GS*9.81)
1900 J=UGAS0^2-(ENRATE*2/GS)
1910 UGAS2=-(J^0.5)
1920 DELGAS=UGAS0-UGAS2
1930 SP=(1-EPS)*(ROEP-ROEG)*9.81*DELX
1940 ROEF=(1-EPS)*ROEP+EPS*ROEG
1950 DELP=DELGAS^2*ROEG/2
1960 DELP=DELP+SP
1970 PTOT=PTOT+DELP
1980 IF X>XSTP(I) GOTO 2010
1990 GOTO 1760
2000 STOP
2010 X2=X
2015 EPS(I)=EPS
2020 PL(I)=PTOT/X2
2030 PRINT "PRESSURE PROFILE", PL(I)
2040 IF XL<LSTP GOTO 1710
2050 PRINT "RETURN FOR TOTAL"
2060 INPUT YES
2070 YES=0
2100 FOR I = 1 TO 13
2110 J=14-I
2120 PT(I)=PL(J)+PLD(I)
2125 PRINT"TOTAL PROFILE",  PT(I)
2130 NEXT I
2140 FOR I=1 TO 12
2141 J=14-I
2142 AVEPS=0.5*(EPS(J)+EPS(J-1))
2143 PRINT "AVEPS", AVEPS
2144 EPS11=(1-AVEPS)/0.55
2145 TRES=-XSTP(J)/UGAS0
2146 CAH=CAH*EXP-(TRES*K1*EPS11)
2147 PRINT "CAH", CAH
2148 NEXT I
2260 END
2270ROEF=486.74
2280DSB=0.15
2290ASB=0.01767
2300 PRINT"CHANGE OF S.B.HEIGHT"
2310INPUT DH
2320VSB=ASB*DH
2330 PRINT"HEIGHT OF SLOW BED"
2340 INPUT HBED
2350 VBED=ASB*HBED
2360 VTOT=0.038
2370 V2=0.038-VBED
2380 R=5.89E-3/V2
2390 PRINT"VOLUME RATIO",R
2400M=VSB*ROEF
2410MR=R*M
2420 SCR1=SCR
2460 US=-UGAS0-0.2
```

```
2470HR=3.0
2480TS1=HR/US
2490M1=TS1*SCR1
2500MD=MR-M1
2510VS=1
2520TSD=HR/VS
2530SCRD=MD/TSD
2540PRINT"SCR IN DOWNFLOW",SCRD
2550 GOTO 1670
2560STOP
2570END
```

APPENDIX G

FLUID JETS

It seems important at this point to introduce the fluid jets, which play an important role in many turbulent mixing operations such as mixing in piping, jet mixing in tanks.

Tollmien (1926) and Ruden (1933) both using piezometric traverse methods across an air-jet, showed that in an axially symetrical jet, the jet appeared to be in the form of a regular cone with its origin some distance behind the nozzle-mouth. In the region close to the nozzle-mouth the axial velocity profile remains constant and the velocity profile gradually changes over from being virtually flat to the Gaussian shape. Some of the features of turbulent jets (Re > 2100) are illustrated in Figure G1. In region I termed the potential core, the velocity is equal to that in the nozzle itself. The potential core is z_c. Region II is an intermediate zone in which the flow is both turbulent and nonturbulent. Region III is the mixing zone that lies between the undisturbed fluid. In region IV the mixing zone and potential core merge and form a totally turbulent pattern.

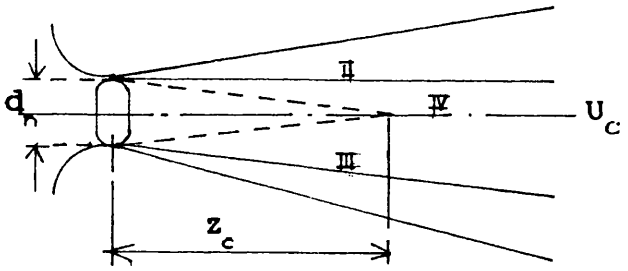

Figure G1

Regarding to the jet angle ie the angle subtended by the cone, various values can be derived from the published data. Tollmien (1926) recomended a complete angle of 24 .

From visual observations, the total jet angle appears to be roughly 14 . Donald and Singer (1959) observed that jet angles increased with kinematic viscosity of the fluid. By considering the design of the 3 distributors used during the experimental work and by assuming that the jet angle is of 14° or 24° , using simple geometry the potential core length can be determined for each orifice diameter of the distributor.

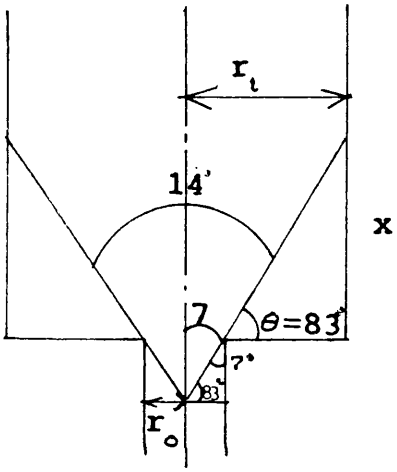

$$\tan\vartheta = \frac{x}{r_t - r_o}$$

$$x = \tan\vartheta\ (r_t - r_o)$$

For $\omega = 14^{\circ}$, $\vartheta = 83^{\circ}$

No. of holes	r_o(cm)	r_t(cm)	x(cm)
1	0.5	2.5	16.3
7	0.19	0.75	4.6
13	0.14	0.625	3.95

1 nozzle case

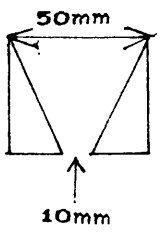

7 hole case

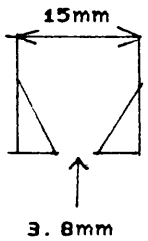

13 hole case

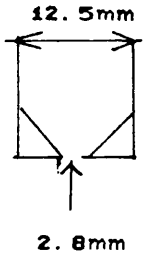

For $\omega = 24^{\circ}$, $\vartheta = 78^{\circ}$

No. of holes	r_o (cm)	r_t (cm)	x(cm)
1	0.5	2.5	9.4
7	0.19	0.75	2.6
13	0.14	0.625	2.3